Forensic Taphonomy:

Investigating the Post Mortem Biochemical Properties of Cartilage and Fungal Succession as Potential Forensic Tools

A thesis presented for the degree of

Doctor of Philosophy

Shawna N. Bolton, B.A. (Hons.), M.Sc.

University of Wolverhampton

Faculty of Science and Engineering

PhD Supervisors: Dr Michael Whitehead and Dr Raul Sutton

Forensic Taphonomy: Investigating the Post Mortem Biochemical Properties of Cartilage and Fungal Succession as Potential Forensic Tools

A thesis submitted in fulfilment of the requirements of the University of Wolverhampton for the award of the degree of Doctor of Philosophy (PhD)

NOVEMBER 2014

Signature: 

Date: 30th November 2014

Abstract

Post mortem interval (PMI – the time elapsed since death and discovery) is important to medicolegal investigations. It helps to construct crucial time lines and assists with the identification of unknown persons by inclusion or exclusion of a suspect's known movements. Accurate methodologies for establishing PMI are limited to about 48-hours. Such methods involve use of increasing levels of potassium in vitreous humour, and algor mortis. This study is two-fold. Firstly, it explores the biomolecular changes in degrading porcine cartilage buried in soil environments and its potential to determine PMI in the crucial two days to two months period. Trotters were interred in a number of graves at two distinct locations exhibiting dissimilar soil environments. Weekly disinterments (for 6 weeks) resulted in dissection for cartilage samples which were processed for protein immunoblot analyses and cell vitality assays. Results demonstrate that aggrecan, a major structural proteoglycan, produces high (230kDa) and low (38kDa) molecular weight cross-reactive polypeptides (CRPs) within cartilage extracellular matrix. The 230kDa CRP degrades in a reproducible manner irrespective of the different soil environments utilised. As PMI increases, aggrecan diminishes and degrades forming heterogeneous subpopulations with time. Immunodetection of aggrecan ceases when joint exposure to the soil environment occurs. At this time, aggrecan is metabolised by soil microbes. The molecular breakdown of cartilage proteoglycans has potential for use as a reliable indicator of PMI, irrespective of differing soil environments, beyond the 48-hours period. Likewise, vitality assays also demonstrated viable chondrocytes for as long as 35 PM days. The second component of this study examined the fungal activity associated with trotters buried below ground. Results indicate that fungal growth was considerably influenced by soil chemistry and changes in the environment. Fungal colonisation did not demonstrate temporal patterns of succession. The results of this study indicate that cartilage has the potential to prolong PMI determination

well beyond the current 48- and 100-hour limitations posed by various other soft tissue methods. Moreover, the long-term post mortem viability of chondrocytes presents an opportunity to explore DNA extraction from these cells for the purpose of establishing a positive identification for unidentified remains. On the contrary, the growth and colonisation patterns of post putrefactive fungi in relation to decomposing porcine trotters proved to be futile for estimating PMI. Therefore, fungi may not be a suitable candidate for evaluating PMI during the early phase fungal activity.

Acknowledgements

When I first embarked on this new chapter of my life, I had no idea where the road ahead would lead me. However, the past four years have been such a blessing. This is owed to the many wonderful staff members and friends who have made my experience far richer than I could have ever imagined. Without their loving support, I could not have made it this far.

Firstly, I would like to express my deepest gratitude to my supervisory team, Drs Michael Whitehead and Raul Sutton for their guidance and support. Thank you for giving me the opportunity to take control of my research and for the constructive criticisms you both have provided during the course of my studies. In doing so, I have learned so much and a great deal about my self. To Dr Jayesh Dudhia of the Royal Veterinary College for providing me with training on how to prepare cartilage samples and perform Western blots, for gifting me the MAb 2-B-6 monoclonal antibody to perform my analyses, and for offering me his advice and support on related subject matter. Thank you to Dr Tim Baldwin for providing me with SDS-PAGE training and for allowing me to use your chemicals and equipment. To the many staff members who have assisted me in more ways than one, Dr Terry Bartlett and Professor John Howl for allowing me to audit their lectures, Drs Andrew Black and Dave Townrow for providing me with transportation to Hilton and data for soil and weather analyses, Mr Robert Hooton for maintaining the burial plot at Compton Park and for constructing the plot at Hilton. Thanks to Dr Angel Armesilla for advice on Western blotting and for gifting the anti-α-tubulin, Dr Mark Morris for his helpful suggestions and black India ink for staining Western blot membranes, Dr Ian Nichol for gifting protease inhibitors, Dr Wei Wang for gifting monoclonal antibodies, anti-vinculin and anti-vimentin, to Professor Craig Williams for assisting me with the interpretations for my soil analysis. Thank you, Drs

Angie Williams and Andrew Black for your assistance with processing orders. Thank you, Ms. Raman Kaur, for taking care of all my research administrative work.

A warm thank you to the lab technicians, Andy Brooke, Bal Bains, Ann Dawson, Nick and Jo Skidmore, Clare Murcott and Henrik for their continued technical assistance with various matters. To Wilma, Jen, and Kate, some of the most wonderful cleaning technicians I have met (thanks for the heart-to-heart conversations), Drs Wera Schmerer, Martin Khechara, and Steve Saffrany for providing me with teaching opportunities. Dr Malcolm Inman, thank you for your help with microscopy, for providing me with photographic images of my fungal plates, and for our much welcomed discussions about life in general, including faith. Thank you Dr Alison McCrea for assisting me with much needed help for statistics and to Rachael Walker, Stephanie Yeoman and Emily Schofield for providing me with additional cartilage samples to assess from their research projects.

Thank you to my "sister-friend," Tinesha Jones, for reminding me about what it means to have faith during difficult times. To my family away from home, Anushree Singh, Nikita Mehta, Tania Pereira, Shaymaa Al-dabagh, who have kept me laughing every single day for four years. And last, but not least, to my wonderful fiancé who has been extremely supportive and for putting up with my extended periods of absence.

To anyone whose name I may have forgotten to mention, my sincerest apologies. Thank you for the years of steadfast support!

Dedication

To my parents, Patricia and Garfield Bolton, who have sacrificed a great deal so that I could follow my heart. To my siblings, Sheldon and Daniella, and my cousin, Kisrene McKenzie, for keeping me grounded. Thank you for believing in me, when at times, I did not believe in myself and for encouraging me to pursue my dreams.

This thesis is dedicated to

Partricia, Garfield, Sheldon, Daniella and Kisrene

Table of Contents

Table of Tables

Table of Figures

List of Abbreviations

ADD	Accumulated degree days
AF	Ammonia fungi
ANOVA	Analysis of variance
BMP-2	Bone morphogenic protein-2
BSA	Bovine serum albumin
C-0-S	Dermatan sulphate
C-4-S	Chondroitin-4-sulphate
C-6-S	Chondroitin-6-sulphate
C	Carbon
CO_2	Carbon dioxide
CBF	Cerebrospinal fluid
Ch'ABC	Chondroitinase ABC
CMP	Compton Park burial plot/soil environment
CPF	Core protein fragments
CRP	Cross reactive polypeptide
CS	Chondroitin sulphate
ECM	Extracellular matrix
EP	Early phase
FGF	Fibroblast growth factor
G	Globular domain
GAG	Glycosaminoglycan
HA	Hyaluronic acid or hyaluronan
HG	Human glioblastoma
HLT	Hilton burial plot/soil environment
HPR	Horseradish peroxidase
IGD	Interglobular domain
IVJ	Intervertebral joint
KS	Keratan sulphate
MAb	Monoclonal antibody
MC	Metacarpal
MCP	Metacarpophalangeal joint
MMP	Matrix metalloproteinase
MSC	Mesenchymal stem cell
MT	Metatarsal
MTP	Metatarsophalangeal joint
N	Nitrogen
NH_4^+	Ammonium
$NO3^-$	Nitrate
OA	Osteoarthritis
PG	Proteoglycan
PM	Post mortem
PMI	Post mortem interval
PPF	Postputrefactive fungi
RA	Rheumatoid arthritis
ROS	Reactive oxygen species
SDS-PAGE	Sodium dodecyl sulphate polyacrylamide gel electrophoresis
TBS-T	Tris buffer saline with tween 20
TGF-β	Transforming growth factor-β
TSD	Time since death
VFA	Volatile fatty acid

Introduction

Chapter 1

1.0 Introduction

1.1 Death and forensic taphonomy: An introduction to forensic investigations

Death is defined as, "[t]he end of life; the permanent cessation of vital bodily functions, as manifested in humans by the loss of heartbeat, the absence of spontaneous breathing, and brain death" (Dictionary.com 2014). When an individual dies, the body gradually loses its ability to support life-sustaining activities and therefore undergoes a series of biochemical changes from within. These changes are governed by an unrestrained production of aerobic microorganisms within the intestinal and respiratory tracts which gradually deplete the body of oxygen. Lack of oxygen inhibits the aerobic (oxygen dependent) metabolism of cells within the body causing its pH to become acidic as the concentration of carbon dioxide (CO_2) increases (Clark *et al*., 1997), resulting in a process known as autolysis.

During autolysis, hydrolytic enzymes such as lipases, amylases, and proteases (Haslam & Tibbett, 2009), are released into the cell's cytoplasm by membrane-bound organelles called lysosomes (Carter *et al*., 2007; Clark *et al*., 1997). At this stage, the cells within the body swell and eventually rupture thereby releasing various nutrients and minerals to the immediate environment (Carter *et al*., 2007; Clark *et al*., 1997; Hopkins *et al*., 2000; Ishii *et al*., 2006). The consequence of these enzymes is cellular destruction and therefore marks the onset of putrefaction, the bacterially induced breakdown of soft tissue (muscles, tendons, blood vessels, and internal organs), which typically occurs 48-72 hours PM (Dent *et al*., 2004; Janssen, 1984).

As time continues forward, these complex changes begin to manifest themselves in ways that become visibly apparent among decomposing bodies. Loss of skin colour, corneal turbidity, rigidity of the body and gravitational pooling of blood are a few examples of such

alterations and are further discussed in section 1.1.1. In conjunction with these post mortem (PM) corporeal modifications, various extrinsic factors also come into play and further alter the body's integrity. Examples of external influences include climate, animal activity, aquatic or burial environment, geographic location, cremation, and commingling (Marks *et al*., 2009; Pokines, 2009; Steadman & Andersen, 2009; Tersigni-Tarrant & Shirley, 2013). Together, these variables result in an ongoing destruction of soft and hard tissue evidence which forensic examiners rely on in order to construct biological profiles for unidentified human remains.

The branch of forensic science concerned with the PM transformations that corporal remains undergo from the moment of death up until the time of discovery is known as forensic taphonomy (Byers, 2005; Marks *et al*., 2009; Willey & Leach, 2009). It involves the investigation of soft tissue changes, decomposition rates and patterns, the dispersion of body parts, and the modifications that occur to both soft tissues and bone. According to Haglund and Sorg (1997, p.3), forensic taphonomy is "the use of taphonomic models, approaches, and analyses in forensic contexts to estimate time since death, reconstruct the circumstances before and after deposition, and discriminate the products of human behaviour from those created by the earth's biological, physical, chemical, and geological subsystems."

Forensic taphonomy is further divided into two subfields: geotaphonomy and biotaphonomy (Nawrocki, 1996). Geotaphonomy is the study of how a person, who buries a body, and how the body itself affects the surrounding geological and botanical environment. Soil disturbances, tool mark impressions found along the walls of burial shafts, footprints at the bottom of graves, disruption of vegetative growth, modification of natural water courses and erosion patterns, and variations in the pH of proximate soil (Ibid) are examples of the PM processes that geotaphonomists are particularly interested in.

Biotaphonomists examine the corporal remains and enquire how decomposition and destruction of the soft and hard tissues came about. Biotaphonomic variables are influenced by environmental (i.e. climate and animals) individual (i.e. age, health and body mass) and cultural (i.e. mortuary practices and autopsy procedures) factors (Nawrocki, 1996). The collection of such data is relevant to forensic investigations in that it is used to provide information about the circumstances surrounding death.

1.1.1 Post mortem interval versus post burial interval

For cases involving the discovery of human remains, establishing a post mortem interval (PMI), an estimate of the amount of time that has elapsed since physiological death and medicolegal examination (Jashnani *et al*., 2010; Knight, 1987; Poloz & O'Day, 2009), is considered crucial to conducting criminal investigations and legal proceedings (Ahi & Garg, 2011; Ferreira & Cunha, 2013; Henßge & Madea, 2007; McDowall *et al*., 1998; Thaik-Oo *et al*., 2002; Zhou *et al*., 2007). Accurate determination of this time frame is necessary for settling civil matters, such as determining the beneficiary of property or whether an insurance policy was in effect (Ahi & Garg, 2011) and most importantly, for conducting criminal investigations (Ahi & Garg, 2011; Kaliszan *et al*., 2009; Pounder, 1995). In the case of the latter, this information presents:

- a time frame for when the individual in question may have died and/or when a crime was likely committed
- creates a reference point for law enforcement officials to conduct well-organized investigations
- confirms or disproves a suspect's alibi by inclusion or exclusion of individuals whose movements are known and

- serves to substantiate witness testimony (Sachdeva *et al*., 2011).

Establishing a PMI provides a timeline of the events surrounding a person's death and can affect the outcome of an investigation (Ferreira & Cunha, 2013; Forbes, 2008; Pounder, 1995).

Unlike PMI, post burial interval (PBI) is concerned with the amount of time that has passed since the burial of remains until their retrieval (Forbes, 2008). It represents only a fraction of the entire post mortem time frame for which an individual has been dead for. For instance, a decedent's body may not be buried until several hours have passed since death. In some cases where deposition of human remains follows immediately after death, PBI and PMI may be synonymous.

1.1.2 Corporal changes and determination of PMI

In forensic situations, PMI is evaluated in one of two ways: 1) by examining the rate of corporal and biochemical changes that occur soon after death; and 2) observing physical evidence found in association with human remains. The biochemical and physical changes that ensue subsequent to death generally occur in a predictable sequence which can be used by forensic pathologists to make inferences about PBI/PMI (Ahi & Garg, 2011; Pounder, 1995). These changes generally occur within 24-48 hours PM and characterise the early postmortem period (Forbes, 2008; Poposka *et al*., 2013).

Within 2-3 hours of dying, skin begins to pallor, sphincter muscles begin to relax resulting in the release of faecal matter, and bodily fluids are released from the gastrointestinal and respiratory tracts (Clark *et al*., 1997; Wilson-Taylor, 2013). The cornea of eyes that remain open after death develop a thin film (approximately 1 hour PM), followed by a hazy white cloudiness (within 2 hours) that becomes densely opaque (as early as 2 hours and is generally established by 6 hours) and is known as corneal turbidity/opacity (Gannon &

Gilbertson, 2014). Each of these soft tissue modifications are classified as early PM changes because they transpire within the first two hours of death when there is a lack of oxygen due to cardiac arrest (Clark *et al*., 1997) and the body is still "flaccid or limp" (Swift, 2010).

Late PM changes are those which occur within the span of several days to months after death and are characterised by the presence of putrefaction; the formation of adipocere, an organic, waxy build-up caused by a saponification process where the fatty tissues of cadavers are converted into a soap-like substance as a result of hydrolysis (Gill-King, 1997); mummification of soft tissues; and "peaty transformations" (Kaliszan *et al*., 2009). Forensic pathologists are able to make inferences about PMI based on the extent of these PM changes.

Additional early PM changes that form methods aiding PMI determination occur among the soft tissues are those that occur 2-4 hours PM. These include the gradual cooling of a body to ambient temperature (*algor mortis*), discolouration of the body due to the settling of blood towards the direction of gravity (*livor mortis*), and the temporary stiffening of muscles (*rigor mortis*) (Clark *et al*., 1997; Kaliszan *et al*., 2009; Wilson-Taylor, 2013). Other methods utilised involve measuring the potassium concentration of the gel-like fluid (vitreous humour) within the eye (Adjutantis & Coutselinis, 1972; Ahi & Garg, 2011; Coe, 1989; Madea *et al*., 1990; Madea & Rödig, 2006; Passos *et al*., 2009), the use of entomological knowledge about the species of arthropods that successively colonise cadavers, the life stages of the insects gathered from or in close proximity to decomposing human remains (Byers, 2005; Haskell *et al*., 1997; Steadman & Andersen, 2009; Turchetto & Vanin, 2004; Voss *et al*., 2008), and the extent of skeletonization and PM modifications that skeletal elements exhibit such as bone weathering (i.e. soil stains, exfoliation, sun-bleaching, cortical exfoliation, and demineralisation) (Behrensmeyer, 1978; Galloway, 1997; Ubelaker, 1997; Wilson-Taylor, 2013).

Table 1.1: Examples of PM corporal changes and circumstantial evidence associated with dead bodies that are used by forensic examiners to make inferences about the decedent's PMI.

Methods Employed for the Determination of PMI Using Various Soft Tissue Indicators			
Method	**Post Mortem Occurrence**	**Additional Characteristics**	**Example**
Skin Pallor	15-30 mins		
Livor Mortis (Gravitational pooling of blood)	1-2 hours	Becomes fixed 8-12 hours	
Rigor Mortis (Muscle stiffening followed by relaxation)	2-4 hours	Lasts up to 24 hours	
***Algor Mortis** (Cooling of body to ambient temperature) Henssge's Rectal Nomogram	Occurs immediately after death	Useful up to 24 hours	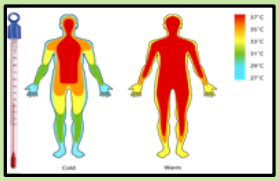
***Vitreous Potassium Humor** (Potassium concentration increases in a predictable manner)	Occurs immediately after death	Increases for up to 100-120 hours PM. Most accurate within 48 hours after death.	
Circumstantial Evidence Used to Aid with PMI Determination			
***Insect Activity** (Life cycle and successive colonization)	Almost immediately after death	Flies alone: 3-13days + Beetles: Up to 25 days Beetles alone: +25 days	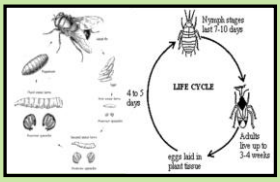

* Methods considered most accurate for determining PMI.

Table 1.1 presents some of the methods employed by forensic examiners that are well-established and considered reasonably accurate for PMI determination. A measure of the body's core temperature at the time of discovery is used to establish PMI using Henßge's rectal temperature nomogram (Henßge, 1988); this method is considered one of the most accurate of the early PM techniques for determining time since death (TSD), especially if used within the 24-hour PMI (Kaliszan *et al*., 2009). It is also deemed the most useful tool in typical forensic situations (Honjyo *et al*., 2005; Kaliszan *et al*., 2009; Nawrocki, 1996). This method assumes a normal body temperature of 37˚C at the time of death and decreases, on average, by 1.5˚C every hour (Clark *et al*., 1997). Analyses of vitreous potassium concentration demonstrate a linear relationship with PMI for approximately 100-120 hours, whereby the concentration of potassium increases as PMI increases (Ahi & Garg, 2011; Drolet *et al*., 1990; Thaik-Oo *et al*., 2002). Vitreous humour is deemed the "most reliable" body fluid for inferring PMI because it is typically well preserved PM, even in cases involving severe trauma. It is least prone to contamination and putrefactive influences unlike blood and cerebrospinal fluid (CBF) (Passos *et al*., 2009; Thaik-Oo *et al*., 2002; Thierauf *et al*., 2009).

Soon after death, bodies are generally invaded by various species of arthropods in a predictable sequence (Voss *et al*., 2008). The most common order of insect to rapidly colonise cadavers is *Diptera*, known as the common fly (Bunch & Shine, 2009; Byers, 2005; Haskell *et al*., 1997). Within 1-2 hours of appearing, these arthropods lay eggs (oviposition) which later develop into larvae and then adult flies. Colonisation of human remains by *Diptera* is succeeded by members of the order *Coleoptera* (beetles) which feed on the eggs and larvae of *Diptera*. Their later arrival and longer life cycles can be used to further extend the PMI estimates obtained from Dipterans (Byers, 2005) (Table 1.1). The use of arthropods for approximating PMI is currently the most precise method available. An extensive amount

of data regarding the developmental rates of cadaver-related arthropods has been collected in natural and controlled environments at varying temperatures. Evaluation of PMI for unidentified remains has been found to be correct within 12 hours of the actual TSD for remains discovered 15-20 days later (Haskell *et al*., 1997). Unlike Henßge's rectal temperature nomogram and evaluation of vitreous potassium concentration, this method can be used for remains discovered past 4 days.

1.1.3 Issues with determining PMI

Despite the relative importance of establishing PMI, the ability for forensic examiners to accurately acquire an estimation of TSD is incredibly difficult and at times evasive (Ferreira & Cunha, 2013; Kaliszan *et al*., 2009; Knight, 1987; Passos *et al*., 2009; Steadman & Andersen, 2009; Steadman, 1997). The majority of the techniques employed by forensic examiners to assess PMI rely heavily upon the presence of soft tissues and fluids which generally undergo rapid biochemical changes. Furthermore, these methods are essentially predisposed to varying degrees of error because the rates at which soft tissue destruction occurs are influenced by a myriad of exogenous and endogenous variables.

The approaches currently used by forensic pathologists to determine TSD are rendered less reliable with increasing PMI. As previously mentioned in sections 1.1 and 1.1.2, this is due to the various extrinsic factors, and to a lesser degree, intrinsic variables such as, ante- or perimortem illnesses (Lange *et al*., 1994; Thaik-Oo *et al*., 2002), manner of death (Muñoz Barús *et al.*, 2002), drug use, trauma sustained around the time of death (Haskell *et al.*, 1997), and age at death which variably impact the rate at which soft and hard tissues decompose. For instance, the rate at which the body temperature of a deceased person reaches equilibrium with its environment is influenced by biological processes (i.e. hypothermia, antemortem struggle which causes an elevation in body temperature,

haemorrhages, and fever) and physical factors (i.e. the presence of clothing, body build, drastic changes in ambient temperature) (Althaus & Henßge, 1999; Dirkmaat & Adovasio, 1997; Henßge, 1988; Kaliszan *et al*., 2009; Nawrocki, 1996; Ubelaker, 1997). Moreover, this method can only be applied to bodies discovered in temperate or cool climates. The PM change in concentration of vitreous potassium is affected by factors such as blood chemistry, chronic illnesses, death by asphyxiation, the decedent's age at death, putrefaction and ambient temperature (Ahi & Garg, 2011; Coe, 1989; Jashnani *et al*., 2010; Rognum *et al*., 1991; Thaik-Oo *et al*., 2002; Zhou *et al*., 2007). Taking these various factors into account, the relationship between biochemical/morphological alterations and PMI progressively diminishes as the integrity of soft tissues become increasingly degraded. As Forbes (2008b) emphasises, "soft tissues are prone to environmental modifications and do not generally survive the decomposition process, rendering the use of morphological characteristics in dating human remains problematic." Therefore, accurate determinations of PMI utilising soft tissue changes is constrained to time frames of 24-48 hours.

In the case of forensic entomology, environmental factors such as inclement weather, the presence of drugs or toxins in the decedent's body at the time of death, the presence of clothing and/or coverings, and the location of a corpse (above ground, below ground, in coffins, etc.), may limit arthropod activity or restrict their access to decomposing bodies (Catts, 1992; Galloway, 1997; Haskell *et al*., 1997). Moreover, estimates of PMI are regarded as sub-standard when skeletal remains are the only available source for construing TSD. In practical forensic situations, human remains are not always discovered above ground, or soon after death for that matter. It may be several days, weeks or years later before a decedent is found. In such instances, the current PM techniques may not be applicable for establishing estimates of TSD for bodies found during the later PM period. As a result, alternative methods that are capable of providing accurate estimations of PMI for

human remains discovered well beyond the 48- and 100-hour limits of soft tissue and biochemical methods, as well as for bodies discovered in buried contexts, are much needed.

1.1.4 Recent research studies exploring new methods for ascertaining late stage PMI

Various studies exploring alternative methods for obtaining late period PMI estimates are currently underway to address these issues. *Odor mortis*, the smell of death (Vass, 2012), involves exploration of the decompositional odours that persist well beyond a time frame of 100 years in soil environments. This study is based on the premise that decomposition of soft tissues results in the time-dependent release of some 478 identified volatile organic compounds into the surrounding soil environment as a result of aerobic and anaerobic processes. In soil environments, 56 of these compounds have been consistently associated with human decomposition (Vass *et al*., 2008). With increasing PMI, these elements undergo changes and migration in soil.

Formulation of universal formulas for PMI determination that take into account both 1) taphonomic processes, such as temperature, moisture, partial pressures of oxygen, and 2) the accumulated degree days (ADD – an accumulation of average daily temperatures collected over a period of time) or burial accumulated degree days (BADD – which is essentially the same as ADDs but factors in the temperature of the burial environment) for which soft tissue decomposition reaches completion (1285 ± 110 ADDs, where 1285 represents the ADDs by which no soft tissues remain or the remaining tissues have completely desiccated and the production of volatile fatty acids (VFA) has ceased) (Vass, 2011). These formulas are presented in Table 1.2.

Table 1.2: Examples of PM corporal changes and circumstantial evidence associated with dead bodies that are used by forensic examiners to make inferences about the decedent's PMI (Vass, 2011).

Formula 1	Formula 2
$PMI_{Aerobic} = \frac{1285 \times (decomposition/100)}{0.0103 \times temperature \times humidity}$	$PMI_{Anaerobic} = \frac{1285 \times (decomposition/100) \times 4.6 \times adipocere}{0.0103 \times temperature \times (soil\ moisture)}$
$PMI_{Aerobic}$ - Used to describe estimates of PMI for human decompostion occuring above ground. Result is in DAYS.	**$PMI_{Anaerobic}$** - Used to describe estimates of PMI for human 'burial' decompostion. Result is in DAYS.
1285 - a constant, representing the empirically determined ADD value at which VFA liberation from soft tissue ceases.	**1285** - a constant, representing the empirically determined BADD value at which VFA liberation from soft tissue ceases.
decomposition - a single value, or range, between 1 and 100, representing the best estimation of the extent of total body soft tissue decomposition.	**decomposition** - a single value, or range, between 1 and 100, representing the best estimation of the extent of total body soft tissue decomposition.
	4.6 - a constant which represents a slowdown in the rate of decomposition due to a lack of oxygen.
	adipocere - a multiplicative value based on the % adipocere estimated to be associated with the corpse.
0.0103 - a constant representing the empirically determined measure of the effect of moisture on decompositional rates.	**0.0103** - a constant representing the empirically determined measure of the effect of moisture on decompositional rates.
temperature - the value in degrees Celcius (˚C) of either the average temperature at the site on the day the corpse was discovered or the average temperature over a period of time.	**temperature** - the value in degrees Celcius (˚C) of the soil temperature in the grave vault at the time of excavation and at the level of the corpse (or the average temperature over a period of time).
humidity - a value between 1 and 100, representing either the average humidity over a period of time.	**Soil moisture** - a value between 1 and 100, representing the soil moisture at the site on the day the corpse was discovered (or the average over a period of time).

The concentration of citrate, a molecule present in the bones of living organisms that is fundamental to the performance of metabolic processes, has been shown to decrease with regularity between 4 weeks to 100 years PM among porcine and adult human remains. With the exception of remains that have been stored at temperatures below 0˚C, the rate of citrate loss was relatively unaffected by factors such as temperatures >0˚C, humidity, and burial depth (Schwarcz *et al*., 2010).

These methods illustrate the kinds of techniques that may be well suited for conducting TSD estimations on human remains discovered long after the early PM period and in buried contexts. However, their ability to be utilised for human remains found immediately after those early PM changes deemed useful for establishing PMIs of up to 48- and 100-hours PM have expired are unclear. A great deal of research is required before the true nature of their forensic value can be determined.

1.1.5 The application of accumulated degree days for PMI determination

As briefly mentioned in section 1.1.4, an ADD is an accrual of mean daily temperatures for a specified interval of time. More precisely, it is defined as "heat energy units that represent the accumulation of thermal energy that is needed for chemical and biological reactions to take place in soft tissue during decomposition" (Megyesi, 2005 in Myburgh *et al*., 2013). ADD calculations were initially employed by farmers to regulate crop and pest management. In this instance, computed values are used to make predictions about the amount of time required for crops to produce yield (Wilson & Barnett, 1983).

In the context of forensic science, the purpose for using ADD is to measure the joint influence that chronological time and temperature have on the PM degradation of remains (Simmons *et al*., 2010). More specifically, the theory governing the use of ADD states that

decomposition occurs when there is a sufficient accumulation of thermal energy necessary to overcome the PM biochemical threshold needed to drive the decay process forward. Therefore, ADD measures the amount of thermal energy that is placed into a system over time, resulting in some particular outcome (Ibid). A degree-day is the average ambient temperature experienced by a region over a period of 24-hours (the mean value for the sum of the maximum and minimum temperatures recorded) minus the minimum threshold temperature at which biochemical processes are capable of proceeding PM. The equation for calculating a degree-day is as follows:

$$[(T_{max} + T_{min})/2] - T_{thd}$$

where T_{max} and T_{min} denote the maximum and minimum ambient temperatures reached in one day, and T_{thd} represents the minimum threshold temperature that the accumulated degree-days are considered (Michaud & Moreau, 2011). The minimum temperature required for the biochemical breakdown of humans to proceed is 0˚C. This is owed to an increase in the body's salt concentration as the soft tissues are destroyed by autolytic processes (Vass *et al*., 1992). Therefore, the minimum threshold temperature used for calculating ADD can be set to 0˚C. ADD is then computed by taking the sum of all degree-days representing the number of chronological days that a corpse has been deceased for (Ibid).

Statistical research conducted by Michaud and Moreau (2011) looked at the effects that different controlled temperatures (at accumulations over 5, 10 and 15˚C) had on the rate of decomposition for pig carcasses over time. The state of decomposition was evaluated using the total body score (TBS) method generated by Megyesi and colleagues (2005 in Myburgh *et al*., 2013). They discovered that a great deal of the variability in decomposition rates between pig carcasses was owed to the combined ADD. This study highlights the importance of considering multiple variables affecting the rate of decomposition at once as

they tend to reflect a more realistic representation of the PM processes that occur in nature. In general, the purpose for using ADD versus PM days is to establish a way for the forensic community to cross-compare the PM outcomes of various experiments that assess methods for deducing accurate PMIs in different forensic contexts. The use of ADD compensates for variables such as, "inter-year, between-season, and within-season variability," and presents opportunities for the "development of prediction models valid throughout the year" for specific geographical locations (Michaud & Moreau, 2011; Simmons *et al*., 2010). The concept of using intricate equations that consider more than one influential variable at a time, such as ADD or the universal equations proposed by Vass (2011) as discussed in section 1.1.4, also demonstrates some of the novel approaches that forensic researchers are taking to increase the accuracy for PMI determination and to substantiate the scientific nature of forensic investigations.

1.2 A research gap in the field of forensic taphonomy

Although a vast amount of forensic literature has explored the practicalities of using various soft tissues as measures of PMI, the pathology of degrading cartilage and its use as a forensic tool had remained relatively overlooked until recently (Alibegović *et al*., 2014; Drobnič *et al*., 2005; Rogers *et al*., 2011). A study conducted by Lasczkowski and colleagues (Lasczkowski, Aigner, Gamerdinger, Weiler, & Bratzke, 2002) was among the first to assess the PM value of cartilage by exploring the viability of chondrocytes (cartilage cells) *ex vivo*. Fluoroprobes were utilised to differentiate between the live and dead cells of cartilage samples that were removed from the knee joints of 13 cadavers. The known PMI for these autopsy samples ranged from 1 day to 2.5 months. Findings yielded an inverse correlation

between chondrocyte loss and PMI; as PMI increased, the percentage of viable cells decreased.

Supplementary research examining the effects of temperature on the viability of chondrocytes *in situ* (*ex vivo*) was conducted in a controlled laboratory setting using a cell nutrient culture medium (Alibegović *et al*., 2014). The authors of this study reported that the viability of PM chondrocytes declined most rapidly at a temperature of 35˚C, followed by samples that were stored at 4˚C, although Athanasiou *et al.* (2013) suggest chondrocytes *in situ* of their cartilage tissue can be stored for multiple days with minimal decrease in the number of live cells. Cartilage incubated at 23˚C demonstrated a gradual decline in the number of viable cells, while those incubated at 11˚C showed prolonged viability establishing this temperature as the most optimal of the four for chondrocyte viability.

In addition to these studies, Rogers *et al.* (2011) examined the morphological and microstructural changes exhibited by cartilage for up to 12 weeks PM. They noted that cartilage degradation occurred gradually with systematic changes in the tissue's colour and robustness with increasing time. These macroscopic observations were also observed by ten Broek (2009). Additional PM observations by Rogers and colleagues (2011) included the on-going destruction of nucleic material and the development of orthorhombic crystals that appeared around 3 weeks PM (Rogers *et al*., 2014) and disappeared by 9 weeks PM.

In a review written by Dent, Forbes and Stuart (2004) about the processes of human decomposition in soil environments, the authors explain that protein degradation occurs as a result of proteases, that are released by the body's cells in response to environmental stressors. Degradation of structural proteins in the body does not occur at a uniform rate. Some proteins degrade earlier than others as a body undergoes decomposition. For instance, proteins among the neuronal and epithelial tissues and the membrane that lines the gastro-

intestinal tract are among the first to be destroyed. On the other hand, the epidermis, muscles, reticulin and collagen proteins prove themselves more resilient to the autolytic and putrefactive processes.

1.2.1 Cartilage

Cartilage is an avascular and aneural connective tissue that is exceptionally flexible, yet strong. It serves as a precursor to bones in developing infants and juvenile children, provides a flexible structure to soft tissues such as the ears and nose, stabilises bones, and provides frictionless movement while acting as a shock-absorbing tissue for joints involved in locomotive activities (Bradley *et al*., 2010; Hoffman, 1987; Knudson & Knudson, 2001; Pratta *et al*., 2000; Pratta *et al*., 2003). The connective tissue is predominantly extracellular matrix (ECM). The ECM components are produced by sparsely populated chondrocytes which comprise the cellular matrix and are intermingled among its collagen fibres and proteoglycan constituents (Dudhia, 2005; Gino *et al*., 2003; Goldring & Marcu, 2009; Kheir & Shaw, 2009; McDevitt, 1973). When moving from the articular surface to the cartilage-bone interface, the volume and proportion of proteoglycan molecules with respect to collagen fibres increases while cell density gradually decreases (Goldring & Marcu 2009). This organisation of the extracellular and cellular matrices is analogous for numerous joints and different species (Moger *et al*., 2007).

The ECM components consist of 70% water (Dudhia, 2005), the most abundant component of cartilage tissue (Nordin & Frankel, 2001; Norkin & Levangie, 1992), and proteins and macromolecules, such as collagens, non-collagenous proteins and proteoglycans (PG). Several forms of collagen are present and include types I, II, VI, IX, X, XI, and XXVII (Goldring & Marcu, 2009; Ismail *et al*., 2010; Moger *et al*., 2007; Rengel *et al*., 2007). Type

II collagen is the predominant collagen type (~90%) and is found exclusively in cartilage tissue (Athanasiou *et al*., 2013; Moger *et al*., 2007). It is responsible for the production of dense, rigid cartilage fibres that endow the connective tissue with its tensile property and represents 60% of the total dry weight for cartilage. The non-collagenous protein components include biglycan, decorin, fibromodulin, the matrilins, and cartilage oligomeric matrix protein (COMP). These cartilage molecules comprise 3-5% of the tissue's weight (Bradley *et al*., 2010) and act as catalysts which support the formation and maintenance of collagen fibrils. PGs that are located within the ECM consist of aggrecan, decorin, biglycan, fibromodulin and lumican. Among these ECM components, aggrecan is the dominant PG and accounts for 30% of the dry weight for cartilage.

Cartilage can be categorised into one of three groups: elastic, fibrous and hyaline (Athanasiou *et al*., 2013). Elastic cartilage contains a considerable amount of elastin which is highly insoluble and maintains a branch-like structure. It is often present among soft tissues that require a great deal of flexibility. For instance, elastic cartilage can be found in the ears, larynx, lungs, skin, heart, and stomach. Fibrocartilage (or fibrous cartilage) forms a network of both fibrous and cartilaginous tissues arranged as thick, compact bundles that run parallel to the direction that tensive forces are typically applied. It is mainly composed of type I collagen and possesses a small quantity of type II collagen. This tissue provides various joints, such as the annulus fibrosus of the intervertebral joint (IVJ) discs, the pubic symphysis, menisci of the knees, and the temporomandibular joint disc (Athanasiou *et al*., 2013), with tensile strength and structural support. It also forms as repair tissue for damaged articular cartilage (Kheir & Shaw, 2009). The term, hyaline, is derived from the Greek word *hyalos* meaning "glass" and describes the glossy, translucent white/bluish-white appearance of cartilage (Figure1.1) belonging to this group (Athanasiou *et al*., 2013). In older individuals, hyaline cartilage appears off-white or cream-coloured. It is the most abundant of

the three types of cartilage (Ibid) and is generally situated on the articular surfaces of bones that form synovial joints.

1.2.2 The basic structure and function of hyaline articular cartilage and its components

Articular cartilage functions as a low-frictional surface that minimises wear to the articulating bones and maintains a biochemical/biomechanical makeup that renders it highly durable. The articulating joints are surrounded by a synovium that is comprised of fibrous tissue that forms a cavity (Norkin & Levangie, 1992). In turn, this joint cavity contains synovial fluid that lubricates the surfaces of the hyaline articular cartilage during joint movement.

Synovial fluid also provides the connective tissue with a means for transporting nutrients that are necessary for maintaining homeostasis and ridding the cartilage of waste products by way of diffusion; the transportation of nutrients and wastes across the synovial membrane is assisted by the compressive action generated by force applied to the articular cartilage (Alibegović *et al*., 2014; Athanasiou *et al*., 2013; Kuettner, 1992; Ogawa, 2011). This system for transporting nutrients and waste products is essential to cartilage preservation, especially since chondrocytes are rather isolated from blood supplies and exhibit a low turnover rate for the replacement of various ECM components. Nonetheless, these same distinguishing features make cartilage less susceptible to weight-bearing damage.

The ability of articular cartilage to withstand prolonged and repeated strains caused by various mechanical factors is further enhanced by its chemicophysical makeup. Its basic morphology consists of four zones that are based on the organisation and shape of the chondrocytes (Figure 1.2):

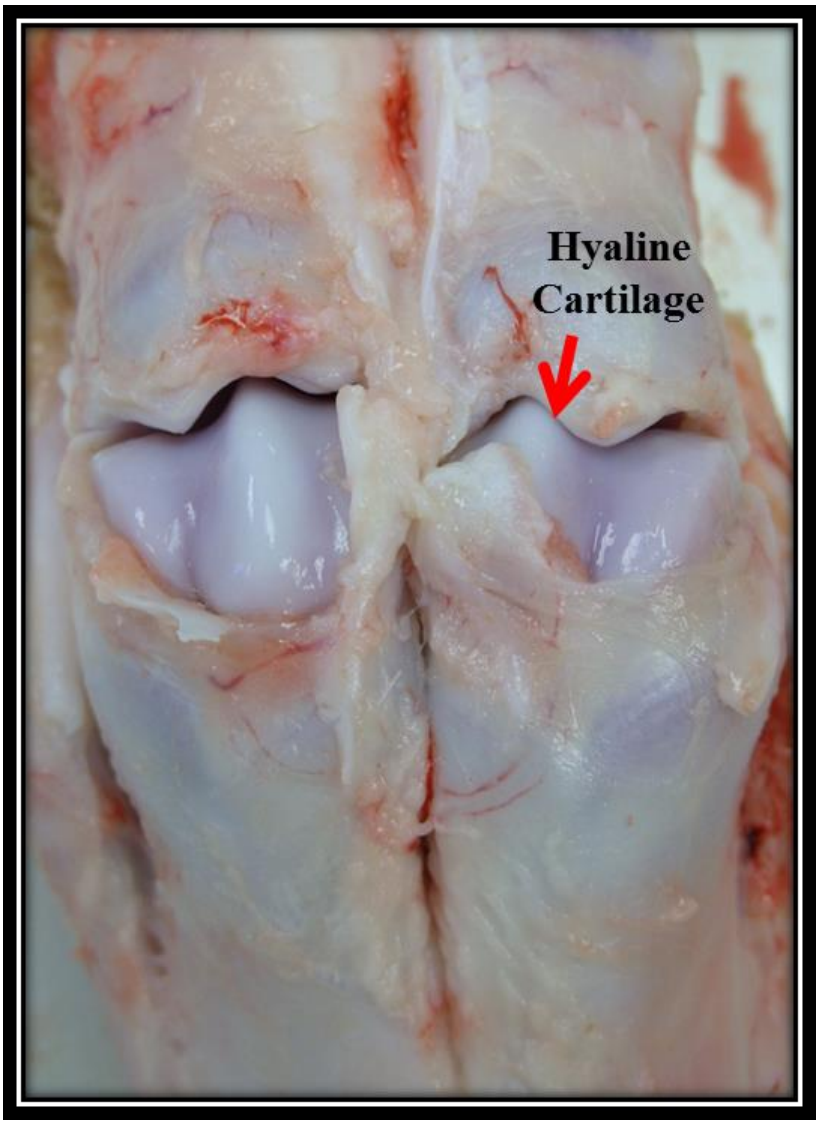

Figure 1.1 Porcine hyaline articular cartilage exposed at the metacarpo-/metatarsophalangeal joint of a trotter. Note the white and bluish white colour of the tissue as well as its glossy appearance.

1. Superficial (tangential) zone – this region comprises the outer portion of the articular surface (the upper 10-20% of the tissue) where the chondrocytes are smallest, circular or ellipsoid-shaped and run parallel to the cartilage surface. PG density and permeability is lowest in this area of the ECM. This zone is principally responsible for dispersing and transmitting the compressive forces generated during movement radially across the surface of cartilage and is 25 times more flexible than its underlying zone (Athanasiou *et al*., 2013; Goldring & Marcu, 2009; Kheir & Shaw, 2009; Pearle *et al*., 2005);
2. Middle (transitional) zone – this area represents 40-60% of the cartilage tissue and is situated directly below the superficial zone. Chondrocytes in this region are slightly larger and are more spherically shaped than chondrocytes in the superficial zone. These cells are arranged in columns that are perpendicular to the articular surface. Type II collagen fibres are also aligned perpendicular to the cartilage articular surface and form arcade-like structures that are intermingled among other haphazardly arranged fibres. Collagen fibrils are thicker and less compact; their function in this region is to support and transmit moderate mechanical forces. The majority of cartilage PGs reside in this zone (Athanasiou *et al*., 2013; Goldring & Marcu, 2009; Kheir & Shaw, 2009; Pearle *et al*., 2005).
3. Deep (radial) zone – Cartilage belonging to this region comprises 30% of the connective tissue volume and rests between the middle zone and cortical bone. The chondrocytes are arranged perpendicular to the articular surface, typically in columnar groups or clusters, are notably larger than chondrocytes in the upper zones, and stretch slightly in the same direction parallel to its surrounding collagen fibrils as they are organised. These large collagen fibres are anchored to the subchondronal bone

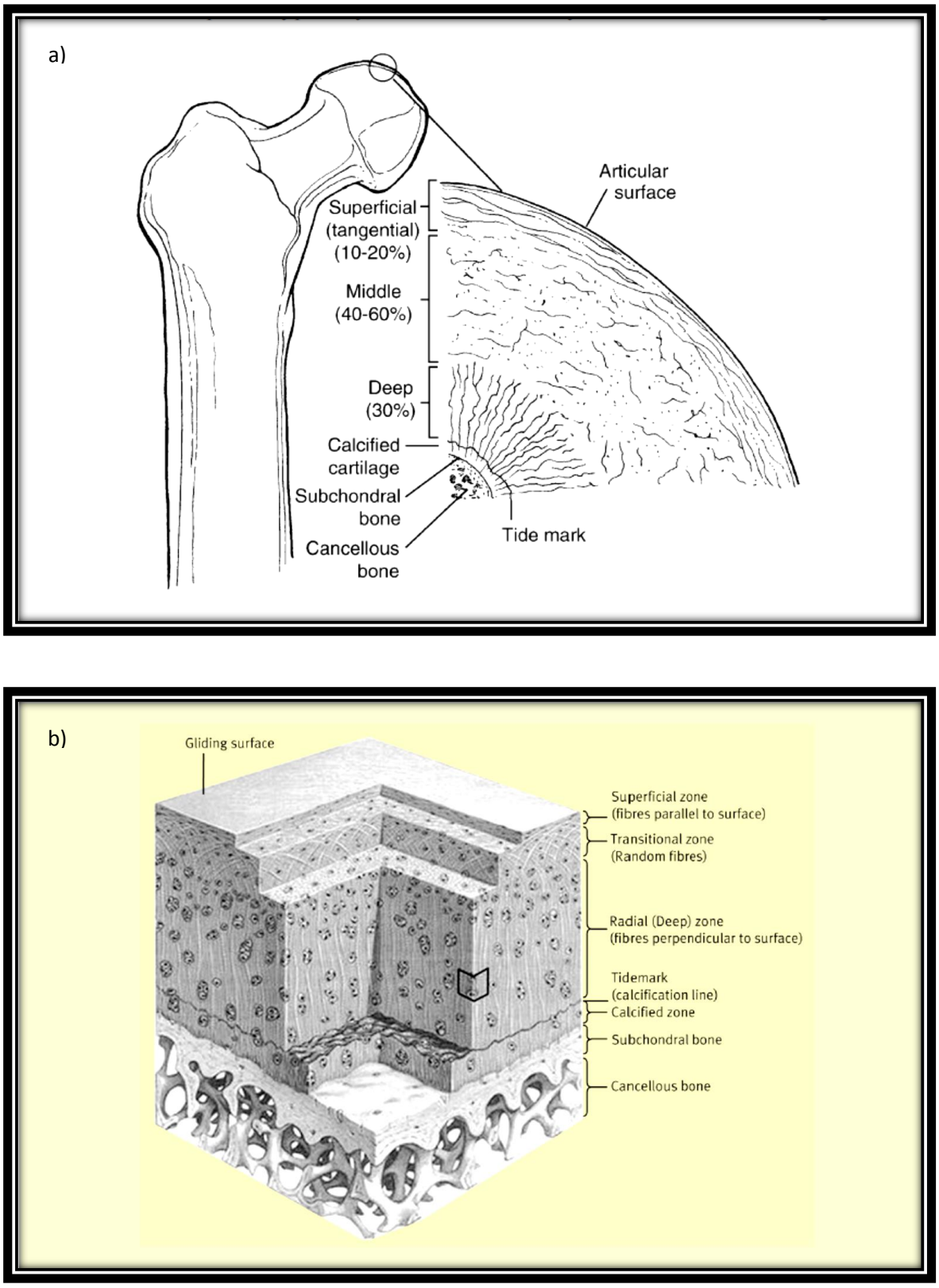

Figure 1.2 Illustrations of the 4 different zones that are represented by hyaline articular cartilage. a) A cross section of hyaline cartilage from the head of a femur. Note. "Reprinted from *Clinics in Sports Medicine*, 24, Pearle, Warren, and Rodeo, Basic science of articular cartilage and osteoarthritis, p. 2, Copyright (2005), with permission from Elsevier." b) A 3D cross section of cartilage collagen and chondrocytes. Note. "Reprinted from *Orthopaedics and Trauma*, 23, Kheir and Shaw, Hyaline articular cartilage, p. 452, Copyright (2009), with permission from Elsevier."

below. Water and PG contents, as well as cell density, are significantly lower in this region when compared with the superficial and middle zones. However, the adjacent tissues are subjected to a substantial amount of shear force during joint articulation. The deep zone is separated from the calcified region of cartilage by a thin line called the tidemark (Athanasiou *et al*., 2013; Goldring & Marcu, 2009; Kheir & Shaw, 2009; Pearle *et al*., 2005).

4. Calcified zone – this area is situated immediately below the tidemark and above the cortical bone surface. This zone is characterised by cartilage that has undergone calcification for transition to subchondral bone. Calcified cartilage acts as a mechanical buffer for uncalcified cartilage and the underlying cortical bone (Goldring & Marcu, 2009). This calcified cartilage continues to persist after union of the bone's growth plates are established.

1.2.3 Type II collagen and aggrecan

In hyaline cartilage, type II collagen and aggrecan are classified as the fundamental structures of the ECM. Type II collagen exhibits a triple-helical structure; it is involved in the formation of fibrils that establish crosslinks with each other to provide stability to the ECM (Dudhia, 2005; Pearle *et al.*, 2005). Its elastic properties buttress the tensile forces that are exerted during locomotion and the build-up of osmotic pressure imparted by proteoglycans, namely aggrecan, trapped between the ECM (Athanasiou *et al*., 2013; Moger *et al.*, 2007). The arch-like orientation of collagen fibrils was first described by Alfred Benninghoff in 1925. Known as the "arcades" or Benninghoff model, collagen fibres are arranged as arch-like structures that are securely embedded in the calcified region of cartilage (Figure 1.3). These fibrils extend vertically through the cartilage ECM, curve obliquely in the middle zone and then adopt an organisation that is parallel with the articulating surface in

the superficial zone. The fibres then proceed to arc over towards the opposite direction (Athanasiou *et al*., 2013; Kheir & Shaw, 2009).

The capacity for cartilage to sustain a great deal of compressive forces is attributed to the large aggregating PG, aggrecan, that exhibits a "comb-like" (McDevitt, 1973) or "bottle-brush" structure (Figure 1.4). Individual PG monomers are non-covalently adjoined to a hyaluronic acid (HA) polymer (also known as hyaluronan) by way of a single small glycoprotein known as link protein (Inagawa *et al.*, 2009; Nguyen *et al.*, 1993; Rengel *et al.*, 2007). The ability for this molecule to perform as a load-bearing and shock-absorbent tissue is dependent upon its volume within the ECM and the polyanionic charge that it bears (Bradley *et al.*, 2010). It is comprised of a protein core with a molecular weight of approximately 230kDa (Athanasiou *et al*., 2013) that is richly populated with long glycosaminoglycan (GAG) side-chains, unbranched polysaccharide chains that exhibit repeated disaccharide units of six-carbon sugar molecules (hexose or hexuronic acid) linked to a six-carbon sugar molecule containing N (hexosamine) (Athanasiou *et al*., 2013; McDevitt, 1973). These GAG side-chains are mostly represented by two types: chondroitin sulphate (CS) and keratan sulphate (KS) (Figure 1.4). CS exists as two different isoforms, chondroitin-4-sulphate (C-4-S) and chondroitin-6-sulphate (C-6-S), whereby the numbers "4" and "6" indicate which C in the hexose sugar-ring the sulphate molecule is attached to (Hilbert *et al*., 2002; McDevitt, 1973). Both forms are present at all times. However, juvenile cartilage is mostly occupied by C-4-S whereas adult cartilage tends to exhibit higher concentrations of C-6-S and KS with age (Athanasiou *et al*., 2013; McDevitt, 1973; Moskowitz, 1984). Although CS and KS are the most prevalent GAGs, other GAGs also include dermatan sulphate (C-0-S) and HA.

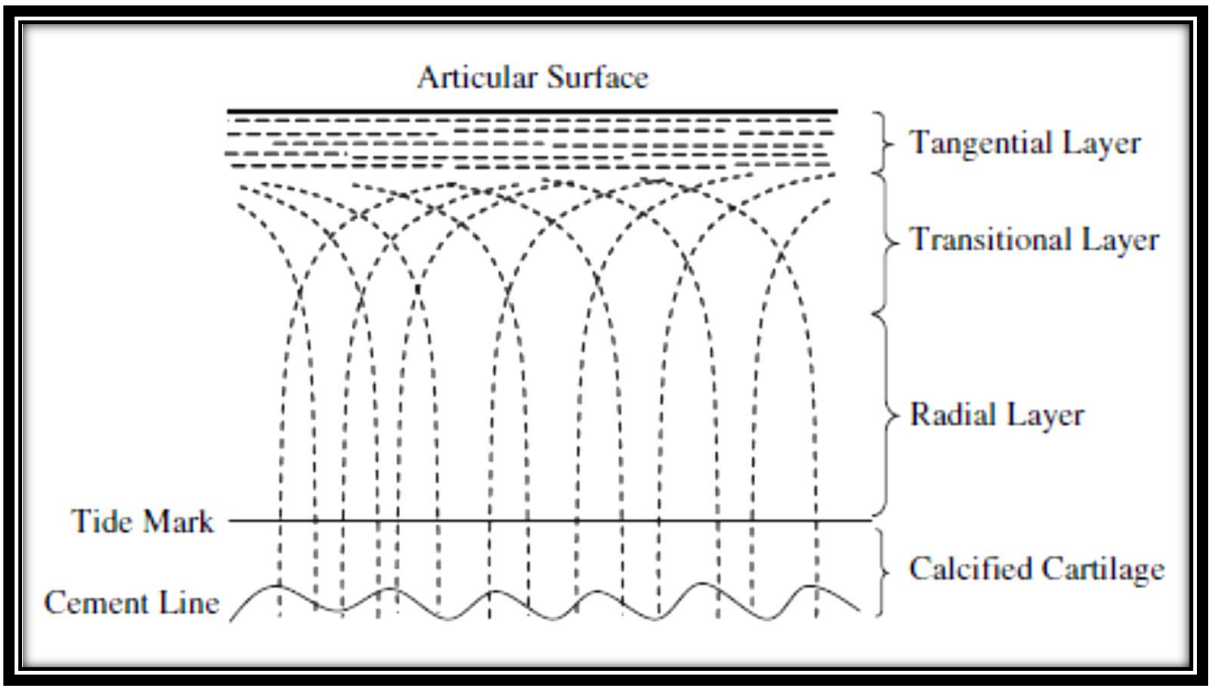

Figure 1.3 Schematic of Benninghoff's model demonstrating the "arcade" arrangement of collagen fibrils in hyaline cartilage. Note. "Reprinted from *Osteoarthritis and Cartilage/OARS, Osteoarthritis Research Society*, 15, Moger *et al.*, Regional variations of collagen orientation in normal and diseased articular cartilage and subchondral bone determined using small angle X-ray scattering (SAXS), p. 683, Copyright (2005), with permission from Elsevier."

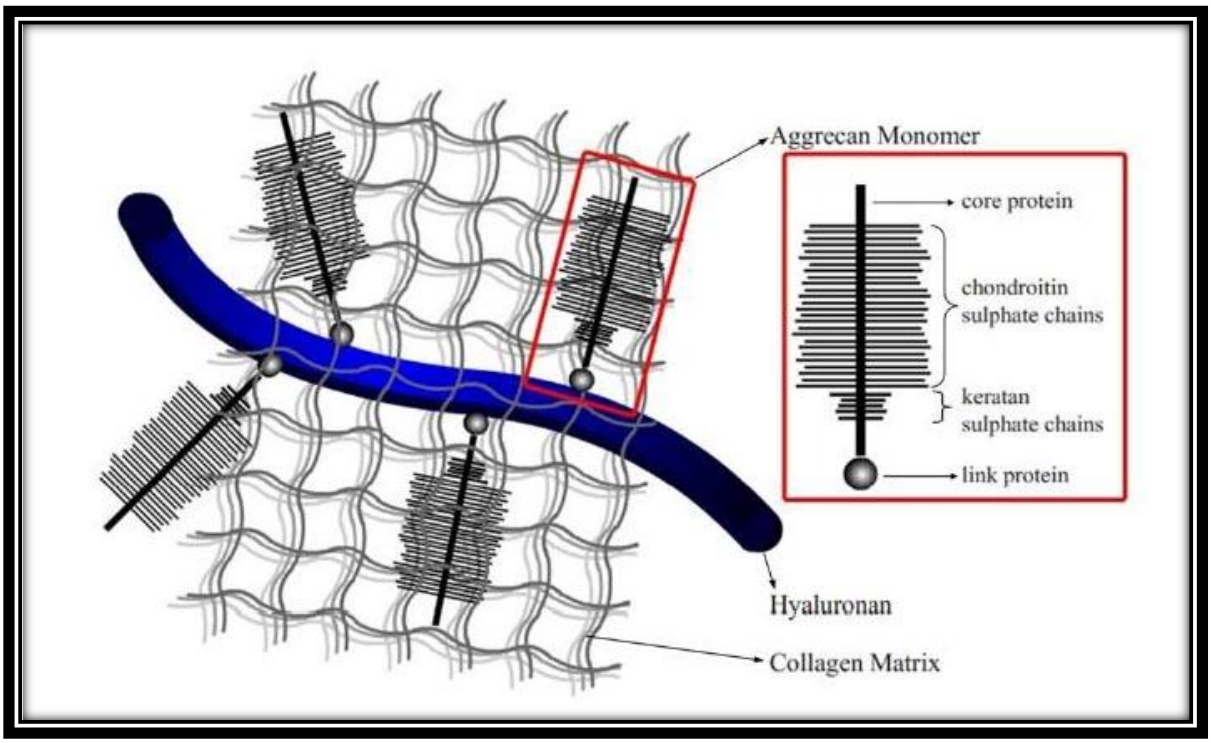

Figure 1.4 A segment of the proteoglycan aggregate exhibiting several aggrecan monomers. The inset shows the basic component of the molecule. Note. "Reprinted from *Nuclear Instruments and Methods in Physics Research Section A: Accelerators, Spectrometers, Detectors and Associated Equipment*, 619, Bradley *et al.*, Synchrotron and ion beam studies of the bone–cartilage interface, p. 331, Copyright (2010), with permission from Elsevier."

The protein core of aggrecan consists of three disulphide-bonded globular domains: G1, G2, and G3 (Figure 1.5). The G1 domain is located at the N-terminal (amino-terminus) of the protein core and is sometimes referred to as the HA-binding region because of its high affinity for interaction with the hyaluronan backbone. G3 is situated at the C-terminal (carboxyl-terminus) of the protein core. These globular domains are interspersed among three extended domains that consist of an interglobular domain (IGD) situated between G1 and G2, and the subsequent KS and CS domains that rest along the lengthy G2-G3 region (Dudhia *et al.*, 1996; Kiani *et al.*, 2002; Wells *et al.*, 2003). The KS and CS domains reflect the primary attachment sites where CS and KS are generally discovered (Bradley *et al.*, 2010; Dudhia, 2005; Roughley, 2006). The CS domain is further subdivided into CS1 and CS2 regions, whereby the CS1 region lies between the KS and CS2 regions (Dudhia, 2005; Roughley, 2006). This domain exhibits uniformly spaced CS chains, whereas CS chains in the CS2 subdomain adopt a clustered arrangement. In this extended G2/G3 region, there are typically 100 CS and 30+ KS GAG side-chains attached to the protein core (Doegesq *et al*., 1991; Dudhia, 2005). Furthermore, CS exists as several different isoforms. Both CS and KS polysaccharides are responsible for endowing cartilage with its highly negative charge that exhibits a strong affinity for attracting and retaining water molecules in the ECM. Water retained by these proteoglycans ensures that cartilage is elastic yet also capable of resisting forces that are generated by friction and mechanical impact (Bradley *et al.*, 2010; Dudhia, 2005; Inagawa *et al.*, 2009; Kheir & Shaw, 2009; Pearle *et al.*, 2005; Pratta *et al.*, 2003).

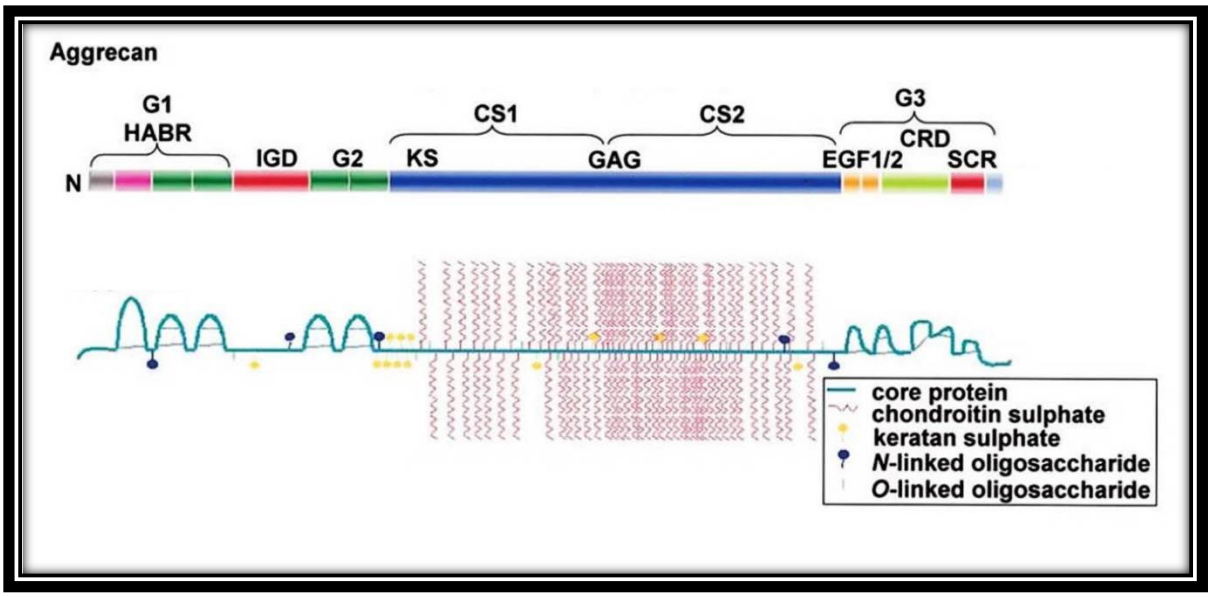

Figure 1.5 Schematic representations of the standardised units, globular domains 1-3 and the extended domains, that make up an aggrecan molecule (upper). The lower image depicts the relative size and positions of the structural components of aggrecan. Notes. Figure modified. From "Aggrecan, aging and assembly in articular cartilage" (Dudhia, 2005, p.2244).

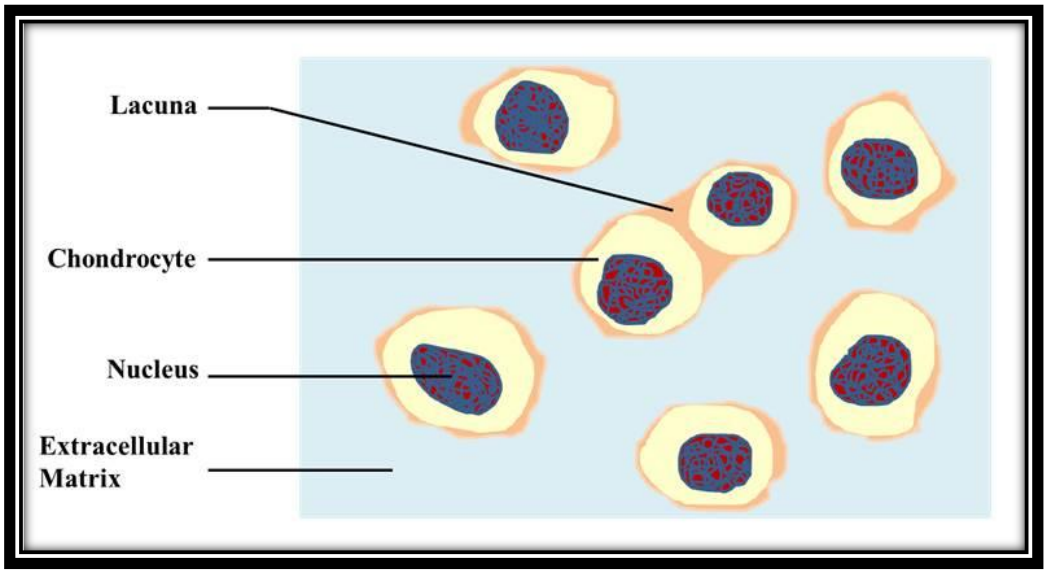

Figure 1.6 A diagrammatic representation of chondrocytes housed within a lacuna.

1.2.4 Chondrocytes and cartilage homeostasis

Chondrocytes occupy less than 5% of hyaline cartilage tissue in humans (Athanasiou *et al*., 2013) and engage in low metabolic activities. In humans, the diameter of chondrocytes falls within a range of 10-13μm where cells in the superficial zone are smallest and increase in size moving towards the deep zone (Ibid). They are responsible for the production of ECM proteins, although their rate of turnover for these matrix proteins is quite slow. This is attributed to several factors: 1) chondrocytes do not divide; 2) they are isolated from one another by ECM components; and 3) they lack access to a blood supply (Goldring & Marcu, 2009). Nonetheless, chondrocytes are capable of subsisting in quite hypoxic environments. Cells that are situated closest to the articular surface can exist at a partial pressure of 10% of atmospheric pressure whereas those located well within the deep zone are able to thrive at partial pressures as low as 1% (Ibid). For these reasons, cartilage relies heavily upon diffusion for transporting nutrients and cellular waste (refer to section 1.3.2) yet maintains remarkable durability.

Chondrocytes are enclosed within microscopic cavities also known as lacunae or chondrons (Figure 1.6). These lacunae are thin, pericellular matrices, regions that immediately surround the chondrocytes which contains fine collagen fibres (Athanasiou *et al*., 2013) that offer the cells hydrodynamic protection. Each lacuna houses a single chondrocyte that is associated with a pericellular matrix containing elevated concentrations of proteoglycans such as HA, biglycans and ECM glycoproteins (Kheir & Shaw, 2009). The cytoskeleton of chondrocytes, like all other eukaryotic cells, possess three types of polymeric filaments: actin microfilaments, intermediate filaments, and tubulin microtubules (Athanasiou *et al*., 2013). Actin microfilaments are the most abundant and smallest of cytoskeletal proteins. In chondrocytes, they are responsible for cellular contraction and maintaining cell structure. Intermediate filaments are intermediary in size with comparison

to actin and tubulin microtubules. Like actin, they assist with counteracting tensile forces and are involved with cell-cell interactions, cell-matrix junctions and the translation of mechanical stimuli into biological responses, a phenomenon called mechanotransduction (Ibid). Vimentin is the most common intermediate filament in chondrocyte. Unlike actin and intermediate filaments, tubulin microtubules are heterodimers (a polypeptide made up of two different amino acid chains) that consist of alpha/beta monomers that have a molecular weight of approximately 55kDa. This polypeptide forms a hollow tube and serves to resist compressive loads rather than tensile forces (Ibid).

Apart from chondrocytes bearing structural features that offer them added protection from imposing mechanical stresses, these cells play an important role in maintaining cartilage homeostasis. This ability to maintain physiological equilibrium is dependent upon the mechanical and biochemical signals that are communicated to chondrocytes by way of cytokines or growth factors (cytokines are protein hormones). Cytokines are small proteins and polypeptides that may be glycosylated or non-glycosylated; they have low molecular weights that range from 10-40kDa (Ikram *et al*., 2004). These molecules are secreted by cells in response to environmental stimuli. They elicit specific or broad biochemical responses which trigger a cascade of events that result in a particular end goal (Ikram *et al*., 2004; Zhang & An, 2007). Cytokines may be classified as autocrines (those which act on the very cells that secrete them), paracrines (cytokines released by one cell type that affects other neighbouring cells) or endocrines (those that must travel some distance to act on cells that are located far away). They may function in one of several ways: 1) to activate cells to stimulate immune system responses; 2) to prompt the production and development of blood cells in bone marrow; 3) to indirectly trigger inflammatory processes; and 4) engage in cytostatic, cytotoxic and antiviral activities (Ikram, Hassan, & Tufail, 2004). In the case of cartilage

maintenance, repair and degeneration, the latter two functions explain the roles that cytokines play in cartilage homeostasis and instability.

Mechanotransduction occurs when mechanical stimulus is applied to articular cartilage. As a result, this mechanical signal causes cytokines to bind to their respective mechanoreceptor which is located along the surface of the chondrocyte membrane. The cytokines are then internalised, thereby activating the production of various enzymes that are released to the ECM or that remain within the cytoplasm. These enzymes may take part in anabolic and/or catabolic activities that either aim to repair cartilage tissue or see to its destruction (Goldring & Marcu, 2009; Ikram *et al*., 2004).

Growth factors are active polypeptides produced by the body that promote cellular division, growth and differentiation (Fortier *et al*., 2011). For the maintenance and repair of cartilage, various growth factors work together to repair the tissue and establish physiological equilibrium. Growth factors are responsible for the synthesis of type II collagen, aggrecan, other PGs, proliferation of mesenchymal stem cells (MSCs) and their differentiation, as well as minimising the effects of catabolic cytokines (Ibid). Example groups of growth factors that play a role in cartilage homeostasis are:

- Transforming growth factor-β (TGF-β) Group (Ibid)
    - Cartilage derived morphogenic protein (CDMP)-1 (also known as GDF-5; growth differentiation factor-5) and CDMP-2 aid in stimulation of cartilage matrix synthesis.
    - TGF-β1 promotes chondrogenesis of synovial lining and bone marrow MSCs and minimises the catabolic activity of Interleukin-1 (IL-1).
    - TGF-β3 stimulates the synthesis of ECM components.

    - Bone morphogenic protein-2 (BMP-2), and BMP-7 are involved in the synthesis of PGs and the reversal of chondrocyte dedifferentiation.
    - Insulin-like Growth Factor-I (IGF-I) generates numerous anabolic activities and decreases catabolic responses. It is involved in extensive repair of damaged cartilage and protects the synovial membrane from constant inflammation.
- Fibroblast growth factor (FGF) Group
    - FGF-2 decreases the activity of the catabolic enzyme aggrecanase.
    - FGF-18 promotes cartilage and synovial thickness while decreasing cartilage degeneration.

According to Goldring & Marcu (2009), the mechanism by which chondrocytes maintain the integrity of cartilage remains elusive, especially since the ability for cartilage to efficiently repair itself is quite limited. For these reasons, damage to the articular cartilage often gives rise to joint impairment that can result in disability (Gendron *et al.*, 2007; Murphy & Lee, 2005).

1.2.5 Cartilage degradation: Loss of homeostasis, roles of proteinases and their mechanisms

The degradation of articular cartilage is initiated when there is a disruption in normal cellular activity within the connective tissue resulting in loss of homeostasis; enzymes generally responsible for the formation, remodelling and repair of connective tissues undergo a "shift in equilibrium between anabolic and catabolic activities" (Goldring & Marcu, 2009; Loeser, 2009; Rengel *et al.*, 2007).

The most frequently studied processes of cartilage degeneration are rheumatoid arthritis (RA) and osteoarthritis arthritis (OA) (Ismail *et al.*, 2010) as they are commonly

observed among the aging population (Loeser, 2009). In humans, the fibrils located in the deep zone of the cartilage take on a bent appearance, while the collagen fibres in the middle region becomes much thicker in appearance and the orientation of fibrils throughout the remaining cartilage zones are markedly noticed; these OA alterations in the organization of the collagen fibres is known as fibrillation (Bradley *et al*., 2010; Moger *et al*., 2007). Moger *et al*. (2007) also noted that changes to cartilage matrix were generally observed in the deeper areas of the tissue while the overlying cartilage maintained a normal appearance.

Cartilage degradation is typically the outcome of elevated proteolytic enzyme activity that is initiated by cytokine-signalling pathways. Cytokines are responsible for the production of proteases which cause PGs in the ECM to catabolise (Gendron *et al*., 2007; Goldring & Marcu, 2009; Yasuda, 2006). Proteases act by cleaving peptide bonds (Madigan & Martinko, 2006). More specifically, articular cartilage aggrecan is destroyed by aggrecanases and matrix metalloproteinases (MMPs) first, followed by the permanent destruction of collagen. In addition, aggrecanases are the first to partake in the catabolism of aggrecan and are followed by MMPs during the later phase of cartilage degradation (Caterson *et al*., 2000; Gendron *et al*., 2007; Inagawa *et al*., 2009; Li *et al*., 2008). Such degradative changes occur when articular cartilage is subjected to an unusual amount of strain caused by mechanical injury, prolonged and repeated use or oxidative stress (Plaas *et al*., 2007). In an immunohistochemical analysis of clonal nests (regions where groups of chondrocyte cells are confined to specific regions) in cartilage exhibiting osteoarthritis, Plaas *et al*. (2007) revealed that these particular cells contained an excess amount of proteins such as RAGE, RUNX-2 and MMP-13, tenascin, annexin VIII, caspases 3 and 9, nitrotyrosine, which serve as indicators of oxidative stress.

Despite the vast amounts of data that have been gathered from numerous studies of diseased articular cartilage, the mechanism through which cells in the ECM undergo

irreversible cellular destruction remains elusive. Moreover, there is no existing information which reveals the temporal and spatial patterns of metalloproteinase clusters found among deteriorating articular cartilage, and hardly any data regarding the series of successive interactions that take place between the various proteinases in terms of time and space is available (Goldring & Marcu, 2009; Moger *et al*., 2007; Plaas *et al*., 2007). In spite of this mystery, recent studies have distinctly identified several enzymes responsible for the destruction of cartilage. These enzymes belong to the MMPs and ADAMTSs (a disintegrin and metalloproteinase with thrombospondin motifs) groups and are responsible for the destruction of cartilage (Arner, 2002; Gendron *et al*., 2007; Goldring & Marcu, 2009; Moger *et al*., 2007; Murphy & Lee, 2005; Plaas *et al*., 2007). MMPs, such as MMP-1, -8 and -13, are considered major mediators of cartilage destruction (Rengel *et al*., 2007), whereby MMP-13 is deemed the most effective (Goldring *et al*., 2011) but also include others, for example MMP-3 and -14 (Goldring *et al*., 2011). They are responsible for destroying the type II collagen matrix; the pathological site of collagen cleavage occurs at the Asn341-Phe342 peptide bond (Caterson *et al*., 2000; Gendron *et al*., 2007). On the other hand, ADAMTSs (ADAMTS-1, -4, -5, -8, -9, and -15), as well as some MMPs (MMP-8, -14, -13), destroy the proteoglycan aggrecan matrix; the chief site of aggrecan cleavage takes place at the Glu373-Ala374 site (Gendron *et al*., 2007; Goldring & Marcu, 2009; Murphy & Lee, 2005; Plaas *et al*., 2007; Rengel *et al*., 2007; Yasuda, 2006). Figure 1.7 illustrates the sites where MMPs and aggrecanases target and cleave the aggrecan protein core.

In general, ADAMTS-4 (aggrecanase-1) and ADAMTS-5 (aggrecanase-2) are identified as the primary proteinases involved in the degradation of aggrecan. Arner (2002), noted that ADAMTS-4 played an important role "during induced breakdown" of the ECM and that ADAMTS-5 appeared to be more concerned with the normal turnover of aggrecan. She states that,

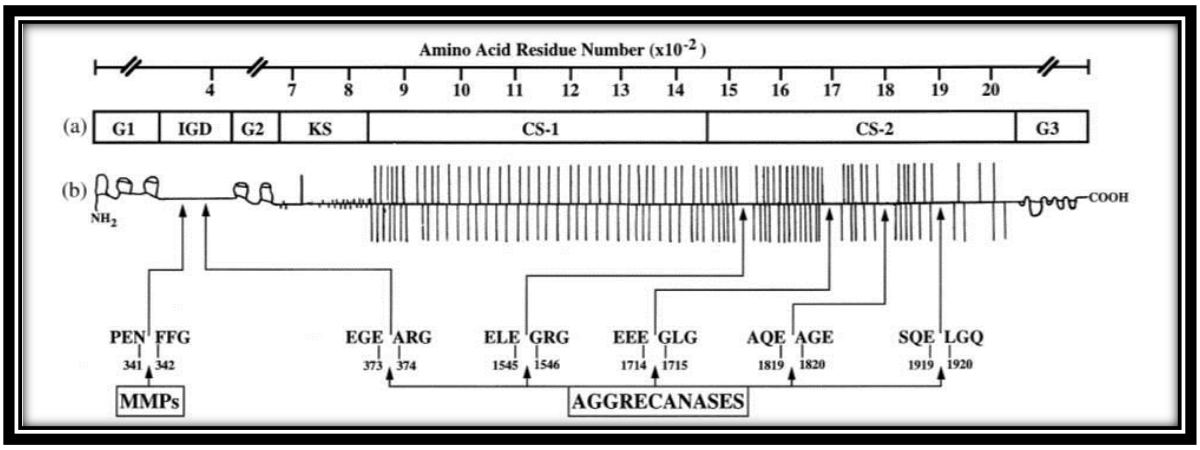

Figure 1.7 Diagrams illustrating a) the locations of the domains pertaining to aggrecan core protein and b) the peptide sequences and relative areas where proteases belonging to the MMP and aggrecanase groups cleave along the protein core. Note. "Reprinted from *Matrix Biology: Journal of the International Society for Matrix Biology*, 19, Caterson *et al*., Mechanisms involved in cartilage proteoglycan catabolism, p. 334, Copyright (2000), with permission from Elsevier."

"…[A]*dditional data regarding post-translational regulation and expression in human diseased and normal tissue is required to determine whether this is indeed the case*."

Gendron and colleagues (2007) appear to be in support of ADAMTS-5 playing the lead role in aggrecan degradation since ADAMTS-4 is efficient in digesting aggrecan core proteins but maintains little energy to perform cleavage of aggrecan at Glu373-Ala374. Results from their studies demonstrated that ADAMTS-5 was more effective than ADAMTS-4 in cleaving the aggrecan core by a 1000-fold. Furthermore, Gendron *et al.*(2007) also discovered that both ADAMTS-4 and -5 maintained optimal activity in environments where pH was between 7.0 and 9.5.

1.2.6 Post mortem cartilage degradation and forensic research

To date, there is very little literature concerning the degradative patterns and mechanisms that hyaline articular cartilage undergoes within the context of PM alterations (see section 1.3). This disparity presents an opportunity for researchers of various disciplines to explore the driving forces behind cartilage degradation. Not only would such information generate useful knowledge that would benefit the forensic database, but it would also be beneficial to clinical studies currently in search for ways to delay, prevent or reverse cartilage degradation in otherwise healthy patients. From the viewpoint of forensic scientists, the aforementioned physical properties of hyaline cartilage (sections 1.3.1-1.3.3) makes this tissue an ideal candidate for forensic research (Alibegović *et al*., 2014; Lasczkowski *et al*., 2002; Rogers *et al*., 2011). Its physical properties render it capable of enduring the immediate degradative effects of autolysis and putrefaction, whereas other soft tissues rapidly succumb to enzymatic and bacterial digestion. Cartilage is highly durable and is afforded

protection from its surrounding soft tissues and bones. The layers of muscles, ligaments, and bone offer this tissue temporary protection from the PM digestive processes and delays exposure of the connective tissue to the immediate environment. As skin, muscle and ligamentous tissues undergo decomposition, the integrity of articular cartilage persists for an extended period of time when compared to these soft tissues.

1.2.7 Research goals for investigation of post mortem articular cartilage

The above literary observations present several key points: firstly, there is a considerable need for investigating the PM degradation of soft tissues in natural environments. This is necessary for obtaining realistic data which reflect the impact that varying environmental factors have on the rate of decomposition; observations made in a contrived laboratory setting does not take into consideration all factors that influence an outcome. Furthermore, such information could be used to improve the accuracy of current post mortem techniques; the current methods employed for establishing estimates of PMI are limited to 48 hours after death which holds no value for bodies found past this time frame; and a great deal is yet to be learned from relatively unexplored soft tissues, like cartilage, which have the potential to expand our knowledge of forensic taphonomic processes that affect human decomposition. Such information may be useful for establishing alternative methodologies and/or improving upon existing ones. For these reasons, a great deal of fieldwork lies ahead of forensic examiners wishing to grasp a better understanding of the ecology of human remains buried in soil environments.

A better understanding of the processes involved in cartilage degradation may yield important useful discoveries that present forensic scientists with additional investigative tools for establishing the identity of unknown decedents, or help generate new research approaches

for finding a solution to osteoarthritic diseases. With regards to cartilage degeneration, Moger *et al*. (2007) states that, "the aetiology of the disease and the interplay of biomechanical and biochemical stimuli and responses [concerning OA] are still poorly understood." Despite this lack of information, a great deal of what is known about the properties and biomechanical and biochemical behaviours of cartilage from a tissue degradation standpoint comes from various studies focused on common joint diseases such as OA and RA (Arner, 2002; Gendron *et al*., 2007; Gino *et al*., 2003; Goldring & Marcu, 2009; Hayes*et al*., 2008; Inagawa *et al*., 2009; Ismail *et al*., 2010; Loeser, 2009; Moger *et al*., 2007; Murata *et al*., 1993; Murphy & Lee, 2005; Plaas *et al*., 2007; Rengel *et al*., 2007). Based on the above research gaps presented in the forensic literature, this study seeks to further investigate the PM decomposition of cartilage over a period of 6 PM weeks. The intent is to determine whether cartilage has potential to overcome the limitations of current soft tissue methods for establishing PMIs beyond 48 hours.

1.3 Forensic mycology

Forensic mycology is the study and applied knowledge of fungi related to cadavers, as well as suspect activity, for the advancement of criminal and legal investigations (Hawksworth & Wiltshire, 2011; Ishii *et al*., 2007; Koshimizu *et al*., 2012; Sidrim *et al*., 2010; Tranchida *et al*., 2014). For years, biologists, ecologists and forensic pathologists performing autopsies have observed the presence of fungi on the surfaces of decomposed animals and human remains (Galloway, 1997; Hitosugi *et al*., 2006; Ishii *et al*., 2006, Ishii *et al*., 2007; Schultz, 1997; Sorg *et al*., 1997; Wilson *et al*., 2007). However, the forensic value of these organisms had not been realised until recent years (Hawksworth & Wiltshire, 2011; Ishii et al., 2007; Sidrim et al., 2010; Mark Tibbett & Carter, 2003).

1.3.1 Forensic investigations involving the application of mycology

Fungi have proven themselves useful in facilitating forensic investigations. They have been used to authenticate the location where a crime was suggested to have taken place, generate a profile for an unknown crime scene environment (Beckett, 2009; Scott *et al*., 2014) and can be utilised to provide an estimate of PMI. Their microscopic organic particles, as well as those originating from plant and animal sources, are classified as palynomorphs. Palynomorphs are reflective of the environments they inhabit and their overall assemblage that consists of different species is particular to an area. Fungi are usually associated with plants or animals. The relationships they have with various organisms may be classified as parasitic, mutualistic, commensal, or pathogenic. Those that obtain their nutrients from decaying organisms are known as saprobes. In most instances, fungal distribution is confined to the limits of their preferred food sources and habitat requirements. As such, they are inclined to grow in specific geographical locations although some moulds are capable of growing just about everywhere (Hawksworth & Wiltshire, 2011). According to Wiltshire and colleagues (2014), "…[N]o two locations have been shown to yield precisely the same palynological profiles, and this makes…a powerful [forensic tool] for differentiating one place from another" (p. 4).

Palynological profiles containing fungal specimens have been generated from trace evidence found in association with cadavers and human activity. When people or objects come into contact with fungi, fungal spores (reproductive cells that develop into new progeny) are transferred to the affected surface. This phenomenon is an illustration of Locard's Exchange Principle which states an exchange of matter is inevitable when two objects touch. In forensic cases, the most commonly observed surfaces affected by the transference of spores are soil, sediments, vegetation, plant litter (Hawksworth & Wiltshire, 2011), articles of clothing worn by perpetrators and cadavers.

There have been several accounts of forensic cases that have successfully utilised trace fungi as a cross-reference for human activity in criminal investigations. For instance, a rape case presented two different accounts from the appellant and the defendant regarding the location where the claimed rape/consensual sex took place (wooded area versus open, manicured park). After having built a palynological profile from both the defendant and appellant's clothing articles, the associated plant and fungal species underwent comparative analyses with ground samples collected from the said locations. Both the suspect and the plaintiff's clothing exhibited palynomorphs characteristic of the forested area corroborating the plaintiff version. More specifically, the number of fungal palynomorphs present at this location was far greater than that exhibited by the park area; the two locations exhibited fungal spores unique to their immediate environment despite being separated by a distance of 130m. As a result of the overwhelming similarities for fungal spores and plant pollen demonstrated in support of the appellant's claims, the defendant pleaded guilty to the rape charges (Wiltshire *et al*., 2014).

In spite of the numerous cases that have successfully utilised palynomorphs like fungi (as described above) to establish/corroborate the geographical location(s) where an alleged crime(s) was said to have taken place, questions have been raised about the precision, reliability and accuracy of analytical techniques used and the robustness of the data gathered (Bryant, 2013). For instance, use of a light microscope to examine the structural features of pollen and spores for identification purposes is restricted to classification at the family level. To obtain a more precise identification of the palynomorphs, use of higher resolution instruments, such as the scanning electron microscope or the transmission electron microscope, are required to accurately identify such specimens at the genus and species level (Milne *et al*., 2005 in Bryant, 2013). The cost and use of such equipment is considerably expensive, time consuming and requires that the forensic palynologist be proficient in using

these machineries. As a result of budget constraints, these methods are not considered practical for many police departments and forensic laboratories (Bryant, 2013; Mason, 2013). Other causes for concern include the "high potential for contamination of pollen and fungal spores" (Mason, 2013), the variability of palynological profiles and the distribution of palynomorphs within a given locale or crime scene, and the statistical significance of the data sample collected from suspect clothing, tools, etc. or sample crime scenes (McKinley & Ruffell, 2007). The inability to control or justify the parameters involved in the collection and analysis of palynological data may result in the inadmissibility of evidence which may potentially thwart the outcome of a criminal proceeding.

Aside from their ability to link an individual(s), corpse(s) and/or object(s) to a crime scene or to determine the movement of these entities, fungi have also been used to establish estimates for PMI. Several researchers were assigned the task of estimating the PMI for a decedent found sitting upright at the bottom of an open well (the average temperature ranged from 12-13˚C with high humidity). The well was devoid of arthropod activity (Hitosugi *et al*. 2006). In their absence, these researchers noted macroscopic evidence of white fungal colonies dispersed across the individual's face (Figure 1.8). Samples of fungi were evaluated and identified as *Penicillium sp.* and *Aspergillus terrous*. Given the physical appearance of the individuals' soft tissue, the decomposed state of various organs and knowledge about the life cycles of the above fungi, the examiners concluded that the individual had been deceased for approximately 10 days. The PMI they established matched that of a person who was reported missing 12 days earlier (Hitosugi *et al*. 2006).

Figure 1.8 Macroscopic evidence of fungi found on a cadaver retrieved from the bottom of a well void of insects (Japan). Note. "Reprinted from *Legal Medicine*, 8, Hitosugi *et al*., Case report: fungi can be a useful forensic tool, p. 241, Copyright (2006), with permission from Elsevier."

Figure 1.9 Macroscopic indications of fungi belonging to the species *Eurotium repens*, found extensively along the surface of human remains discovered on the floor of an abandoned house (Japan). Note. "Reprinted from *Legal Medicine*, 8, Ishii *et al*., Brief communication: analysis of fungi detected in human cadavers, p. 189, Copyright (2006), with permission from Elsevier."

Another examination conducted by the same researchers involved the visible appearance of white and yellow fungal colonies along the surface of a mummified body found on the concrete floor of an abandoned home (Ishii *et al*. 2006). The species of fungi were identified as *Eurotium repens* and *Eurotium rubrum*. The former fungus produced yellow coloured ascomata (the sac-like fruiting structures of fungi belonging to the phylum Ascomycota that arises from vegetative filaments, hyphae, after sexual reproduction has been initiated (Purves, 2001) and an anamorphic stage (the stage for which there is a gradual change in form from one type to another during the evolution of a group of organisms) (Collins English n.d.) of *E. repens* (*Aspergillus repens*) that formed white asexual conidia (spores) (Figure 1.9).

Although the above case reports illustrate some of the ways in which fungi have been used to assist criminal investigations, their associations with human remains are not fully understood and information that does exist about the roles these saprobes play in the on-going decay of cadaveric tissues is limited. At present, forensic research is currently investigating the ecology of fungi within the context of human decomposition.

1.3.2 Fungi

Fungi are a very diverse group of microorganisms that share similar characteristics with plants and animals, but more so with their evolutionary relatives of the animal kingdom (Badauf & Palmer, 1993 in Deacon, 2006; Hawksworth & Wiltshire, 2011). They are comprised of various mushrooms, moulds, mildew, lichens and yeasts. Despite the common features they share with both plants and animals, they warrant enough differences to be classified as a kingdom of their own. In particular, fungi are characterised as eukaryotes because they bear membrane-bound nuclei and cytoplasmic organelles. They typically develop as hyphae with growth occurring at the apex of these structures. However, some fungi reproduce as single-celled yeasts by formation of buds. Other species are capable of expressing both hyphal and yeast growth phases dependent upon

environmental conditions. Fungi are non-photosynthetic heterotrophs and therefore require "pre-formed organic nutrients" as they are incapable of physically ingesting and converting natural food sources into useful energy. Moreover, the cell walls of fungi are not primarily composed of cellulose, which is the basic structural component of plant cell walls, but is comprised of chitin, a uniquely strong polysaccharide that also forms the exoskeleton of arthropods (Deacon, 2006; Madigan & Martinko, 2006). Lastly, their reproductive strategies may be classified as sexual, asexual or both depending on the stage of their life cycle (Ishii *et al*., 2006; Madigan & Martinko, 2006) and results in the formation of spores which provide protection to, and allow for the dispersal of, new reproductive cells that give rise to new fungi.

The variety of fungal species on earth is estimated at more than 1.5 million (Hawksworth, 2001; Suzuki & Bärlocher, 2009). In the UK, there are approximately 14,000 known species of fungi with an addition of 40-50 newly identified species that are incorporated into the UK Fungal Research Database each year (Hawksworth & Wiltshire, 2011). The environments that various fungi inhabit are just as diverse and range from tropical to glacial regions, aquatic to terrestrial, and may be extremely basic or acidic.

1.3.3 Fungi and human decomposition

On account of the numerous fungal species, their habitats and reproductive behaviours, little is known about soil fungi and their relationship with decomposing human remains, the amount of metabolic activity these microorganisms generate in response to the addition of cadaveric resources (Howard *et al*., 2010), or how the relationship of human remains and fungi influence various ecosystems. It is known, however, that the decomposition of a cadaver is largely owed to extrinsic factors, such as scavengers, insect, bacterial and fungal activity, rather than the autolytic and putrefactive processes that initiate the process from within (Carter & Tibbett, 2008a). In the case of microbes, saprophytic fungi classified as biotrophs and necrotrophs (further discussed in section

1.3.5) assist the decay process by breaking down organic compounds comprising the human body. These reduced compounds are then released to the immediate environment where they are recycled by other organisms. Although the above questions concerning the ecology of fungi and human remains arose from studies exploring the decay of human cadavers above ground, they are equally valid for decomposition occurring below ground (Carter *et al*., 2007). Moreover, few studies have reported the identity of different fungal species that are present at each decompositional stage and across geographical regions (Sidrim *et al*., 2010). At present, forensic mycologists are examining the ways that fungal communities interact with human remains, especially with remains that are buried in clandestine graves (Sagara *et al*., 2008).

1.3.4 The ecology of fungi, human remains and the soil environment

When human remains are introduced to the terrestrial environment, the surrounding ecosystem undergoes various transformations (Hawksworth & Wiltshire, 2011). Vegetation directly beneath the corporal remain(s) is destroyed and then proceeded by new growth. This is due to corporal smothering and the overabundant release of leachate that is comprised of water, carbon (C), and nutrients such as nitrogen (N) and phosphorus (P) which are deposited to the soil below (Carter & Tibbett, 2008a). This release of high-quality nutrients to the surrounding environment provides sustenance for other organisms to thrive. The excretory gases and fluids that evolve from human remains and other cadaveric matter results in the deposition of additional compounds into an ecosystem that "has evolved over millions of years to exploit those nutrients" (Pokines, 2009). Soil enriched by these decompositional by-products form what Carter, Yellowlees and Tibbitt (2007) classify as a "cadaver decomposition island" (CDI). CDIs are characterised by an influx of soil microorganisms, microbial activity and an abundance of nematodes (Carter *et al*., 2007). At such sites, numerous insects, plants and microbes compete with each other for cadaveric resources. The

metabolic processes that are carried out by these microorganisms alters the chemical and physical composition of the surrounding ecosystem (Madigan & Martinko, 2006).

The overall effects that purged fluids have on below ground ecology, the condition of soil nutrients, and the microbial communities that are present during active decay (rapid mass loss and cadaveric fluids are released to the soil), as well as the communal changes that occur among these assemblages, are poorly understood or unknown, especially from a forensic point of view (Carter *et al.*, 2007; Sagara *et al.*, 2008; Suzuki, 2002). Moreover, the species of fungi found growing on human cadavers have been poorly documented (Hawksworth & Wiltshire, 2011). In an attempt to understand the interactive effects of decomposing remains on soil chemistry and microbial activity, a number of studies have looked at the chemical components of soil before and after the interment of bodies, the effect that varying soil pH has on the rate of decomposition, and the microbial activity that takes place below ground as a result of purged fluids.

The burial of three pigs in shallow graves composed of drift and tertiary clay, lead Hopkins and colleagues (2000) to discern that elevated concentrations of C, nitrogen (N), ammonium (NH_4^+), amino acid, soil pH level (the pH of the control soil samples were between 3.5 and 3.8, while the grave soil samples were between 3.8 and 5.6), biomass and respiratory activity found in the grave soils had increased. Surprisingly, biomass and respiratory activities were prolonged for up to 430 days after burial (Ibid).

The decomposition of human remains in soil is facilitated by physical, chemical and environmental processes (Galloway, 1997). However, the majority of cadaver breakdown is owed to the activities of scavengers, invertebrates and, namely, bacteria (Carter & Tibbett, 2008a) which are responsible for the conversion of organic nutrients derived from corpses into inorganic compounds, such as NH_4^+, NO_3^- and CO_2. These compounds are utilised by plants and other organisms like fungi (Anderson, Meyer, & Carter, 2013). This process causes the proximal soil

environment to gradually undergo changes in its chemical composition and microbial fauna over time (Carter *et al.*, 2007). Soon after the deposition of cadavers in terrestrial environments, the surrounding soil becomes basic as a result of soft tissue decay that is facilitated by insect and microbial activity (Carter & Tibbett, 2008b). Dent, Forbes and Stuart (2004) provide a generalised overview of the PM interactions that transpire between human cadavers, the proximal soil environment, and fungi. During autolysis (aerobic), the human body which is comprised of 64% water and 36% nutrients (10% fat, 20% protein, 1% carbohydrate and 5% minerals; Dent *et al*., 2004) undergoes soft tissue modifications. These changes result in the expulsion of minerals, lipids, proteins and carbohydrates to the immediate soil environment. This discharge causes the soil's pH (alkalinity) and its nitrogen concentration to increase (Carter *et al*., 2007; Galloway, 1997; Hopkins *et al*., 2000) establishing conditions favourable to anaerobes, as well as fungi (Dent *et al*., 2004), that facilitate the putrefactive stage of decomposition. As microbial respiration continues within the CDI, oxygen within the soil environment is gradually depleted and CO_2 levels simultaneously rise (section 1.3.5). This process causes the soil's pH to shift from basic to acidic, gradually transforming the microbial assemblage with time (Carter *et al*., 2007). Janaway (1996 in Hopkins *et al*., 2000) was first to describe this succession from aerobes to anaerobes with affiliation to cadaver decomposition. Section 1.3.5 describes the pattern of fungal activity that occurs in relation to cadaver decomposition in terrestrial environments.

1.3.5 Fungi as indicators of clandestine graves and PBI

Most fungi associated with cadaver decomposition are aerobic (Dent *et al*., 2004). They are observed on the surface of skin, where lesions occur and can also be found growing within the digestive tract and other cavities. Moulds are typically observed on the surfaces of decomposing remains within the first week of deposition (Hawksworth & Wiltshire, 2011). Those that grow on bodies found within graves develop at a slower rate (Evans, 1963 in Dent *et al*., 2004). Fungi that

have been found particularly useful for estimating PBI are ordinary decomposer or spoilage fungi capable of colonising cadavers (Dent *et al*., 2004).

Fungi live cooperatively amongst different microbial communities. In CDIs, for example, majority of cadaver soft tissue decay is owed to the activities of bacteria and invertebrates. The waste products generated by bacteria that are present during the early PM stage of decomposition generate nutrients that are utilised by fungi to sustain their metabolic processes (Haelewaters, 2013; Sagara *et al*., 2008). Hard tissues (bones, hair, nails, horns, hooves, feathers, and bills) that continue to persist long after the soft tissues have perished exhibit a particular assemblage of fungi. This collaborative PM relationship between bacteria and fungi has rendered the latter group of organisms potentially useful forensic tools for detecting clandestine graves and for estimating PBI. In 1976, Sagara noted the presence of *Hebeloma vinosophyllum*, an ectomycorrhizal fungus (fungi that colonise the roots of host plants, such as tree roots, extracellularly), in association with the corpse of a cat and dog that were both found at different locations. It is considered to be a possible "corpse-finding" fungus that emerges approximately 2-3 months after urea or ammonium has been introduced to the soil environment (Haelewaters, 2013; Hawksworth & Wiltshire, 2011). This fungus continues to produce sporophores (hyphal structures known as the fruiting bodies that bear reproductive spores), for up 2 years. Expounding upon this notion of using fungi as clandestine grave markers and as estimates of PBI estimates, Carter and Tibbett (2003; Mark Tibbett & Carter, 2003, 2008) describe two groups of fungi associated with cadaver decomposition: ammonia fungi (AF) and post-putrefactive fungi (PPF).

Hebeloma vinosophyllum is an example of AF that arises when a deliberate, sudden and excess amount of urea or ammonium is deposited to the soil environment causing the soil's alkalinity to increase. In soil containing high amounts of alkali and alkaline-earth substances, ammonia may be spontaneously or biologically liberated to the soil environment as a result of microbial processes (Carter & Tibbett, 2003; Sagara *et al*., 2008). This group of fungi produces

fruiting structures that appear on the soil surface. On the other hand, PPF are found naturally growing on human remains or in soil after cadavers or excreta have been introduced to the terrestrial environment (Ibid). Both groups of fungi essentially generate the same species population and sequence of fruiting bodies.

Suzuki (2009) points out that the reproductive structures of ammonia fungi show up in a sequential manner after there is a large increase in the amount of nitrogen associated with the alkalinisation of the soil. Changes that occur among the fungal species assemblages are classified as fungal succession (Suzuki, 2002). The taxa of AF found growing on urea-/nitrogen-treated soil and the order of their appearances are as follows (Sagara *et al.*, 2008):

> Mitosporic fungi (formerly Deuteromycetes) → Ascomycetes (cup fungi –predominantly Discomycetes) → Basidiomycetes (primarily Agaricales).

For PPF fungi, the order of fungal succession is much like that above but is considered a larger set that is inclusive of the AF and occurs in the following manner (Carter & Tibbett, 2003; Suzuki, 2009):

> Zygomycetes → Ascomycetes (cup fungi) → Agaric fungi consisting of small basidiomycetes → Agaric fungi that consist of larger basidiomycetes.

The patterns of succession for these fungi can be categorised as early phase (EP) or late phase (LP). EP fungi are categorised as saprobes whereas LP fungi are mainly biotrophs (Suzuki, 2009), pathogens that obtain their nutrients by feeding on the tissues of their living host by way of special nutrient-absorbing structures, but can also consist of necrotrophs (pathogens which kill their host by releasing toxins or degradative enzymes that destroy the tissue they then feed on) and the occasional saprotroph. During the EP of fungal succession, moulds (Deuteromycetes) are the first to make an appearance followed by disk or cup-shaped fungi (Discomycetes), and then small gilled-fungi (Agaricales).

LP fungi consist of large and small gilled-fungi, such as *Hebeloma vinosophyllum* as previously discussed. Carter, Yellowlees and Tibbett (2007) state that cadavers representative of the dry (desiccated soft tissues or little evidence of flesh/connective tissues remaining) and the remains (completely skeletonised artefacts of remains) decomposition stages (the two are sometimes difficult to distinguish) that are found in contact with nitrogen rich soil demonstrate associations with the presence of fruiting bodies that are members of the PPF group. These EP fungi fruit in response to high concentrations of ammonia for 1-10 months after nitrogen addition. LP PPF fruit in response to organic nitrogen and high concentrations of ammonium and nitrate (NO_3^-). Late Phase fungi may be present for up to 4 years after the addition of nitrogen (Sagara, 1992). Suzuki (2009) also noted that AF are capable of colonising soil under acidic conditions.

According to Yamanka (2002 in Sagara *et al*., 2008), the successional change from EP to LP fungi in urea treated plots may be rationalised in the following manner. Soil treated with ammonium-nitrogen (NH_4^+–N) will first attract EP fungi because they have a preference for this compound which produces ideal alkaline conditions for them. They are also capable of extracting C sources saprotrophically from the organic components of soil in the absence of roots from live trees. Consequently, these EP fungi find the soil environment unsuitable when a build-up of nitrate-nitrogen (NO_3^-–N) level occurs and the existing soil conditions become increasingly acidic due to microbial respiration. Consequentially, EP fungi are gradually replaced by LP fungi that are capable of utilising both NO_3^-–N and NH_4^+–N, prefer acidic soil environments, and form mutualistic relationships with ectomycorrhizal tree roots in order to obtain C sources for their development.

Griffin (1960) provided a detailed report of more than 30 different genera of fungi that were associated with the PM colonisation and destruction of hair samples collected from several decedents. These samples of hair were sterilised before coming into contact with soil from three

different environments. He noted that these species of fungi had populated the hair samples at different time periods. The order in which these fungi successively colonised the hair samples was also described. Saprophytic fungi that were highly competitive in nature and expressed the ability to exploit simple nutrients from the hair substrate were the first colonisers. The species involved were Fusarium spp., Penicillium spp. and members of the Mucorales which are characteristic of this stage. Their presence overlapped with the second phase of fungal species that successively colonised the hair samples. These successive species were identified as *Chaetomium cochlioides*, *Gliocladium roseum*, *Humicola spp*. and other *Penicillia*. Griffin (1960) states that their emergence may in part be due to their ability to process the more resilient components of the substrate.

The sequence of fungal succession associated with cadaver decomposition in soil environments may provide an alternative means for determining PMIs/PBIs in situations where other methods, such as arthropod succession, are rendered useless. If the time frame for which various fungal fruiting bodies make their appearances is known, as well as the timing of their reproductive sequence (life cycle, season for which they appear), then it may be possible to obtain more useful PMIs/PBIs given that PPF are not in competition with other microbes or plants.

1.3.6 Recurring fungal taxa typically observed among PM remains

More than 70 different taxa of PPF (including AF) have been documented from studies of soil treated with urea and/or nitrogenous components and from observations of naturally occurring PPF associated with cadaver remains or animal excreta (Suzuki, 2009). A study conducted in Ceará, Brazil (Sidrim *et al*., 2010) reported the fungal species isolated from the hair, skin, lungs and the mucus-lined orifices of human cadavers at various decompositional stages; the bloat stage (n = 34 cadavers) which is represented by corporal swelling due to a build-up of gases that are generated as a result of autolytic processes, the putrefactive stage (n = 6 cadavers), and the

skeletonised (dry/remains) stage (n = 20 cadavers). The authors reported that the fungi predominantly found in association with cadavers assessed during the bloat and putrefaction stages were of the genuses *Aspergillus*, *Penicillium*, and *Candida*. Cadavers that were examined during the skeletonised phase consisted of fungal populations mostly belonging to the *Apergillus*, *Penicillium*, and *Mucor* genuses. However, two species of *Mucor* fungi were present among the 143 different fungi observed from cadavers representing the bloat stage.

A similar study conducted by ten Broek (2009) reported observations of fungal succession found on pig trotters disinterred from a soil (sandy loam silt) environment. The species observed by the author and the order of their appearances involved fungi from the *Mucor*, *Aspergillus* and *Penicillium* genera. The species of *Mucor* was detected at 8 days *post*-burial and persisted until 40 *post*-burial days had lapsed. Fungi representative of the *Penicillium* genus appeared after 28 days *post*-burial and was succeeded by species belonging to the genus *Aspergillu*s at 40 days post-burial.

In Buenos Aires, Argentina, Tranchida, Centeno and Cabello (2014) conducted research on control soil samples that were collected from soil that had been resting directly below human remains that were 24 days PM (test sample). The head of the individual was completely skeletonised, whereas the appendages illustrated signs of advanced decay. Control soil was collected 15m away from the location where the cadaver was found. Interestingly, fungi of the *Penicillium*, *Aspergillus* and *Mucor* genuses were observed among control samples of soil but were completely absent from the test soil situated below the remains. Observations of rain puddles from the previous day's rainfall or soil pH (Section 1.3.5) may serve as underlying explanations for the absence of these genera from soil in direct contact with the remains. However, the authors fail to make mention of the soil's composition. Table 1.3 lists the fungal species that were present in the soil beneath the discovered remains.

Various studies from countries such as Australia (Griffin, 1960), Belgium (van de Voorde & van Dijck, 1982), Canada (Huculak & Rogers, 2009), Japan (Hitosugi *et al*., 2006; Ishii *et al*., 2006, 2007), and the United Kingdom (Hawksworth & Wiltshire, 2011; Janaway *et al*., 2008 in Hawksworth & Wiltshire, 2011; Rogers, 2010; ten Broek, 2009; Wilson *et al*., 2007) have reported detection of *Aspergillus spp.*, *Penicillium spp.*, both or some combination of these fungi accompanied by the presence of fungal species classified as *Candida spp*. and/or *Mucor spp*.

Other fungal species found in association with human remains reported by these studies are presented in Table 1.3. The fungal species listed in this table are solely for comparative purposes and do not serve as prototypes for each country presented. They merely reflect the species of fungi that have been documented for cadavers found in distinct locations.

Table 1.3: A list of the fungal species found in relation to decomposed remains discovered in different countries and in various forensic contexts.

Location	Author(s)	Environment	Fungal Species Observed
Argentina	Tranchida, Centeno and Cabello (2014)	Terrestrial (field with puddles from previous day's rainfall)	*Dichotomomyces cejpii*, *Talaromyces trachyspermus*, *Talaromyces flavus*, and *Talaromyces sp.*
Australia	Griffin (1960)	Laboratory (Sterile human hair in contact with surface soil from 3 distinct locations)	30+ different Genera. Examples of genera present among hair interred in all three soil types include *Cunninghamella cochlioides*, *Fusarium spp.*, *Gymnoascus gypseum*, *Keratinomyces ajelloi*, *Mortierella spp.*, *Penicillium spp.*, and *Streptomyces spp.*
Belgium	van de Voorde & van Dijck, 1982	Room (with constant temperature of 12˚C)	*Cladosporium sp.*, *Fusarium sp.*, *Geotrichum candidum*, *Hormodendron sp.*, *Mortierella sp.*, and *Penicillium chysogenum* (as *P. notatum*)
Canada	Huculak & Rogers, 2009	Terrestrial – Soil (buried and above ground)	*Aspergillus spp.*, and *Penicillium spp.*
Japan	Hitosugi *et al.*, 2006	Abandoned House (mummified remains; humidity approximately 100%, constant temperature 12-13˚C)	*Aspergillus terreus* and *Penicillium sp.*
United Kingdom	Hawksworth & Wiltshire, 2011	Body of water	Species of *Fusarium*, *Geotrichum*, *Mucor*, and *Pythium*
United Kingdom	Hawksworth & Wiltshire, 2011	Closed Flat, blood from corpse on carpet sample	*Mucor plumbeus*, *Penicillium brevi-compactum*, and *P. citrinum*
United Kingdom	Janaway, Percival & Wilson, 2008	Terrestrial	Moulds, *Candida sp.*
United Kingdom	Rogers, 2010	Terrestial - Soil (buried)	*Aspergillus fumigatus* and *Penicillium sp.*
United Kingdom	ten Broek, 2009	Terrestial - Soil (buried)	Mucor, Penicillium, Aspergillus nidulans or Aspergillus glaucus

1.4 Research objectives and aims

This study is two-part. It examines the proteolysis of decomposing cartilage from porcine trotters buried in soil environments and the fungi that are present among these specimens, including their patterns of growth and species succession with time. The overall objective for these studies is to determine whether the PM processes that govern the decay of cartilage and the colonisation of cadavers by various fungi can be used as forensic tools to estimate PMI beyond 48 hours. Pig trotters were chosen as models of human decomposition as their biogeochemistry strongly mirrors that of humans (Dent *et al*., 2004; Forbes *et al*., 2002; Turchetto & Vanin, 2004).

1.4.1 Intended goals for the investigation of post mortem articular cartilage

In light of the observations made in sections 1.1.3 and 1.1.4, the aims of this investigation are to 1) explore the forensic value of PM cartilage from a biomolecular standpoint, 2) determine whether decomposition of this tissue has potential use for estimating PMI beyond the current limitations of 48-hours that are imposed by other soft tissue, and 3) provide additional information about the PM processes involved in the destruction of aggrecan, the structural component of cartilage.

1.4.2 Research objectives for forensic mycology section

The research findings presented in sections 1.2.5 and 1.2.6 illustrate the groundwork that forensic mycologists have established in recent years. Macroscopic and microscopic observations of fungi associated with the decomposition of cadavers, and the sequence of their appearances shows that these organisms have the potential to provide estimates of PBI. Nonetheless, a considerable amount of data concerning the roles that fungi play in facilitating human

decomposition is necessary for the establishment of alternative methods that are capable of providing reproducible and sound estimates of PBI.

In keeping with the current goals of forensic mycology, the aims for the mycology research section was to determine whether various morphological forms of fungi found in association with buried porcine trotters in soil environments could be selected as candidates for future identification, to observe the rate and extent of their growth, and to determine whether the colonising species involved appeared in particular sequences.

Materials and Methods

Chapter 2

2.0 Materials and Methods

2.1 Study sample

Subject samples consisted of dismembered adult porcine (*Sus scrofa*) trotters and the tail of an adult bovine (*Bos taurus*). Trotters were obtained from F.A. Gill Ltd., a local abattoir (Parksfield, Wolverhampton), and dismembered at the carpal/tarsal joint, or superiorly along the limb bone proximal to this area. The specimen of bovine tail, collected from Crown Butchers (Stourbridge, West Midlands), was received stripped of its skin and dermis in accordance with the UK Food Standards Agency's (FSA) health and safety regulations (Annex III to Regulation (EC) No 853/2005 – Section I, Chapter IV), thereby exposing the underlying muscle tissues. Both porcine and bovine samples were collected from their respective abattoir and butcher shop within hours of being slaughtered.

Cartilage extracts were removed from specimens of porcine metacarpaophalangeal (MCP)/metarsophalangeal (MTP) joints (hyaline articular cartilage) and bovine coccygeal (tail) intervertebral joints (fibrous cartilage) hours after slaughter and were appointed control samples. These extracts were labelled "0 days PM". Samples interred below ground for various lengths of time were designated experimental samples and labelled according to the number of PM days spent interred. For instance, if an experimental sample had spent 14 days below ground it was labelled '14 days PM'.

2.2 Burial sites

Interments were carried out at two distinct burial sites: The University of Wolverhampton's Crop Technology Unit at Compton Park (Wolverhampton, West Midlands, UK; SO888988), and the Grange Farm Bungalow in Hilton (Shropshire, UK; SO781949). The burial plot at Compton Park (CMP) was located in an urbanized residential area and situated at ground level. The Hilton

(HLT) burial plot was erected at the top of a hill (approximately 66m above sea level) on a rural farm. Both plots were contained by wood and chain-linked fences that extended 60cm below ground to minimise animal scavenging/disturbances. Soil was classified as sandy loam at both CMP (Vaz, 2001) and HLT (using thermogravimetric, x-ray fluorescence and X-ray diffraction analyses; see Results section 3.1). However, CMP exhibited moist and nutrient rich soil whereas HLT consisted of dry and nutrient deficient soil (lacking a sufficient amount of humus).

For the duration of each interment, the ambient temperatures (high and low) for Wolverhampton were recorded daily (www.accuweather.com). Weekly collections of data consisting of the amount of precipitation (mm) were also obtained from the University of Wolverhampton's meteorological station located proximal to the Hilton Grange Farm burial plot.

2.3 The sequestering of cartilage samples for Western blot analyses (and live/dead cell assays)

2.3.1 Interment and disinterment of porcine and bovine specimens

Experimental samples were interred in graves approximately 12cm apart with dimensions of 30.5cm x 20.0cm x 30.5cm (length x width x height). The amount of time that PM specimens remained below ground was measured in days. Several experiments were conducted for Western blot and live/dead cell analyses over the course of 28 months (March 2, 2011 – August 5, 2013) and, during this period, experiments were carried out at various times of year and subjected to different seasons (Table 2.1).

A specimen of bovine tail was disarticulated along several intervertebral joints producing 5 segments encasing one to several undisturbed joints. The fragment bearing the smallest circumference (severed from the most inferior aspect of the tail) was used for the control sample. The remaining tail fragments were buried so that fragments of increasing circumference were sequentially placed in graves adjacent to each other. Larger samples bearing more muscle tissue

Table 2.1:
A list of the experiments conducted, the location of their burial, the duration of weekly disinterments, and the dates for which the experiments occurred.

Experiment Type and Burial Location	Length of Experiment	Dates of Occurrences	Average Ambient Temperatures (˚C) High |Low|| Overall
Long-term EXPT 1 (CMP vs HLT)	7-42 Days PM	Mar. 28 – May 10, 2011	16.9 | 6.8 || 11.9
Long-term EXPT 2 (CMP vs HLT)	7-42 Days PM	Jun. 20 – Aug. 2, 2011	21.6 | 13.5 || 17.6
Short-term Trotters EXPT 3 (CMP – Daily)	1-7 Days	Oct. 31 – Nov. 7, 2011	13.4 | 6.5 || 10.0
Long-term EXPT 4 (HLT)	7-32 Days	Sept. 17 – Oct. 19, 2012	13.6 | 6.7 || 10.5
Long-term EXPT 5 (HLT)	7-42 Days PM	Oct. 8 – Nov. 19, 2012	14.5 | -0.7 || 6.9
Air, Tap and Sea Simulated Exposed Trotters EXPT 6	12 Days PM (Air), 35 Days PM (Tap & Sea Exposed)		N/A
Long-term EXPT 7 (HLT)	28-44 Days PM	Feb. 11 – Mar. 27, 2013	5.0 | 0.0 || 2.5
Long-term EXPT 8 (HLT – LIVE/DEAD)	7-42 Days PM	Apr. 15 – May 28, 2013	14.0 | 5.0 || 9.5
Long-term EXPT 9 (HLT – LIVE/DEAD)	7-42 Days PM	Jun. 3 – Jul. 15, 2013	20.0 | 9.0 || 14.5
Long-term EXPT 10 - Bovine (HLT – LIVE/DEAD)	10-31 Days PM	Jul. 4 – Aug. 5, 2013	21.0 | 11.0 || 16.0

were used for later PM samples to minimise the early onset of joint exposure to the immediate environment.

Disinterment of PM samples was executed with a gardening spade to remove the bulk of soil and then with a small hand-held trowel to gently lift away proximal dirt to avoid damaging the specimens. Samples removed from their graves were photographed with a scale (using a Samsung S850 or Canon IXUS 115 HS) to illustrate their size and appearance at the time of disinterment. Observations about the physical state of specimens were recorded (see sections 3.2.5-3.3.3). Specimens were placed in securely-sealed biohazard bags and transported to a laboratory. Residual soil was gently rinsed away from the soft tissues and photographed to detail the extent of soft tissue changes undergone by PM samples.

2.3.2 Extraction of hyaline articular cartilage from trotter samples

Trotters were dissected with surgical blades using the method set out by Rogers *et al.*(2010) with slight modification:

1. Incisions parallel to the metacarpal (MC)/metatarsal (MT) and first phalange joints were made to pass through the dermis and extended from the lateral to medial aspects of the trotter. The dermis and tendons situated along the anterior, medial and lateral portions of the trotter were removed to expose the underlying bone;
2. the synovial membranes encasing the MCP/MTP and phalanges 1 and 2 joints were carefully perforated to expose the articular cartilage, which was then photographed;
3. cartilage samples were excised from the exposed joint surfaces with a scalpel so that slivers were removed and stored at -20˚C.

2.3.3 Extraction of fibrous cartilage samples from the intercoccygeal joints of bovine

This required scalpel removal of muscle tissue as vertical strips extending the length of the tail fragment followed by manipulation of the tail to determine joint location. Once located, an incision was made extending through the anterior surface of the joint towards the posterior. When contact was made with the transverse and spinous processes, slight downward incisions were continued through until complete disarticulation of the joint was achieved. Cartilage samples were excised by creating several deep slices which penetrated through to the cartilage-bone interface, forming a cross-hatched pattern (4mm x 4mm), and then severed by drawing the scalpel transversely along the surface of bone until the specimens of cartilage were removed completely. Samples were stored in labelled 25ml plastic universal vials at -20˚C.

2.3.4 Cartilage water content

Weights of empty 25ml plastic universal vials were recorded prior to, and again after, the introduction of cartilage samples, which were then frozen at -20˚C. Subsequently the samples were lyophilised (Edwards Modulyo EF4 Freeze Dryer), whereupon the vials and contents were re-weighed in order to measure the dry weights of the cartilage samples, and to facilitate the extraction of ECM PGs.

Percentage water loss was calculated (Table 3.1) with one-way ANOVA (Table 3.2) and paired samples t-test (Table 3.3) analyses being performed on the results.

2.3.5 Proteoglycan extraction and sample preparation

Freeze-dried samples of control and PM cartilage underwent proteoglycan (PG) extraction using the protocol set out by Dudhia *et al.* (1996) with 25mM EDTA and 1% w/v Protease Inhibitor Cocktail I (Calbiochem). Approximately 30mg of samples were weighed in 1.5ml Eppendorf tubes (the weights for each sample were recorded). For each microgram of sample, 30µl of 4M guanidine hydrochloride extraction buffer containing 50mM sodium acetate (pH 6.8) was added. Samples were then placed on a rotating wheel (Stuart Model SB2 Rotator) in a cold room (4˚C).

Preliminary tests were conducted with control samples to determine the incubation time for which optimal PG extraction was achieved. Thus, control samples were subjected to 8, 16, 24, 40 and 48-hour protein extractions. The optimal time for PG extraction was established as 24-hours. Therefore, all control and experimental cartilage samples were extracted with 4M guanidine hydrochloride buffer for 24 hours.

Protein suspensions for each sample were measured in volumes of 200µl and placed in 1.5ml Eppendorf tubes. PG extracts were precipitated with 1300µl of a 1:100 5M sodium acetate: 95% ethanol precipitation buffer solution (precipitation buffer) at -80˚C for 2 hours, followed by centrifugation (13,000 rpm) for 10 minutes (Progen Genfuge 24D Microcentrifuge) at room temperature and supernatants discarded. The remaining PG deposits were subjected to three more precipitations. However, protein extracts were mixed with 1000µl of precipitation buffer on a rotating wheel (4˚C) for 10 minutes and incubated at -80˚C for 30 minutes before centrifugation. Residual PGs were dried in a 37˚C heating block. The desiccated protein samples were reconstituted by adding 200µl of 50mM Tris, 60mM sodium acetate, pH 8.0 (Tris acetate buffer) to each sample and placing them on a roller mixer (Orthodiagnostic Systems Ortho-Mini Mixer) for 3 hours at 4˚C.

Re-suspended protein samples (5µl) were digested with 0.05 units of Chondroitinase ABC from *Proteus vulgaris* (Sigma-Aldrich, UK), 0.01 units of Keratanase from *Psuedomonas sp*. (Sigma-Aldrich, UK) and 11.25µl of Tris acetate buffer overnight in a heating block (37˚C). The protein concentration (µg protein/cm^3) for each sample was determined by Bradford assay (1976) using the modified protocol established by Zor and Selinger (1996). The computed concentrations for each sample were divided by a dilution factor of 4 to compensate for the 3:1 ratio of digestion buffer to reconstituted protein solution. These values were used to calculate the desired amount of sample protein (x µg) to be ran subsequently in a volume (x µl) of 1X loading buffer (Zor & Selinger, 1996) for Western blot analysis.

2.4 SDS- PAGE and Western Blot analyses

Digested cartilage samples underwent SDS-polyacrylamide gel electrophoresis (SDS-PAGE) [41] using 9%, 10% or 8-18% (w/v) gels. Polyacrylamide gels were prepared using cassettes with internal dimensions of 75mm x 100mm x 0.75mm (length x width x depth) and 0.75mm 15-wells spacer combs (3.35mm wide wells with a 20µl maximum capacity per well). Gradient gels (8-18%) were cast using a gradient pump (Gilson Minipuls 3) set to 20 rpm. For each experimental run, uniform measures of protein per volume of solution were loaded in their respective wells (approximately 20µg protein/10µl 1X sample buffer) alongside one or two protein molecular weight marker mixtures, 4µl of Prestained Protein Marker, Broad Range, 7-175kDa (New England Biolabs) and 3µl of BLUeye Prestained Protein Ladder, 9-235kDa (GENEFLOW). Both porcine and bovine samples were loaded at a mass concentration of 20µg of cartilage protein (measured by Bradford assay using the revised protocol described by Zor and Selinger in 1996) in 10µl of sample buffer, unless

specified otherwise. Protein samples were electrophoresed at 165V for 48-55 minutes until the bromophenol dye fronts were approximately 1cm from the bottom of the gel. Western blot transfers of proteins to polyvinylidene difluoride (PVDF) membranes (Millipore) (Towbin, Staehelin, & Gordon, 1979) were conducted at 100V for 70 minutes. Protein-bound membranes were then treated to non-specific protein binding using a 10% milk/2% bovine serum albumin (BSA) solution or 5% milk solution depending upon the primary antibody used (see section 2.4.1).

2.4.1 Probing of PVDF membranes with monoclonal antibodies

Monoclonal antibody 2-B-6 conjugated to HRP

PVDF membranes were blocked overnight by immersion in 10% skimmed milk 2% aqueous BSA solution at 4˚C. The milk/BSA solution was then poured away and the membrane rinsed three times at 10-minute intervals with a 1× Tris buffer saline and Tween 20 (0.025%) solution (TBS-T). Incubation with a 1:500 dilution of monoclonal antibody (MAb) 2-B-6 (mdbioproducts, UK) in 5ml of 10% skimmed milk/2% BSA blocking solution occurred for one hour in sealed bags. Removal of membranes from solution was proceeded by three 10-minute rinses with TBS-T (0.025%), followed by a one-hour incubation with horseradish peroxidise (HRP)-linked anti-mouse IgG antibody (1:1000 dilution, Cell Signaling Technology) in 5ml of 1X TBS-T (0.025%). Finally, membranes were rinsed three times for 10 minute intervals with 1X TBS-T (0.025%) and remained in rinse buffer solution until ready for chemiluminescence.

Anti-α-Tubulin

The methodology used in 2.4.1 was adapted for membranes probed with anti-α-tubulin and involved minor changes. This antibody recognises α-tubulin, a small globular protein that forms microtubular structures located within cellular membranes. PVDF membranes were blocked with 5% skimmed milk in a 1×TBS-T (0.05%) solution for 40 minutes at 4˚C. Rinses were conducted five times before and after primary and secondary incubations with 1× TBS-T (0.05%) for intervals of five minutes. Membranes were incubated overnight at 4˚C with a 1:2500 dilution of anti-α-tubulin (primary antibody) made with 1× TBS-T (0.05%). Secondary anti-mouse was diluted in1× TBS-T (0.05%) for one hour. Membranes were kept moist in 1× rinsing buffer until they were ready to be visualised by chemiluminescence.

Anti-Vimentin and Vinculin

Using the protocol in 2.4.1 for membranes probed with MAb 2-B-6, pilot tests for anti-vimentin (Santa Cruz Biotechnology) and vinculin (Sigma-Aldrich, UK) antibodies were conducted on Chondroitinase ABC digested samples of control cartilage. For anti-vimentin, a dilution of 1:2500 was used, and 1:8000 for vinculin. Each antibody experiment was subjected to overnight incubations with a 5% skimmed milk blocker and another using 10% skimmed milk/2% BSA, also testing for non-specific binding. Experiments using smaller dilution factors for anti-vimentin (1:400 and 1:200) and vinculin (1:350 and 1:200) were subjected to non-specific protein blocking for 45 minutes in a 5% skimmed milk solution. Membranes were placed in primary antibody solutions for overnight incubation. Rinses with 1× TBS-T (0.05%) were subsequently carried out before and after primary and secondary antibody incubation at 5-minute intervals.

2.4.2 Visualisation of targeted proteins

Immobilised target proteins were made visible by autoradiography using a horseradish peroxidase (HRP) chemiluminescence detection kit (EZ- ECL; Geneflow), Kodak Biomax MS Film, developer and fixer (Kodak GBX; Sigma) (Towbin *et al.*, 1992). Membranes probed with HRP-conjugated anti-mouse IgG antibodies were incubated for 2 minutes in a 1:1 stabilised peroxidase and luminol substrate solution, unless indicated otherwise. Subsequently, excess substrate was removed and the protein-bound membranes were then wrapped in cling film. Membranes were secured to a cassette and covered with x-ray film. Film exposure occurred for a specific amount of time that was empirically determined.

2.5 Sample preparations for live/dead cell assays

2.5.1 Cartilage cross-sections for pilot and experimental studies

Preliminary tests were conducted on control cartilage extracted from trotters collected within hours of slaughter. Cartilage samples were aseptically excised from the MCP/MTP joints of porcine trotters using the methods outlined in "Section 2.3.2." Samples were taken from five distinct locations on the distal surface of the MC/MT joint of one trotter to determine a sample area presenting the greatest number of live cells at 0 days PM for conducting vitality assays on experimental samples. The surface areas involved in this experiment were:

1. the most inferior aspect of the joint (the ridge),
2. the groove situated lateral to this ridge, and
3. the lateral, medial and posterior surfaces of the joint.

Cross-sections of these cartilage samples (approximately 0.8mm thick) were created using two double-edged razors taped on opposite sides of a sheet of acetate paper. The cartilage

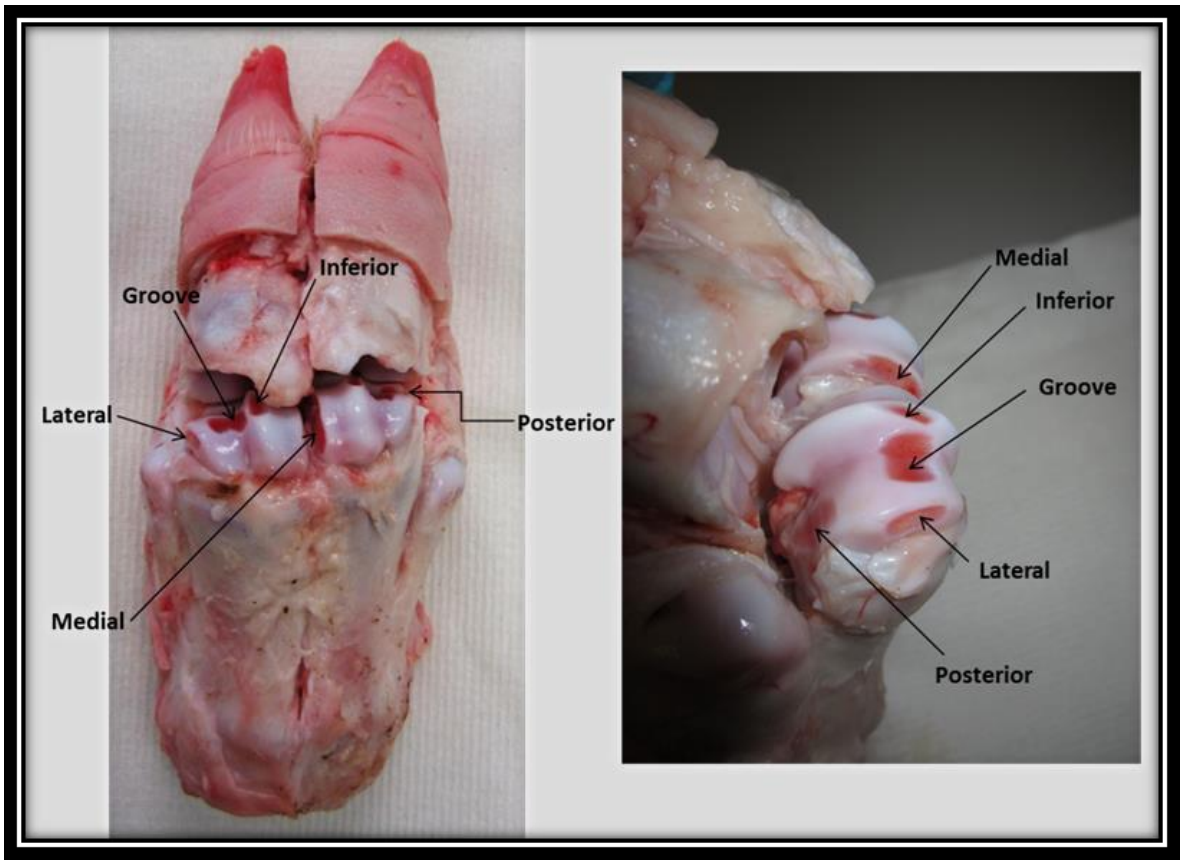

Figure 2.1 Frontal and lateral views of a dissected control (0 days PM) trotter. The images illustrate the distal surfaces of the MCP/MTP joints from which cartilage samples were excised for preliminary vitality assays. Cross-sectional samples were obtained from 5 different areas along the distal surfaces of the MCP/MTP bones (the most inferior aspect of the joint (ridge), groove, medial, lateral and posterior surfaces) to determine a surface area least affected by mechanical activity/damage to achieve a reliable count of live cells.

cross-sections were separated according to pig trotter specimen and joint number. Samples were rinsed in phosphate buffer saline (PBS) solution containing glucose (5.6mM), calcium (0.9mM), and magnesium (0.5mM) and then temporarily placed in 0.5ml Eppendorf tubes containing 500µl of Dulbecco's Modified Eagle Medium (DMEM) (Life Technologies, UK). Experimental outcomes dictated that cartilage samples removed from the inferior ridge of the distal MC/MT joint were the most ideal area for collecting test samples. Therefore, samples of PM cartilage were collected from this area only.

2.5.2 Cell vitality assay

Cartilage cross-sections were placed in 0.5ml Eppendorf tubes containing 500µl of PBS. To each test tube, one microlitre of propidium iodide (Sigma-Aldrich, UK) (1mg/ml stock solution, dissolved with dimethyl sulphoxide) and Calcein AM (1mg/ml) (Merck Millipore) were added to achieve a 1:500 dilution of both fluoroprobes and incubated at 4˚C for 1 hour to conserve cell viability (wrapped in foil). Propidium iodide (Sigma-Aldrich, UK) was used to detect the nuclei of ruptured cells and fluoresces red (λ_{ex} 540nm, λ_{em} 608nm) when bound to nucleic material. Calcein AM identifies live cells by transporting across the cell membrane and staining the cytoplasm fluorescent green; (λ_{ex} 495nm, λ_{em} 515m).

In a darkened room, cartilage cross-sections were gently transferred to double cavity slides (Fisher Scientific), with a diameter of 15mm and a depth of 1.2mm to 1.5mm. Approximately 130µl of 1× PBS buffer solution was added to each cavity. Samples were covered with a glass coverslip and sealed with clear nail varnish. Simultaneous images of live (green) and dead (red) chondrocytes at the superficial and tangential/deep (central region) zones of the cartilage cross-sections were taken using a fluorescence microscope

(Olympus BX61). Observations of live cells were conducted with a fluorescein isothiocyanate (FITC) filter which emits a blue light (excitation wavelength of 467-498nm; emission wavelength of 513-556nm) that detects green fluorescent proteins. Dead cells were detected using a Texas Red filter which gives off a yellow light that detects red fluoroprobes (λ_{ex} = 542-582nm; λ_{em} = 604 – 644nm).

The percentage of viable cells was calculated by counting the number of live and dead cells that fell within the perimeters of a self-determined/-designed tally window to establish a consistent field of view (Fig. 2.2). This tally window was placed centrally to the medial and lateral peripherals of the inferior ridge with its upper and lower borders in line with the photo image captured (Fig. 2.3). Statistical analyses (Pearson's correlation, ANOVA and multivariate analysis) examining the relationships between PMI, average weekly temperature (˚C), average weekly precipitation (measured in mm) as independent variables, and the percentage of live chondrocytes (as the dependent variable) were performed in order to determine the nature and degree of correlation between these variables.

2.6 The collection, inoculation and observations of post mortem fungal samples

The needle point of a dissecting probe, sterilised on site with ethanol (70%), was placed in direct contact with white hyphal growth. The fungal sample was then inoculated on a malt extract agar (MEA) Petri dish (MEA: 0.5% Ampicillin sodium salt, 1.5% Agar No. 2, 2% Malt extract) by carefully lifting the lid and gently wiping the needle across an isolated section. MEA is typically used as it assists with the isolation and identification of fungi and yeasts. This medium provides fungi with various nutrients, carbon and protein which are required for growth. The presence of ampicillin ensures that bacterial growth is prohibited.

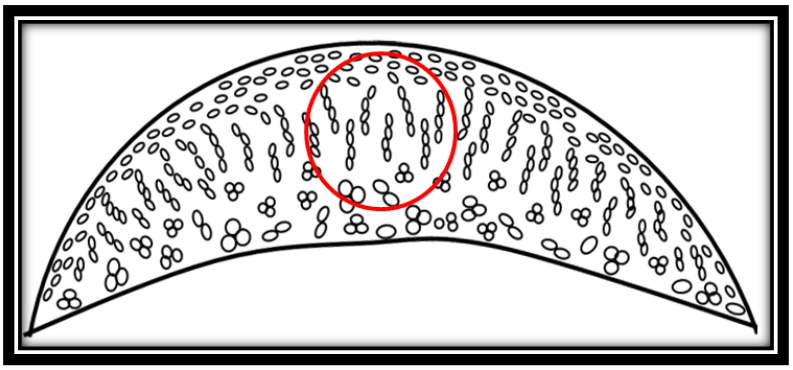

Figure 2.2 A schematic diagram of a cartilage cross-section collected from the most inferior aspect of the distal MCP/MTP joint (the ridge). The red circle indicates the area of the cross-section considered most central on the specimen sample and viewed under the microscope's field of view.

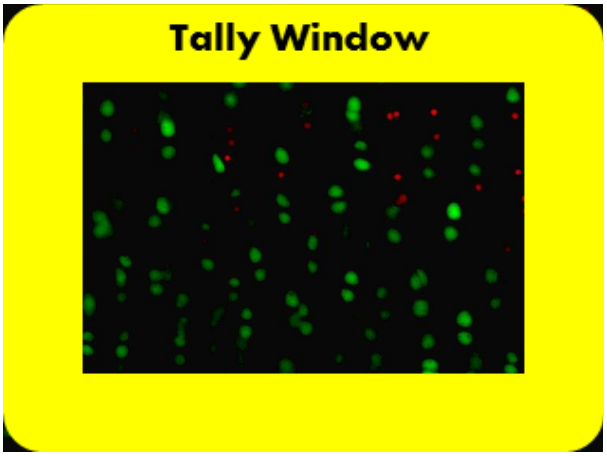

Figure 2.3 A tally window superimposed on a photographic image displaying live (green) and dead (red) chondrocytes, as captured from the camera of a fluorescence microscope (Olympus BX61).

Inoculated Petri dishes were incubated for 2-3 days at 25˚C and fungal growth monitored to minimise species cross-contamination. At the appearance of distinct fungal colonies, each specimen was re-inoculated on fresh MEA medium using the streak plate inoculation technique. This process was repeated as many times necessary to achieve pure, isolated colonies. Colony samples were mounted onto microscopic slides containing a drop of lactophenol cotton blue stain, a mounting fluid which preserves the structural integrity of fungal specimens while staining the chitin within their cell walls so that they are discernible under a light microscope. Fungal samples were then observed under a light microscope (Kyowa UNILUX-12) at 40X magnification. The appearance of the sporulating structures for each fungal specimen was then compared with a fungal key to establish a possible identification at the genus level.

Results

Chapter 3

3.0 Results

3.1 Soil, post mortem cartilage and water content

Soil at CMP was characterised as sandy silt loam (Vaz, 2001) with an average pH of 5.54 (Rogers, 2010). Soil from HLT underwent thermogravimetric, X-ray fluorescence, and X-ray diffraction analyses to determine the soil type. Results from the thermogravimetric analyser (Perkin Elmer TGA7) demonstrated a 2.99% loss of organic material at 329˚C, a considerably low percentage indicative of soil lacking fertilization with humic material (Figure 3.1). The small peak at 533˚C is representative of the soil's clay component. Low potassium (1.43%) and phosphorus (0.06%) levels presented by X-ray fluorenscence (Spectro Xepos) lend further support for poorly fertilized soil (Table 3.1), whereas the high percentage of silicon (29.9%), attributed to the 74% SiO_2 (silica, the sand component) composition (Table 3.2), characterized the soil as sandy loam. The soil's pH was 7.06.

Twelve pairs of trotters were interred at CMP and HLT for experiments 1 (EXPT 1) and 2 (EXPT 2) as detailed in Section 2.3.1 and Table 2.1 (ADDs calculated for each PMI can be found in Table A.1 for EXPT 1 and A.2 for EXPT 2 in the Appendix). Empirical observations of post mortem articular cartilage revealed a gradual reduction in the tissue's integrity over time (Figure 3.2). Systematic changes in colour and robustness were visibly noted. With increasing PMI, the colour of cartilage progressively changed from white to dark pink and finally beige while the tissue became thinner and gradually receded from the cartilage tidemark. These observations were in accord with reports made by Rogers *et al.* (2010) and ten Broek (2009). The percent water content for PM porcine hyaline cartilage was investigated at weekly intervals for a period of six weeks (sections 2.3.1–2.3.4).

Two experiments involving the weekly collection of PM cartilage samples from CMP and HLT were conducted during March 28-May 10, 2011 (EXPT 1) and June 20-August 2,

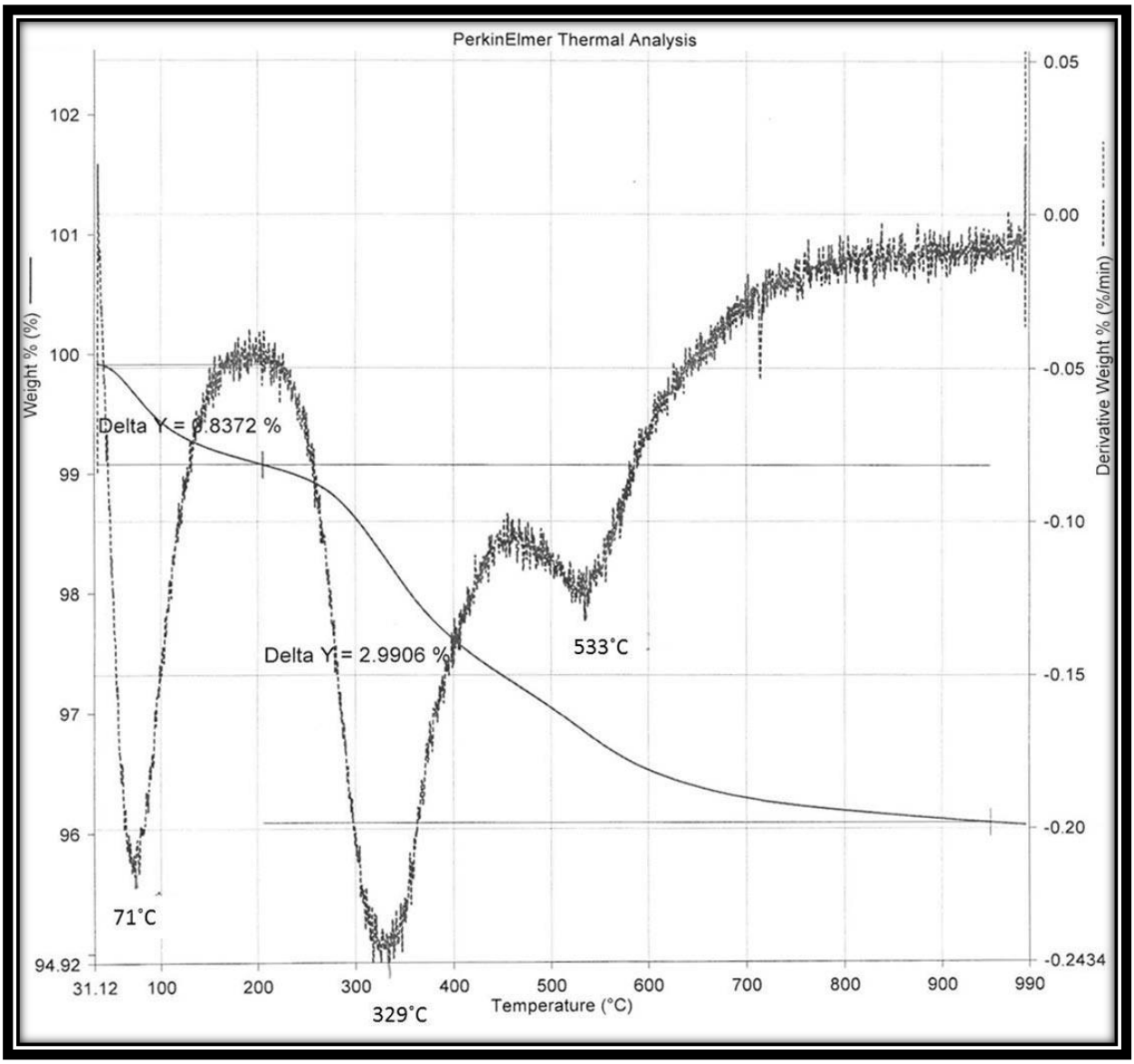

Figure 3.1 Thermogravimetric output for soil collected from the Hilton burial plot. The peak situated at 329˚C corresponds to a small 2.99% loss of organic material and denotes soil that is lacking in nutrients. The peak at 533˚C resulted from a loss of the soil's clay component. At 71˚C, little water loss was observed (0.84%) indicating that the soil was relatively dry.

Table 3.1: X-ray fluorescence analysis for soil from Hilton.

Symbol	Element*	Concentration (%)	Abs. Error (%)
Na	Sodium	2.06	0.99
Al	Aluminum	5.99	0.04
Si	Silicon	29.90	0.06
P	Phosphorus	0.06	0.002
K	Potassium	1.43	0.014
Fe	Iron	1.82	0.008

* Only elements whose percent concentration was greater than one are included in this table. All other elements are considered negligible.

Table 3.2: X-ray diffraction analysis of soil from Hilton

	Card ID	Match Score	Relative Mass Score	Relative Intensity [%]	Display [µm]	Formula
1	33-1161	29.41	0.82	74	25	SiO_2
2	03-0418	15.94	0.59	4	131	Ca-Mg-Al-Si-O
3	23-0493	5.90	0.54	6	12	K_2O

(Philips Diffractometer; model PW170)

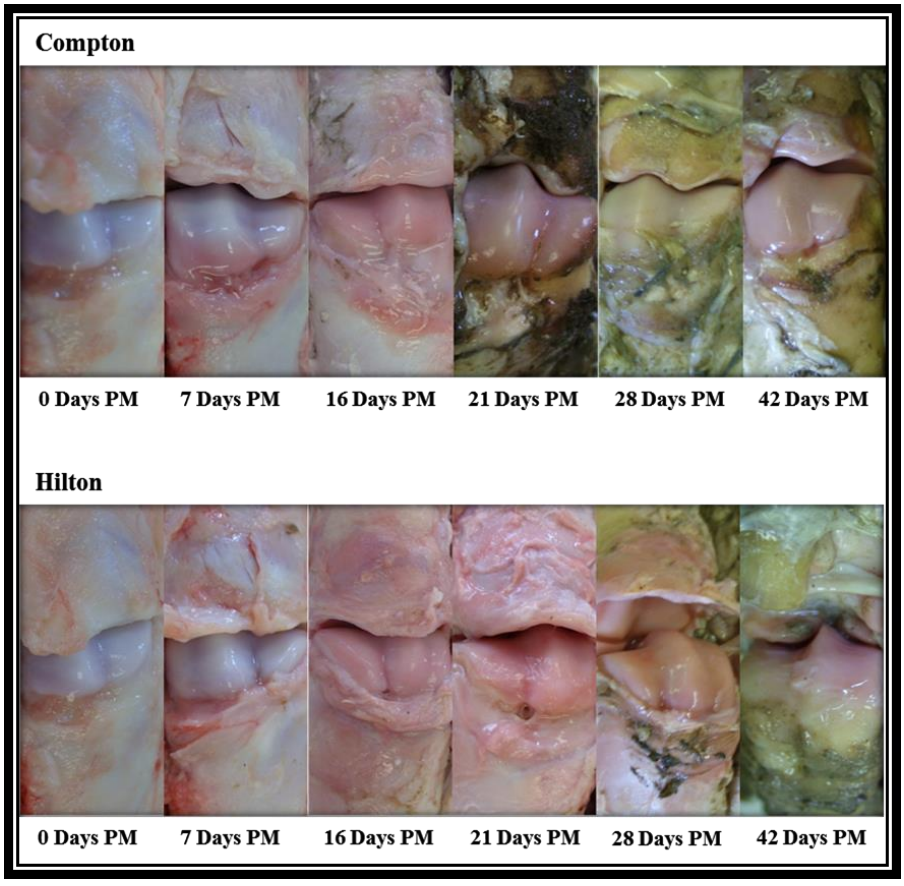

Figure 3.2 The physical appearance of post mortem cartilage observed 0-42 days PM after death. With increasing PMI, there is a gradual change in the colour of the tissue from pearly white to pink and evidence of resorption at later intervals.

2011 (EXPT 2) respectively. The aims of these experiments were to 1) determine whether the water content of PM cartilage would change with increasing PMI, and 2) observe whether soil environment would influence the percentage of water retained by PM cartilage samples collected from two different burial plots (CMP – moist soil; HLT – dry soil). The null hypotheses (H_0) for these experiments were that 1) no changes in the water content of articular cartilage would be observed with increasing PMI, and 2) that differences in soil environment would have no influence on the water content of PM cartilage samples. Conversely, the alternative hypotheses (H_A) stated that 1) changes in the percentage of water content for articular cartilage would occur as PMI increased, and 2) that differences in soil environment would influence variations in the water content of PM articular cartilage collected from distinct burial plots. For each experiment, control samples of cartilage (0 days PM) were taken from two dismembered trotters and pooled together. Control samples represented a mean of articular cartilage samples collected from two different pigs. After lyophilisation, the change in weight for EXPT 1 control cartilage yielded a water content of 70.50% and 71.15% for EXPT 2 control samples (70.83% average). The result of this analysis is seen in Table 3.3. The mean values obtained for EXPT 1 and EXPT 2 control articular cartilage samples are well within the range of that reported for human cartilage by Dudhia (2005), Lüsse *et al.* (2000), Armstrong & Mow (1982), Mow, Ratcliffe, & Poole (1992), and Kheir & Shaw (2009).

For EXPT 1 and EXPT 2 (see Table 2.1 for details), experimental cartilage samples (7-42 days PM) collected from trotters disinterred at the CMP and HLT burial plots were extracted and weighed in the same manner as the control samples (0 days PM). The percent water content of experimental samples collected for EXPT 1 showed values ranging from 65.48% to 73.29% between the two soil environments. Apart from the samples collected at 7 days PM from CMP (65.48%) and at 28 days PM from HLT (65.80%), the water content of

Table 3.3: Weekly evaluations of post mortem cartilage samples collected from CMP and HLT burial plots for experiments 1 and 2 (Microsoft Excel 2010).

	Control Sample	7 Days PM	14 Days PM	21 Days PM	28Days PM	42 Days PM *
% Water Content CMP (EXPT 1)	70.5	65.48	69.18	71.34	71.24	72.53
% Water Content HLT (EXPT 1)		66.85	70.69	69.03	65.8	73.29
% Water Content CMP (EXPT 2)	71.15	72.51	72.04	71.93	74.82	72.38
% Water Content HLT (EXPT 2)		70.59	71.34	71.63	71.8	72.48
Mean Percent of Water Content (%)	70.83	68.86	70.81	70.98	70.92	72.67
Standard Error	0.33	1.63	0.61	0.66	1.88	0.21

* Data omitted for 35 days PMI as no trotters were collected from EXPT 2 at this interval for comparison with EXPT 1 samples.

Table 3.4: A one-way ANOVA statistical analysis of the mean percent water content for samples collected from both CMP and HLT at weekly intervals. The test illustrates that there are no significant differences in the mean water content for PM cartilage samples as PMI increases (Microsoft Excel 2010).

SUMMARY

Groups	Count	Average	Variance
Control Sample	2	70.83	0.21
7 Days PM	4	68.86	10.59
14 ($+2_{EXPT\ 3}$) Days PM	4	70.81	1.49
21 Days PM	4	70.98	1.76
28 ($+2_{EXPT\ 2}$) Days PM	4	70.92	14.10
42 Days PM	4	72.67	0.17

ANOVA

Source of Variation	Sum of Squares	Degrees of Freedom	Mean Square	F	P-value	F crit
Between Groups	29.25	5	5.85	1.11	0.40	2.85
Within Groups	84.55	16	5.28			
Total	113.79	21				

Table 3.5: Statistics showing the pooled calculated mean percent water content for PM cartilage samples collected from the CMP and HLT burial plots at each weekly PMI (experimental replicates = 2). The grand mean for each burial site, as well as the corresponding skew values are shown (Microsoft Excel 2010).

Experiments 1 & 2	7 Days PM	14 (+2$_{EXPT\ 3}$) Days PM	21 Days PM	28 (+2$_{EXPT\ 2}$) Days PM	42 Days PM	Grand Mean	Skew
Mean % Water Content for Compton	68.99	70.61	71.63	73.03	72.46	**71.34**	**-0.74**
Mean % Water Content for Hilton	68.72	71.01	70.33	68.80	72.88	**70.35**	**0.69**

Table 3.6: Paired samples T-test illustrating the statistics and significance of differences between the mean percent water content for PM cartilage samples obtained for samples collected from CMP and HLT burial plots at weekly PMI (SPSS v. 20).

PAIRED SAMPLES STATISTICS

		Mean	N*	Standard Error Mean
Pair 1	**Mean % Water for Compton**	70.3480	5	.77124
	Mean % Water for Hilton	71.3440	5	.71589

* N refers to the number of observations

PAIRED SAMPLES T-TEST

		Paired Differences				t	Degrees of Freedom	P-value
		Mean	Standard Error Mean	95% Confidence Interval of the Difference				
				Lower	Upper			
Pair 1	**Mean % Water for Compton** / **Mean % Water for Hilton**	-.99600	.86695	-3.40305	1.41105	-1.149	4	.315

PM samples fell within the range for the mean percentages (68.86% - 72.67%) observed for both comparative experiments (EXPT 1 and EXPT 2). The percent water values obtained for all experimental cartilage samples from EXPT 2 fell within this range of overall means. A one-way ANOVA (Table 3.4) revealed that there were no significant changes in the mean water content of articular cartilage with increasing PMI ($F = 1.11$, $df = 5/16$, $p > 0.05$, $\eta^2 = 0.26$; $F_{critical} = 2.85$).[1]

A two-tailed paired samples t-test evaluated the means obtained for percent water content from weekly PM samples collected from CMP and HLT. No significant difference was observed among the mean water contents for PM cartilage collected from CMP (M = 71.34) and HLT (M = 70.35), t (4) = -1.15, $p > 0.05$, $\eta^2 = 0.51$ (Tables 3.5 and 3.6).[2] Despite increasingly visible signs of progressive decay, especially among cartilage samples collected at later PMIs, the tissue's water content remained relatively stable up to six weeks PM.

3.2 Immunological examination of the extracellular matrix component, aggrecan

3.2.1 Protein extraction

Control cartilage extracts digested with Chondroitinase ABC (Ch'ABC) enzymes were subjected to SDS-PAGE using low percentage gels (9% and 10%). These gels were stained with Coomassie Blue Brilliant R (Triple Red Laboratory Technology, UK) to examine CRP patterns for porcine. Numerous CRPs were detected.

---

[1] F – Observed value; df – Degrees of freedom (between and within; df_B/df_W) where df_B represents the degrees of freedom between the observed populations and df_W, the degrees of freedom within each of the groups observed; p – Significance level; η^2 – Effect size. The measure of strength of relationship; $F_{critical}$ – The factor used to compute the margin of error.

[2] M – Mean; t (df) – Observed t value.

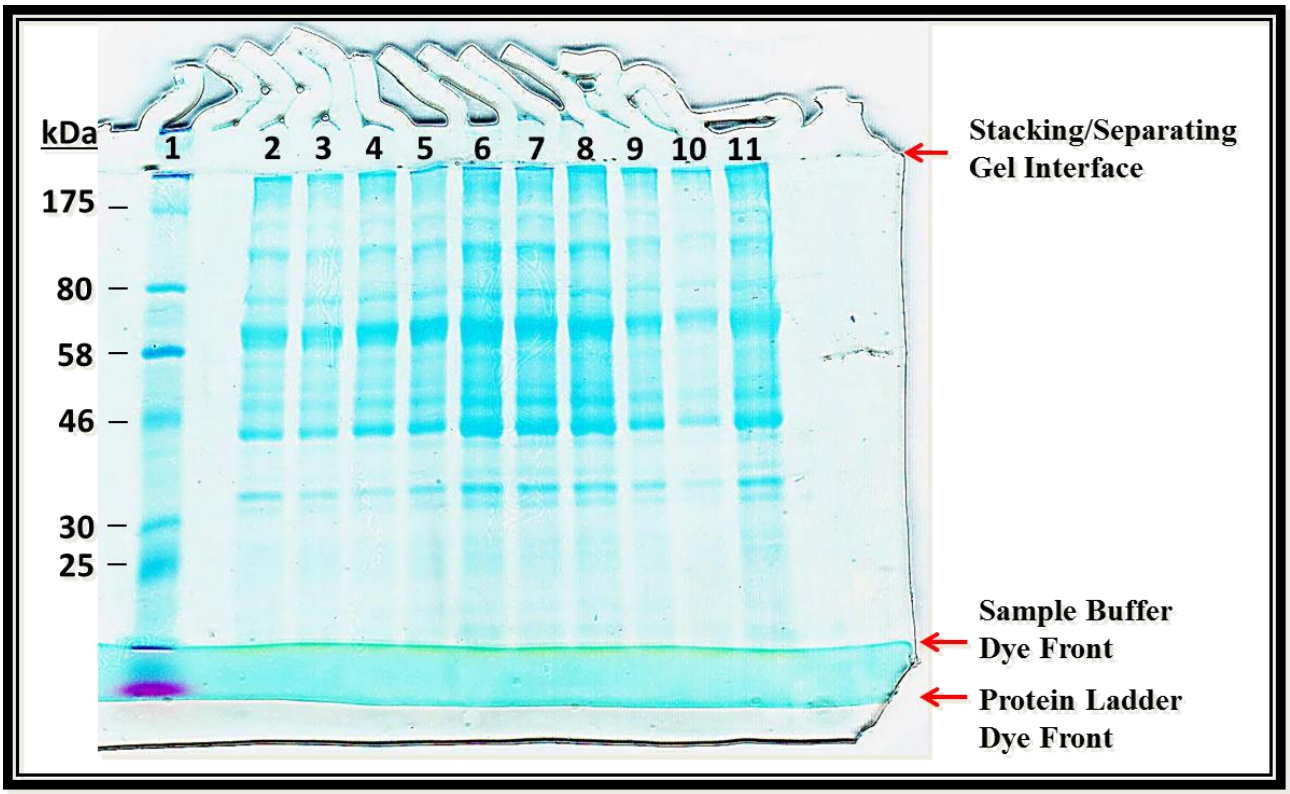

Figure 3.3 Coomassie stained SDS-PAGE gel illustrating the intensities of cartilage protein extracts conducted on samples excised from two random trotters. Protein extractions were carried out for 8, 16, 24, 40 and 48 hours. Lane 1 – Protein marker (7-175kDa); Lane 2 – Trotter 1, 8-hours extraction; Lane 3 – Trotter 2, 8-hours extraction; Lane 4 – Trotter 1, 16-hours extraction; Lane 5 – Trotter 2, 16-hours extraction; Lane 6 – Trotter 1, 24-hours extraction; Lane 7 – Trotter 2, 24-hours extraction; Lane 8 – Trotter 1, 40-hours extraction; Lane 9 – Trotter 2, 40-hours extraction: Lane 10 – Trotter 1. 48-hours extraction: Lane 11 – Trotter 2. 48-hours extraction.

Determining the time frame for which optimal protein extraction was achieved involved cartilage extracts collected from two control trotters of unknown specimen origin/sample. Samples extracted for 8, 16, 24, 40 and 48 hours illustrated the most intense CRPs among samples extracted for a minimum of 24 hours (Figure 3.3). Therefore, all cartilage samples underwent PG extraction for 24-hours.

3.2.2 Western blot analysis of fresh control samples

Fresh control samples of porcine articular cartilage were obtained from five forelimbs dismembered from five different pigs 3-4 hours after slaughter. Samples were processed to determine whether inter-individual variation occurred among tissue samples collected from different pigs. Isolated protein samples were treated with MAb 2-B-6 for the detection of aggrecan core protein, the major subunit of the PG monomer (sections 2.4 and 2.4.1). Cross reactive polypeptides (CRPs) (the term "CRP" will be used in reference to immunodetected polypeptides made visible by cross-reaction with a specified monoclonal antibody and HRP chemiluminescence solutions) were observed indicating positive cross-reactivity between the monoclonal antibody and porcine aggrecan extracts. Figure 3.4 shows little inter-individual variation among control porcine cartilage samples. The control samples generated images of high molecular weight CRPs greater than 175kDa and are representative of whole, deglycosylated core proteins. Aggrecan core proteins stripped of their polysaccharide side-chains possess a molecular weight of approximately 230kDa [45, 46, 47]. Between the 175kDa and 80kDa marks, four lower molecular weight CRPs that successively faded were observed. These CRPs were accompanied by a CRP at approximately 50kDa and an intense CRP situated around 38kDa (Figure 3.3).

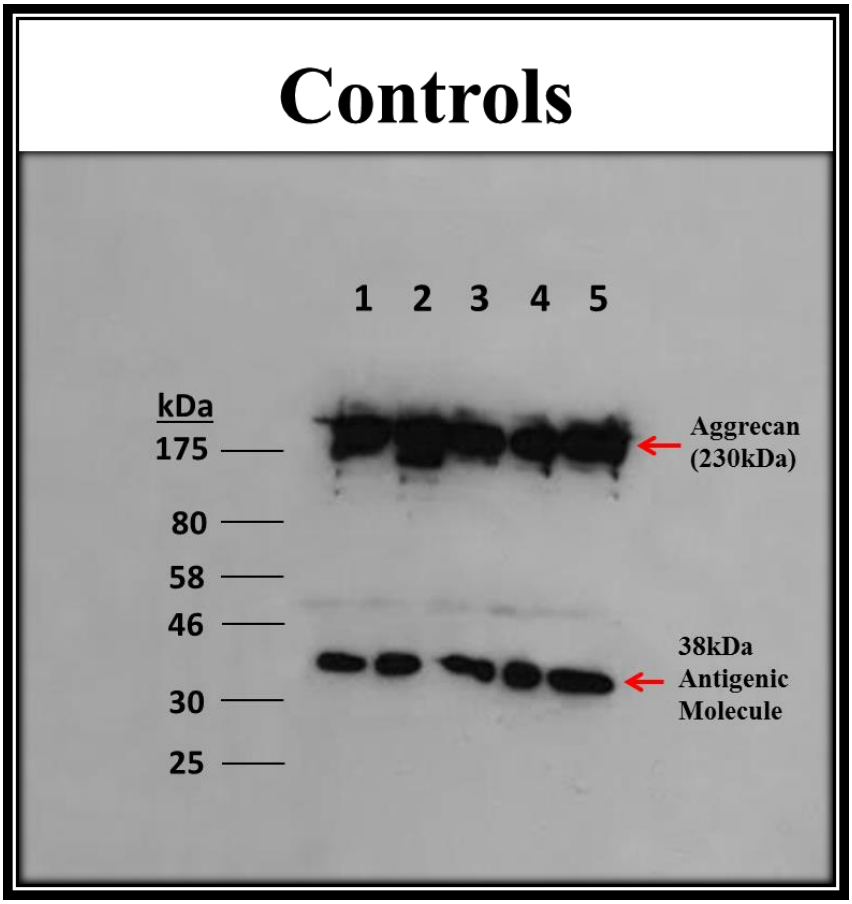

Figure 3.4 Control cartilage obtained from the forelimbs of five randomly selected pigs for the evaluation of inter-individual variation. Protein samples (20µg) were separated using a 9% polyacrylamide gel and then transferred to PVDF membranes by Western blotting. Membranes were probed with MAb 2-B-6 and treated with HRP chemiluminescence. Lane 1 – Control 1; Lane 2 – Control 2; Lane 3 – Control 3; Lane 4 – Control 4; Lane 5 – Control 5.

3.2.3 Digested versus undigested cartilage samples

To verify the images obtained for control samples 1-5 (Figure 3.4) were valid MAb 2-B-6 cross-reactions with the C-4-S neoepitopes (C-4-S stubs), protein extracts for control samples 1-5 were untreated with Ch'ABC enzymes prior to Western blot analysis. No CRPs were visible around the 230kDa, 50kda and 38kDa marks (Figure 3.5a) as was previously seen among control samples 1-5 digested with Ch'ABC (Figure 3.4). Experimental samples were compared against cartilage protein extracted from Control 1 trotter treated (+ Ch'ABC) and untreated (– Ch'ABC) with chondroitin sulphate (CS) digestive enzymes (Figure 3.5b). A MAb 2-B-6 CRP was present for the + Ch'ABC protein extract however, no lower molecular weight CRPs were seen beyond 230kDa as presented in Figure 3.4. The appearance and disappearance of these lower molecular weight CRPs will be considered further in the discussion section. The – Ch'ABC sample for the same cartilage protein extract did not display any observable CRPs.

3.2.4 Short-term burial of trotters

Cartilage protein extracts taken from trotters disinterred daily for seven days (EXPT 3) were electrophoresed using an 8-18% gradient gel (refer to Table A.3 in the Appendix for ADDs). A Western blot of samples one to seven days PM presented 230kDa CRPs for aggrecan core protein made visible by immunodection with MAb 2-B-6 (Figure 3.6). The length of these CRPs extend below 175kDa and are likely composed of several smaller protein as seen amongst the control samples in Figure 3.4. No notable differences were observed in the day-to-day degradation patterns for aggrecan core protein and no CRPs were present at 38kDa.

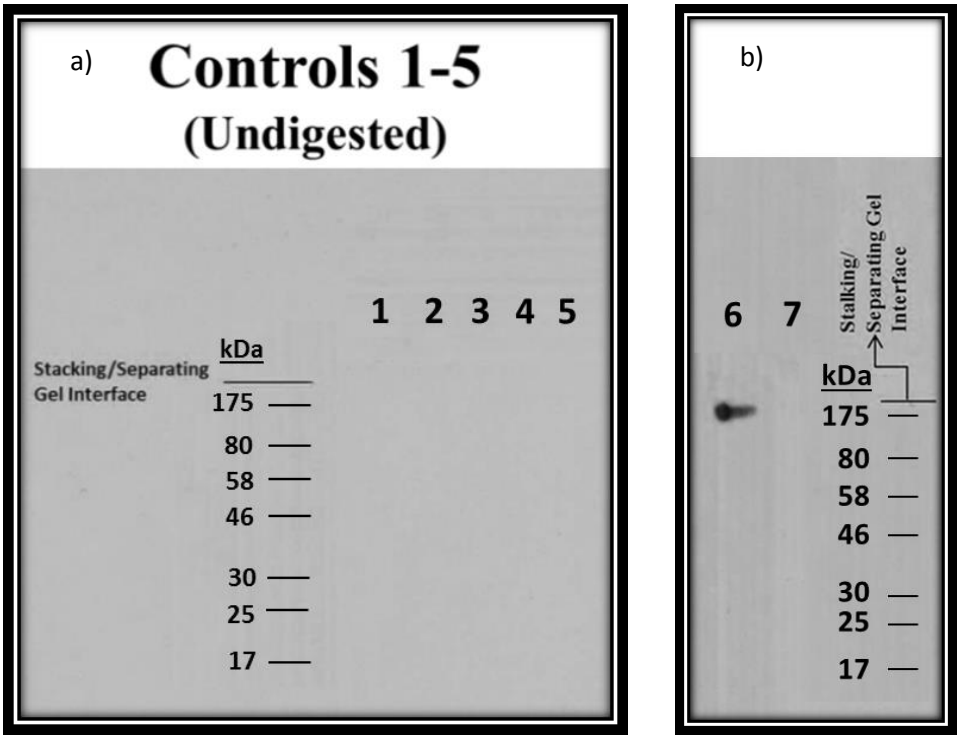

Figure 3.5 Western blot images of aggrecan a) untreated with chondroitinase ABC (Lane 1 – Control 1; Lane 2 – Control 2; Lane 3 – Control 3; Lane 4 – Control 4; Lane 5 – Control 5) compared with b) digested (+Ch'ABC – Lane 6) and undigested (-Ch'ABC – Lane 7) Control 1 samples. Each sample contained 20µg of protein and were ran on 10% polyacrylamide gels.

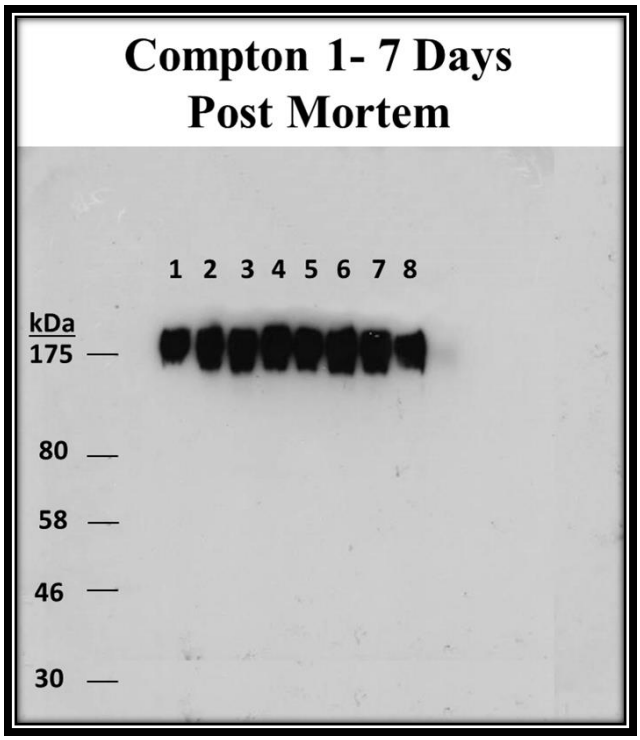

Figure 3.6 Western blot of aggrecan degradation for cartilage samples collected from trotters disinterred daily for a period of 7 days. Each sample of Ch'ABC digested cartilage contains 20ug of protein. Samples were separated on an 8-18% gradient gel and transferred to PVDF membrane. Immunodetection was performed with MAb 2-B-6 (mouse IGg) and HRP chemiluminescence. Lane 1 – Control (0 days PM); Lane 2 – 1 day PM; Lane 3 – 2 days PM; Lane 4 – 3 days PM; Lane 5 – 4 days PM; Lane 6 – 5 days PM; Lane 7 – 6 days PM; Lane 8 – 7 days PM.

3.2.5 Comparative Western blot analyses of post mortem cartilage interred in Compton and Hilton soil environments

Comparative analyses of PM samples collected from CMP and HLT soil environments were conducted during the spring (EXPT 1 – March 28-May 10) and summer (EXPT 2 – June 20-August 2) of 2011. For a period of six weeks, pairs of trotters were disinterred weekly from each burial plot. Their physical state at the time of disinterment, and upon removal of residual soil prior to dissection, was recorded. In general, the skin of decaying trotters thinned while muscle tissues and tendons gradually became frail and liquefied. These changes were most apparent at 30 days PM. At this PMI, skin was quite delicate and vulnerable to tearing upon handling, or exhibited breaks in areas surrounding the joints. Muscles and tendons were typically much softer at 30 days PM and exhibited signs of liquefaction in comparison with trotters disinterred 7-21 days PM.

Cartilage samples buried in CMP and HLT soil environments during the spring (EXPT 1) showed slight differences in appearance for control and PM protein CRPs representing aggrecan. For samples collected from CMP, intense CRPs of aggrecan weighing 230kDa were consistently present for control and experimental samples up to 21 days PM (Figures 3.7a). Aggrecan CRPs (230kDa) were much more intense for samples collected at seven and 14 days PM compared to the corresponding control sample (0 days PM). The 230kDa CRP situated at 14 days PM had extended further down the gel than the CRP representing 7 days PM. Samples 21 days PM presented a less intense CRP around 230kDa and were accompanied by a couple of densely packed, thinner CRPs weighing between 230kDa and 170kDa. Less intense CRPs approximating 130kDa and 93kDa were also present at this PMI. CRPs weighing approximately 38kDa were present among samples 7-21 days PM. This CRP was absent for the control sample.

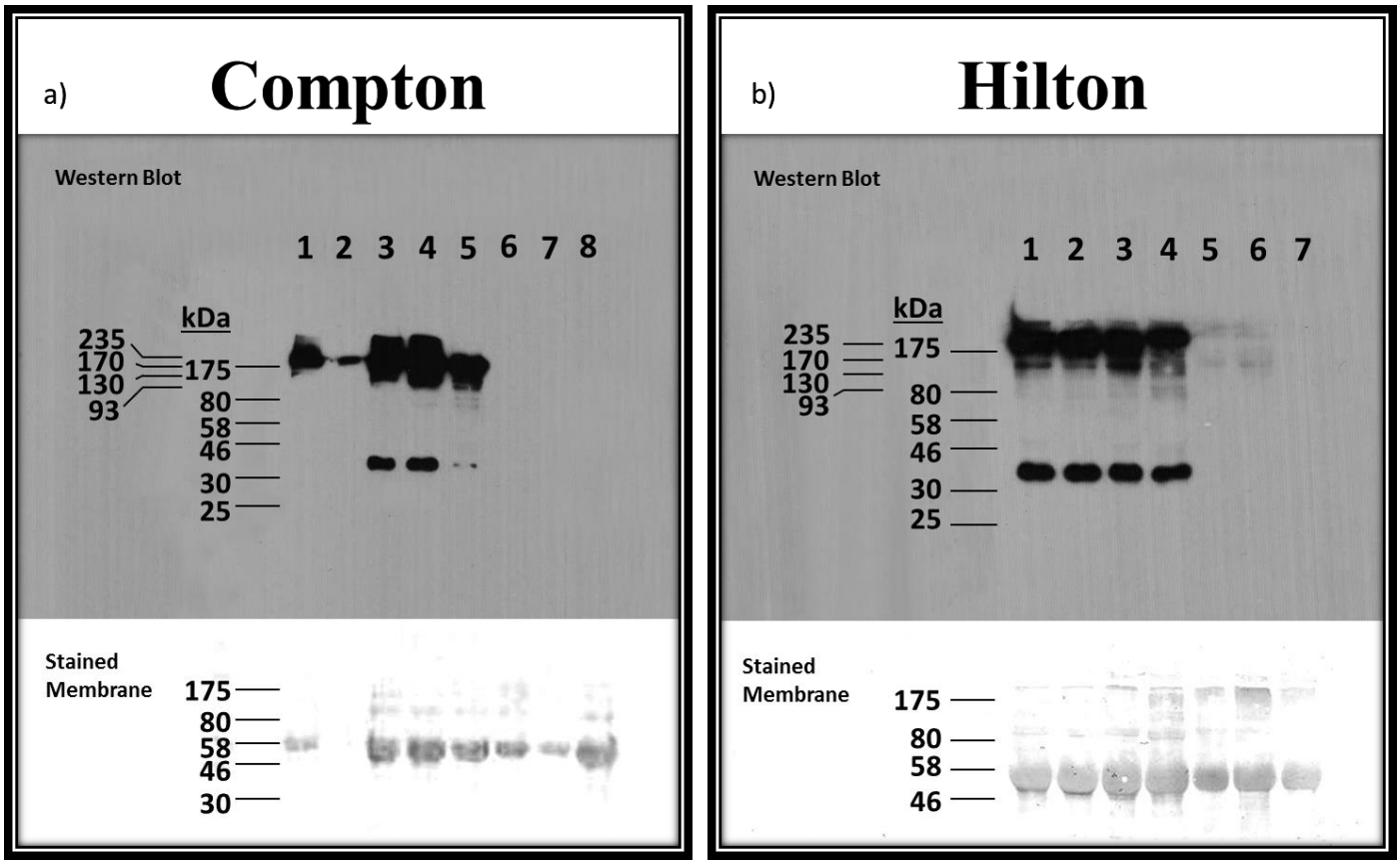

Figure 3.7 EXPT 1 - Comparative analysis of a) CMP and b) HLT aggrecan protein gathered from samples collected during spring 2011. Each PM sample contained approximately 20µg of protein and were electrophoresed on 10% polyacrylamide gels. Western blots underwent immunodetection for aggrecan using MAb 2-B-6. Aggrecan (~230 kDa) is seen up to 21 days PM for samples collected from both CMP and HLT burial plots. Stained membranes illustrate the amount of sample protein loaded. A) Lane 1 – Control (0 days PM); Lane 2 – spillage of protein from Lane 1; Lane 3 – 7 days PM; Lane 4 – 14 days PM; Lane 5 – 21 days PM; Lane 6 – 30 days PM; Lane 7 – 36 days PM; Lane 8 – 42 days PM). B) Lane 1 – Control (0 days PM); Lane 2 – 7 days PM; Lane 3 – 14 days

PM trotters disinterred from HLT presented 230kDa CRPs representative of aggrecan for up to 21 days PM (Figure 3.7b). Additional CRPs of various molecular weights were also discernible between 175kDa and 58kDa. These CRPs showed incremental changes in heterogeneity and intensity (Figure 3.7b); with increasing PMI, aggrecan molecules showed continued reduction to lower molecular weight by-products gradually extending towards the 58kDa mark. Samples 0, 7 and 14 days PM exhibited 230kDa CRPs bearing the greatest antibody-binding properties with a distinct CRP weighing approximately 160kDa. At 14 days PM, this CRP appeared more intense than earlier PM samples. Aggrecan CRPs (230kDa) and degradation gradients situated between 175-58kDa showed the same PM trend for intensity. At 21 days PM, the 230kDa CRP is notably less intense and additional degradation CRPs of aggrecan core protein emerge between 230-70kDa (Figure 3.7b). The intensity of these CRPs diminishes with increasingly lower molecular weight fragments.

As PMI increased, so did the number and intensity of visible aggrecan by-products between 230kDa-70kDa for PM samples collected from CMP and HLT. Samples disinterred from HLT presented degradation CRPs that were well discernible in comparison with samples collected from CMP (Figure 3.7 a and b). For both soil environments, samples collected 7-21 days PM during the spring (EXPT 1) illustrated core protein fragments that intensified with increasing PMI and was most pronounced for samples collected at 21 days PM. A prominent reduction in the intensity/amount of intact aggrecan molecules (~230kDa) to lower molecular weight CRPs of increasing intensity was observed at this PMI. For control and PM samples collected from CMP and HLT, no additional aggrecan degradation by-products were observed beyond those situated at the 38kDa mark. Results obtained for both soil environments were reproducible.

Comparative analyses of PM samples from CMP and HLT soil environments during the summer of 2011 (EXPT 2 – June 20-July 2) yielded similar results as those obtained for

PM samples collected earlier in the spring. Aggrecan remained present up to 21 days PM and did not appear for samples collected 30-42 days PM (Figure 3.8). Distinct CRPs with molecular weights approximating 230kDa and 38kDa were present for samples collected from both soil environments. Unlike control cartilage (0 days PM) extracted for CMP EXPT 1 which did not display a MAb 2-B-6 CRP at 38kDa, this CRP was present for control collected for CMP EXPT 2.

EXPT 2 samples from CMP showed distinct CRPs at 230kDa and 38kDa for specimens 0-21 days PM (Figure 3.8a). A degradation gradient of far less intensity was observed between 230kDa and70kDa. PM samples from HLT also presented Western blot images of CRPs weighting 230kDa for up to 21 days PM (Figure 3.8b). CRPs at 230kDa showed successive lengthening across samples 0-14 days PM. At 21 days PM, the intensity of this CRP was notably reduced and accompanied by the development of faintly emerging CRPs situated between 230kDa and 70kDa. Gradients of degradation by-products situated between 230kDa and 70kDa for samples 0-21 days PM gradually extended towards the 70kDa mark and intensified with increasing PMI (Figure 3.8b). The observed trends for this experiment (HLT) are consistent with those seen among Western blot images for CMP and HLT of EXPT 1 (Figure 3.7).

The Western blot for CMP EXPT 2 PM samples presented a slightly different image where the 230kDa CRPs highlighting aggrecan successively thinned with increasing PMI and the antigenic molecule of protein situated at 38kDa increased in intensity for samples collected 0-14 days PM (Figure 3.8a). At 21 days PM, this CRP was notably thinner for PM samples 7 and 14 days old. However, at this PMI a gradient of decomposed aggrecan core protein was faintly seen between 230kDa and 70kDa.

Western blot images of PM cartilage samples collected from CMP and HLT burial sites during the spring (Figure 3.7) and summer (Figure 3.8) periods displayed MAb 2-B-6

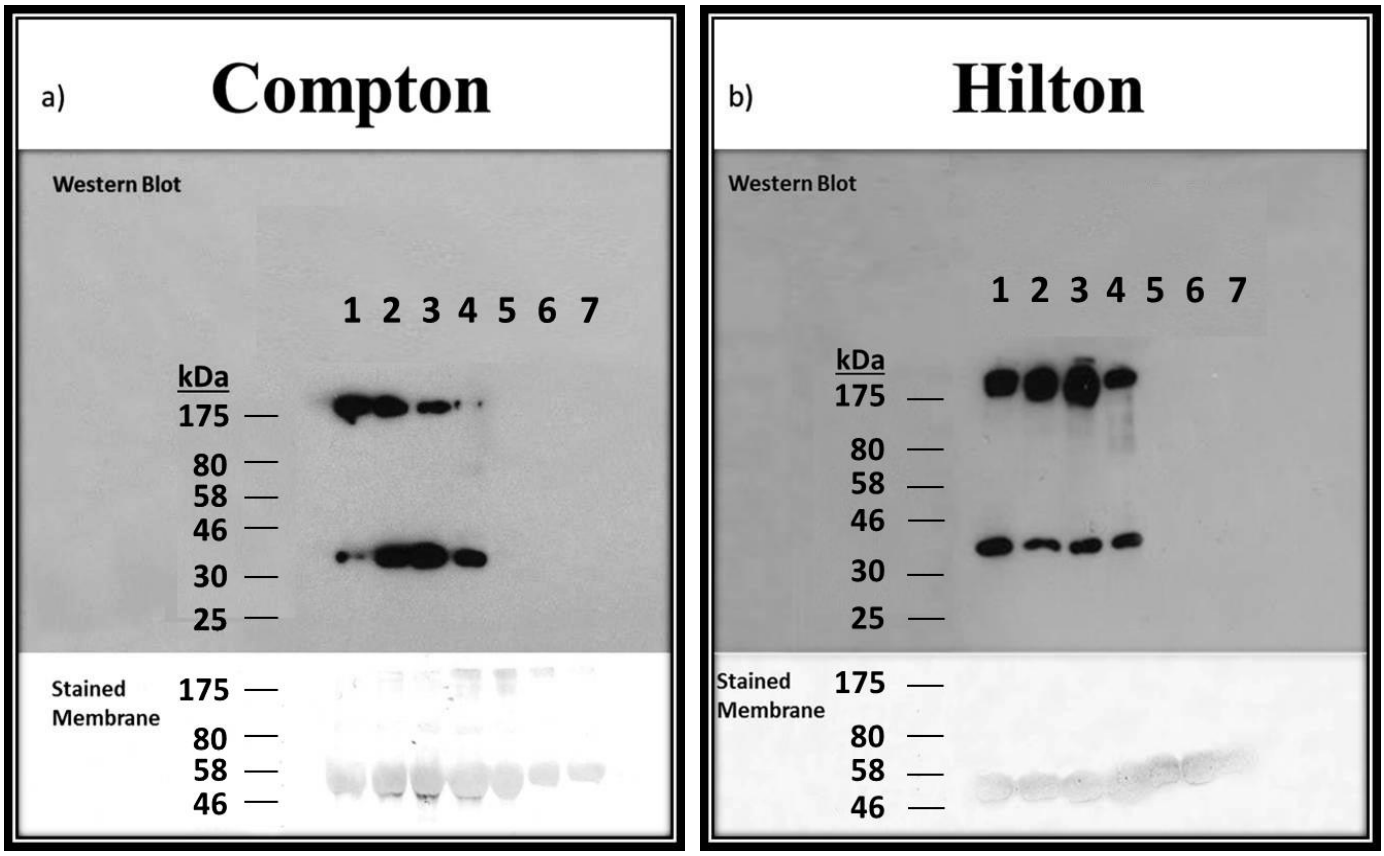

Figure 3.8 EXPT 2 – Comparative analysis of a) CMP and b) HLT 230kDa CRPs gathered from samples disinterred during the summer of 2011. Roughly 20µg of cartilage protein were run on 10% polyacrylamide gels. Aggrecan was detected using MAb 2-B-6 and can be seen up to 21 days PM for samples collected from both sites. Stained membranes show the amount of protein samples loaded. Images a) CMP and b) HLT: Lane 1 – Control (0 days PM); Lane 2 – 7 days PM; Lane 3 – 14 days PM; Lane 4 – 21 days PM; Lane 5 – 30 days PM; Lane 6 – 36 days PM; Lane 7 – 42 days PM.

CRPs with molecular weights approximating 230kDa and 38kDa. Both CRPs were present for control and experimental samples for up to 21 days, with the exception of the control sample collected at 0 days PM from CMP during the spring (Figure 3.7a). This pattern is in agreement with those seen among the five test control samples in Figure 3.4. For samples extracted at PMIs of 30-42 days, 230kDa CRPs were virtually unseen.

In general, PM samples collected at 21 days from both soil environments during the spring and summer of 2011 presented aggrecan CRPs at 230kDa that were less intense than samples collected at earlier PMIs (Figures 3.7 and 3.8). At this PMI, a less intense CRP weighing 230kDa was accompanied by notably more and intense lower molecular weight subpopulations of MAb 2-B-6 immunoreactive by-products that closely approached 70kDa in comparison to samples collected 0-14 days PM. The CRPs located at 38kDa for 21 days PM were also notably less intense than those seen for samples collected at 7 and 14 days PM (Figures 3.7a and 3.8a). However, the intensity of the CRPs for PM samples disinterred from HLT (EXPT 1) remained relatively unchanged for each PMI (Figures 3.7b and 3.8b). Furthermore, no degradation by-products were observed below the antigenic molecules situated at 38kDa for samples collected from soil environments 1 and 2 (Figures 3.7 and 3.8).

3.2.6 Narrowing the PMI at which relative levels of aggrecan protein become diminished

Six pairs of trotters were interred at HLT from September 17, 2012 to October 19, 2012 (EXPT 4). Their disinterment occurred at weekly intervals for 21 PM days and biweekly thereafter. The ADDs are listed in Table A.4 of the Appendix. CRPs weighing 230kDa were visibly detected with HRP chemiluminescence for cartilage samples 0-28 days PM (Figure 3.9). The intensity of these CRPs successively increased for samples 0, 7 and 14 days PM. At 21 days PM, the intensity of the 230kDa CRP was considerably diminished in

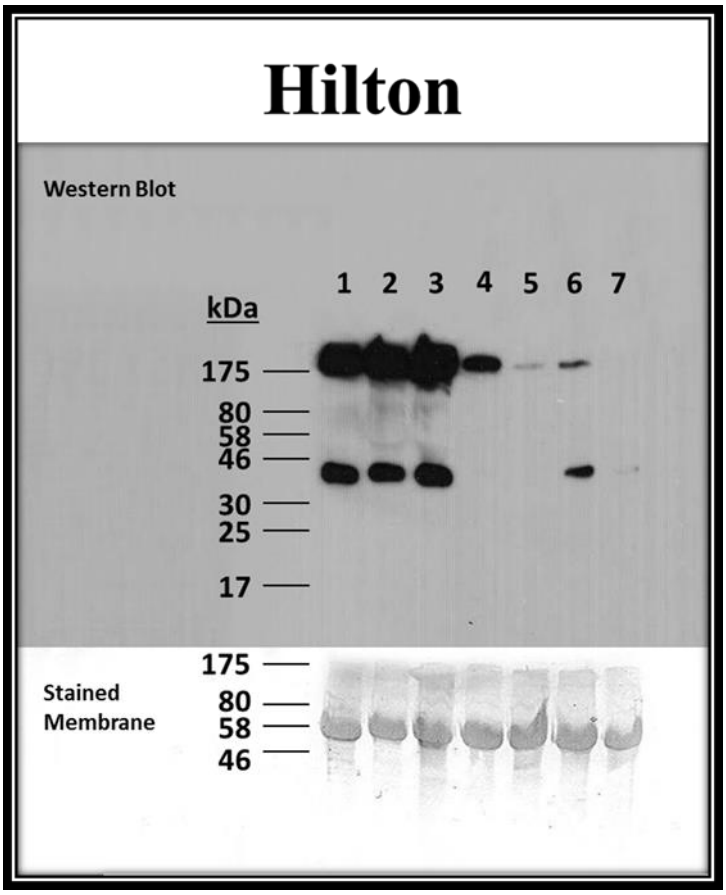

Figure 3.9 EXPT 4 – Western blot of PM cartilage extracts (20µg protein, 10% polyacrylamide gel) collected weekly up to 21 days PM and biweekly thereafter up t 32 days PM (September to October 2012) to determine whether aggrecan was n longer detectable between 21 and 28 days PM. Unlike previous experiments wher the 230kDa CRPs were undectable after 21 days PM, CRPs were detected until 28 day PM. Lane 1 – Control (0 days PM); Lane 2 – 7 days PM; Lane 3 – 14 days PM; Lane 4 21 days PM; Lane 5 – 24 days PM; Lane 6 – 28 days PM; Lane 7 – 32 days PM.

comparison to the CRP for control (0 days PM). The 230kDa CRP seen at 24 days PM was notably less intense than that at 21 days PM. However, the 230kDa CRP was seen at 28 days. The faint emergence of distinct MAb 2-B-6 degraded CRPs situated between 230kDa and 70kDa were first seen at 7 days PM and intensified for protein extracts 14 days PM (Figure 3.9). These degraded CRPs are absent for samples 21 days PM and beyond. The CRP located at 38kDa was present for samples 0-14 and 28 days PM, but absent for protein extracts collected 21, 24 and 32 days PM. The CRP representing this molecule was notably less intense at 28 days PM than samples collected 0-14 days PM. The intensity of the CRPs for PM samples collected 0-14 days PM appeared uniform. No breaks were observed among the skin of trotters disinterred at 21 days PM. At a PMI of 24 days, the skin was notably thinner and exhibited visible breaks around several joints (Figure 3.10). Cartilage samples extracted from trotters collected at this PMI presented a single thin CRP at 230kDa that emitted a very weak signal. On the contrary, the skin of the trotters disinterred at 28 days PM was not as thin as that belonging to trotters disinterred at 24 days. Furthermore, trotters disinterred at 28 days PM showed little disruptions across the skin surfaces and did not occur in close proximity to the joints. Therefore, no joints were exposed to the soil environment. The physical state of trotters disinterred at 32 days PM was marked by extremely thin skin with large, penetrating breaks across the MCP/MTP joint interface that resulted in joint exposure to the soil environment (Figure 3.10).

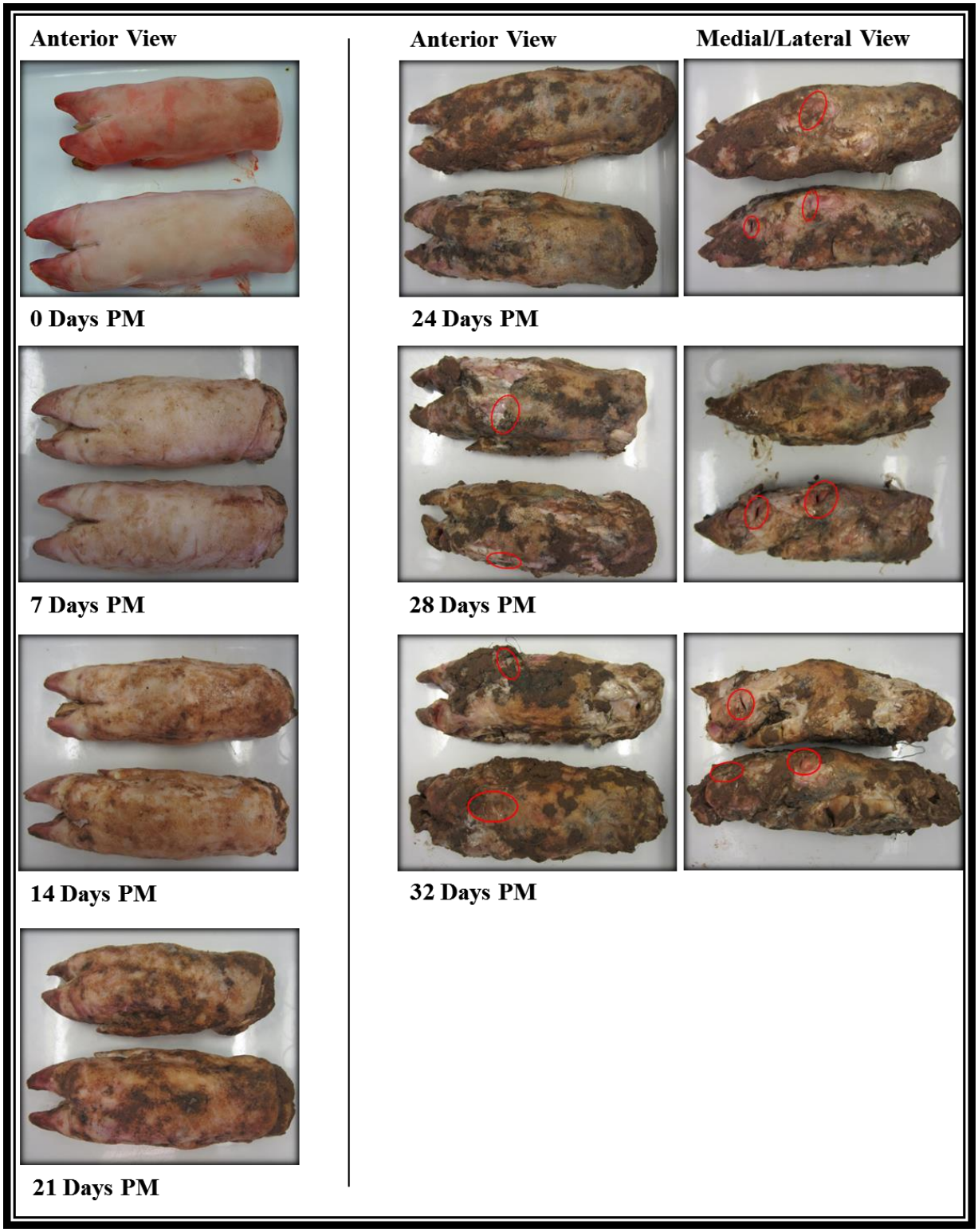

Figure 3.10 EXPT 4 – The physical state of PM trotters disinterred weekly (0-21 days PM) and bi-weekly (24-32 days PM) from September 17 to October 19, 2012. The skin and flesh of PM trotters remained fully intact for up to 21 days. Trotters disinterred 24-32 days PM, presented breaks in the skin exposing the joints to the immediate soil environment and are highlighted by red circles.

3.2.7 The effects of temperature upon the degradation of aggrecan

The appearance of CRPs beyond 21 days PM, as seen among EXPT 4 PM samples (Figure 3.9), prompted an inquiry regarding the influences of temperature on the decompositional process of cartilage. The overall average ambient temperature for the time period which these trotters were buried was 10.5˚C (a mean of 13.6˚C high and 6.7˚C low). EXPT 5 was conducted with six pairs of trotters that were interred from October 8, 2012 to November 19, 2012. Disinterments occurred at weekly intervals. During the time frame that the trotters remained below ground, the average ambient temperature was 6.9˚C (high: 14.5˚C, low: -0.7˚C). Table A.5 in the Appendix provides the ADDs experienced by EXPT 5 trotters.

Unlike the results obtained for the comparative analyses conducted during the spring and summer of 2011 (EXPT 1 and EXPT 2), CRPs of aggrecan situated at 230kDa were present for up to 35 days PM for EXPT 5 (Figure 3.11). CRPs for samples 0-15 days PM were the most intense whereas CRPs for samples 22-42 days PM were much less intense. The 230kDa CRP at 22 days PM was slightly more intense than that for 35 days PM. The latter, in turn, was more intense than samples extracted at 29 days PM. At 38kDa, the antigenic glycopolypeptide was intensely seen at 8 days PM and less so at 0 and 15-42 days PM. Both 230kDa and 38kDa CRPs were the least intense for cartilage samples extracted at 42 days PM.

Trotters disinterred at 8 and 15 days PM were deemed well preserved. They remained fully intact, exhibiting skin, muscle tissue and tendons that remained as robust as trotters observed at 0 days PM. No breaks were noted along the surfaces of their skin. In contrast with previous PM experiments, trotters disinterred at 22 days PM presented skin and muscle tissues that were notably thinner with breaks around and through the MCP/MTP and phalangeal joints.

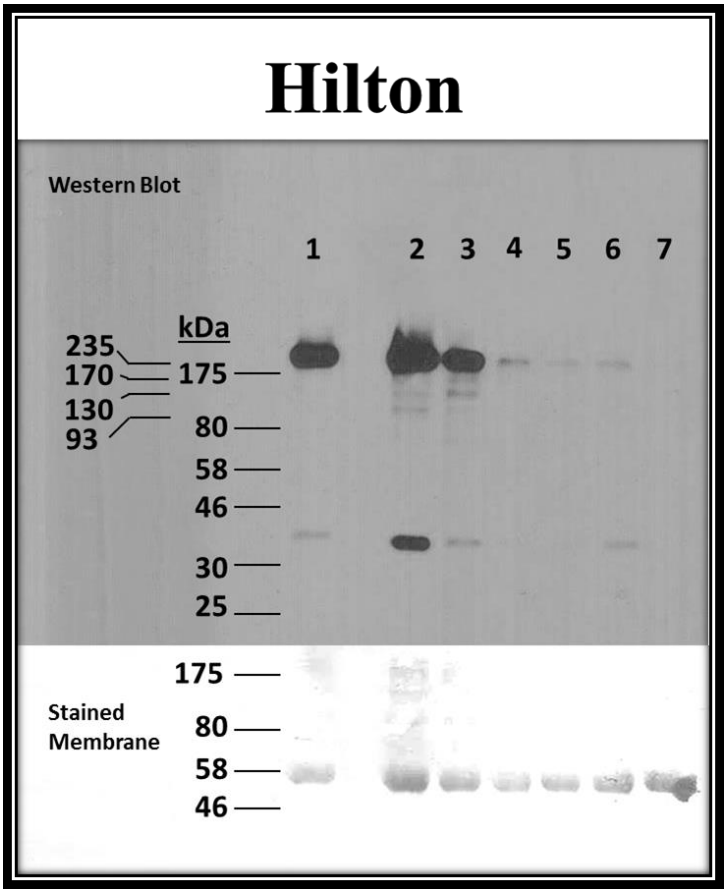

Figure 3.11 EXPT 5 – Cartilage extracts from PM samples collected from October t Novemer 2012. Cooler ambient temperatures resulted in the presence of 230kD CRPs seen beyond 21 days PM. Less intense CRPs are visible for cartilage sample collected 22-35 days PM. Lane 1 – Control (0 days PM); Lane 2 – 8 days PM; Lane 3 15 days PM; Lane 4 – 22 days days PM; Lane 5 – 29 days PM; Lane 6 – 35 days PM Lane 7 - 42 days PM.

3.2.8 Mummified and water submerged trotters: Investigating the effects of different environments on aggrecan degradation

EXPT 6 trotters were placed in a greenhouse and left to decay in open air and in tanks containing tap water or simulated sea water. By 12 days PM, trotters left exposed to the air had mummified resulting in the complete desiccation of soft tissues. Therefore, trotters were soaked in water for approximately one hour before attempting dissection. No visible lacerations were found along the surface of the skin and no joints were exposed to the external environment. Insect colonisation, in the form of maggots, was present after tissue rehydration.

Water submersed trotters were left in their respective tap and simulated sea water tanks for 35 days. These trotters had developed a very strong and putrid odour, as well as a thin layer of adipocere. The trotters were still fairly robust and did not present any breaks in the skin. Therefore, no joints were exposed to the immediate water environments.

Dissection of the MCP/MTP joints of air exposed trotters at 12 days PM presented cartilage that was as white in colour and robust as control cartilage. Trotters submerged in tap water and simulated sea water for 35 PM days exhibited cartilage that was light pink and maintained a rigid structure, although not as rigid as samples extracted at 0 days PM.

Western blot images of MAb 2-B-6 CRPs were seen for control (0 days PM), mummified (12 days PM), tap water and simulated sea water submerged specimens (35 days PM) (Figure 3.12). CRPs weighing 230kDa were clearly visible for control, mummified and tap water submerged specimens. The 230kDa CRP was absent for cartilage samples extracted from trotters submerged in simulated sea water. This CRP was most intense for control and air exposed (12 days PM) samples, especially for cartilage removed from mummified trotters which presented a slightly more intense CRP than the control. For tap water submerged trotters, the 230kDa CRP was notably less intense than that representing

control and air exposed trotters, yet comparatively more intense than CRPs seen for samples previously collected at 35 days PM from CMP and HLT soil environments (EXPT 1, 2, 4 and 5; Figures 3.7-3.9 and 3.11). The 38kDa CRP was observed among control, air exposed and tap water submerged cartilage extracts. For each of these PM sample, the relative intensity of this CRP followed the same trend corresponding to the 230kDa CRP. The 38kDa CRP was most intense for control and mummified trotter extracts, with the latter bearing the greatest intensity, whereas extracts taken from tap water submerged trotters presented a far less intense CRP. No 38kDa CRP was observed for the simulated sea water cartilage extracts. For 35 days PM trotters submerged in tap water and simulated sea water, additional CRPs and degradation gradients were observed between 230kDa and 70kDa as among EXPT 1 and 2 samples 14-21 days PM. The intensity of the CRPs situated between 230kDa and 70kDa decreased in order of reduced molecular weight.

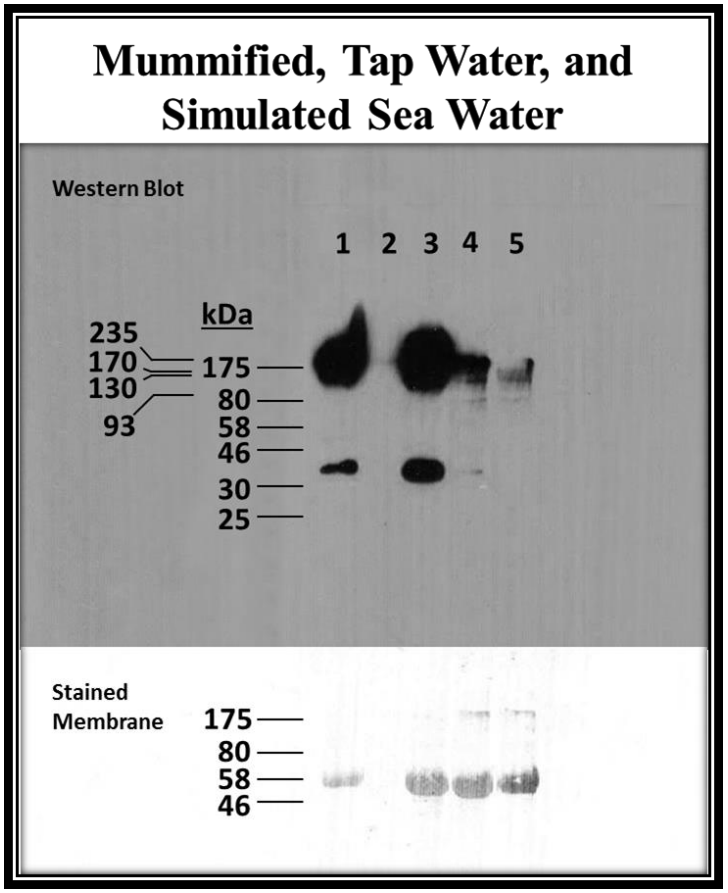

Figure 3.12 EXPT 6 – Trotters exposed to air and water environments (tap water and simulated sea) yielded 230kDa CRPs (20µg of protein loaded per sample; samples ran on 10% polyacrylamide gel). Mummified extracts exhibited the most intense CRP, followed by tap water samples. Simulated sea samples did present a CRP at 230kDa. Lane 1 – Control (0 days PM); Lane 2 – Sample spillage; Lane 3 – Air exposed trotters (12 days PM); Lane 4 – Tap water exposed trotters (35 days PM); Lane 5 – Simulated sea water exposed trotters (35 days PM).

3.3 Cartilage degradation at the cellular level: Investigating the post mortem properties of chondrocytes

3.3.1. Anti-α-Tubulin

The ability for aggrecan molecules to persist long after the catabolic processes of death ensue generated an inquiry about cartilage degradation at the cellular level. With an extremely low cell density in comparison to other tissues of the body, perhaps chondrocyte degradation would mimic the gradual and ordered breakdown witnessed for aggrecan with increasing PMI.

Investigation of PM cartilage was conducted at the cellular level using the monoclonal antibody, anti-α-tubulin. Western blots for protein samples probed with anti-α-tubulin (Sigma, UK) were first performed on 20μg of heat-treated (denatured) and untreated samples of control cartilage (0 days PM) from porcine to determine whether protein samples were immunoreactive and further denatured, thereby enhancing their visualisation. These samples were compared with human glioblastomas (HG) cells (heat-treated), known to positively react with the antibody. Porcine samples positively cross-reacted with the antibody and presented CRPs in line with the 50-58kDa CRPs present for HG (Figure 3.13). These CRPs fell within the expected range for humans (Abeyweera *et al.*, 2009; Herreros *et al.*, 2000; Ley *et al.*, 1994; Raoet *et al.*, 2001).

Western blots of PM cartilage samples collected for EXPT 4 to EXPT 10 (Table 2.1) underwent immunodetection with anti-α-tubulin. PM samples consisted of 40μg of protein from porcine hyaline articular cartilage and 60μg from the fibrous intervertebral cartilage of bovine specimens. Alpha-tubulin CRPs were detected for porcine cartilage extracts and exhibited molecular weights identical to the HG cells (Figures 3.14, 3.15, and 3.19). CRPs for bovine experimental samples were virtually undetected (Figure 3.19).

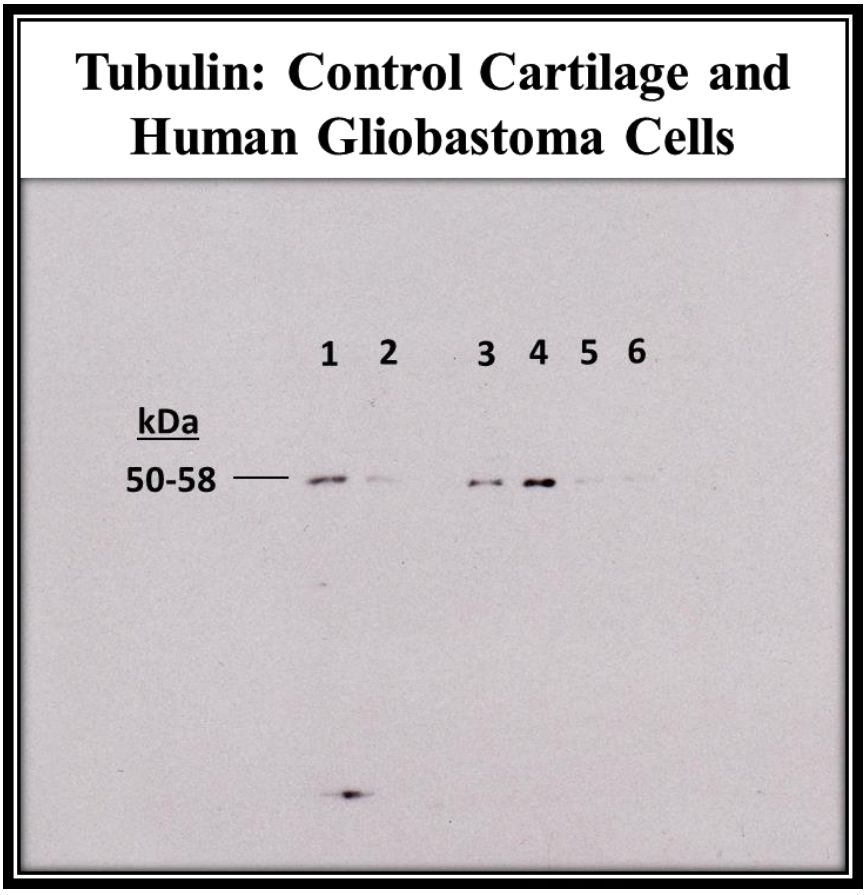

Figure 3.13 A comparison of heated verus non-heated proteoglycan extracts (0 days PM) with control human glioblastoma to test for the cross-reactivity of porcine chondrocytes with anti-α-tubulin. Porcine samples demonstrated CRPs. However, protein extracts further denatured with heat appeared more intense than non-heated extracts. CRPs of porcine tubulin appear in line with the control sample from human. Lane 1 – Heated Control (0 days PM); Lane 2 – Non-heated Control (0 days PM); Lanes 3-6 – Human glioblastoma cells.

A Western blot of EXPT 4 (Table 2.1) PM porcine samples collected from HLT presented CRPs for α-tubulin (Figure 3.14a) when developed. Alpha-tubulin CRPs were present for samples 14-32 day PM (Figure 3.14). No CRPs were detected for control (0 days PM) and 7 days PM samples (Figure 3.14). The stained membrane demonstrated fairly equal loading of protein samples with the exception of the 7 days PM sample that was slightly overloaded.

Unlike the Western blot image obtained for EXPT 4 samples (Figure 3.14), the results obtained for weekly porcine samples collected from HLT for EXPT 5 (Figure 3.15) showed α-tubulin CRPs present for control and experimental samples, 8-42 days PM. CRPs seen at 8 and 15 days PM were less intense than PM samples collected at later intervals. In contrast, the control sample of cartilage protein extract generated an α-tubulin CRP of greatest intensity. The CRP's intensity coincides with the heavily stained membrane-bound proteins that demonstrate an overload of sample buffer when compared with experimental samples showing lighter staining and relatively equal loads of sample buffer.

A series of experimental trotters were interred at HLT over the course of several months to assess cell vitality. These trotters were also utilised for the extraction of PM cartilage to conduct Western blot analyses with the monoclonal antibody, anti-α-tubulin. For EXPT 7, trotters were disinterred weekly from February 11, 2013 to March 27, 2013 (average temperature: 2.5˚C; Table 2.1). Cartilage extracts were collected solely from trotters disinterred 28, 35 and 44 days PM. The resulting Western blot image yielded α-tubulin CRPs for each of the available samples. As PMI increased, the intensity of the 50-58kDa CRPs decreased so that the CRP represented at 44 days PM was dimly seen (Figure 3.16).

Weekly disinterments of EXPT 8 PM samples gathered April 15, 2013 – May 28, 2013 (average temperature: 9.5˚C; Table 2.1) displayed CRPs for α-tubulin from cartilage extracted 22-35 days PM. The α-tubulin CRP for control cartilage (0 days PM) was barely

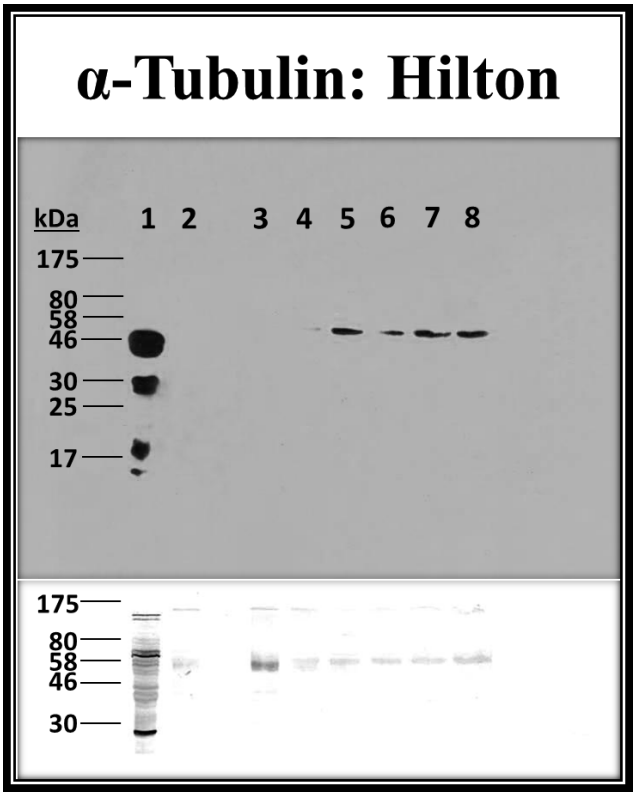

Figure 3.14 EXPT 4 – Human glioblastoma (*HG) (10µg protein) ran alongside 40µg of protein extracted from porcine hyaline cartilage (0, 7, 14, 21, 24, 28 and 32 days PM). Images of α-tubulin CRPs are distinctly present for samples 21 days PM and older, although the CRP begins to make an appearance at 14 days PM. Lane 1 – Human glioblastoma control; Lane 2 – Porcine control (0 days PM); Lane 3 – 7 days PM; Lane 4 – 14 days PM; Lane 5 – 21 days PM; Lane 6 – 24 days PM; Lane 7 – 28 days PM; Lane 8 – 32 days PM.

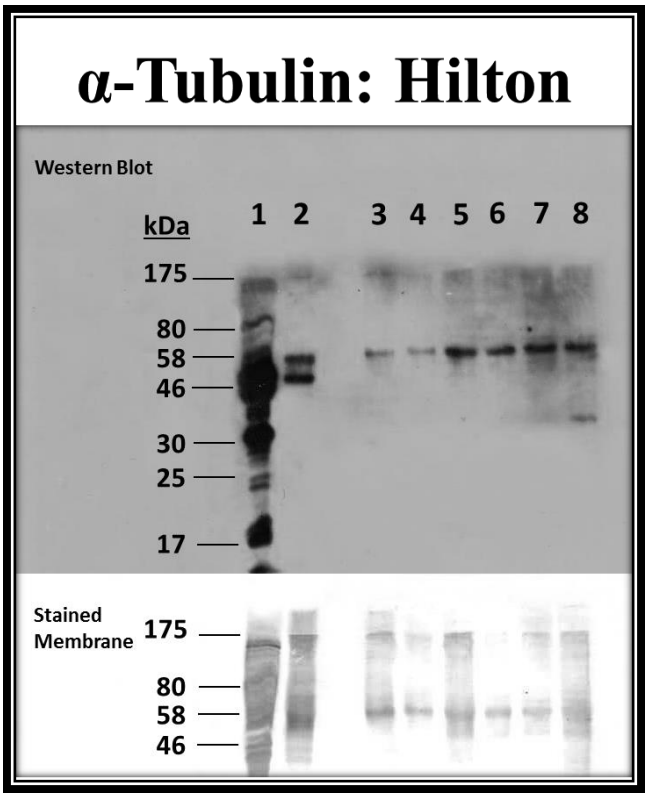

Figure 3.15 EXPT 5 – Alpha-tubulin CRPs are present for samples (40µg protein/sample) collected October 8 – November 19, 2012. CRPs at 8 and 15 days PM are notably less intense in comparison to a clearly visible control and samples obtained 22-42 days PM. The stained membrane below illustrates relatively equal loading of PM samples. Lane 1 – Human glioblastoma control; Lane 2 – Porcine control (0 days PM); Lane 3 – 8 days PM; Lane 4 – 15 days PM; Lane 5 – 22 days PM; Lane 6 – 29 days PM; Lane 7 – 35 days PM; Lane 8 – 42 days PM.

visible. A trace amount of α-tubulin was detected for cartilage extracted 7 days PM. Alpha-tubulin distinctly appeared at 22 days PM. For samples 28 and 35 days PM, these CRPs were darker and of equal intensity. A CRP of less intensity than samples 22 days PM was observed at 43 days PM. Like EXPT 7, no CRP was visible for cartilage samples extracted 14 days PM (Figure 3.17).

A Western blot of EXPT 9 cartilage extracts collected June 3, 2013 to July 15, 2013 (average temperature: 14.5˚C; Table 2.1) yielded α-tubulin CRPs for samples 0-42 days PM. An intense α-tubulin CRP was present for control cartilage (0 days PM). The amount of protein loaded for this sample was in excess of protein loaded for samples 7-42 days PM. This is highlighted by the darkened protein track visible on the stained PVDF membrane (Figure 3.18). For protein extracts collected from cartilage 7 days PM, the α-tubulin CRP was the least intense while samples 14 days PM showed greater intensity. Protein samples 21-42 days PM illustrated α-tubulin CRPs bearing the greatest intensity while maintaining uniformity with increasing PMI (Figure 3.18).

Cartilage extracts collected from PM specimens of bovine vertebrae (EXPT 10; average temperature: 16.0˚C) did not display α-tubulin CRPs for control (0 days PM) and experimental samples (10, 17, 24, and 31 days PM) (Figure 3.19). The total amount of protein loaded for each PM samples was 60μg per 25μl of 1X sample buffer.

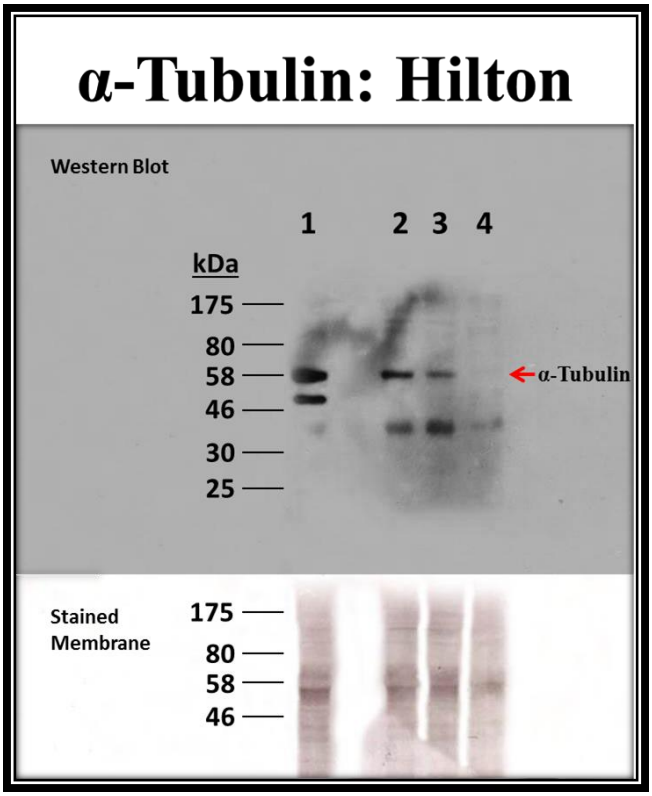

Figure 3.16 EXPT 7 – Cartilage protein extracts (40µg protein/sample) from PM trotters collected 28-44 days PM. The joints of PM trotters remained fully intact and were unexposed to the immediate soil environment. Alpha-tubulin CRPs were seen for control and experimental samples collected at 28 and 35 days PM. AS PMI increased, the intensity of the 50-58kDa CRPs diminished and was barely discernible at 44 days PM. Lane 1 – Porcine control (0 days PM); Lane 2 – 28 days PM; Lane 3 – 35 days PM; Lane 4 – 44 days PM.

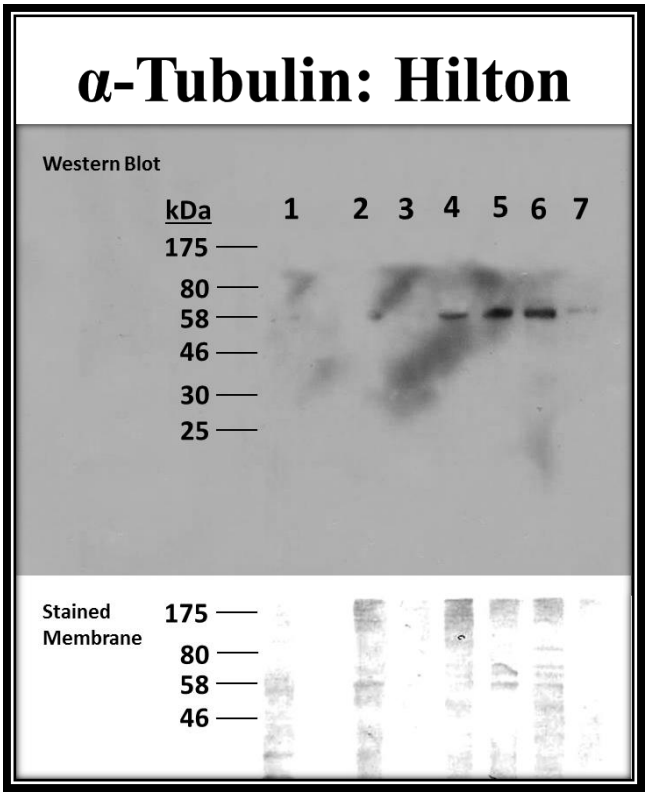

Figure 3.17 EXPT 8 – PM cartilage extracts (40µg protein/sample) were acquired from trotters disinterred April 15 – May 28, 2013 and displayed α-tubulin CRPs for cartilage samples 22, 28, 35 and 42 days PM. The trace of a CRP can be seen for samples gathered at 7 days PM. Lane 1 – Porcine control (0 days PM); Lane 2 – 7 days PM; Lane 3 – 14 days PM; Lane 4 – 22 days PM; Lane 5 - 28 days PM; Lane 6 – 35 days PM; Lane 7 – 43 days PM.

Figure 3.18 EXPT 9 – PM cartilage extracts (40µg protein/sample) collected June 3 – July 15, 2013) displayed CRPs of α-tubulin for cartilage samples 0- 42 days PM. The 230kDa CRP representative of samples collected at 7 days PM was the least intense followed by samples collected at 14 days PM. Cartilage samples collected 21-42 days PM were uniformly the most intense. Lane 1 – Porcine control (0 days PM); Lane 2 – 7 days PM; Lane 3 – 14 days PM; Lane 4 – 21 days PM; Lane 5 – 28 days PM; Lane 6 – 35 days PM; Lane 7 – 42 days PM.

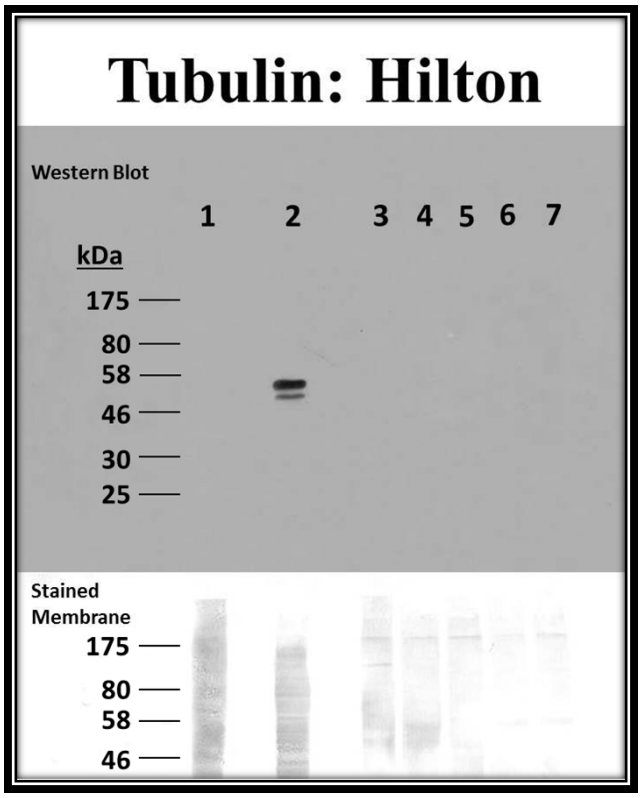

Figure 3.19 EXPT 10 – PM bovine cartilage extracts acquired from coccygeal intervertebral joints (60µg protein) electrophoresed alongside porcine (40µg protein) and human glioblastoma (10µg protein). No CRPs indicative of α-Tubulin were visible for porcine or bovine samples. Lane 1 – Porcine control (0 days PM); Lane 2 – Human glioblastoma; Lane 3 – Bovine control (0 days PM); Lane 4 – 10 days PM; Lane 5 – 17 days PM; Lane 6 – 24 days PM; Lane 7 – 31 days PM.

3.3.2 Vimentin and vinculin

Western blots of control cartilage protein were exposed to varying dilutions of the antibodies, anti-vimentin (1:2500 to 1:200) and anti-vinculin (1:8000 to 1:200). No CRPs were detected for vimetin or vinculin. Figure 3.20, Lanes 1 and 2, illustrate Western blots of control cartilage protein subjected to concentrated solutions of anti-vimentin and anti-vinculin (1:200) antibodies.

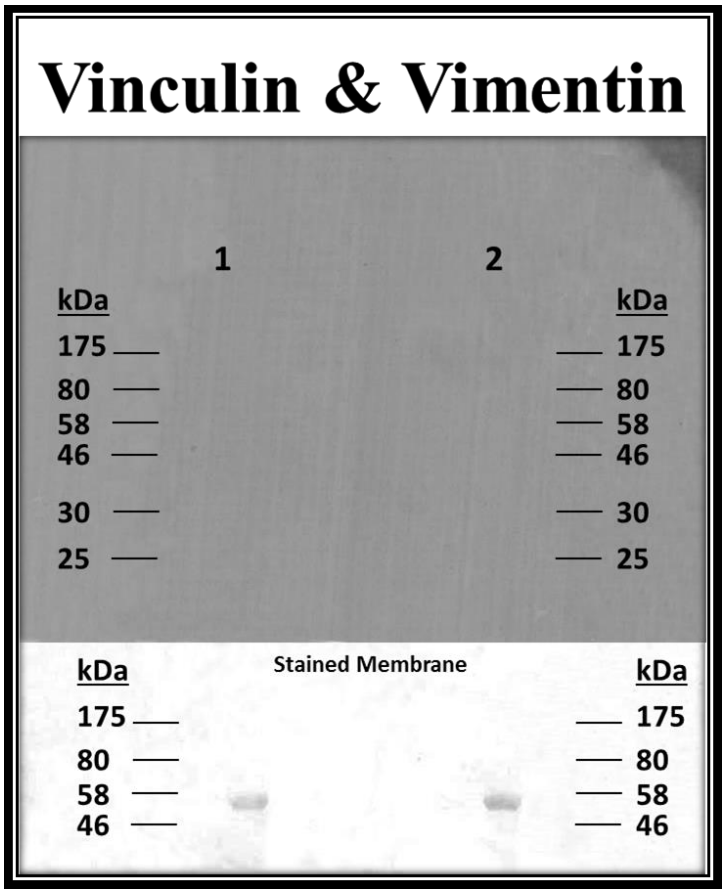

Figure 3.20 Western blot analysis of control porcine cartilage (20µg protein) subjected to immunodetection with monoclonal antibodies anti-vinculin (Lane 1) and anti-vimentin (Lane 2). Antibodies were prepared as 1:200 dilutions. No CRPs representative of vinculin or vimentin were noted.

3.3.3 Cell vitality assays

a) *Preliminary observations using a control sample to determine the best surface area for conducting cell viability tests*

Live/dead cell assays were conducted on cartilage slivers collected from five different regions along the distal end of the MCP/MTP bones for two trotters (a total of four joints examined). The areas examined were: the most inferior aspect of the bone (the ridge), the lateral groove situated next to the ridge, and the medial, lateral and posterior surfaces of the joint (Figure 2.1). They were chosen because of the assumed protection afforded to the joint surfaces as a result of their location in relation to surrounding structures.

Propidium iodide and calcein AM stained cartilage cross-sections were removed from dismembered trotters within two to three hours of death (0 days PM control). Cartilage cross-sections from various surface locations demonstrated that sample area is an important factor to consider when conducting live/dead cell assays. Some areas were more suitable than others presenting little or no dead cells within hours of slaughter (Figure 3.19). For cartilage cross-sections viewed centrally (Figure 2.2) so that the middle/tangential zone was the primary focal point, the ridge (labelled "Inferior" in Figure 2.1) proved to be the most ideal sample area where little to no dead cells were observed at 0 days PM. For this particular surface area, nearly 100% of the chondrocytes were viable. Cross-sections of the remaining four surface areas presented variable amounts of dead cells (Figure 3.21). Of these four regions, cross-sections of the lateral groove appeared to possess the least proportion of dead cells, followed by the posterior, medial and lateral surface areas, with the lateral region possessing the greatest. Cartilage was thickest along the ridged surface of the MCP/MTP joint whereas, cartilage collected from the four other

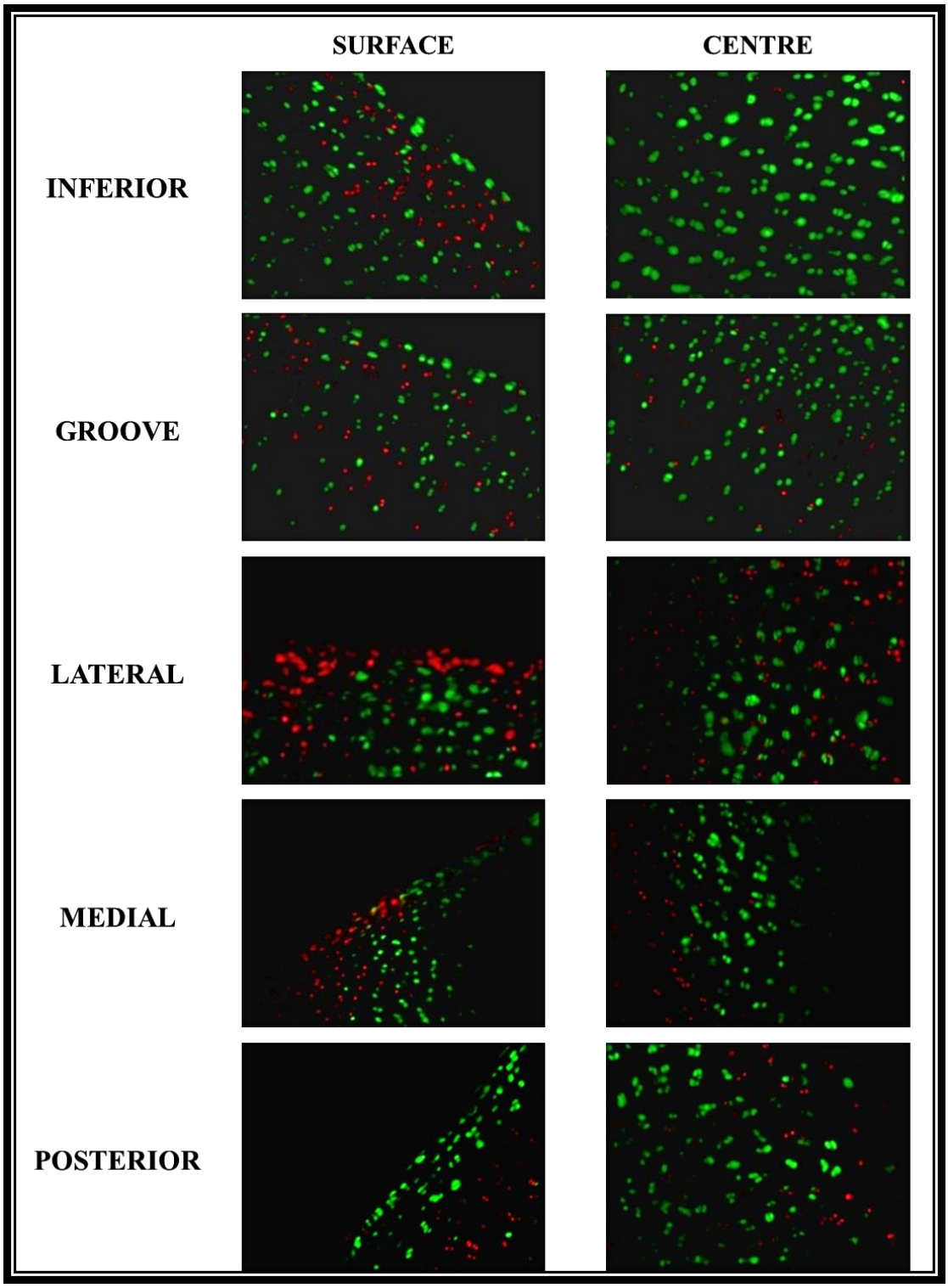

Figure 3.21 Photographic images of the live/dead cell assays conducted for 5 selected areas along the distal end of the MCP/MTP joint (the inferior ridge or apex, the groove situated lateral to the joint's ridge, and the lateral, medial and posterior joint surfaces). The top row of images is representative of the most central aspect of the cartilage cross-sections obtained, whereas the bottom row illustrates the surface area of these cross-sections.

regions were notably thinner, especially cartilage samples extracted from the medial and lateral aspects of the joint.

The cartilage ridge, lateral groove, medial, lateral and posterior facets presented a clustering of dead cells along their articular surfaces. The lateral and medial articular surfaces showed that majority of dead cells were situated along the articular surfaces and extended into the middle/tangential zone, intermingling with the live cells beneath. A single layer of live cells along the outermost region of the superficial zone outlined the ridge and lateral groove articular surfaces above intermingling live and dead cells below. Cartilage extracts taken from the posterior aspect of the joint presented a thick layer of live cells along the articular surface with numerous dead cells situated below at the superficial-middle zone interface. In general, a mixture of live and dead cells occupied the periphery of cartilage cross-sections.

b) *Cell viability test for HLT post mortem samples collected February 11th to March 27th, 2013 (EXPT. 7)*

Six pairs of trotters interred February 11th, 2013 (EXPT 7) were disinterred on a weekly basis for six weeks (until March 27, 2013). During this experimental period the average ambient air temperature was 2.5˚C (high of: 5.0˚C; low of 0.0˚C). Table 3.7 shows the weekly average ambient high and low temperatures that interred trotters experienced each week, and an overall average high and low temperature for the duration of the entire experiment. The rate of decomposition was evidently slower than observed for previous experiments; skin gradually became thinner at a PMI of 36 days in comparison to previous experiments (EXPTs 1, 2, 4, and 5) where notably thinner skin was observed 21-24 days PM (Figure 3.22). These observations prompted Western blot analyses of cartilage samples obtained 30 days PM and beyond to investigate the presence of chondrocytes and aggrecan beyond 21 PM days. For this experiment,

skin remained fully intact for up to five weeks PM. At six weeks PM, the skin of trotters exhibited small breaks. However, the joints remained unexposed to the soil environment.

Table 3.7: The average weekly and overall high and low ambient temperatures experienced by PM trotters collected February 11 to March 27, 2013. Temperatures are rounded to the nearest whole number.

PMI (Days)	Ambient Temperature (˚C)	
	High	Low
0	1	0
7	5	0
14	4	-1
21	6	0
28	7	1
36	6	-2
44	4	0
AVERAGE	**5**	**0**

Unlike previous Western blot analyses involving use of MAb 2-B-6 where CRPs were not visible beyond 21-28 days PM (Figures 3.7 to 3.10), the above cartilage samples extracted at 28, 36 and 44 days PM yielded very intense CRPs for chondroitinase digested aggrecan (230kDa) and the 38kDa CRPs (Figure 3.23). This indicates that detection of aggrecan can be further extended to 44 days PM under circumstances where joint exposure has been delayed as a result of cooler climates. Between 175kDa and 58kDa, additional CRPs of degradation products were observed. These CRPs intensified and additional lower molecular weight particles increased with increasing PMI.

Live cell assays and for cartilage cross-sections excised from the most inferior ridge of the distal MCP/MTP joint were conducted within 1-2 hours of disinterment. Corresponding cartilage extracts were subjected to Western blot analysis with MAb 2-B-6 for cross-comparison with aggrecan degradation. Figure 3.24 illustrates the physical appearance of PM cartilage prior to sample extraction. The experimental collection consisted of samples collected at 0, 7, 14, 21, 28, 36 and 44 days PM (Figure 3.22 depicts the physical state of the trotters from which PM

Figure 3.22 EXPT 7 – The physical state of PM trotters disinterred 0-44 days PM from February 11 to March 27, 2013. The skin of PM trotters remained unbroken for up to 36 days PM. Muscle tissues and tendons remained relatively firm at this PMI. At 44 days PM, the skin and underlying soft tissues were thinner and softer than previous PM samples. No joint exposure was observed. Superficial breaks in the skin are denoted by red circles.

Figure 3.23 EXPT 7 – Western blot of control and PM samples collected at 28, 36 and 44 days PM from trotter samples interred for live cell assays. These PM samples were subjected to protein analysis after noting that the surrounding soft tissue around the joints remained relatively intact in contrast to previous trotters left in the ground for similar lengths of time. Lane 1 – Porcine control (0 days PM); Lane 2 – 28 days PM; Lane 3 – 36 days PM; Lane 4 – 44 days PM.

cartilage cross-sections were excised). Immediate observations of live cell images revealed the presence of viable cells up to 36 days after death. A significant decrease in the number of live cells was most apparent at 36 days PM (Figure 3.24b). At this time period, approximately one third of the chondrocytes maintained viability. The percentage of live cells located centrally to the apex of cartilage cross-sections was calculated for each PMI (Table 3.8).

A graph illustrating the PM trend for the percentage of live chondrocytes with increasing PMI is presented below (Figure 3.25). The plotted data presents a sigmoidal graph for which the number of live cells at 0 days PM is 95% followed by a plateau where the percentage of live cells fall between 60-65% for PM samples collected at 7, 14 and 21 days PM. Beyond 21 days PM, a steady decline in the percentage of live cells is observed. At 28 days PM, the percentage of live cells remaining is nearly half the value of PM samples that fall within the plateau of the graph and is followed by a six-fold decrease in the percentage of live cells at 36 days PM. By 44 days PM, nearly all chondrocytes have died with approximately 1% of cells still viable.

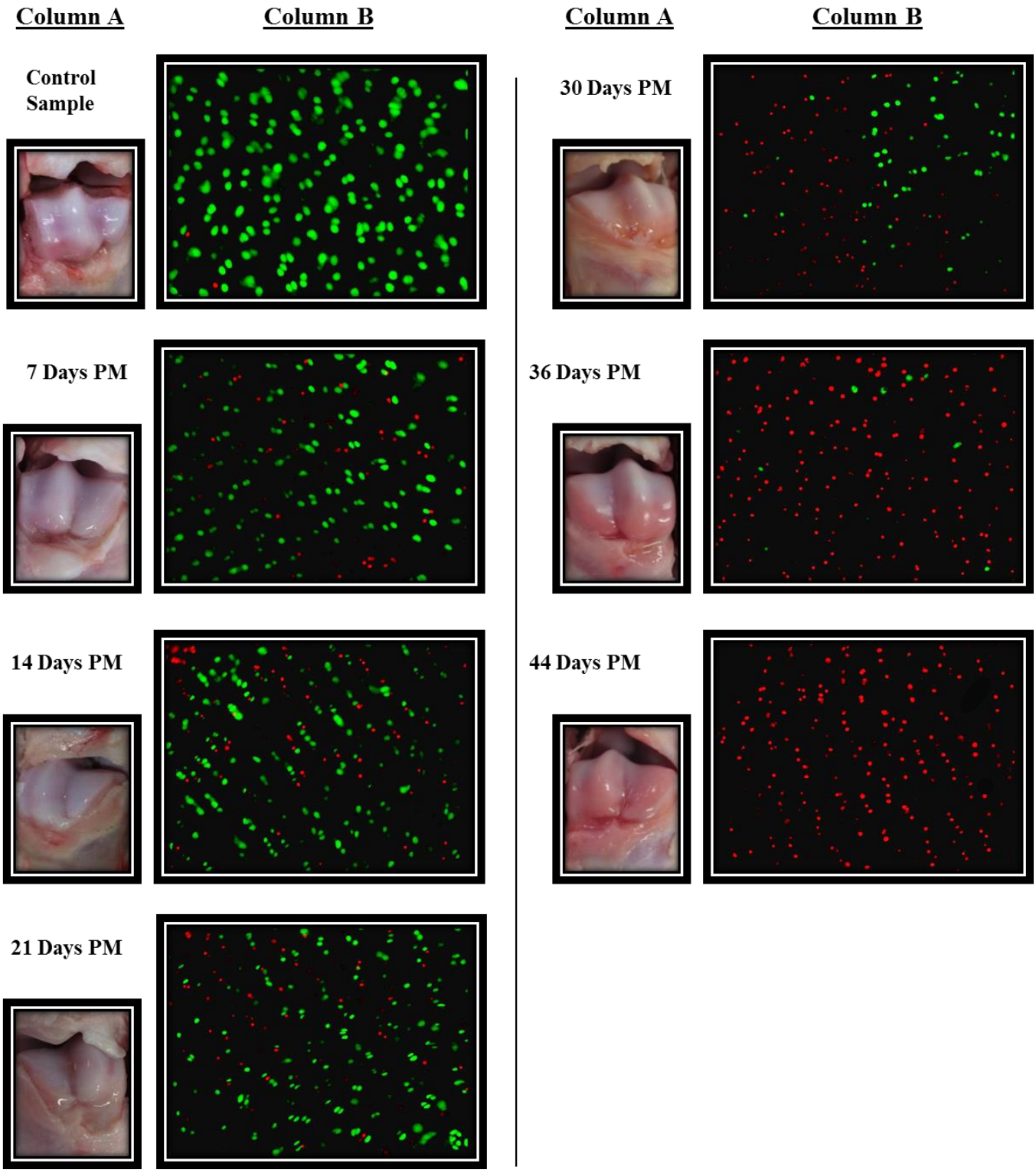

Figure 3.24 EXPT 7 – Column A presents images displaying the appearance of PM cartilage (0-44 days PM) exposed at the MCP/MTP joints for trotters disinterred weekly from February 11 to March 27, 2013. Column B shows live/dead cell images of PM cartilage taken with a fluorescence microscope (Olympus BX61) using FITC (for detection of live cells using calcein AM – green fluorescence) and Texas red (for detection of dead cells using propidium iodide – red fluorescence). A substantial decrease in the number of viable cells was observed at 36 days PM.

Table 3.8 Weekly tabulations of the dates for which trotters were disinterred, the number of days each sample spent below ground, the accumulated degree days each specimen experienced, and the percentage of live chondrocytes present on the day of disinterment (EXPT 7 - February 11 to March 27, 2013).

Date of Extraction	Number of Days PM	Accumulated Degree-Days (ADD)	Percentage of Live Chondrocytes (%)	Standard Deviation (+/-)
February 11	0	1*	95	6.0
February 18	7	22	64	14.3
February 25	14	32	65	7.2
March 4	21	64	60	11.2
March 13	30	90	36	14.8
March 19	36	108	6	7.6
March 27	44	115	1	0.8

* This ADD value was not taken into consideration for control cartilage extracted on the day of slaughter but was included among calculations for all experimental trotters disinterred.

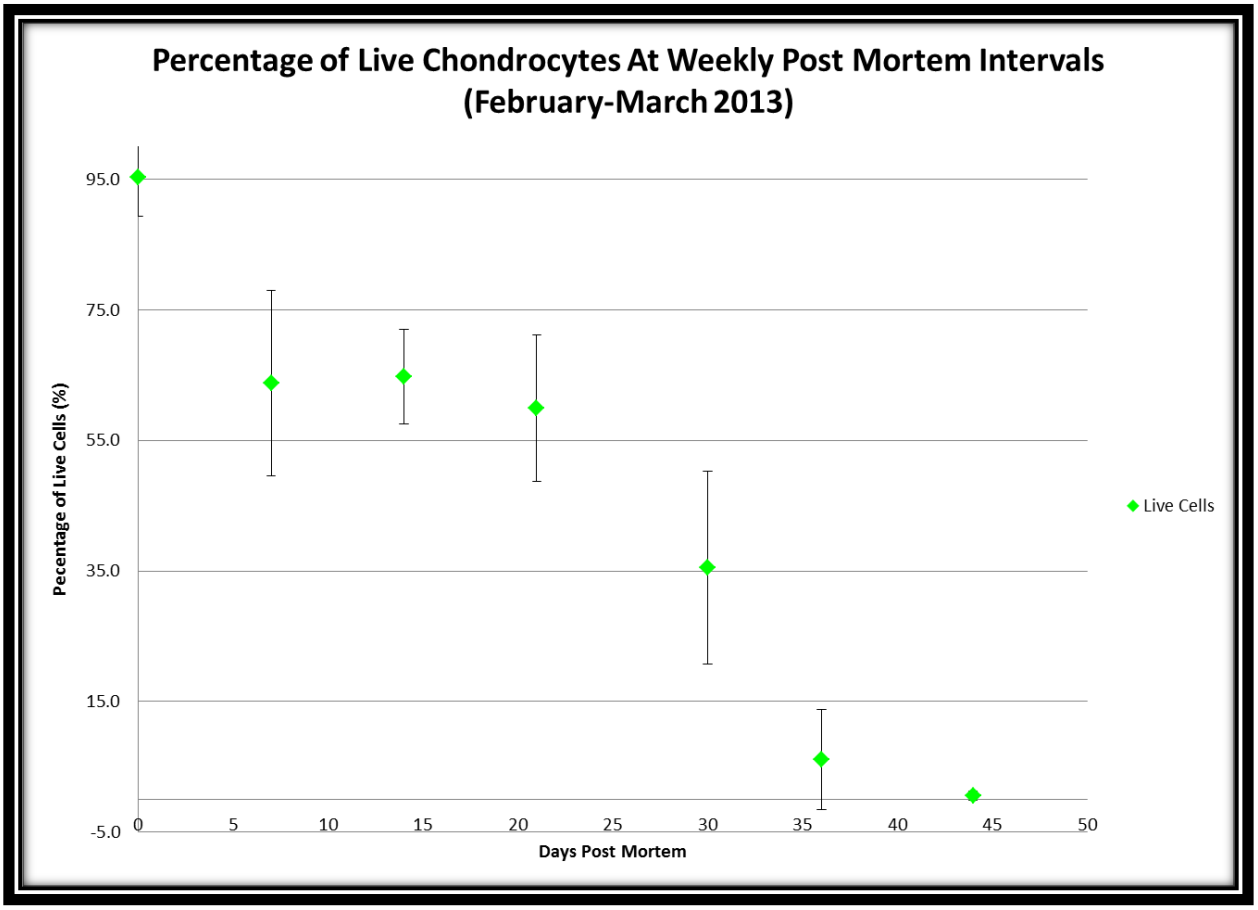

Figure 3.25 EXPT 7 – For cartilage samples collected 0-44 days PM, the percentage of live chondrocytes that persisted each week were plotted in a graph. A sigmoidal curve was observed. At 7 days PM, a 30% decrease in the percentage of viable cells was observed when compared to the percentage of viable cells present at 0 days PM. From 7-21 days PM, the percentage of viable cells remaining was approximately 60% and remained relatively constant for 2 weeks. After 21 days PM, the percentage of viable cells proceeded to decline by a factor of two for 30 and 36 days PM, and then rapidly thereafter.

c) *Cell viability test for HLT post mortem samples collected April 15th to May 28th, 2013 (EXPT. 8)*

A second cell viability experiment was conducted for six pairs of trotters that were disinterred weekly from April 15, 2013 to May 28, 2013. Over the course of these six weeks, ambient temperatures reached an average high of 14.0˚C and an average low of 5.0˚C (average temperature: 9.5˚C). In comparison with the previous cell viability assays conducted April 15 to May 28 (2013), cartilage samples disinterred for this experiment (EXPT 8) experienced temperatures that were, on average, 9˚C (high) and 5˚C (low) warmer (Table 3.9).

Table 3.9: The average weekly and overall high and low ambient temperatures experienced by PM trotters collected April 15 to May 28, 2014. Temperatures are rounded to the nearest whole number.

PMI (Days)	Ambient Temperature (˚C)	
	High	Low
0	16	9
7	13	4
14	13	4
22	16	3
28	16	6
35	13	4
43	13	6
AVERAGE	**14**	**5**

Soft tissue degradation occurred more rapidly among EXPT 8 trotters. Skin and joints were fully intact at 22 days PM. Joint exposure was first noted among trotter samples at 28 days PM (Figure 3.26), mirroring earlier observations of joints exposed to the immediate soil environment at this PMI (Sections 3.2.5, Figures 3.7 & 3.8).

A Western blot of EXPT 8 cartilage extracts was performed for cross-comparison of extracellular (aggrecan) (Figure 3.27) and cellular (chondrocyte) (Figure 3.28) degradation activities. CRPs approximately 230kDa were plainly visible for control and experimental samples 7, 14 and 22 days PM, and demonstrated additional CRPs below (between 230kDa-

70kDa). The 38kDa CRP appeared among these samples. However, the CRP representing this molecule for control cartilage was very intense, whereas the 38kDa CRPs that appeared for samples 7, 14 and 22 days PM were less intense. Control, 7 and 14 days PM samples showed additional CRPs amidst a degradation gradient that extended towards 70kDa while PM samples collected at 22 days presented CRPs that approached 93kDa. For control cartilage, these additional CRPs appeared slightly less intense than samples collected at 7 days PM. As PMI increased, these CRPs for samples extracted 7-22 days PM gradually became less intense and appeared fewer in number. However, the 38kDa CRPs for these PM samples showed little increase in intensity. For PM samples disinterred after 28, 35 and 43 days below ground, remnants of aggrecan by-products could be seen, displaying very faint CRPs at 230kDa for samples 35 days PM and even more faintly at 43 days PM.

Live cell assays performed on cartilage samples gathered from EXPT 8 trotters presented viable chondrocytes for as long as 22 days PM (Figure 3.28). At this PMI, the live chondrocytes comprised 7%. This value was lower than the previous experiment for which the percentage of live cells amounted to 60% at 21 days PM, signifying an approximate nine-fold decrease in the percentage of viable cells.

Table 3.6 displays the percentage of live cells observed at each PMI. At 28 days, 1% of the chondrocytes were viable whereas a 3% increase in vitality occurred at 35 days PM. No live chondrocytes were present at 43 days PM. A time course graph of cell viability for EXPT 8 cartilage samples closely resembled the graph obtained for EXPT 7 samples where the data plots formed a polynomial curve approaching a sigmoid-shape (Figure 3.29). However, no distinct plateau was observed as seen around 7-21 days PM for EXPT 7 (Figure 3.25). For samples 0-14 days PM, the graph shows a steady decrease in the percentage of live cells. From 14 to 21 days

PM, a substantial decrease in live cells amounted to 57%. Beyond 21 days PM, the percentage of live cells steadily levelled off so that 0% of live cells remained at 43 days PM.

Evaluation of live cell assays performed on samples disinterred during April and May of 2013 (EXPT 8) with their respective α-tubulin Western blots (Figure 3.16) did not reflect similar temporal patterns for degradation of the cellular matrix.

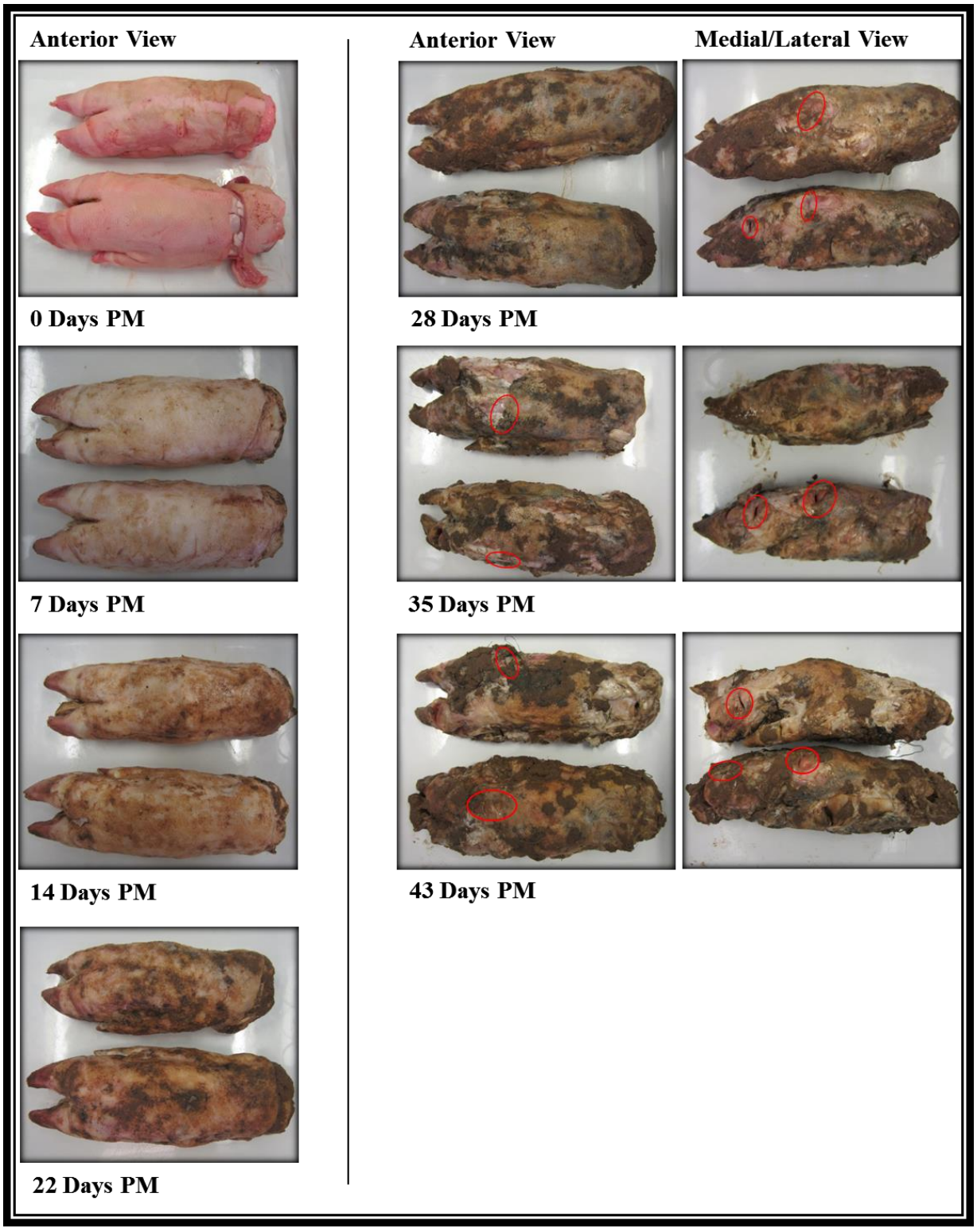

Figure 3.26 EXPT 8 – The physical state of trotters disinterred 0-43 days PM from April 15, 2013 to May 28, 2013. For 22 days, the skin of PM trotters remained unbroken. By 28 days PM, superficial discontinuities in the skin and some joint exposure were observed and underlying soft tissues felt notably thinner and softer. Joint exposure to the surrounding soil environment was observed at 35 days PM. Superficial breaks in the skin and joint exposure are denoted by red circles.

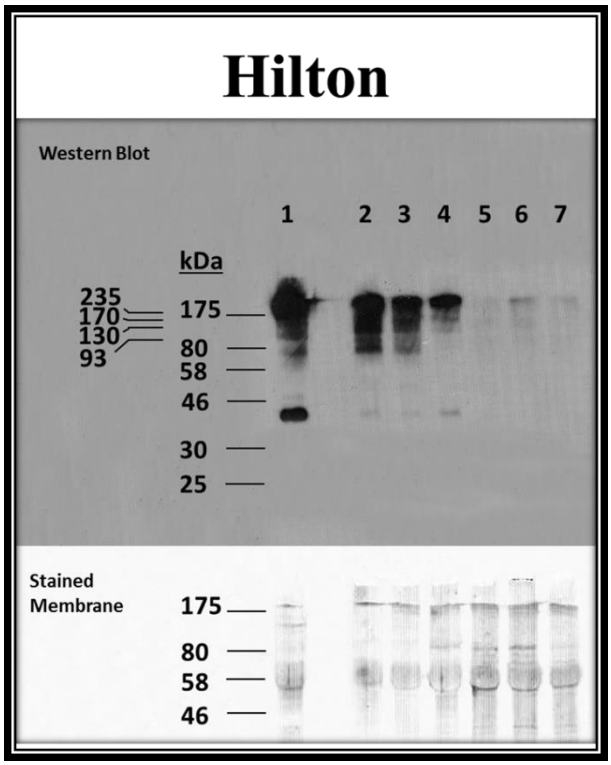

Figure 3.27 EXPT 8 – A Western blot image of PM porcine cartilage extracts (30µg protein/10µl 1X sample buffer) acquired from trotters disinterred weekly from April 15-May 28, 2013 for a second cell viability experiment. The samples are representative of 0, 7, 14, 22, 28, 35 and 43 days PM aggrecan detected with MAb 2-B-6. Lane 1 – Porcine control (0 days PM); Lane 2 – 7 days PM; Lane 3 – 14 days PM; Lane 4 – 22 days PM; Lane 5 – 28 days PM; Lane 6 – 35 days PM; Lane 7 – 43 days PM.

Table 3.10 Weekly tabulations of the dates for which trotters were disinterred, the number of days each sample spent below ground, the accumulated degree days each specimen experienced, and the percentage of live chondrocytes present on the day of disinterment (EXPT 8 - April 15 to May 28, 2013).

Date of Extraction	Number of Days PM	Accumulated Degree-Days (ADD)	Percentage of Live Chondrocytes (%)	Standard Deviation (+/-)
April 15	0	13*	99	1.9
April 22	7	73	79	12.1
April 29	14	145	64	5.8
May 7	22	295	7	2.6
May 13	28	354	1	1.4
May 20	35	420	4	3.3
May 28	43	494	0	0

* This ADD value was not taken into consideration for control cartilage extracted on the day of slaughter but was included among calculations for all experimental trotters disinterred.

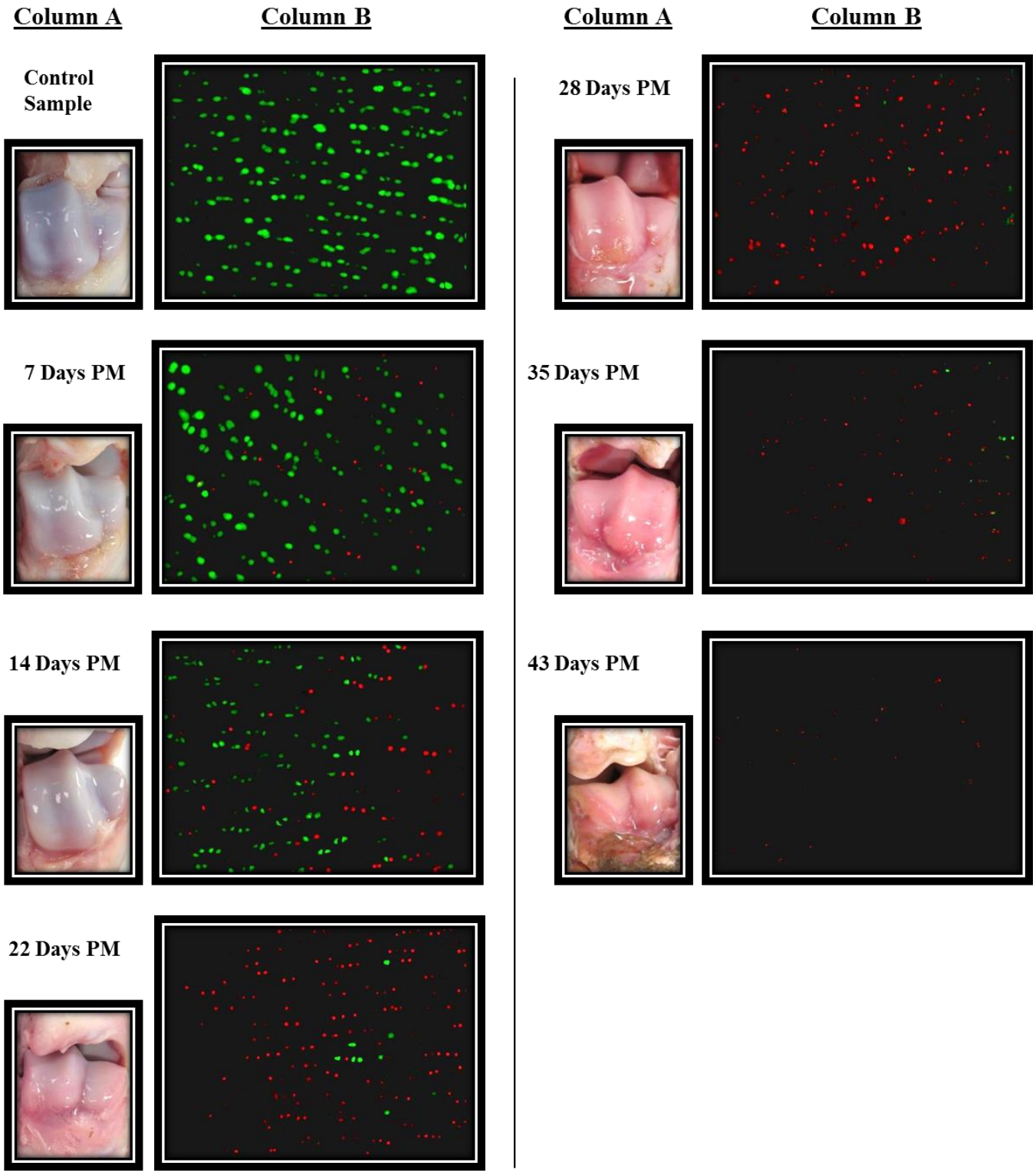

Figure 3.28 EXPT 8 – Images of PM cartilage (0-43 days PM) at the MCP/MTP joint from trotters collected weekly from April 15 to May 28, 2014 are situated under Column A. With increasing PM, the pearly white tissue gradually turned dark pink and finally pale by 43 days PM. Column B displays the live/dead cell images taken with a fluorescence microscope (Olympus BX61) that correspond to each weekly sample of PM cartilage listed in Column A. Live cells appear green and dead cells red. At 22 days PM, the number of viable cells had dramatically decreased by nearly 90%.

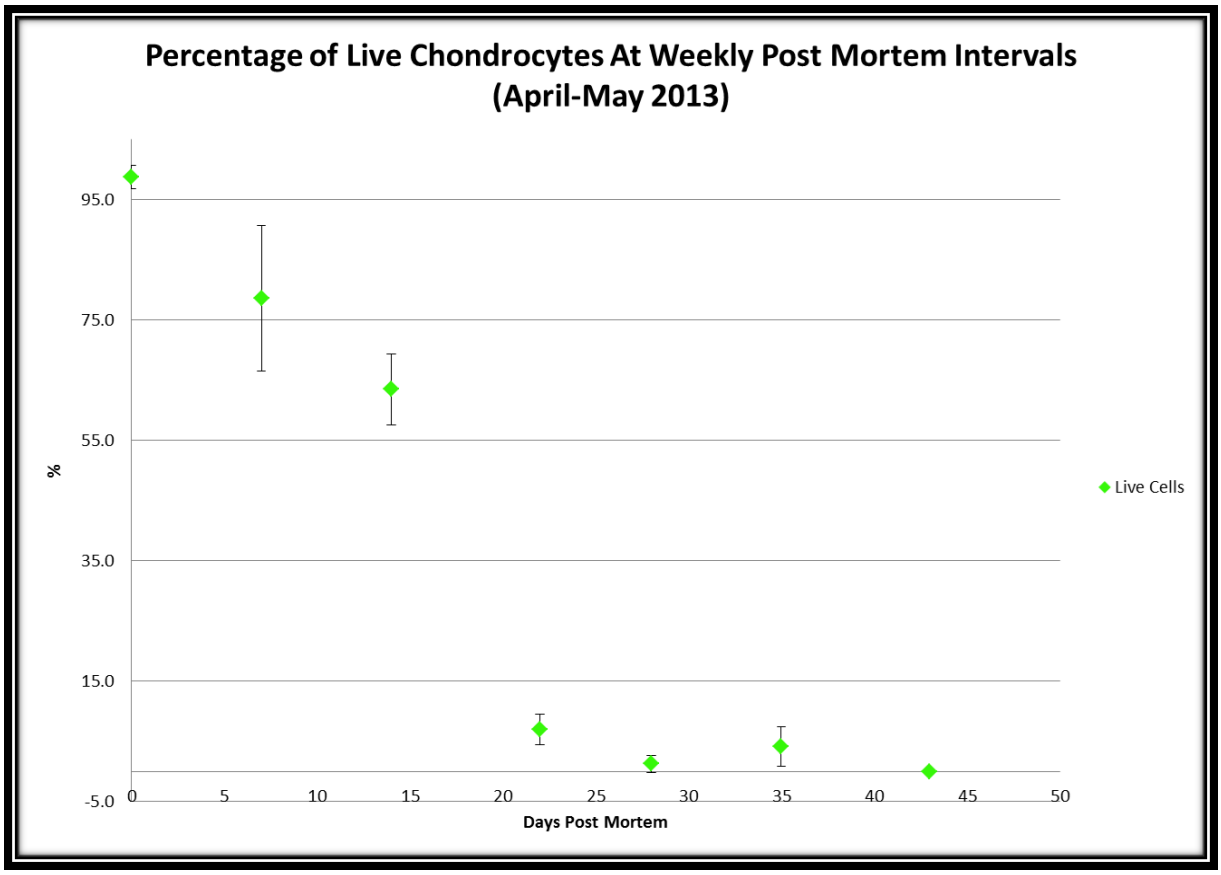

Figure 3.29 EXPT 8 – For cartilage samples collected 0-43 days PM, the percentage of live chondrocytes tha persisted each week were plotted in a graph. A sigmoidal curve was observed. Over the course of 14 days, th percentage of live cells appears to steadily decrease in a near linear fashion and then rapidly decreased b approximately 90% between 14 and 22 days PM. From 22-43 days PM, the percentage of viable cells remainin steadily decreased from 7-0%.

d) Cell viability test for HLT post mortem samples collected June 3rd to July 15th, 2013 (EXPT. 9)

Cell viability assays and Western blots were performed on cartilage samples collected from trotters disinterred weekly from June 3 to July 15, 2013. During this period the overall average ambient temperature was 15.0˚C (high: 20.0˚C, low: 9.0˚C) (Table 3.11). The rate of soft tissue degradation was observably more rapid (Figure 3.30) than previous experiments conducted for cell vitality assays and Western blotting. By 14 days PM, trotters were pallid with wrinkles along various areas of thinning skin. The skin of one trotter was broken around the medial MCP/MTP joint. Joint exposure was observed at 21 days PM. At this PMI, cartilage was visibly pink and had begun to recede from the cartilage-bone interface. The cartilage maintained some rigidity but was softer to cut through in comparison with cartilage extracted at 0 days PM.

Table 3.11: The average weekly and overall high and low ambient temperatures experienced by PM trotters collected June 3, 2013 to July 15, 2013. Temperatures are rounded to the nearest whole number.

PMI (Days)	Ambient Temperature (˚C)	
	High	Low
0	20	6
7	19	7
14	16	9
21	19	12
28	19	10
35	22	11
42	25	11
AVERAGE	**20**	**9**

Examination of the PM ECM properties for the samples obtained was conducted with MAb 2-B-6. A Western blot of PM samples extracted 0-42 days showed the presence of 230kDa CRPs for samples 0-14 days PM (Figure 3.30). Additional CRPs were seen between 230kDa and 70kDa among samples 0-14 days PM. The intensity of the 230kDa CRP diminished with increasing PMI. From 0-7 days PM, the number of CRP protein fragments increased as did

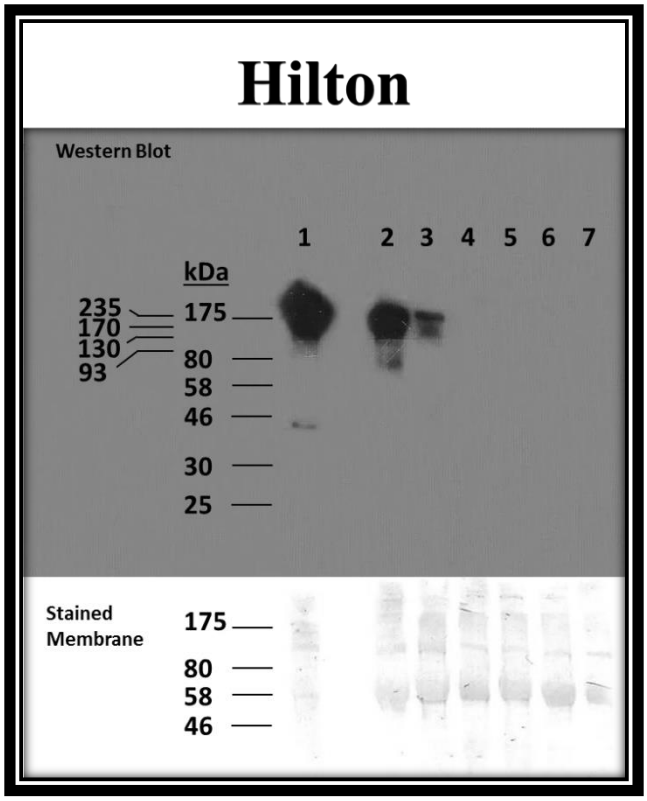

Figure 3.30 EXPT 9 – Western blot of PM porcine cartilage extracts (20µg protei acquired from trotters disinterred weekly (June 3 to July 15, 2013). Aggrecan wa detected for samples 0-14 days PM using MAb 2-B-6. No CRPs were seen amor samples collected 21-42 days PM. The absence of these CRPs coincides with joi exposure to the soil environment. The stained membrane demonstrates relative equal loading of samples. Lane 1 – Porcine control (0 days PM); Lane 2 – 7 days PM Lane 3 – 14 days PM; Lane 4 – 21 days PM; Lane 5 – 28 days PM; Lane 6 – 35 day PM; Lane 7 – 42 days PM.

the length of undefined degradation by-products. PM cartilage extracted from trotters that remained below ground for 14 days was accompanied by a grade of reduced aggrecan by-products weighing as little as 130kDa. A 38kDa CRP only appeared for control cartilage. No 38kDa CRPs were seen for PM samples collected beyond 14 days PM.

Cell viability assays for PM samples gathered weekly from 0-42 days showed no live cells beyond 14 days (Table 3.12). The percentage of live cells dramatically decreased from 95% at 0 days PM to 52% for samples 7 days PM. Only 2% of the chondrocytes detected at 14 days PM were viable. No chondrocytes were viable at 21-42 days PM and the number of dead chondrocytes (red fluorescence) visible at 21 days PM had greatly diminished so that only several were seen at the most central aspect of the cartilage cross-sections. For samples collected beyond this PMI (28-42 days PM), there were no evidence of chondrocytes; no live or dead cells were visibly detected with the fluorescence microscope (Figure 3.32). Non-fluorescent images of the cartilage cross-sections highlighting the same area of the fluorescent figures for samples 28 and 42 days PM were taken to illustrate the presence of lacuna which previously housed cellular material for live and dead chondrocytes (Figure 3.33). Interestingly, a Western blot of these PM samples subjected to α-tubulin immunodetection indicated that the cellular component, tubulin, remained present up to 42 days PM (Figure 3.18) despite the lack of fluorescence for live and dead cells. Figure 3.34 presents the data in Table 3.12 as an exponential graph of chondrocyte viability over time.

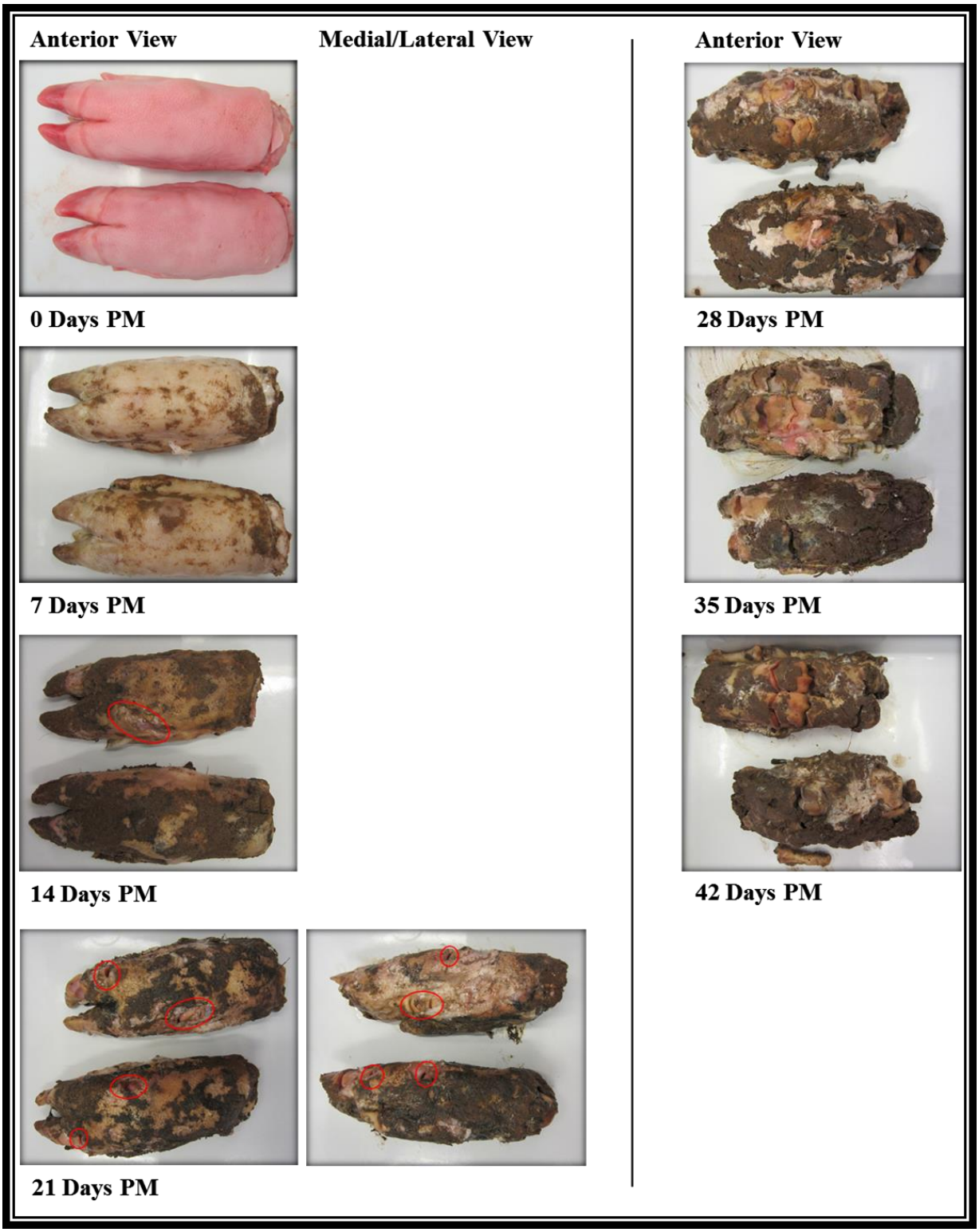

Figure 3.31 EXPT 9 – The physical appearance of trotters disinterred 0-42 days PM from June 3 to July 15, 2013. At 14 days PM, a superficial break was observed in the skin of a trotter. The joints of PM trotters disinterred at this PMI remained unexposed to the immediate soil environment. Joint exposure was first noted for PM totters disinterred after spending 21 days below ground. Superficial breaks in the skin and joint exposure are highlighted by red circles for clarification. Joint exposure was observed up to 42 days PM.

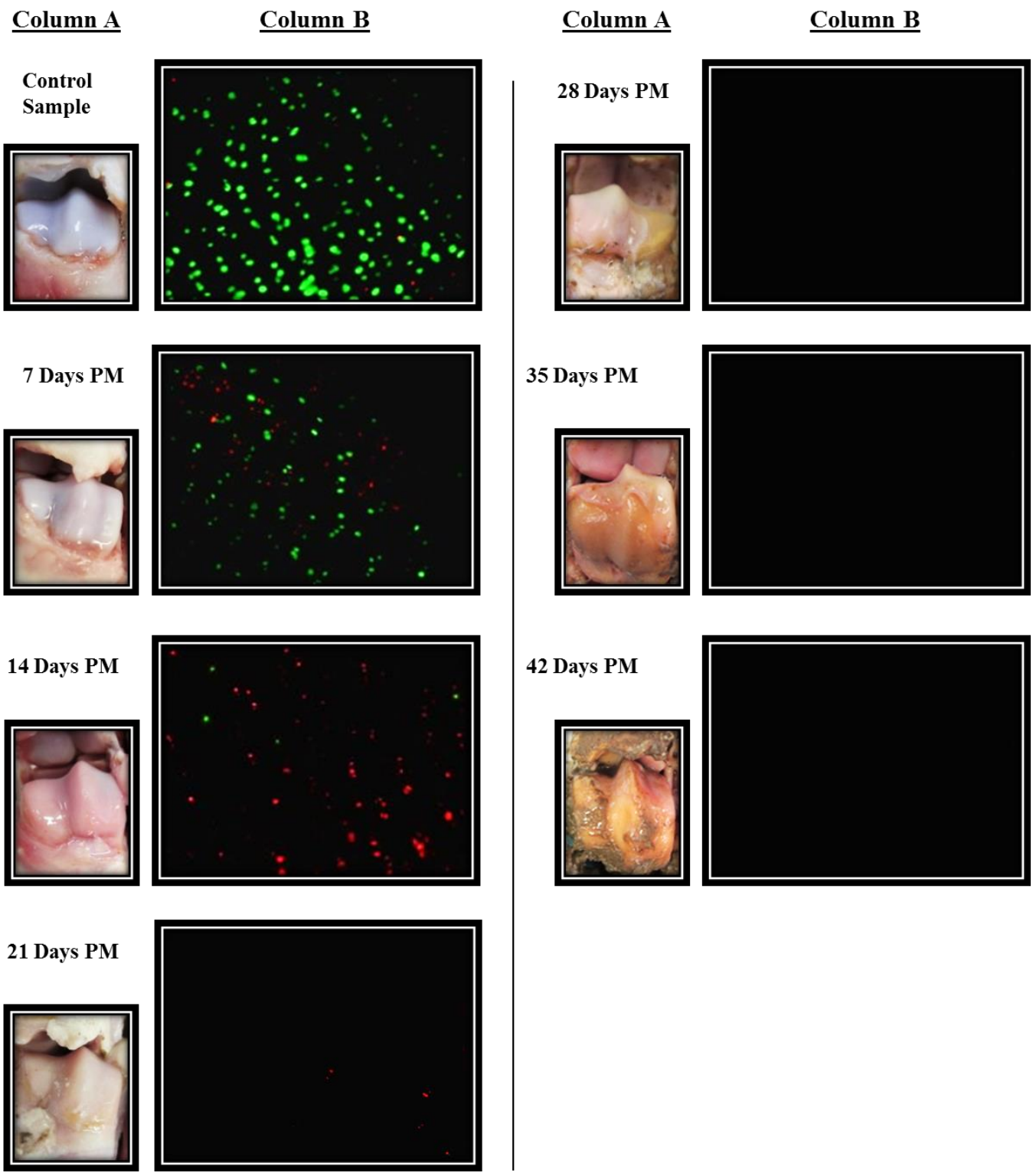

Figure 3.32 EXPT 9 – Images of PM MCP/MTP joint cartilage (0-42 days PM) collected from trotters disinterred weekly during June 3 to July 15, 2013 are shown under Column A. Cartilage appeared pink at 14 days PM. At 21 days PM, cartilage developed pallor and began to retreat from the cartilage/bone interface. Corresponding live/dead cell images (Column B) were captured with a fluorescence microscope (Olympus BX61) and showed that live chondrocytes (green) were absent by 21 days PM. Nuclei, representative of dead cells (red), were completely disintegrated by 28 days PM.

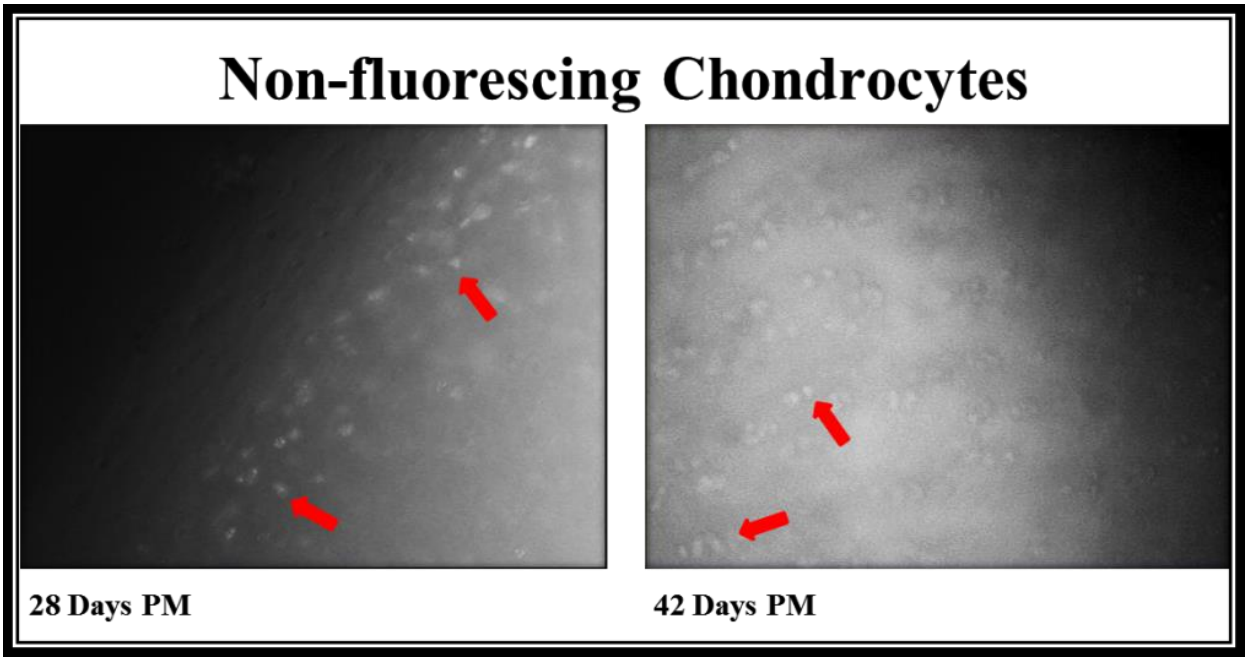

Figure 3.33 EXPT 9 – Non-fluorescing microscopic images of PM MCP/MTP joint cartilage at 28 and 42 days PM. Images were taken with both FITC (for detection of green fluorescence) and Texas Red (for detection of red fluorescence). Neither red, nor green fluorescent colours were detected and suggest complete degradation of cytoplasmic and nucleic material. Red arrows point to light ovid shapes which indicate the presence of empty lacuna which once contained live chondrocytes.

Table 3.12 Weekly tabulations of the dates for which trotters were disinterred, the number of days they spent below ground, the accumulated degree days experienced by each, and the percentage of live chondrocytes present at the time of disinterment (EXPT 9 - June 3, 2013 to July 15, 2013).

Date of Extraction	Number of Days PM	Accumulated Degree-Days (ADD)	Percentage of Live Chondrocytes (%)	Standard Deviation (+/-)
June 3	0	13*	95	3.4
June 10	7	99	52	6.1
June 17	14	192	2	2.1
June 24	21	299	0	0
July 1	28	403	0	0
July 8	35	521	0	0
July 15	42	650	0	0

* This ADD value was not taken into consideration for control cartilage extracted on the day of slaughter but was included among calculations for all experimental trotters disinterred.

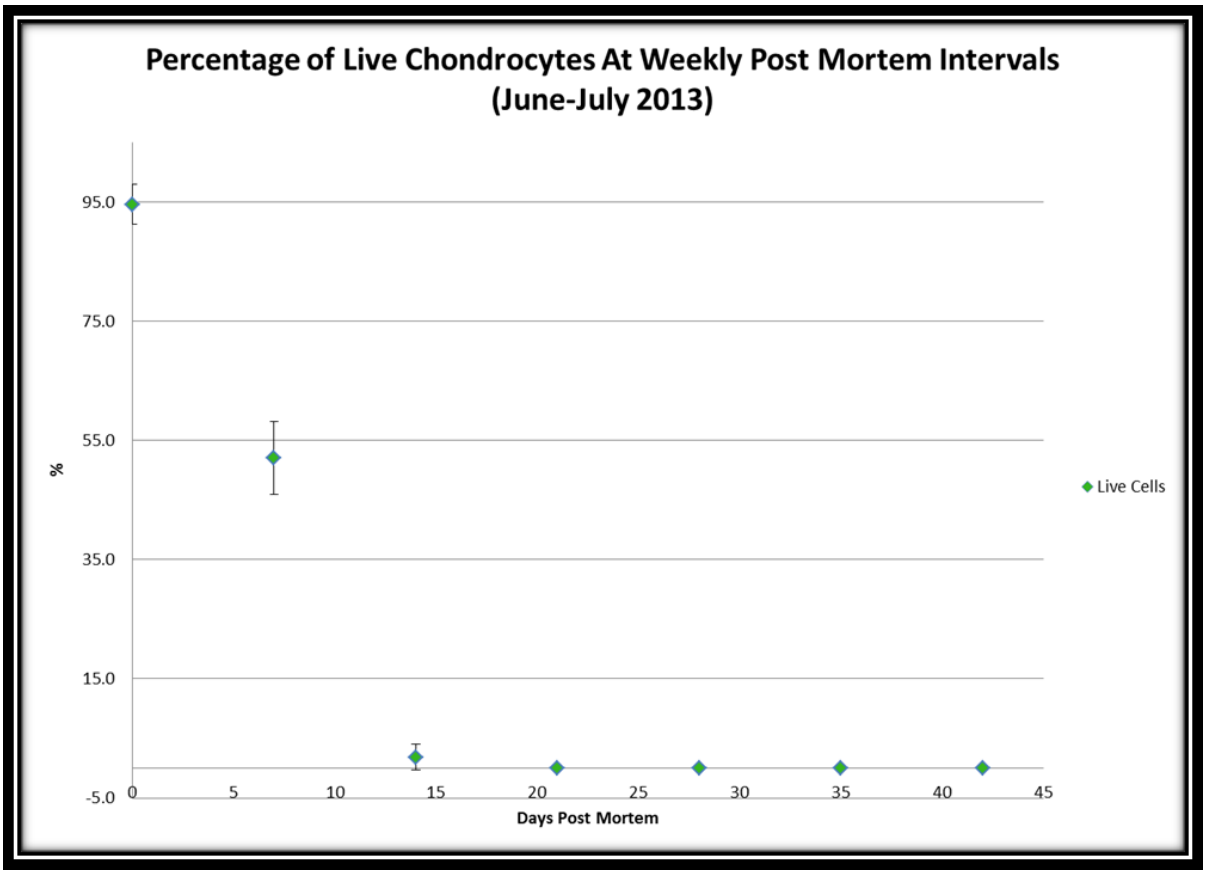

Figure 3.34 EXPT 9 – A graph illustrating the PM trend for the percentage of live chondrocytes with increasing PMI for cartilage samples collected weekly 0-42 days PM (June 3 to July 15, 2013). The curvature is vaguely sigmoidal, appearing exponential. After 7 days PM, half the initial percentage of live cells present at 0 days PM persisted. At 14 days PM, only 2% of the chondrocytes are viable. At 20 days PM, no viable cells were observed thereafter.

e) Cell viability test for HLT post mortem bovine samples collected July 4th to August 5th, 2013 (EXPT. 10)

PM cartilage extracts removed from the intervertebral joints of dismembered ox-tail were subjected to the same cell viability assays and Western blot experiments as those that were performed on cartilage samples extracted from porcine trotters. Experimental samples were obtained Thursday July 4th, 2013, interred July 8th, 2013, and disinterred weekly from July 15th, 2013 to August 5th, 2013. For the duration of this experiment, the overall average ambient temperature was 18˚C (high: 25˚C, low: 11˚C; Table 3.13). Since the specimen of dismembered bovine tail was obtained without skin, it was not possible to assess and appreciate the degradative changes that would have occurred along the skin's surface with increasing PMI.

Table 3.13: The average weekly and overall high and low ambient temperatures experienced by PM segments of ox tail collected July 4 to August 5, 2013. Temperatures are rounded to the nearest whole number.

PMI (Days)	Ambient Temperature (˚C)	
	High	Low
0	4	4
10	25	11
17	27	13
24	26	14
31	21	14
AVERAGE	**21**	**11**

The unearthed segments of PM bovine tail displayed evidence of soft tissue degradation over time (refer to Figures 3.35 and 3.37, Column A). At 0 days PM, muscle tissues were vibrant red and firm to the touch. Tendons and intervertebral cartilage were white in colour, robust and flexible. Upon disinterment, the 10 days PM tail segment was incrusted with soil that was difficult to thoroughly rinse away and white hyphal growth was observed along the surface of the tail that was in contact with the ground below. Two other morphologically different microorganisms were present: that which was small, circular (an approximate diameter of 1mm) and white; and the other, a blackened film randomly dispersed along the surface of the muscle

tissue. The segment of 17 days PM ox-tail, disinterred the following week, also possessed encrusted soil on the muscles. Muscle tissue and tendons were softer with respect to the sample disinterred 10 days PM. The muscle surface proximal to the surrounding soil environment was either soil stained or became pallid. The inner tissues remained bright red but were slightly darker than the control sample. The outer concentric rings of the fibro-cartilaginous joint tissue were light pink in colour while the centre remained white.

At 24 days PM, the ox-tail exhibited very soft muscle tissues, especially along its periphery, and experienced several rainfalls since the previous sample's disinterment. The outer soft tissues (muscles, tendons, and fat) had begun liquefying. At the time of disinterment, clumps of soil and soft tissue fell away from the tail segment upon removal from its grave. Exposure of the intervertebral joints displayed uniformly pink cartilage that was darker than cartilage extracted at 17 days PM.

The final segment of ox-tail disinterred at 31 days PM was entirely covered in moist soil. The outer muscles, tendons and fat were extremely degraded and demonstrated an increased amount of liquefaction in comparison to the specimen of tail disinterred 24 days PM. Upon handling, soil and liquefied soft tissue fell away quite readily. Muscle tissue had become uniformly pallid, appearing much duller than the specimen observed at 24 days PM. Tendons were quite flaccid and exhibited no elasticity. The onset of skeletisation for the tail segment was perceived by exposure of the transverse and spinous processes of the vertebrae through the muscles and tendons. The outer concentric rings of the fibro-cartilage were a darker pink than intervertebral joint cartilage observed at 24 days PM. The central aspect of the cartilage was creamy yellow or beige in colour. Cartilage at this PMI maintained elasticity but was softer, and required less force to cut away from the joint surface.

Western blot images of PM bovine intervertebral cartilage were performed with MAb 2-B-6 (Figure 3.36). Variable results were obtained. A Western blot conducted with 30µg of cartilage protein yielded 230kDa aggrecan CRPs for control (0 days PM) and experimental samples 10, 17, 24, 31 days PM (Figure 3.36a). At 0 days PM the 230kDa CRP was dimly seen. The 230kDa CRPs present for experimental samples were intense. Like PM samples of porcine cartilage, bovine intervertebral cartilage extracted at 10 days PM presented degradation by-products situated between 230kDa and 70kDa. For cartilage samples 17 days PM, these by-products reached as far as 58kDa and were far more intense than those observed at 10 days. By 24 and 31 days PM, the 230kDa CRPs of aggrecan demonstrated a gradual reduction in their intensity with comparison to the previous samples. The 38kDa CRP was present for samples 0-31 days PM. No particular trend was observed for the intensity of this molecule as PMI increased. The Western blot results obtained for these specimens of bovine intervertebral cartilage mirrored results obtained for porcine cartilage that presented aggrecan (230kDa) for up to 21 days PM.

A second Western blot using protein extracts from the same control and experimental samples was performed using 20µg of protein sample (Figure 3.36b). MAb 2-B-6 CRPs were visible for samples 0, 10 and 17 days PM. No CRP indicative of aggrecan was situated at the 230kDa mark for the control sample. Like the previous results obtained for control IVJ cartilage obtained from a bovine specimen, a low molecular weight CRP weighing 38kDa appeared. This CRP was absent for all experimental samples (10-31 days PM).

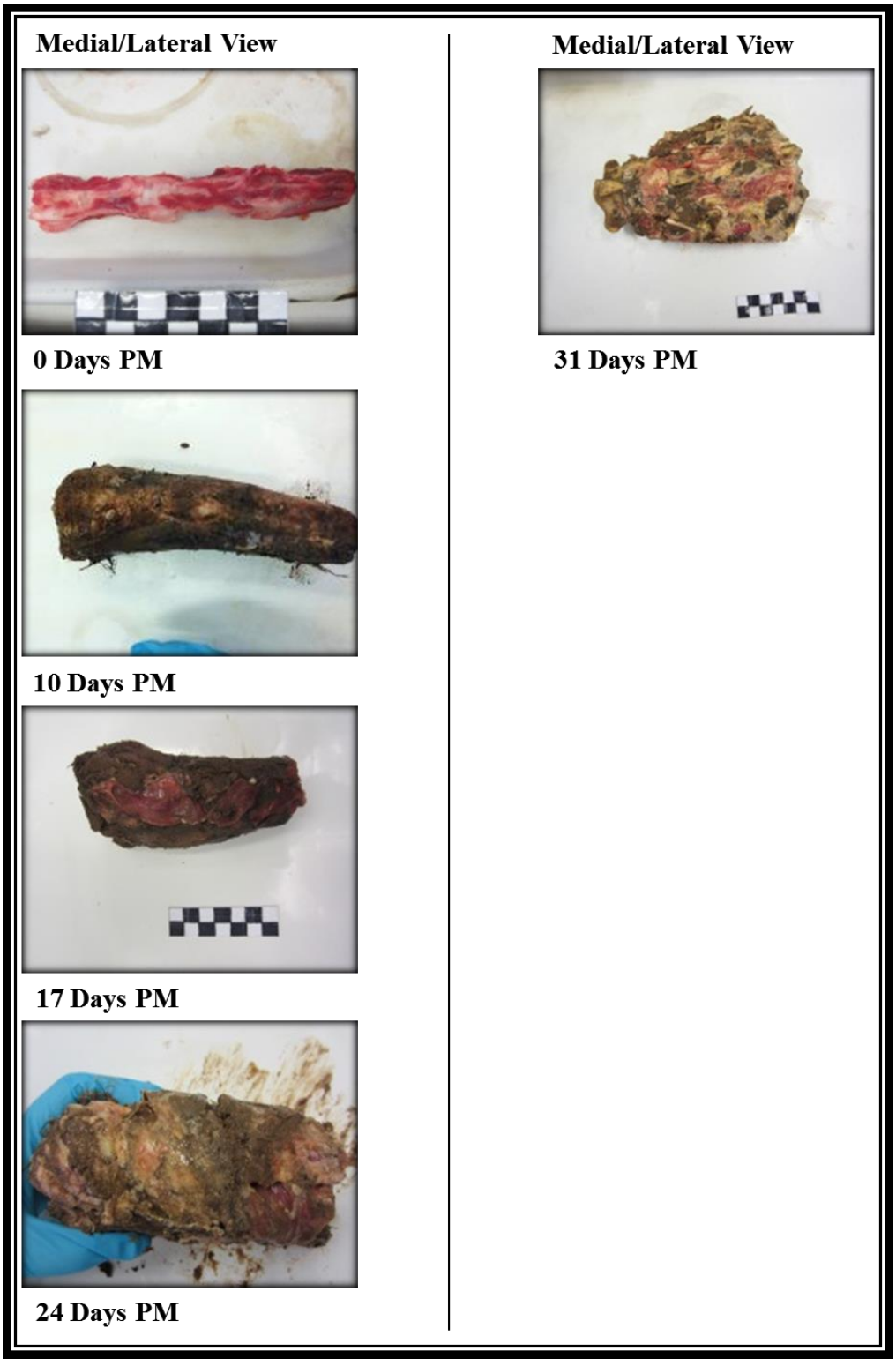

Figure 3.35 EXPT 10 – The physical state of PM bovine tail segments disinterred 0-31 days PM (July 4 t August 5, 2013). In the absence of skin, the intervertebral joints of the tail segments disinterred 10-24 day PM remained relatively unexposed to the immediate soil environment. At 31 days PM, superficial muscle and tendons were notably liquefied in comparison with the tail segment disinterred at 24 days PM. Th transverse and spinous processes were exposed to the surrounding soil.

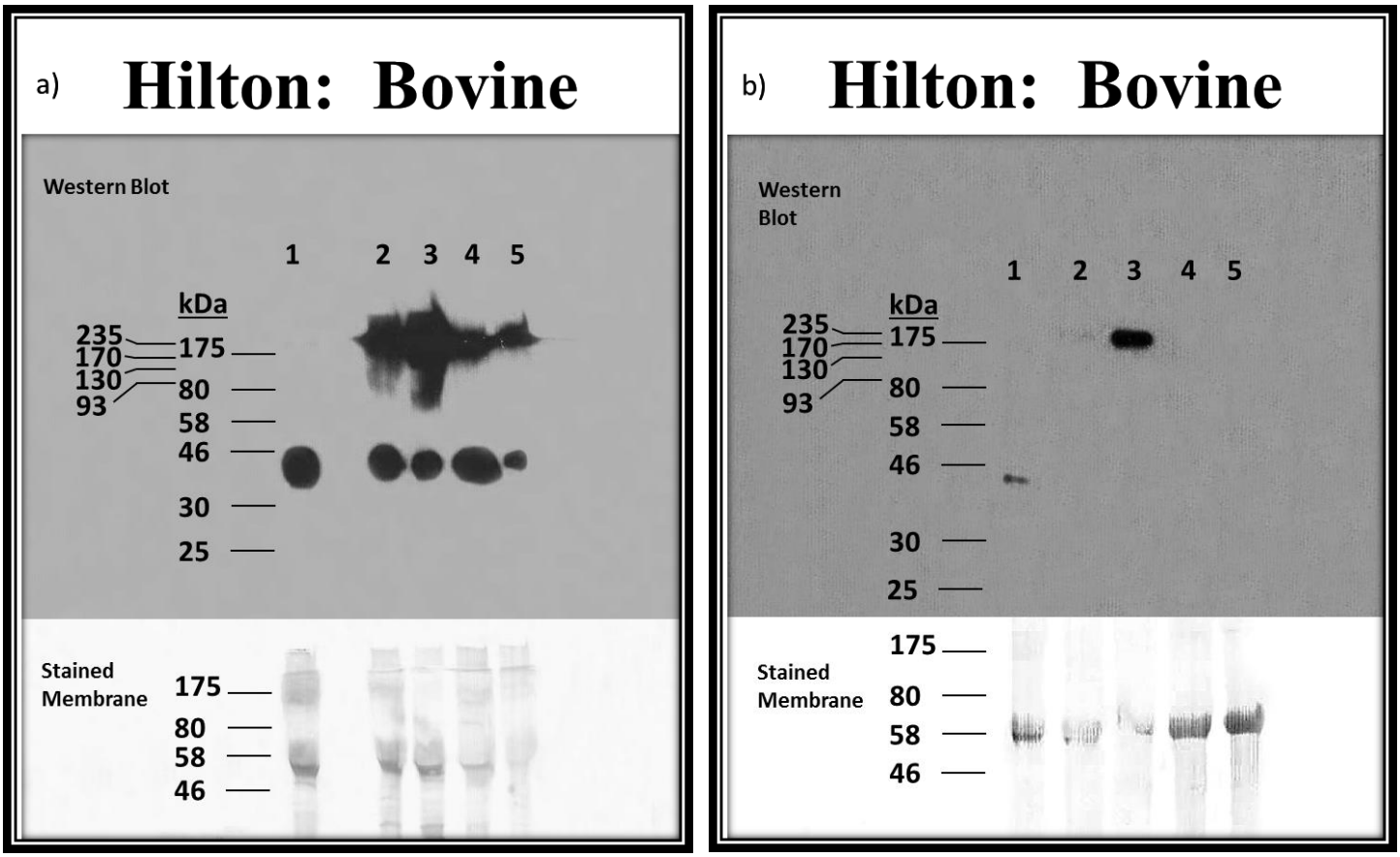

Figure 3.36 EXPT 10 – Western blots of PM bovine cartilage extracts acquired from the intervertebral joints of tail segments disinterred weekly (July 4 to August 5, 2013). Immunodetection of aggrecan was performed using MAb 2-B-6. A) Aggrecan (35µg protein per PM sample), represented at 230kDa, was detected for samples 0-31 days PM. CRPs weighing 38kDa were seen among samples 0-31 days PM. B) Bovine cartilage extracts (20µg protein per PM sample) using the same PM samples presented aggrecan (230kDa) for samples collected at 10 and 17 days PM. A single 38kDa CRP presented itself for the control sample. Lane 1 – Bovine control (0 days PM); Lane 2 – 10 days PM; Lane 3 – 17 days PM; Lane 4 – 24 days PM; Lane 5 – 31 days PM.

For samples 10 and 17 days PM, 230kDa CRPs were visible. The 230kDa CRP for PM cartilage extracted 10 days PM was far less intense than the CRP representing cartilage samples 17 days PM.

A live/dead cell assay was performed for fibro-cartilage samples extracted from bovine intervertebral joints 0-31 days PM (EXPT 10). Table 3.14 lists the percentage of cells that were viable at each of the PMIs examined. The percentage of live cells present for the control sample (0 days PM) of cartilage was 100%. At 10 days PM, 80% of chondrocytes remained viable while live cells were absent for samples collected 17-31 days PM (Figure 3.37). For cartilage samples 17-31 days PM, the number of dead chondrocytes (red) decreased with time. The timing of absolute cell death for chondrocytes derived from bovine intervertebral joints appeared to overlap with that for chondrocytes originating from articular cartilage extracted from the MCP/MTP joints of porcine trotters (EXPT 9). Both EXPT 9 and EXPT 10 were conducted around the same time period and were affected by similar climate (see Tables 3.11 and 3.13). Figure 3.38 presents a graph of the data in Table 3.14. The shape of the graph is polynomial bearing the slight semblance of a sigmoidal curve.

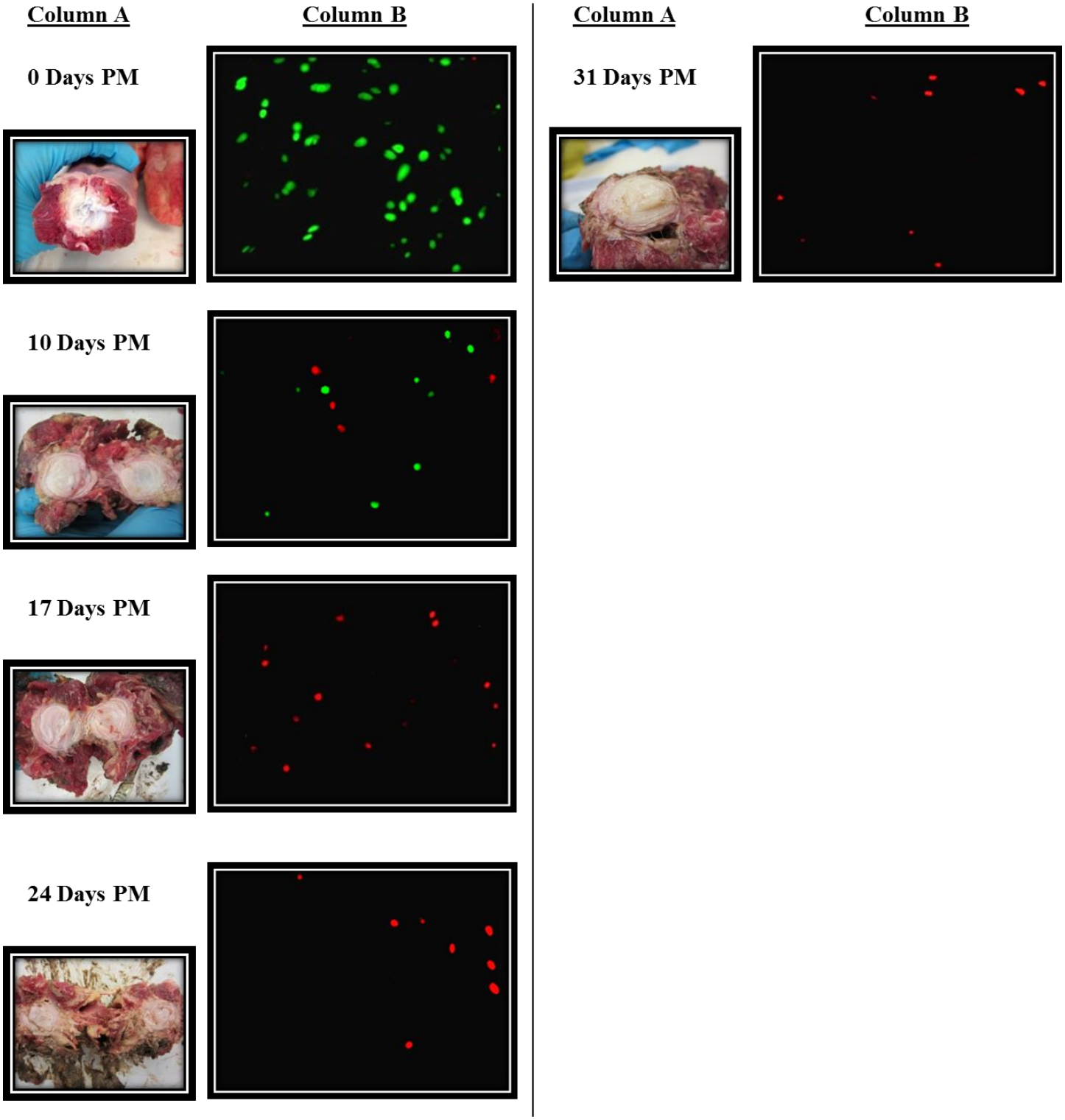

Figure 3.37 EXPT 10 – Column A shows images of 0-31 days PM bovine intervertebral cartilage (fibrous) disinterred weekly (July 4 to August 5, 2013). Like PM samples of porcine articular cartilage, the intervertebral cartilage of bovine tail demonstrated a gradual change in the tissue's colour. As PMI increased, cartilage changed from white to pink and finally beige. A fluorescence microscope (Olympus BX61) was used to capture corresponding live/dead cell images (Column B). Live chondrocytes (green) were present up to 10 days PM. Nuclei stained red (dead cells), were solely present 17-31 days PM. Their numbers decreased with increasing PMI.

Table 3.14 Weekly tabulations of the dates for which tail segments were disinterred, the number of days they spent below ground, the accumulated degree days experienced by each, and the percentage of live chondrocytes present shortly after disinterment (EXPT 10 – July 4, 2013 to August 5, 2013).

Date of Extraction	Number of Days PM	Accumulated Degree-Days (ADD)	Percentage of Live Chondrocytes (%)	Standard Deviation (+/-)
July 4	0	17*	100	0
July 15	10	168	80	31.4
July 22	17	310	0	0
July 29	24	447	0	0
August 5	31	576	0	0

* This ADD value was not taken into consideration for control cartilage extracted on the day of slaughter but was included among calculations for all experimental trotters disinterred.

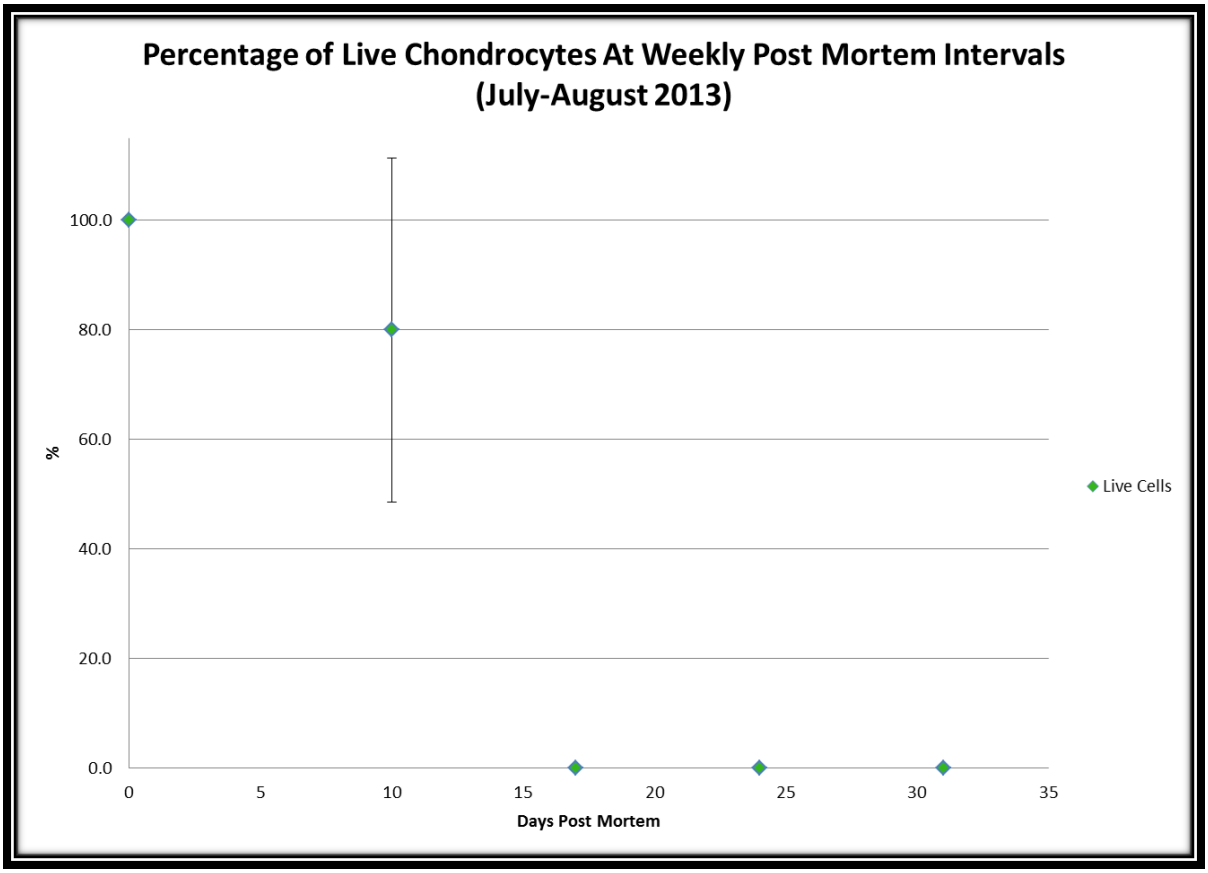

Figure 3.38 EXPT 10 – A graph illustrating the PM trend for the percentage of live chondrocytes at weekly intervals for bovine coccygeal intervertebral cartilage extracted 0-31 days PM (July 4 to August 5, 2013). The curvature of the graph is sigmoidal. At 0 days PM, all chondrocytes (100%) are viable. This proportion decreased to 80% by 10 days PM and then drastically to 0% for samples collected 10-31 days PM. Rate of cell death occurred rapidly between 10 and 17 days PM.

3.3.4 Statistical reports on the measures of association for independent variables PMI, average temperature and average precipitation with the percentage of live cells

Descriptive statistics for the dependent (percentage live cells) and independent variables are presented in Table 3.15. Pearson product-moment correlation coefficient tests measured the relationship of each independent variable (PMI, average temperature, and average precipitation) with data collected for the percent of live cells (dependent variable). Table 3.16 illustrates the computed correlation regression (r) values for each independent variable. A significantly strong negative relationship was observed between PMI and the percent of live cells, $r\,(21) = -0.85$ ($p < 0.001$).[3] Comparison of average temperature and percent of live cells presented a moderately negative correlation between the two variables, $r\,(21) = -0.32$ ($p > 0.05$). A weak negative correlation between percent live cells and average precipitation was observed among the variables, $r\,(15) = -0.14$ ($p > 0.05$).

A multiple linear regression analysis was performed to compute the relative relationships of the independent variables (PMI, average temperature and average precipitation) to chondrocyte survival (%) and to evaluate the strength of their influence. The analysis revealed that PMI was the most significant factor bearing the greatest influence for changes in the percent of viable cells with time, $R^2 = 0.94$, $F(3, 11) = 60.27$, $p < 0.05$, whereas average ambient temperature and average precipitation were found to have no significant effect on the percent of live PM chondrocytes (Table 3.17). A Durbin-Watson test was performed for this regression analysis (Table 3.17). A value of 2.25 indicates that no autocorrelation exists among the independent variables that would influence an over- or underestimation of this regression analysis.

[3] r (df) – correlation regression value with degree of freedom located between the parentheses; p – significance value.

Table 3.15: Descriptive statistics for the dependent (percent live cells) and independent variables.

Statistics		Percent Live Cells (%)	PMI (Days)	Average Temperature (˚C)	Average Precipitation (mm)
N	Valid	21	21	21	15
	Missing	0	0	0	6
Mean		35.3152	21.2381	9	16.1333
Standard Error of Mean		8.40224	3.17423	1.20317	4.07415
Median		6.95	22	9	12
Mode		0	.00[a]	13	0
Skewness		0.45	0.007	-0.123	0.765
Standard Error of Skewness		0.501	0.501	0.501	0.58

a. Multiple modes exist. The smallest value is shown

Table 3.16: Correlation between the percentage of live cells and other variables.

Parameter	N	Regression Coefficient (r)	
PMI	21	-0.85	**
Average Temperature	21	-0.32	
Average Precipitation	21	-0.14	

** Significant at the 0.01 level.

Table 3.17: Statistical outputs for measures of the regression model fit and scoring of coefficient variables, statistical significance of model (ANOVA test), and estimates of the amount of variation and statistical significance of independent variables with comparison to the percent of live cells.

Multiple Regression Model Summary for Predictor Coefficients[a] and the Dependent Variable[b]

Model	R	R Square	Adjusted R Square	Standard Error of the Estimate	Durbin-Watson
PMI, Avg Temp, Avg Ppt vs % Live Chondrocytes	.971[a]	0.943	0.927	10.754	2.254

a. Predictors: (Constant), PMI, Average Temperature, Average Precipitation
b. Dependent Variable: Percent Live Chondrocytes

ANOVA Test for the Overall Multiple Regression Model for Percent Live Chondrocytes

Model		Sum of Squares	Degrees of Freedom	Mean Square	F	P-value
1	Regression	20909.893	3	6969.964	60.267	.000[a]
	Residual	1272.162	11	115.651		
	Total	22182.056	14			

a. Predictors: (Constant), PMI, Average Temperature, Average Precipitation

Estimates and Statistical Significance of Coefficients[a]

Coefficients	Unstandardized Coefficients		Standardized Coefficients	t	P-value	95.0% Confidence Interval for B		Collinearity Statistics	
	B	Standard Error	Beta			Lower Bound	Upper Bound	Tolerance	VIF
(Constant)	108.680	6.750		16.101	0.000	93.824	123.536		
PMI	-2.456	0.187	-0.947	-13.104	0.000	-2.868	-2.043	0.998	1.002
Average Temp	-0.946	0.512	-0.133	-1.846	0.092	-2.074	0.182	0.997	1.003
Average Precip	-0.401	0.182	-0.159	-2.198	0.050	-0.802	0.001	0.998	1.002

a. Dependent Variable: Percent Live Chondrocytes

3.4 Post mortem trotters and fungal activity in soil environments

Although the CMP and HLT burial plots shared the same soil type, the effects of their contrasting soil environments (CMP exhibiting moist soil, whereas soil at HLT was extremely dry) were seen first-hand in patterns of hyphal growth. Weekly collections of fungal samples removed from soil encrusted trotters disinterred from CMP and HLT demonstrated growth characteristic of Zygomycota and Ascomycota. Characteristically, zygomycota are filamentous and fast spreading, whereas the mycelia of Ascomycota are closely interwoven together and exhibit slower growth rates.

For PM trotters disinterred weekly from the CMP and HLT burial plots (June 20 to August 2, 2011), fungal samples were collected from the adhering soil. Images of these soil covered trotters were taken to illustrate the presence or absences of hyphal (zygomycota) growth (Figures 3.39 and 3.40). At 7 days PM, the presence of hyphae (white and cotton-like growth) was clearly visible at the dismembered end of the trotters collected from CMP. The presence of this fungal growth is highlighted by a red oval in Figure 3.39. Trotters disinterred 14-42 days PM did not appear to exhibit hyphal growth when viewed first-hand.

Trotters disinterred weekly from Hilton during the same time period exhibited hyphae at 7-21 days PM (Figure 3.40). With increasing PMI, observation of this fungal growth gradually diminished and was no longer visible from 30 days PM and onwards. In comparison to trotters disinterred from CMP, fungal growth was far less extensive at 7 days PM. Although growth was minimal for trotters disinterred from HLT, the appearance of this fungus persisted for 3 weeks.

EXPT 2 - CMP Soil Environment

a)

b)

7 Days PM

14 Days PM

21 Days PM

30 Days PM

36 Days PM

42 Days PM

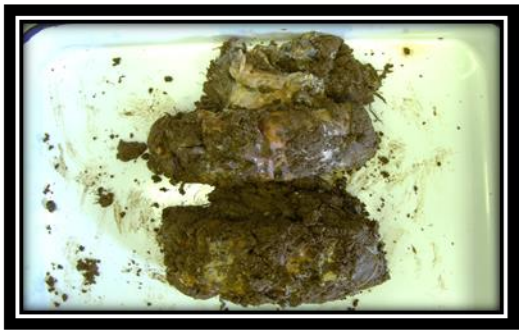

a) Partial overview of graves.
b) Trotters upon disinterment.
Red circles indicate areas of visible hyphal growth.

Figure 3.39 EXPT 2 – Images of PM trotters at the time of their disinterment. The appearance of fungal colonies were denoted by the presence of hyphal growth (white cotton-like growth) found in close proximity to pig trotters disinterred at the Compton locale June 20 - August 1, 2011). Hyphae were seen among trotters disinterred after 7 days PM and were absent from all other PM trotters (14-42 days PM).

EXPT 2 - HLT Soil Environment

a)

b)

7 Days PM

14 Days PM

21 Days PM

30 Days PM

36 Days PM

42 Days PM

a) Partial overview of graves.
b) Trotters upon disinterment.
Red circles indicate areas of visible hyphal growth.

Figure 3.40 EXPT 2 – Weekly disinterments of PM trotters disinterred from the Hilton burial plot (June 21 - August 2, 2011). The images containing red circles highlight the presence of fungal colonies detected by signs of hyphal growth (white cotton-like appearance) found in close proximity to soil covered porcine trotters. The presence of hyphae was seen among trotters disinterred 7-21 days PM.

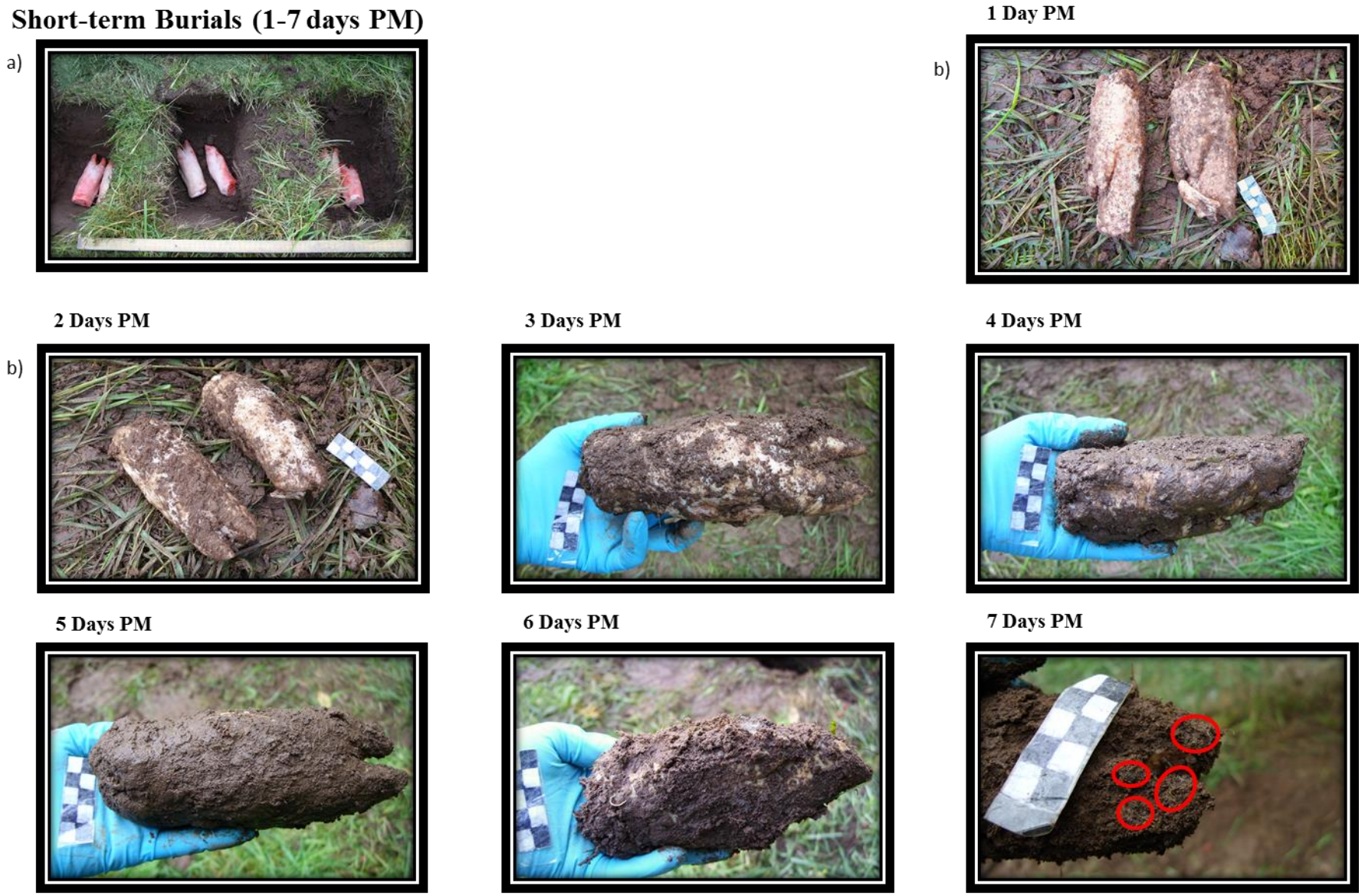

Figure 3.41 Short-term burial – PM trotters disinterred daily over a period of 7 days from the Compton burial site. Hyphal growth was not readily distinguished until 7 days PM as is indicated by red circles that highlight their occurrences.

The short-term burial conducted over 7 days involving daily disinterments of trotters was also examined for the presence of zygomycota (Figure 3.41). PM samples disinterred 1-6 days PM did not exhibit discernible hyphae. At 7 days PM the commencement of such growth were seen around and between the hooves of the trotters. The amount of growth was far less than that which occurred at the same time interval for EXPT 2 trotters disinterred from CMP. In an environment that is dry and nutrient deficient little hyphal growth was observed. However, the same was true for trotters buried in damp, nutrient rich soil where too much moisture restricted hyphal growth. Hyphae appeared to flourish in nutrient rich soil that was moist but not saturated.

Comparative analysis of the fungal growth for trotters disinterred at 7 days PM for EXPTs 2 and 3 (CMP) showed that the extent of hyphal growth for EXPT 3 was far less than that which appeared for trotters disinterred for EXPT 2. The soil environment for EXPT 2 was moist. For EXPT 3, the moisture content of the soil was considerably damper and rather muddy. Photographed images (Samsung S850) illustrating the extent of fungal growth and relative differences in soil moisture are presented below in Figure 3.42.

3.4.1 Fungal inoculations gathered from soiled trotters upon disinterment

Fungal samples inoculated on MEA media immediately after disinterment were subjected to incubation at 25˚C. One or several different colonies were typically noted within 2-3 days of incubation and were separated for re-inoculation in order to achieve pure colonies.

Figure 3.42 Images illustrating the differences in soil consistency and the extent of fungal growth (red circle) on trotters disinterred from CMP at 7 days PM (Samsung S850). a) The soil environment for EXPT 2 trotters is moist and b) demonstrates a notable amount of hyphal growth at the dismembered end of the trotter, whereas the c) soil environment for EXPT 3 trotters is saturated and exhibits a muddy texture and d) the amount of visible hyphal growth is minimal.

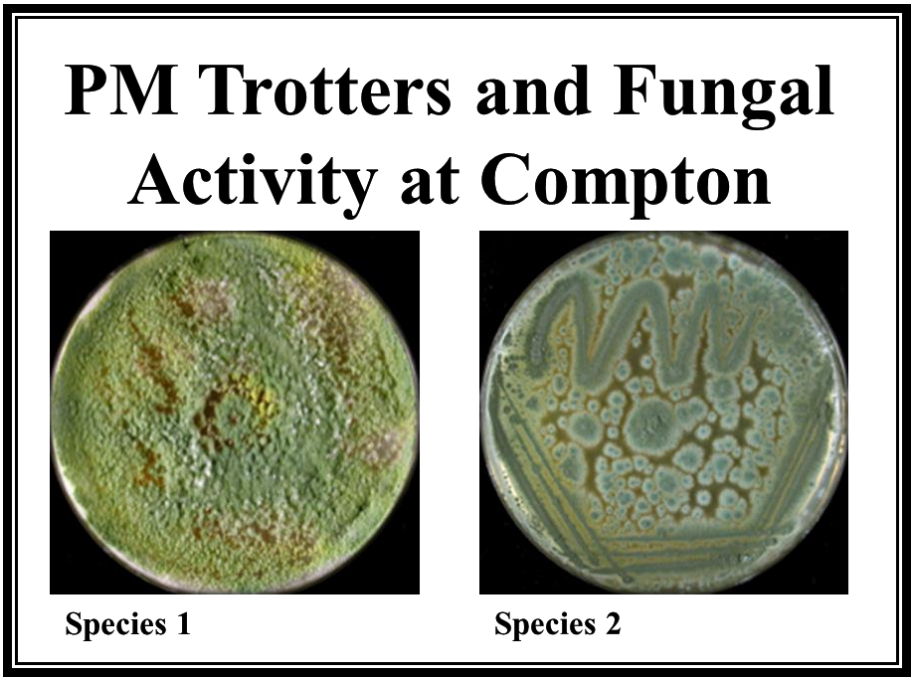

Figure 3.43 Fungal colonies collected from PM trotters that were disinterred at CMP. Species 1 produced rapidly spreading white hyphae that generated yellow and then green spores. Species 2 (an Ascomycota) generated discrete white colonies that dispersed and developed blue-grey spores. Photographic images courtesy of Dr Malcolm Inman.

EXPT 2 PM trotters disinterred from CMP, presented two characteristically different species of fungi that were consistently observed among samples collected weekly at 7-42 days PM (Figure 3.43) and were labelled Species 1 and 2. Species 1 initially appeared as white hyphae that rapidly covered the media plate. This fungus was succeeded by yellow and then green pigmented growths that overlaid the hyphae. On the other hand, Species 2 started out as discrete white colonies that became blue-grey. With the exception that fungal samples were not collected for trotters disinterred 36 days PM, fungi resembling Species 2 were not detected among trotters that were disinterred 14 and 21 days PM. Likewise, Species 1 was not discovered on trotters that had been unearthed after spending 30 and 42 days PM below ground. Images of fungal species acquired from PM trotters disinterred weekly at CMP are presented in Figure 3.44.

Three distinct fungal species were found in association with PM trotters disinterred from HLT (EXPT 2). Cross-comparison of these samples with those collected from CMP during the same time period indicated that two out of the three fungi observed from HLT (Species 1 and 2) were the same growth exhibited by trotters from CMP (Figure 3.43 and 3.44). The third fungal species that was observed, Species 3 (Figure 3.45), formed discrete black colonies that were succeeded by a tough olive green growth. Species 1 was detected among trotters 7-28 days PM. Species 2 was present for trotters 7-21 and 42 days PM, whereas Species 3 was found in association with trotters 49 days PM (Figure 3.46).

For the short-term burial that occurred for 7 days, PM trotters presented fungal Species 1, 2 and 3. An additional fungal colony, Species 4 (Figure 3.47), was observed at 6 days PM (Figure 3.48). Its growth was brown and "sandy-looking." Of the fungal samples

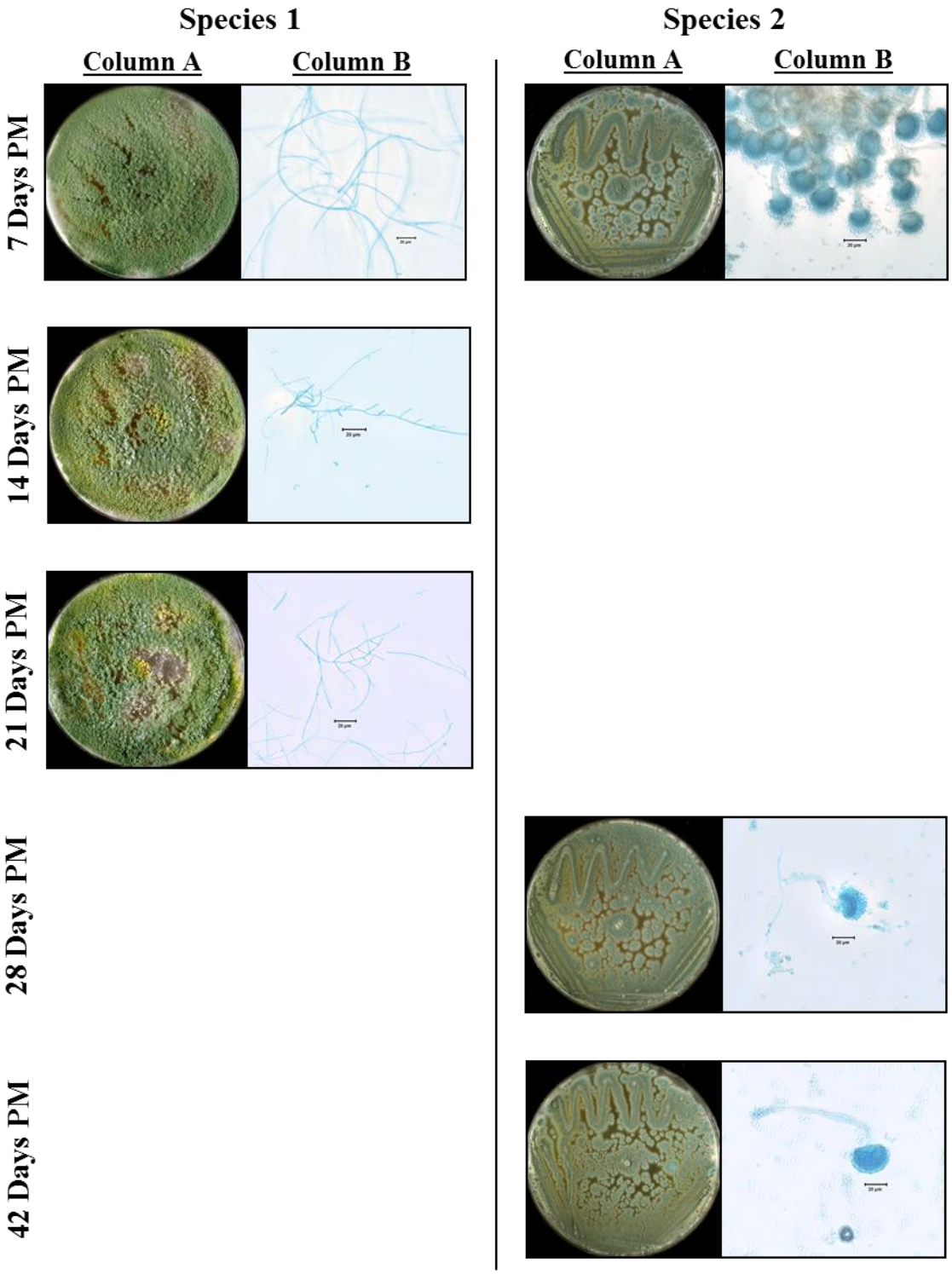

Figure 3.44 EXPT 2 – Images of MEA petri dishes inoculated with fungal samples collected from PM trotters at CMP are presented under Column A (images courtesy of Dr Malcolm Inman). Species 1, a member of the zygomycota, produced rapidly spreading white hyphae that generated yellow and then green spores. Species 2 generated discrete white colonies that dispersed and developed blue-grey spores. Column B presents microscopic images (Nikon Eclipse ME60) taken at 400X that illustrate the morphological features of spores.

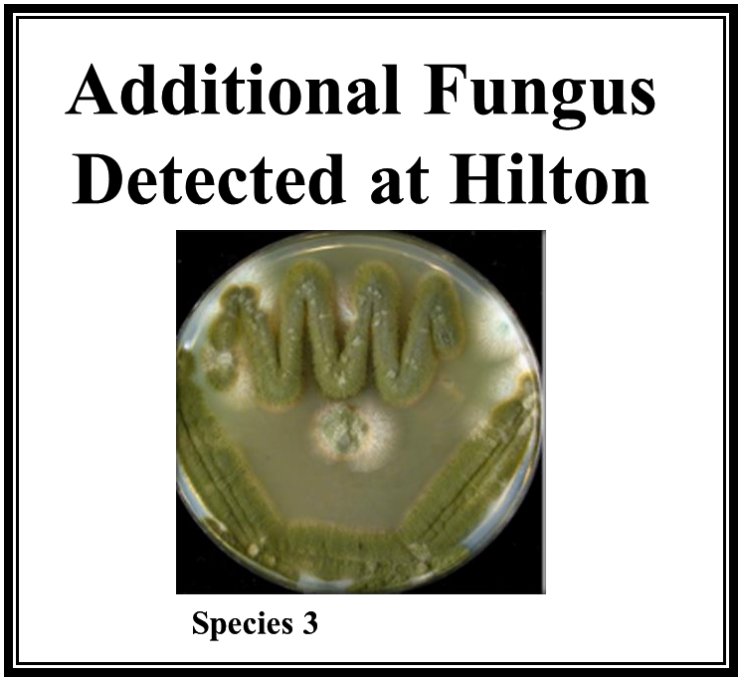

Figure 3.45 Fungal species 3 detected solely among PM trotters disinterred from the HLT soil environment. Species 3, an Ascomycota, initially presented black, discrete colonies that later appeared olive green in colour and that were rigid (Image courtesy of Dr Malcolm Inman).

collected for this short-term experiment, Species 1 and 2 were the prominent colonisers. Species 1 was detected among 3, 5 and 7 days PM trotters while Species 2 was collected from trotters 1, 4, and 7 days PM (Figure 3.48).

Figures 3.44, 3.46 and 3.48 also present microscopic images of the fungal specimens taken at a magnification of 400X. These images illustrate the sporulating structures that are typically used to aid with the classification of unknown fungi. Cross-comparisons of Species 1 to 3 with like samples of fungi from different experiments presented identical microscopic images for each unknown species. Figure 3.49 presents enlarged microscopic images representing the spore structure of each fungus. A fungal key, *Illustrated Genera of Imperfect Fungi (3rd Edition)*, was referred to in an attempt to identify the genuses of these species. Species 1 was classified as belonging to the genus *Varicosporium sp.* on account of the following description: "No sharp distinction between conidiophores and conidia, conidiophores simple or sparingly branched near the apex, bearing conidia apically; conidium (blastospore) consisting of a main elongated axis with 2 or 3 laterals on one side; each lateral is septate and branched again, hyaline; saprophytic, aquatic or in soil" (Barnett & Hunter, 1972, pp. 136). Species 2 was characterised as a member of the genus *Aspergillus sp*. owing to the appearance of conidiophores that were "upright, simple, terminating in a globose or clavate swelling, bearing phialides at the apex or radiating from the entire surface; conidia (Figure 3.47).

Figures 3.44, 3.46 and 3.48 also present microscopic images of the fungal specimens taken at a magnification of 400X. These images illustrate the sporulating structures that are typically used to aid with (phialospores) 1-celled, globes…, basipetal chains." (Barnett & Hunter, 1972, pp. 136). For species 3, the fungal structure and its pigmentation looked characteristic of the fungi belonging to the genus *Monilochaetes sp*. According to

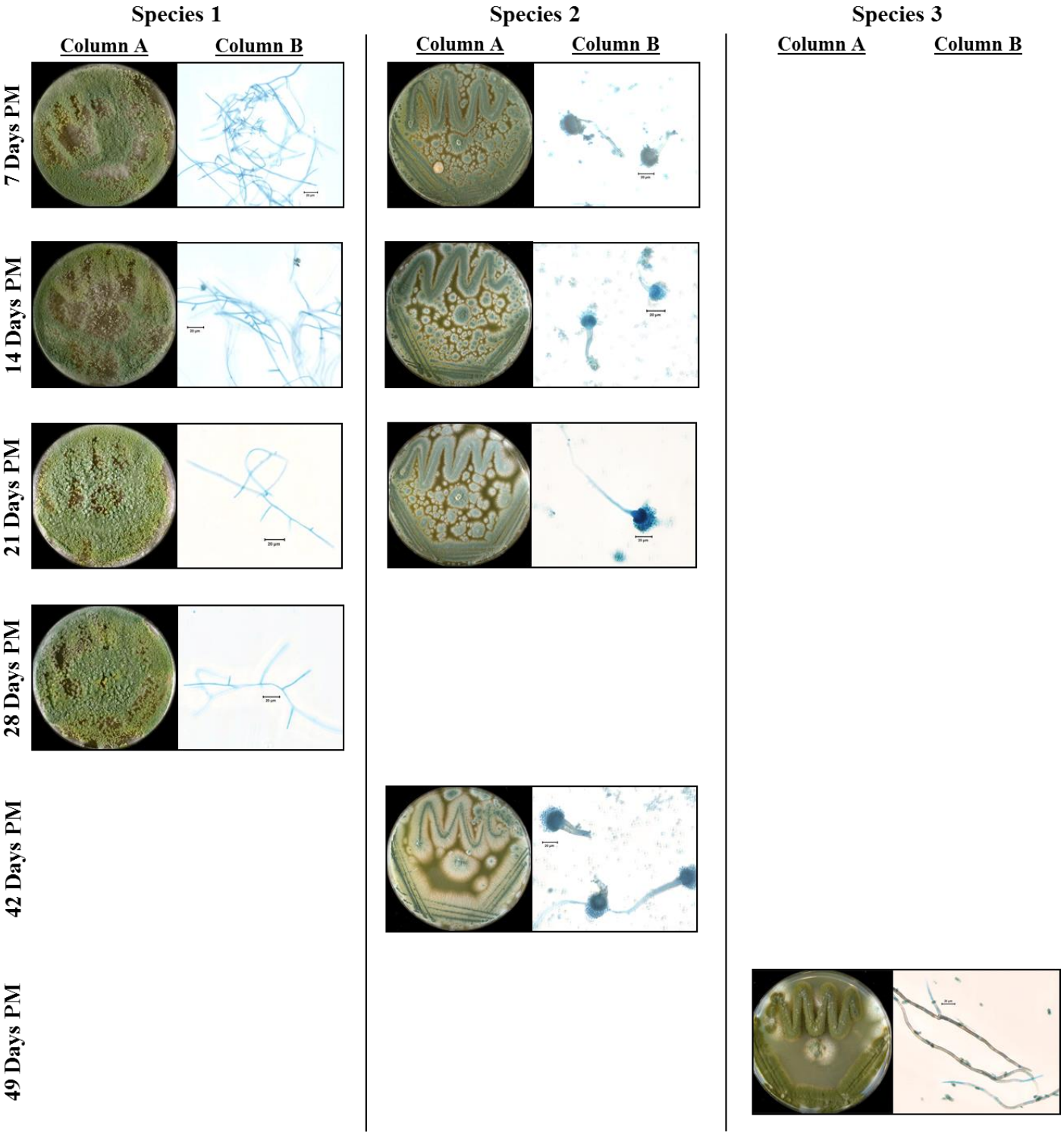

Figure 3.46 EXPT 2 – Column A: MEA petri dishes inoculated with fungal samples from PM trotters disinterred from HLT (images courtesy of Dr Malcolm Inman). Species 1 and 2 appear to be the same species observed for specimens collected from the CMP burial plot; the physical appearance and growth patterns of these microorganisms exhibited the same characteristics as the fungal samples obtained from CMP. Column B: detailed microscopic images (Nikon Eclipse ME600) of the corresponding fungus' spores at 400X. The scales presented in the images measure 20µm.

Barnett & Hunter (1972), members of this genus bear conidiophores that are dark in colour, "erect, slender, [and are] usually simple, septate" (pp. 82). The conidia are either hyaline (glass-like) in appearance or develop pigment with increasing age. They are generally produced individually at the apex of the conidiophore. However, when subjected to environments where the amount of humidity is high, the conidia are produced in chains (Barnett & Hunter, 1972). Genus determination for Species 4 was not attempted due to difficulties with visualising clear and detectable microscopic images detailing spore structure.

No particular trend was observed for the temporal colonisation of the various fungal species observed. Species 1 and 2 were the most prominent fungi found in association with decomposing trotters buried in soil environments and appeared to colonise the samples within a few days of interment. Species 3 demonstrated rare occurrences among the sample populations investigated for the CMP and HLT burial site, whereas Species 4 was solely observed from HLT. Species 3 was present among PM samples disinterred at 49 days PM (EXPT 2) and 2 days PM (short-term experiment). Fungi representative of Species 4 was associated with 6 days PM trotters disinterred from HLT.

Figure 3.47 Fungal species 4 was discovered among 6 days PM trotters collected from CMP. This fungal species is a member of the phylum, Ascomycota. Its hyphal growth was cream/tan coloured with dark spores and exhibited a sand-like appearance (image courtesy of Dr Malcolm Inman).

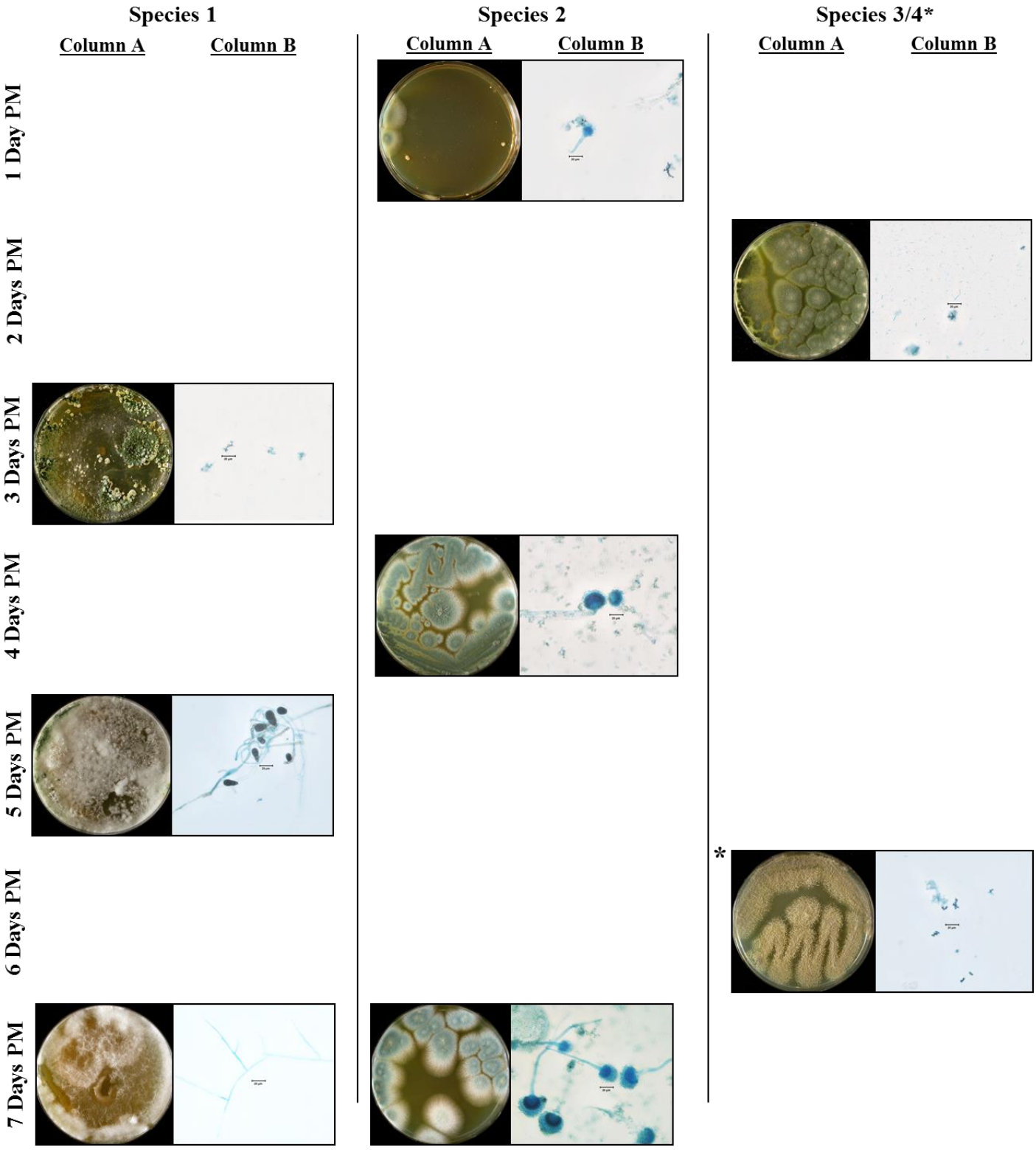

Figure 3.48 Short-term burial – Column A illustrates the fungi found in association with PM trotters disinterred from CMP on MEA nutrient plates. These specimens of fungi were collected from PM trotters that were disinterred daily for a period of 7 days (images courtesy of Dr Malcolm Inman). Species 1 to 3 were present among the fungal samples observed, in addition to a fourth (species 4, differentiated by an asterisk above for 6 days PM trotters) that was not observed for the previous experiments. Column B shows a 400X magnification of the corresponding fungus' spore morphology (Nikon Eclipse ME). The scale present measures 20µm.

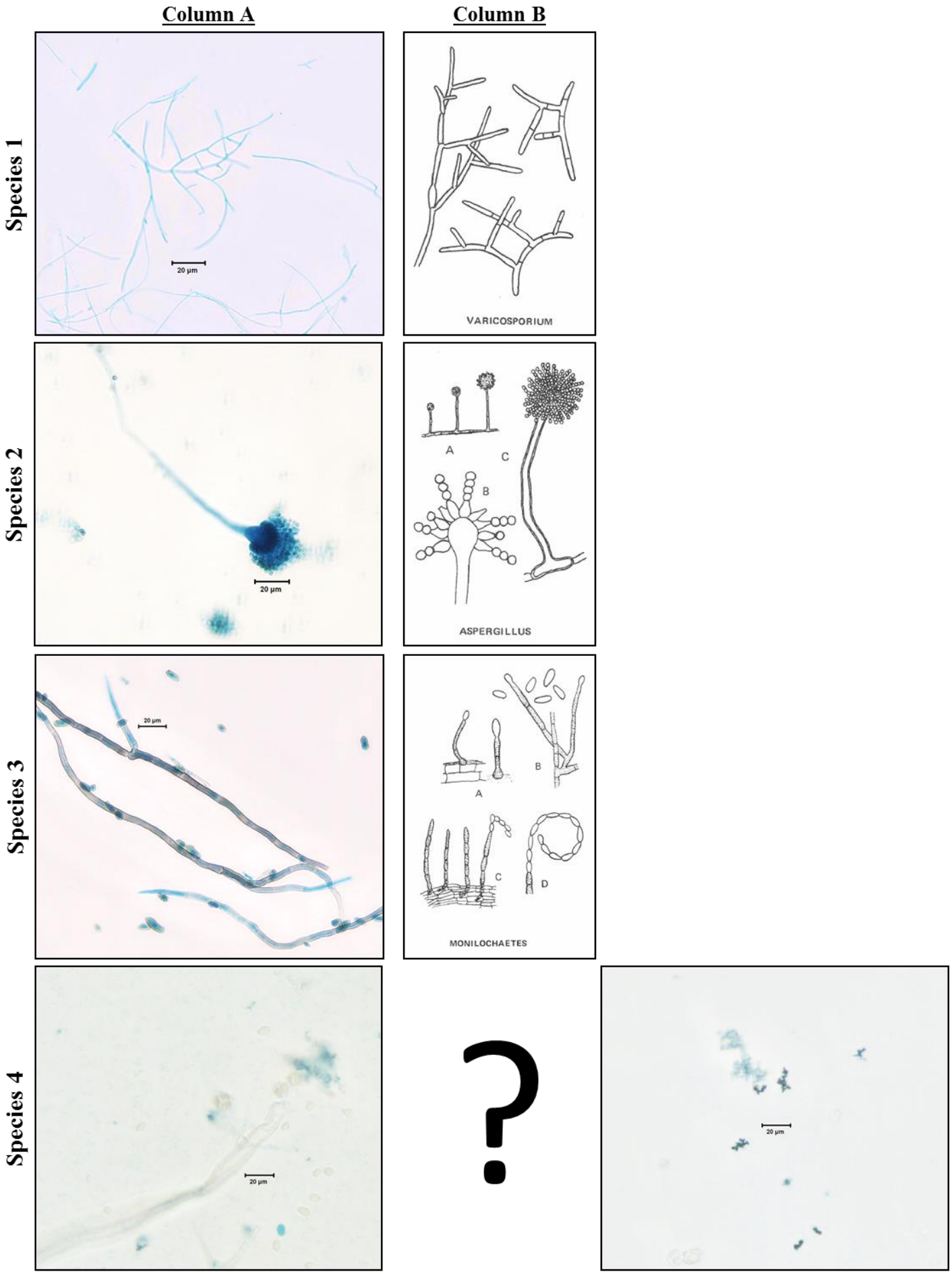

Figure 3.49 Enlarged images representing the microscopic features (Nikon Eclipse ME) of fungal spores for species 1-4 at 400X (Column A) and representations of each genus as depicted in the fungal key, *Illustrated Genera of Imperfect Fungi* (Barnett & Hunter, 1972) for comparative value (Column B).

Discussion

Chapter 4

4.0 Discussion

4.1 Evaluating the post mortem properties of degraded cartilage

The data gathered from this pilot study offers novel insights about the biochemical properties of PM cartilage collected from trotters that were buried in soil environments. These results have proven to be quite interesting and are worthy of further consideration. They illustrate that the PM destruction of cartilage is an orderly process that occurs over a protracted timescale, unlike other soft tissues, such as skin, muscles, ligaments, and nerve and blood vessels, which undergo rapid biochemical changes that impact the rate of decomposition in what misleadingly appears as an ostensibly unpredictable and chaotic manner (Powers, 2005). Rivers and Dahlem (2014) describe autolysis as one of the governing PM processes that disrupts cellular homeostasis, thereby "driving the intracellular environment towards chaos." The ability to witness the decelerated process of PM decay as demonstrated by cartilage is owed to its low cell density and slow metabolic rate. The results presented in this study are the first to explore the molecular breakdown of PM cartilage and its possible applications for forensic investigations. Results obtained for water content, aggrecan destruction and chondrocyte viability suggest that PM cartilage is a fairly stable tissue in death as it is in life. This attribute is likely owed to its biochemical properties and structural organisation.

4.1.1 The macroscopic properties of post mortem cartilage

Systematic changes in the colour and robustness of PM cartilage were observed and demonstrated that the soft tissue gradually changes from white or bluish-white to dark pink before finally exhibiting a cream or beige colour. Osteoarthritic cartilage is known to change

from a “pearly white color to yellow or brownish” (Athanasiou *et al*., 2013). Simultaneously, the tissue becomes flaccid and undergoes resorption, slowly retreating away from the cartilage bone interface as PMI increases. These observations were consistent with those reported by Rogers (2010) and ten Broek (2009). They reflect the oxidative stress that cartilage undergoes in extremely hypoxic environments. Although cartilage requires a hypoxic environment with a partial pressure of ~7-10% of atmospheric pressure (Goldring & Marcu, 2009; Henrotin *et al*., 2005) to support homeostasis, oxygen is still required by mitochondria for basal metabolic activity to continue. Consequently, chondrocytes located in the superficial zone contain a high mitochondrial density with comparison to other zones (Henrotin *et al*., 2005). In a review (Henrotin *et al*., 2005), the effects of oxygen and reactive oxygen species (ROS) were examined, including “molecules like hydrogen peroxide (H_2O_2), ions like the hypochlorite ion (OCl^-), radicals like hydroxyl radical ($\bullet OH$) or the superoxide anion (O_2^-) which is an ion and a radical at the same time,” and their impact on articular cartilage homeostasis. ROS are known for the role they play in intracellular signalling and cell physiology. They are responsible for the activation and proliferation of cells, and cell death (Carlo & Loeser, 2003; Martin & Buckwalter, 2006; Roughley & Mort, 2014). Henrotin *et al*., (2005) reported that a partial atmospheric pressure of approximately 5% did not induce chondrogenesis in rat articular cartilage. The same observation was made for rabbit articular cartilage (Portron *et al*., 2013). However, Henrontin *et al*. (2005) state that when ROS are present in excess amounts, there is a disruption in the normal balance between oxidants and antioxidants resulting in “oxidative stress” that leads to the catabolism of cartilage. The exact nature of this observed colour change in PM cartilage (white to dark pink) is not yet understood and requires further investigation. However, Athanasiou *et al*. (2013) state that an increase in PG destruction results in the emergence of an irregular

tidemark that becomes punctuated with blood vessels. The emergence of blood vessels resulting from enzyme/ROS activity may explain the colour change among PM cartilage.

4.1.2 Post mortem cartilage and water retention

Observations of the above macroscopic changes exhibited by cartilage samples 0-42 days PM generated questions about the tissue's water content over time. It was hypothesised that the percentage of water constituting cartilage would decrease with increasing PMI. The rationale for this assumption was that the perceived loss in tissue robustness and the gradually diminished surface area of cartilage along its subchondral bone was due in part to water loss resulting from ECM degradation. Furthermore, it was assumed that the proteolysis of aggrecan would result in the release of water molecules bound to GAGs to facilitate the process of hydrolysis (Hopkins, 2008). This process was expected to participate in the on-going destruction of aggrecan peptide bonds that would result in tissue destruction and perhaps the inability for GAGs to retain water. Loss of water retention with increasing PMI would serve as a plausible explanation for the lack of structural stability and rigidity among the ECM. This was witnessed in later PM samples of cartilage that appeared notably pink in colour, and became increasingly softer and progressively thinner.

Several experiments were conducted to determine whether soil environment would have an impact on the percent water content of cartilage with increasing PMI. The average percent water content for control porcine cartilage was computed and a value of approximately 70% was obtained. This percentage is well within the range of those reported for human articular cartilage by Dudhia (2005) (~70% wet weight), Lüsse *et al*.(2000) who provide a range of 70-75% for "bound and unbound water," and Mow *et al*. (1992), as well as Kheir and Shaw (2009), who established much broader ranges (60-85%). One-way ANOVA

and paired-sample t-test statistics revealed that there were no significant differences in the mean percent water content as PMI increased from 0-42 days PM, and that the overall differences in mean percent water content for samples interred at CMP (71%) and HLT (70%) were not significant; the null hypothesis stating that no change in water content would be observed was accepted. Therefore, it was concluded that soil environment (moist and nutrient-rich versus dry and nutrient-deficient) and PMI did not impact the water content of PM cartilage for buried trotters.

The percent water content for cartilage extracts collected weekly from 0-42 days PM for EXPTs 1 and 2 remained relatively constant with increasing PMI for both soil environments. Values for the water content of PM cartilage was collectively gathered from both comparative experiments (EXPT 1 & EXPT 2) and presented as mean percentages ranging from 69% to 73%. These values imply that PM cartilage continues to retain water despite obvious signs of tissue degradation; GAGs that remain within the ECM of PM cartilage continues to function normally as their polyanionic properties remain preserved. The GAG side-chains of aggrecan monomers possess polar negative charges that form hydrogen bonds with water molecules present in cartilage (Dudhia, 2005; Lüsse *et al*., 2000; Wang *et al*., 2013). According to Dudhia (2005), the consequence of such large aggregating PGs is the natural uptake of large volumes of water which is owed to the CS and KS side-chains. This feature is quintessential for maintaining hydration levels in articular cartilage, providing the tissue with weight-bearing properties, and explains why the percent water content of PM cartilage was conserved despite increasing PMIs.

EXPT 1 presented cartilage samples with percent water content values that fell below the lower limits of the range established for mean percent water content (refer to paragraph above). Cartilage specimens collected at 7 days PM from CMP possessed an average water content of 65%, while cartilage collected from HLT at 28 days PM had a water content of

66%. Since these outliers fall below the range established for mean percent water content, their lower values may be attributed to loss of water during sample preparation or a microenvironment that promotes faster breakdown.

Cartilage is composed of two types of water: water that is bound to GAGs which forms an integral part of the PG and collagen network, and interstitial water that is free to traverse the porous ECM when osmotic pressure is applied due to mechanical movement (Mow *et al*., 1992; Wang *et al*., 2013). During dissection, it was noted that cartilage samples dehydrated quite rapidly (within a timespan of approximately 10 minutes at room temperature) when not immediately secured in sealed containers and left exposed to air. Water content varies within the ECM of cartilage. As stated by Mow *et al*. (1992), the articular surface of human cartilage exhibits the highest water content (approximately 80% of the total wet weight volume) and decreases to approximately 65% in the deep zone. When cartilage is not subjected to mechanical stress, the negatively charged GAGs achieve a state of electrostatic equilibrium. This is where the excess charges imparted by the GAGs exert repulsive forces on neighbouring GAGs that are minimised by achieving an ideal amount of distance away from each other. When cartilage is in a state electrostatic equilibrium, the majority of its water remains dissociated from the GAGs (Lüsse *et al*., 2000). Theoretically, if PGs trapped within the ECM of PM cartilage exhibit GAGs that have endured autolytic and putrefactive processes, then the tissue should remain in a permanent state of electrostatic equilibrium. If this is the case, then discrepancies in the values obtained for the percent water content of PM cartilage samples collected at 7 days PM (CMP) and 28 days PM (HLT) can be attributed to a loss of unbound water by way of the porous ECM upon prolonged exposure to air. According to Wang *et al*. (2013), the destruction of PGs increases the porosity and permeability of the ECM. This phenomenon would explain why dissected cartilage dehydrates when exposed to air.

The observed water retention in PM cartilage, despite evidence of tissue degradation (i.e. colour change, flaccidity and tissue loss), may in fact be ascribed to ECM components that have not yet undergone PG destruction. It is likely that cartilage degradation is governed by a gradual and ordered process whereby destruction of PGs results in the systematic removal of collapsed tissue. When PG monomers that form large aggregates in cartilage undergo destruction, they are broken down into smaller, unstable fragments that are expelled from the ECM (Wang *et al*., 2013). In injured and OA hyaline articular cartilage (Kheir & Shaw, 2009; Wang *et al*., 2013), as well as IVJ cartilage (Iatridis *et al*., 2012), the concentration of PG is reduced. Loss of PGs results in modification of the collagen network and increased hydration (Athanasiou *et al*., 2013; Iatridis *et al*., 2012; Kheir & Shaw, 2009; Wang *et al*., 2013). In turn, increased water content and porosity leads to softening of the cartilage tissue (Kheir & Shaw, 2009). These degenerative structural changes were macroscopically observed among notably degraded samples of PM cartilage. Therefore, it may be that the mechanisms responsible for degenerative joint diseases are the same or similar to the ones that govern the PM destruction of articular cartilage.

4.2 Post mortem changes within the cartilage extracellular matrix

4.2.1 An evaluation of control cartilage proteoglycan

A preliminary experiment to determine the minimum time required to achieve optimal PG extraction from unprocessed (samples not subjected to pulverisation) cartilage samples was conducted. The purpose of using unprocessed cartilage extracts was to minimise the amount of mechanical destruction that pulverisation would generate, thereby diminishing artificially destroyed aggrecan. Extractions were conducted for 8, 16, 24, 40 and 48 hours. A Coomassie blue stained SDS-PAGE gel illustrated protein bands that reached maximum

intensity by 24-hours. Protein bands for samples extracted for 40 and 48 hours presented protein bands of relatively equal intensities with the exception of trotter 2 samples extracted for 40 hours and trotter 1 samples extracted for 48 hours. The intensities of these protein bands were notably reduced and are likely the result of improper solubilisation of protein samples after drying protein precipitates. In such solutions, the protein sample forms globules that are difficult to re-suspend in solution. The protein solution is not homogenised and generates a sample solution where the concentration of protein extracts is markedly lower and therefore, the amount of protein added to the loading buffer is less than anticipated.

Fresh samples of cartilage were extracted from five randomly selected forelimbs attained from five different pigs within 3-4 hours of slaughter. Protein extracts derived from these cartilage samples were subjected to Western blot analysis and probed with MAb 2-B-6 for detection of individual variation among aggrecan molecules. The presence of high and low molecular weight CRPs were seen at approximately 230kDa and 38kDa. The presence of lower molecular weight CRP subpopulations situated between the 175kDa and 58kDa markers were also visible. These CRPs fall within the limits for observing the structural and catabolic neoepitopes of aggrecan that has been probed with MAb 2-B-6 (Caterson *et al.*, 2000). The presence of these CRPs will be further discussed later. In general, the results indicate that no notable discrepancies exist in the pattern of aggrecan CRPs present for control samples 1-5. The CRPs for control samples 1-5 demonstrate uniformity in their appearance. To establish that the chondroitinase ABC enzymes were viable and that the results obtained for these samples were not due to some unforeseen PM process or shared immunogenicity, Western blots were performed for undigested and chondroitinase ABC digested protein samples. No CRPs were seen among undigested samples. However, control cartilage digested with chondroitinase ABC yielded a CRP confirming the validity of the results obtained for controls 1-5. These tests concluded that the images obtained for control

samples 1-5 in Figure 3.4 were in fact depictions of aggrecan-related bands and that the digestion protocol used was successful. The results of this test, and that conducted for PM samples later on (image not shown), also imply that C-4-S chains remain intact throughout the processes of PM decay and that the neoepitope is specifically generated in response to enzymatic digestion with chondroitinase ABC. Therefore, any variations observed among PM samples of cartilage would be deemed genuine artefacts of aggrecan degradation.

Visibility of CRPs for control samples 1-5 signified that the cross-reactivity of MAb 2-B-6 was not exclusive to human cartilage. Cross-reactivity of this antibody with the chondroitinase digested aggrecan motif presented by porcine specimens was indicative of structural homology with humans. The presence of this C-4-S motif is quite conserved among higher mammals (Doege *et al.*, 1991). Likewise, the majority of the amino acid sequences in aggrecan are highly conserved among many different species (Doege *et al.*, 1991; Kiani *et al.*, 2002). This is especially true for amino acid sequences that constitute major proteolytic sites. Such sites include those that are cleaved by MMPs (FVDIPEN) and aggrecanase (NITEGE) (Doege *et al.*, 1991; Flannery *et al.*, 1998; Little *et al.*, 2002; Yasumoto, 2003). Cross comparison of the amino acid sequences for various species showed that the MMP cleavage site was highly conserved among humans, pigs, horse, sheep, dog, rat and mouse, whereas the amino acid sequence for the aggrecanase cleavage site was conserved among human, pig, horse, cattle, sheep, rabbit, and rat. The shared amino acid sequences for these cleavage sites among humans and pigs, as well as the chondroitinase ABC digested C-4-S neoepitope, increases support for the use of pigs as human models in forensic investigations.

4.2.2 Post mortem changes in aggrecan are not detectable within the first PM week

A short-term experiment examining the PM activity of aggrecan within the first week of interment demonstrated no notable changes across samples disinterred daily over a 7-day period. This suggests that the concentration of catabolic cytokines (proteases) had not yet reached a critical threshold sufficient enough to elicit disruptions in the homeostatic equilibrium of the cartilage matrices. Subsequently, the commencement of aggrecan degradation is postponed. It is also possible that the effects of aggrecanolysis occurring within this time period were not significant enough to be to be detected by Western blot analysis. Taking into consideration the physical properties and structures of cartilage, it is highly likely that the tissue's low cell density and tough collagen fibres (Athanasiou *et al*., 2013; Dent *et al*., 2004; Goldring & Marcu, 2009; Kheir & Shaw, 2009; Moger *et al*., 2007; Pearle *et al*., 2005) are truly viable in the short term (see later) and capable of enduring a considerable amount of physiological and environmental stress before exhibiting signs of breakdown. An extremely low population of chondrocytes trapped within a thick ECM translates into delayed transport of cytokines to initiate catabolic pathways (Ikram *et al*., 2004; Zhang & An, 2007) which postpones cartilage destruction.

4.2.3 Soil environment does not influence differences in the post mortem degradation of cartilage

The basis for having interred trotters below ground is that the rate of decomposition is approximately 8 times slower, especially for bodies buried in shallow graves, than that for remains situated above ground (Jaggers & Rogers, 2009; Rodriguez, 1997; Vass *et al*., 2004; Vass, 2011). This reduction in the rate of decomposition below ground can be ascribed to an environment that is typically cooler in temperature and exhibits little or no insect activity (Vass, 2011). Such environmental conditions made it possible to gradually observe the PM

processes that cartilage extracellular and cellular matrices undergo for a period of up to 44 days PM. Furthermore, the rate of decomposition is also slowed as a result of reduced insect and scavenger activity (Carter & Tibbett, 2008a).

Comparative analyses of PM cartilage samples collected from trotters interred in different soil environments (CMP – moist, nutrient-rich; and HLT – dry, lacking humic material) are representative of samples collected during the spring (EXPT 1) and summer (EXPT 2) months of 2011 (overall average ambient temperatures = 11.9˚C for EXPT 1 and 17.6˚C for EXPT 2). Western blots of aggrecan degradation over the span of 42 days (for EXPTs 1 and 2) display MAb 2-B-6 CRPs with molecular weights approximating 230kDa and 38kDa (Figures 3.7 and 3.8). These high and low molecular weight CRPs were present among control and experimental samples for up to 21 days PM, with the exception of samples collected at 0 days PM for the CMP spring experiment. For this particular sample, no 38kDa CRP is present (Figure 3.7a). Semi-quantitative assessments of these CRPs show that with growing PMI, there is a corresponding increase in the intensity of the 230kDa CRP. This trend implies that the volume of intact aggrecan decreases as the number or volume of lower molecular weight heterogeneous subpopulations accumulates. On the other hand, the 38kDa CRPs do not express any particular trend with increasing PMI aside from samples collected from the CMP soil environment during the summer for EXPT 2 (Figure 3.8b). This particular Western blot suggests that a rapid conversion of degraded aggrecan subpopulations occurred to produce a final product weighing 38kDa. This 38kDa antigenic glycopolypeptide gradually accumulates with time while the protein core of aggrecan simultaneously disintegrates.

The heterogeneity of PM aggrecan, as seen among these Western blots, shows the distinct emergence of bands representing CRPs for samples disinterred from HLT, whereas PM samples collected from CMP presents gradients situated between 175kDa and 58kDa.

These slight differences in the appearance of the heterogeneous subpopulations of aggrecan may be attributed to differences in the moisture content of the soil environment. As section 4.1.2 alludes, water is an essential component for the process of decomposition. The PM destruction of proteins is dependent upon the activity of enzymes to break apart peptide bonds. In order for this process to take place, enzymes require a set amount of water to maintain their structural integrity in order to perform their function(s). They also require the assistance of water molecules to break apart peptide bonds (Hopkins *et al*., 2000). The smooth transition of aggrecan by-products to a final 38kDa derivative is likely facilitated by a moist soil environment that promotes ideal conditions for proteolysis. Conversely, a dry soil environment may cause bodily fluids to be leached to the surroundings and therefore, prolong proteolytic events (Hopkins, 2008).

An experiment conducted by Kashiwagi *et al*. (2004) examined the proteolytic effects that modified versions of ADAMTS-4, had on aggrecan degradation. Aggrecan samples incubated with this enzyme for long periods of time presented a number of low molecular weight subpopulations of aggrecan that were made visible with MAb 2-B-6. The appearance of aggrecan subpopulations among the control and experimental samples examined in this study may also be attributed to prolonged enzymatic digestion (Kashiwagi *et al*., 2004) or small quantities of degraded aggrecan known to accumulate in aged cartilage (Bayliss & Ali, 1978a; Dudhia, 2005; Dudhia *et al*., 1996). Overall, the general appearance of the CRPs present for the comparative samples collected for EXPTs 1 and 2 (Figures 3.7 and 3.8) are in agreement with those seen among the five test control samples in Figure 3.4. CRPs bearing the greatest intensities are present at 230kDa and 38kDa. With increasing PMI, these CRPs are accompanied by less intense heterogeneous subpopulations of aggrecan that grows in number and intensity as time goes on.

The presence of these high and low molecular weight bands have been described in a report written by Bayliss and Ali (1978b) and describes the sedimentation profiles of cartilage PG extracts removed from human specimens of various ages. The authors noted the presence of "protein-polysaccharide light (PP-L) and protein-polysaccharide heavy (PP-H) fractions" that were present in variable amounts. Cartilage samples extracted from elderly patients yielded higher volumes of the low molecular weight PG (PP-L), whereas cartilage extracts from younger individuals exhibited higher volumes of the high molecular weight PG (PP-H) and little or no PP-L. The molecular weights of these PGs elements were not provided. Although the methodology employed by Bayliss and Ali (1978b) involved gel chromatography, whereas the results obtained for this study utilised polyacrylamide gel electrophoresis, they have yielded analogous results. An article written several years later by Dudhia and colleagues (1996) also examined the age-related changes in human aggrecan and noted the presence of both high and low molecular weight PGs. The high molecular weight PG was identified as glycosylated aggrecan (~250kDa) while the low molecular weight PG was identified as the C-terminal G3 domain of the aggrecan protein core. In this current study, the high molecular weight band situated at approximately 230kDa is associated with deglycosylated aggrecan that has not undergone proteolytic cleavage of its protein core (Heinegård & Oldberg, 1989; Knudson & Knudson, 2001; Watanabe, Yamada, & Kimata, 1998). The molecular weight of the G3 domain was not provided in the above reports (Bayliss & Ali, 1978b; Dudhia, 2005; Dudhia *et al*., 1996). However, based on the amino acid sequences that comprise the G3 domain, Aspberg (2012) predicted a molecular weight of 36kDa for this C-terminal structure. The value of the low molecular weight CRP peptide observed among control and PM porcine aggrecan was determined to have a molecular weight approximating 38kDa. This value is near identical to that which has been calculated by Aspberg (2012). As observed by Dudhia and colleagues (1996) and among PM cartilage

samples in the experiments carried out in this study, this CRP did not present additional heterogeneous subpopulations with increasing PMI. However, in order to conclude the exact identity of this low molecular weight CRP, it is necessary for PM protein samples to undergo further immunohistological evaluation with antibodies that are designed to detect the C-terminal G3 domain.

Western blots for EXPTs 1 and 2 also illustrated an increase in the heterogeneity of aggrecan and its degradation products and the intensity of its subpopulations with increasing PMI. These heterogeneous subpopulations of CRPs were observed between 175kDa and 58kDa. In general, PM samples collected from CMP exhibited a continuous gradient of degradative by-products bearing progressively lower molecular weights as PMI increased. In a similar manner, PM samples of aggrecan collected from HLT demonstrated discernible bands of heterogeneous CRPs. The appearance of these increasingly heterogeneous CRPs were also observed among human cartilage samples by Bayliss & Ali (1978a) and Dudhia *et al*. (1996). These authors noted that the composition of aggrecan became increasingly heterogeneous with age. According to Dudhia and colleagues (1996), this age-related change is owed to several factors:

- Inverse changes in the size and number of CS chains (decreased) and KS chains (increased);
- Changes in the patterns of GAG sulphation;
- Proteolysis of the aggrecan core, especially in the IGD region; and
- Destruction of the G3 domain.

Articular cartilage "exhibits extensive heterogeneity both in terms of molecular size and chemical modifications" with increasing age and therefore, affects its ability to function as an aggregate (Dudhia, 2005). The presence of these increasingly heterogeneous CRPs suggests

that PM degradation of cartilage is an ordered process that occurs in a step-wise manner which mimics normal aggrecan turnover as seen among aged samples of human cartilage.

For samples extracted at PMIs of 30-42 days, CRPs were virtually unseen with the exception of faint bands that appeared for PM samples collected at 30 and 36 days from HLT in spring (Figure 3.7b). An absence of MAb 2-B-6 CRPs for these cartilage extracts implies that the aggrecan core protein has undergone complete disintegration. If there were fragments remaining that are too small to be resolved in 9-10% gels they would have likely been detected at the gel dye-front. However, no CRPs were observed at this location. Lack of visible CRPs during these later PM intervals shows overlap with signs of extreme soft tissue degradation (trotter skin, muscles and tendons) subsequent to complete perforation of the synovium exposing the joint cavity to the immediate soil environment. The skin of trotters disinterred 30-42 days PM became significantly thinner, with muscles and tendons showing increased amounts of liquefied tissue, and the start of bones (metacarpals/metatarsals and phalanges) disarticulating at the epiphyseal-diaphysis junction. In general, the soft tissue damage observed among PM trotters disinterred from CMP was more extensive than that of trotters disinterred from HLT. This acceleration in soft tissue decomposition is due, in part, to the moisture content of the soil environment. The moisture level of soil environments affects the metabolism of soil microbes (Carter & Tibbett, 2008a). Likewise, changes in the moisture content of soil causes fluctuations in microbial activity; a rise in moisture level results in increased microbial biomass, whereas water loss is accompanied by a reduction in microbial activity (Hopkins, 2008). Furthermore, the deposition of remains in soil environments also provides additional moisture (and nutrients) to the surrounding soil, which also influences the proliferation of soil microbes (Carter *et al*., 2007; Hopkins, 2008). Although the porcine samples used in this research consisted of limbs and not whole pigs that release large quantities of leachate (as a consequence of autolytic and

putrefactive processes), the autolysis of dismembered trotters results in the discharge of decomposition fluids in far less volumes, nonetheless. According to Vass (2011), the human body is overall comprised of 55-56% water. However, various other soft tissue constituents, apart from fat and muscles, maintain water levels that exceed 85%. Moreover, water facilitates the transport of microbes and their proteolytic secretions into the soft tissues of decomposing remains. Soft tissue degradation revealing the joint exposure exposes cartilage to various soil microbes. In turn, these microbes metabolise digested ECM cartilage proteins (Carter & Tibbett, 2008a; Dent *et al.*, 2004) and cause rapid deterioration of the tissue. This phenomenon explains why aggrecan is not detected beyond 21 days PM among Western blots for EXPTs 1 and 2.

Although trotters were buried in distinctly different soil environments (CMP burial plot – located at ground-level, exhibiting moist, nutrient rich soil; HLT burial plot – situated at the top of a hill and consisting of dry, nutrient deficient soil), the degradative patterns displayed by samples of cartilage protein with corresponding PMIs proved to be astonishingly similar. It was assumed that the PM biochemical breakdown of cartilage would exhibit uncontrolled breakdown as a result of various environmental factors influencing the rate of its decomposition. Despite this assumption, samples from CMP and HLT burial plots demonstrate that different soil environments have little influence on the PM appearance of this decomposing cartilage protein. The Western blots produced for these comparative experiments (Figures 3.7 and 3.8) illustrate that the PM destruction of large PG aggregates occurs in an orderly fashion. Aggrecan monomers that become dissociated from their native PG aggregate progressively break down into smaller fragments that accumulate within the ECM. This process continues to take place until soil microbes gain access to the cartilage when the joint cavity becomes exposed to its surrounding environment. At this point, soil derived microorganisms metabolise aggrecan quickly. The appearance and disappearance of

heterogeneous subpopulations of aggrecan breakdown products that arose from PM trotter samples bearing intact joints may be attributed to a combination of factors. For example, age-related changes that reduces aggrecan to low molecular weight fragments, and the available water content in the immediate soil environment which impacts the ability for enzymes to efficiently carry out their proteolytic activities.

4.2.4 The relative rate at which post mortem aggrecan degrades is dependent upon climate

Comparative Western blots for EXPT 1 and EXPT 2 trotters, disinterred from CMP and HLT over the course of 42 days, presented images of CRPs representing aggrecan for up to 21 days PM (Figures 3.7 and 3.8). This discovery prompted a four and a half week experiment involving 6 pairs of trotters that were interred at HLT (EXPT 4). Disinterment of these trotters occurred weekly for 3 weeks and then twice weekly thereafter. The purpose of this experiment was to estimate the time frame for which relative amounts of aggrecan diminished and were no longer detectable between 21 and 28 days PM. Unlike EXPTs 1 and 2 for which CRPs are present for 0-21 days PM, CRPs weighing 230kDa and 38kDa are distinctly visible for samples 0-28 days PM (Figure 3.8). The PM presence of aggrecan is further seen for an additional week. This observation coincided with notably cooler, overall ambient temperature (10.5˚C) during the autumn (September to October, 2012). The physical state of PM trotters disinterred during this experiment demonstrated obvious signs of soft tissue degradation with increasing PMI. Breaks in the skin were observed among trotters disinterred 24 days PM and onwards. Interestingly, the soft tissues of trotters disinterred at 24 days PM appeared much more degraded in comparison to trotters that were disinterred 28 days PM. The Western blot image for this experiment (Figure 3.9) reaffirms this observation. A faint CRP weighing 230kDa is present for cartilage samples extracted at 24 days PM, whereas the 230kDa and 38kDa CRPs that are present for the 28 days PM sample exhibits a

greater relative intensity. The nature of this outcome might be credited to a soil microenvironment that favoured quicker breakdown for a number of reasons, such as loosely packed soil, variations in the loam/clay soil contents (Jaggers & Rogers, 2009) and water retention properties (Fitzpatrick, 2008; Jaggers & Rogers, 2009). However, soils that possess a high clay content are known to delay the decomposition of remains (Carter & Tibbett, 2008b; Carter *et al*., 2007; Forbes, 2008a; Pounder, 1995). Since trotters disinterred at 24 days PM were notably more degraded than those collected at 28 days PM, it is unlikely that the clay content of the soil played a substantial role in its decomposition unless it was lower in this microenvironment. The soil type for both CMP and HLT burial plots is classified as sandy loam silt (sections 1.3.6, 2.2 and 3.1). This soil type, according to Fitzpatrick (2008), "is sandy to touch" and has a 10-20% clay composition. Therefore, it is most probable that the sandy loam soil, repeated rainfalls that occurred during this interment period and loosely filled grave were contributing factors that served to accelerate the decomposition of trotters that were gathered at 24 days PM. When the soil environment contains more than 85% moisture, the rate of decomposition is accelerated. On the other hand, the rate at which remains decompose is decelerated when the soil's moisture content falls below 85% (Vass, 2011).

Display of the 38kDa CRPs did not present any notable trends among the PM samples and reflects the same randomness as seen among PM samples extracted for EXPTS 1 and 2. Likewise, gradients of heterogeneous subpopulations of aggrecan breakdown were also seen (Figure 3.9). These results are consistent with those previously discussed in section 4.1.5.

Another set of 12 trotters were interred at HLT for EXPT 5 (October 8 to November 19, 2012). The time at which this interment was carried out overlapped with EXPT 4 for a period of 12 days. Trotters for EXPT 5 experienced an average ambient temperature of 6.9˚C which was a few degrees cooler than that experienced by EXPT 4 specimens. This condition

resulted in the visibility of CRPs for up to 35 days PM, further extending the PM presence of aggrecan for an additional 7 days. Samples collected 0-15 days PM exhibited intense CRPs, whereas those seen for samples extracted 22-35 days PM were considerably less intense. Trotters that were disinterred 22-35 days PM presented skin that was much thinner with breaks occurring along its surface, and underlying muscles and ligaments exhibited liquefaction. However, these joints remained unexposed to the soil environment. Cartilage protein extracted at 8 days PM demonstrated the most intense 230kDa CRP among these samples. The intensity of this CRP is owed to an excess amount of protein that was loaded onto the SDS-PAGE gel (refer to the stained membrane in Figure 3.11). The integrity of the soft tissues for trotters disinterred at 8 and 15 days PM were found to be well preserved when compared with control trotters. Their robust appearance can be partly ascribed to the moisture content and the cooler climate of the soil environment they were interred in (Rodriguez, 1997; Rogers *et al.*, 2011). Soils that possess high water levels and the ability to retain moisture (the smaller the soil particles, the greater the water retention properties of soil) promote waterlogging and the formation of adipocere which delay the decompositional processes (Carter & Tibbett, 2008a; Forbes, 2008a; Rodriguez, 1997). Likewise, colder climates also postpone the decomposition of remains (Carter & Tibbett, 2008a; Rodriguez, 1997). Janaway (2008) further explains that although cold environments inhibit most of the microbial activity that takes place within soil, low temperatures that are above freezing simply slows the metabolic activities of these microbes. In general, microbes are less active during the winter (Carter & Tibbett, 2008a). On the contrary, an experiment conducted by Carter, Yellowlees and Tibbett (2008) examined the effects of temperature on microbial activity in differing soil environments and the influences they exerted on cadaver decomposition. They noted that as temperature increased, cadavers experienced a rapid loss in mass. Cadavers that were buried in three different sandy soil environments exhibited

thinner and more flaccid soft tissue by 28 days PM, irrespective of temperature (29˚C, 22˚C and 15˚C) (Carter *et al.*, 2008). Changes in temperature also affects the activities of enzymes and chemical reactions that take place within the soil environment (Carter *et al.*, 2008).

The low intensity CRPs seen among cartilage samples 22-35 days PM coincides with the increasingly liquefied soft tissues. This suggests that a water saturated soil environment may have also facilitated the transport of soil microbes through the skin which resulted in the soft tissue degradation presented as liquefaction and that the cooler climate may have decelerated their metabolic activities. This might explain the faint presence of aggrecan for a longer period of time and reinforces the assumption that microbial digestion also facilitates the PM destruction of aggrecan.

The greater range of aggrecan breakdown products seen among the 8 days PM sample are more numerous in comparison to PM samples of cartilage protein extracted 15 days PM. This example illustrates that subpopulations of aggrecan breakdown products are present in cartilage as early as 8 days PM and possibly even earlier. However, they are present in such small quantities that they may be difficult to detect even by HRP chemiluminescence. This outcome further supports the assumptions made in section 4.1.5 that the heterogeneity of PM aggrecan samples is associated with age-related changes that take place in the cartilage during life (Bayliss & Ali, 1978a; Dudhia, 2005; Dudhia *et al.*, 1996), and that these changes are also reflected in PM processes. Although all samples were subjected to the same incubation times with chondroitinase ABC enzymes, the effects of prolonged enzymatic digestion cannot be dismissed as a possible factor affecting the appearance of these CRP subpopulations. As with previous PM samples, the 38kDa CRPs did not appear in any particularly meaningful order or exhibit notable changes that could be attributed to PM degradation. A marginally cooler climate resulted in the presence of CRPs for yet another additional week, so that aggrecan was visible for up to 35 days PM.

4.2.5 Mummified and water submerged trotters

Both mummified and water submerged trotters were left to decompose in an open-door, greenhouse environment where the ambient temperatures were notably warmer in comparison to the natural outdoors. Trotters left exposed to the surrounding environment had completely mummified by 12 days PM. Trotters did not exhibit visible lacerations in the surface areas of skin protecting the joints. Cartilage for this sample appeared pearly white. Water submersed trotters were left in their respective tap and simulated sea water tanks for 35 days. These trotters developed a very strong and putrid odour, as well as a thin build-up of adipocere. At the time of their recovery, they were still robust and showed no visible disruptions in their skin; joints remained unexposed to the water environments. Remains submerged in aquatic environments take nearly twice as much time to decompose than remains exposed to air. This delay is caused by the water's cooler temperature and a lack of insect activity (Rodriguez, 1997). Bacterial content and water salinity also influence the rate at which bodies decompose (Ibid.), whereby bodies of water containing low levels of bacteria reduce the rate of decomposition. In a similar manner, saltwater sources (i.e. oceans) limit the amount of bacterial action and prolong the decay process. Sea water generally contains a high salt content where the concentration of NaCl ranges from 3.4-3.7% (Kakizaki *et al.*, 2008). At 35 days PM, the cartilage of water submersed specimens appeared light pink and the tissue maintained its robustness. The Western blot image for PM samples 0-35 days PM show that cartilage extracted from the mummified trotters at 12 days PM bear the greatest intensity for the 230kDa CRP with respect to PM samples obtained from water submersed trotters at 35 days PM. This outcome is expected since the mummified trotter samples were extracted 23 PM days earlier than the water submersed trotters. The latter were expected to have a diminished appearance as seen among late stage PM cartilage samples collected from trotters buried below ground.

Assessment of the water submersed samples displays a markedly less intense 230kDa CRP for the tap water specimen than that which is present for mummified samples. The 230kDa CRP is absent for the simulated sea water specimen. Its absence, in relation to the CRP present for the tap water specimen may be owed to the concentration of salt that is present in the simulated aquatic environment. Heterogeneous subpopulations of aggrecan were clearly seen among these late PM samples (Figure 3.12). Several authors assert that aggrecanase, an enzyme responsible for the destruction of aggrecan *in situ* (Arner, 2002), demonstrates sensitivity to salt (Arner *et al*., 1999; Gendron *et al*., 2007). Arner and colleagues (1999) state that the enzyme achieves optimal activity when the NaCl concentration is about 100mM. At a concentration of 250mM, enzyme activity decreases by approximately 50% and is completely inhibited when the salt concentration is 500mM. Another study examining the differential effects of NaCl on both ADAMTS-4 and ADAMTS-5 aggrecanases indicated that the proteolytic capability of ADAMTS-4 was dramatically affected by changes in the concentration of NaCl in contrast to that for the ADAMTS-5 enzyme (Gendron *et al*., 2007). Optimal enzyme activity for ADAMTS-4 was observed with NaCl concentrations ranging from 12.5-50mM. When the NaCl concentrations surpassed 50mM, this enzyme ceased to function: "At 150mM NaCl, only 20% of the maximal activity was detected; essentially no activity was detected at or above 200mM NaCl" (Ibid). Gendron *et al*. (2007) observed that the functionality of ADAMTS-5 was considerably influenced by salt concentrations, but not in the exact manner as that for ADAMTS-4. ADAMTS-5 activity was decelerated when concentrations of NaCl were below 50mM or exceeded 500mM. Optimum enzyme activity for this species of aggrecanase occurred when the NaCl concentration was 200mM, with 80% of its functionality sustained at a concentration of 150mM NaCl (Gendron *et al*., 2007). The difference in the concentration of NaCl required by ADAMTS-4 and ADAMTS-5 to achieve optimal enzymatic activity is

attributed to the ionic nature of their interactions with the sulphated GAGs of aggrecan. ADAMTS-5 has a much stronger affinity for aggrecan than ADAMTS-4 (Ibid.) and can therefore continue to carry out its proteolytic functions in environments that contain high concentrations of NaCl. In contrast, ADAMTS-4 exhibits a much lower threshold for coping with NaCl concentrations that exceed 500mM. Therefore, this enzyme is much more sensitive to physiological salt concentrations than ADAMTS-5 (Ibid). If the tap water environment contains little salt (concentrations below 50mM) or none at all, then ideally the proteolysis of aggrecan by ADAMTS-5 should be decelerated according to the results mentioned above. This may serve to explain the presence of the 230kDa CRP that is visible for cartilage extracts removed from tap water submerged trotters and its absence among samples subjected to a saltwater environment. Gendron and colleagues (2007) express that:

> *The reason for the relatively little activity of ADAMTS-5 against aggrecan at low NaCl concentrations is presently unclear, but it may be due to structural changes within the enzyme itself or to increased unproductive interactions between ADAMTS-5 and the substrate. Nonetheless the activity of ADAMTS-5 on deglycosylated aggrecan was about 500 times stronger than that of ADAMTS-4 under the physio-logical salt concentration. Thus, differences in aggrecanase activity between ADAMTS-4 and -5 may lie in both the intrinsic activity of their catalytic domains and their affinities for aggrecan.*

Furthermore, aggrecanase activity is also affected by temperature and therefore ceases to operate at 56˚C and above (Arner *et al*., 1999). Consequently, loss of the 230kDa CRP for trotter samples submersed in simulated sea water may have transpired at slightly accelerated rates than that of tap water submersed samples as a result of warm temperatures elicited by the greenhouse and optimal NaCl concentrations in the simulated sea water. Nonetheless, the

presence of saltwater microbes capable of entering the synovium by way of osmosis cannot be dismissed as a possible contributing factor for the early decay of PG aggregates with respect to fresh water specimens that displayed a 230kDa CRP. The results obtained for these water submerged samples are representative of bodies submersed in stagnant waters that are devoid of microbial and floral fauna. Whether or not these factors and continuous water flow will impact the rate of decomposition requires future investigation. Furthermore, the PM life span of aggrecan from mummified trotters was only examined after 12 days PM and could not be cross-compared with the rates of decomposition for different water environments. The premature extraction of cartilage from mummified trotters arose from concerns that anticipated difficulties with dissecting the joints of trotters whose skin and muscle tissues were completely desiccated, and possibly cartilage that might have also been dehydrated. However, upon rehydrating these trotters for a couple hours, dissection proceeded as normal and the cartilage encountered still remained fresh and easy to dissect. Therefore, the same experiment should be conducted to evaluate whether similar outcomes would recur for trotters submerged in different water environments and to examine the PM appearance of aggrecan from mummified trotters bearing the same PMIs.

The results obtained for this and the above analyses further strengthen the argument that cartilage has forensic potential. Its PM presence is relatively unaffected by different environments. It is capable of being immunodetected among samples with PMIs that greatly exceed the current 48-hour limitations that other soft tissues comprising the body impart.

4.3 Investigating the degradative properties of cartilage at the cellular level: The post mortem viability of chondrocytes

With an extremely low cell density compared to other tissues of the body, it was hypothesised that the catabolic effects of proteolytic enzymes released from chondrocytes would require time to be transported through the cartilage ECM. Over time, an accumulation of these enzymes would initiate the process of autolysis whereby the extracellular and cellular matrices of cartilage would undergo destruction. This mechanism would serve to explain the gradual breakdown of aggrecan and its ECM components. Western blots were conducted to determine whether chondrocyte death mirrored the gradual and ordered breakdown of aggrecan as witnessed with increasing PMI.

4.3.1. Immunodetection of α-tubulin for the investigation of cellular degradation

PM cartilage samples that were collected for EXPTs 4 to 10 (Table 2.1) and subjected to Western blot detection of aggrecan using MAb 2-B-6 also underwent immunodetection with anti-α-tubulin to determine whether the pattern of cellular degradation mirrored a process similar to that of its ECM component, aggrecan. PM samples consisted of cartilage extracts obtained from the articular joints of porcine trotters and the IVJs of bovine tail. Alpha-tubulin CRPs were visible among extracts of porcine cartilage containing 40μg of protein per 10μl of sample buffer. The molecular weight of these CRPs is equivalent to that of human tubulin, weighing approximately 58kDa as comparatively illustrated with control HG cells as seen in Figures 3.13 to 3.15 and 3.19. Visible CRPs for porcine samples reinforces claims that pigs are adequate models for forensic studies. Conversely, CRPs were virtually unseen for cartilage samples containing 60μg of protein extracts from bovine vertebrae with the exception of control HG (Figure 3.19).

4.3.2 Heat-treated versus non-heated cartilage protein and the visibility of α-tubulin

A preliminary test was conducted with heat-treated and non-heat treated samples of cartilage protein mixed with sample buffer to determine whether heating protein samples would improve the visibility of CRPs. Heated samples of control cartilage protein dissolved in 1X sample buffer resulted in a notably more intense CRP indicative of α-tubulin than was seen for the non-heated control sample. Samples of cartilage protein prepared with SDS sample buffer would require heat to accelerate the cleavage of its sulphur bonds, thereby disrupting and straightening the secondary, tertiary and quaternary globular structures in order to facilitate their unhindered movements through the polyacrylamide gel. The rationale for this test was based on the understanding that cartilage maintains a low cell density. Performing a comparative Western blot of heat-treated and non-heated cartilage protein samples confirmed that heat would be required to enhance visualisation of cartilage's underpopulated cellular components.

4.3.3 Alpha-tubulin CRPs reveal the post mortem perseverance of chondrocytes

Protein extracts from cartilage collected September 17 – October 19, 2012 (average temperature: 10.5˚C) for EXPT 4 (Table 2.1) demonstrated an absence of α-tubulin CRPs for samples 0 and 7 days PM (Figure 3.14). However, samples 14-32 days PM presented α-tubulin CRPs. Lack of α-tubulin CRPs for cartilage samples 0-7 days PM suggests that chondrocytes are trapped within the cartilage ECM during this time period; the cells are not easily accessible as the ECM still remains tightly packed (Alibegović *et al*., 2014; Mow *et al*., 1992; Pearle *et al*., 2005). The vague appearance of the CRP representing cartilage after 14 days PM indicates that the structural integrity of the ECM has been compromised, resulting in the soft tissue's collapse. As discussed in section 4.1.2, the destruction of PGs causes the ECM to weaken and lose its structural stability (Athanasiou *et al*., 2013; Iatridis *et*

al., 2012; Kheir & Shaw, 2009; Wang *et al*., 2013). Consequently, these changes create a much more permeable ECM (Kheir & Shaw, 2009). In relation to the development of OA cartilage, Athanasiou and colleagues (2013) indicate that during the early stage of this disease, "no visual, functional or mechanical alterations appear detectable." The lack of visible α-tubulin CRPs for cartilage samples 0-7 days PM and its faint emergence at 14 days PM serve as a case in point. Changes in the biochemistry and physical structure of PM cartilage have proven to be a gradual process (sections 4.1.1, 4.1.2 and 4.2.3). The effects of degradation do not become visibly apparent until a substantial amount of destruction has taken place within the cartilage matrix. This is further illustrated by the presence of α-tubulin CRPs that are distinctly seen for samples 21-32 days PM. These CRPs are of relatively equal intensity and do not demonstrate heterogeneous subpopulations as seen among degraded aggrecan. It should be noted that the Western blots carried out for α-tubulin required longer developing times with HRP chemiluminescence substrate than was the case for immunodetection of aggrecan. Hence why the multiple and very intense CRPs are seen for HG samples containing a fourth of the protein concentration (10μg) that was used for porcine articular cartilage samples which contained 40μg of protein. The extended time that was required to develop images of cartilage α-tubulin reflects the low cellular density of the tissue (Athanasiou *et al*., 2013; Kheir & Shaw, 2009; Pearle *et al*., 2005).

EXPT 5 samples (Table 2.1) presented α-tubulin CRPs for cartilage samples extracted 0-42 days PM (Figure 3.15) despite trotters experiencing a slightly cooler average temperature (6.9˚C) than EXPT 4 samples. Alpha-tubulin CRPs were least intense for samples 8-15 days PM with succeeding PM samples displaying the greatest, and relatively equal, intensities. Of all the PM samples represented for α-tubulin, the control sample exhibited the greatest intensity. This is due to an overloading of protein sample as demonstrated by the stained membrane. The presence of CRPs for PM samples collected at 0

and 8 days was unexpected. It was anticipated that the cooler climate would result in the appearance of α-tubulin CRPs at later PMIs as seen for EXPT 4. Bearing in mind that the soil environment was very damp for the duration of interment and that the physical state of PM trotters was notably degraded as described in sections 3.2.7 and 4.2.4, it is possible that the early appearance of these CRPs are owed to microbial activity. However, the physical state of PM trotters disinterred at 8 and 15 days exhibited robust and uninterrupted skin. Furthermore, an α-tubulin CRP and an accompanying lower molecular weight subspecies are seen at 0 days PM. This suggests that the immunoblot was overexposed to chemiluminescence substrates or that relatively more protein was loaded (see Figure 3.15, lanes 2, 3, 5 and 8 of stained membrane). The former explanation is most probable since background noise is seen amidst the CRPs. CRPs present for samples 0-15 days PM indicates that small quantities of liberated chondrocytes do exist within the ECM but may not be easily detected by HRP chemiluminescence. Overall, the Western blot image for EXPT 5 shows a similarity in the trend observed for EXPT 4. Chondrocytes appear to be fairly restricted within the ECM during the first two PM weeks (8 and 15 days). Once the ECM begins to deteriorate, the chondrocytes become more readily accessible as is demonstrated by the presence of α-tubulin CRPs from 22-42 days PM. In addition, the presence of α-tubulin for up to 42 days PM (although possibly overloaded) suggests that chondrocytes are quite resilient (Alibegović *et al*., 2014; Drobnič *et al*., 2005; Lasczkowski *et al*., 2002) despite clear evidence of PM changes that have occurred among cartilage tissues.

For PM samples of cartilage that were extracted from trotters 28-44 days PM which experienced an overall average temperature of 2.5˚C (EXPT 7), α-tubulin CRPs were present and for extracts collected at 0 days PM (Figure 3.16). Again, the presence of an α-tubulin CRP and a subspecies for the sample collected at 0 days PM can be attributed to a combination excess protein and overexposure to chemiluminescence substrate as discussed

above. The presence of CRPs for samples 28 to 44 days PM was expected given that climate was considerably cooler at the time this experiment was conducted. The rate of soft tissue decomposition was markedly slower than witnessed for previous experiments. With increasing PMI, the intensity of the α-tubulin CRPs for samples 28-44 days PM decreased. By 44 days PM, the CRP was vaguely seen. As there were breaks in the skin of trotter samples collected up to 44 days PM, the increasingly dim CRPs seen at 35 and 44 days PM indicates that chondrocyte α-tubulin was undergoing PM destruction.

PM samples of cartilage protein from EXPT 8 were subjected to Western blot analysis for α-tubulin. The average ambient temperature during the time frame for this interment was 9.5˚C, one degree cooler than the average temperature computed for EXPT 4 (Table 2.1). Alpha-tubulin CRPs were clearly present for 22-35 days PM. At 43 days PM, this CRP was dimly seen. These results closely mirror those seen for EXPT 4 samples which demonstrate the appearance of α-tubulin at precisely the same PMI and similar overall temperature, and EXPT 7 which illustrates the disappearance of this microtubule protein as a result of PM processes.

Alpha-tubulin CRPs were seen among EXPT 9 cartilage samples extracted 0-42 days PM. The overall ambient temperature experienced by these trotters while interred was 14.5˚C, warmer conditions than earlier experiments presented in this section. Alpha-tubulin CRPs were visible for cartilage samples extracted 0-42 days PM (Figure 3.18). The α-tubulin CRP seen for sample extracts collected at 0 days PM was due to protein overload (refer to lane 1 in the stained membrane for Figure 3.18). At 7 days PM, a CRP faintly emerged and possibly corresponds to the warmer climate and increased rate of decomposition observed for these trotters. From 7-21 days PM, the intensity of the α-tubulin CRP grew as PMI increased. Cartilage samples collected 21-42 days PM showed the greatest intensity and remained uniformly so during this time frame. In the previous Western blots for detection of α-tubulin,

the investigated protein appeared to begin the process of degradation within a time span of 35-44 days PM. Unlike these previous experiments, the intensity of the α-tubulin CRP seen at 42 days PM remained relatively the same as those for samples collected 21-35 days PM for EXPT 9. This result may imply that warmer ambient temperatures are ideal for the prolonged PM survival of α-tubulin. Additional CRP were seen, very faintly across lanes 2-6, above the 175kDa mark and represent protein samples that did not enter the gel on account of residual aggrecan protein that did not undergo thorough deglycosylation.

Finally, cartilage removed from the IVJs of PM bovine tail was also subjected to Western blot analysis for the detection of α-tubulin (EXPT 10). To reiterate, the interment of these samples overlapped with that for porcine trotters from EXPT 9 and the average ambient temperature experienced by the specimens of bovine tail was 16.0˚C (Table 2.1). No CRPs demonstrating the presence of α-tubulin were visible among the 60μg of fibrocartilage protein ran in this experiment, except for that which was visible for HG control (Figure 3.19). This lack of visible CRPs for α-tubulin despite running samples that contained three times the amount of protein used for hyaline articular cartilage extracted from porcine specimens, provides further support that far fewer chondrocytes exist within the fibrocartilage situated between the vertebrae (Masuda *et al*., 2003; Roughley, 2006). For this this reason, detection of α-tubulin was not possible. This may also have to do with the sample area from which cartilage samples were collected. For this experiment, cartilage samples were gathered from the entire articular surface. Intervertebral cartilage exhibits phenotypic chondrocytes that produce aggrecan and collagen type II fibres in the central region of the cartilaginous disc, known as the nucleus pulposus. The outer region of this disc is known as the annulus fibrous (Masuda *et al*., 2003; Sive *et al*., 2002). To quote Roughley (2006),

> *"The nutritional and repair problems of articular cartilage are magnified in the intervertebral discs, which in the lumbar spine are the largest avascular and least cellular tissues in the body."*

Further tests should be conducted using only the nucleus pulposus of IVJ cartilage to determine if results are achievable.

4.3.4 Vimentin and vinculin: Determining the post mortem presence of other cell membrane components

Control samples of porcine articular cartilage underwent preliminary Western blot analyses using the MAbs, anti-vimentin and anti-vinculin, for detection of vimentin and vinculin which are filaments located in the membranes of chondrocytes. CRPs were not detected among control samples that were probed with vimentin or vinculin. Despite their lack of appearance, the anti-vimentin and anti-vinculin antibodies were only tested on control samples. Experimental samples were not examined due to time constraints. Like α-tubulin, vimentin and vinculin are membrane-bound cytoskeleton proteins. Immunodetection of α-tubulin among PM samples of cartilage protein was not typically observed from 0-14 days PM or were not seen as intensely as PM samples collected 21 days PM and beyond. It is most probable that vimentin and vinculin were not detected at 0 days PM as the ECM had not yet degraded to the point where enough chondrocytes which house these micro proteins could be accessed. Based on the results obtained for Western blots of α-tubulin, the conjecture is that vimentin and vinculin may be detected at later PMIs, mimicking the results obtained for α-tubulin.

Labelling intensity studies of vimentin and tubulin in normal and osteoarthritic rat cartilage indicated average labelling percentages of 63.9% for vimentin and 37.4% for tubulin. In osteoarthritic chondrocytes, these percentages showed a 37.1% reduction for

vimentin and 20.1% for tubulin in OA-induced rat cartilage (Capín-Gutiérrez *et al.*, 2004). In light of these observations, the PM decrease in the percentage of chondrocyte cytoskeletal proteins may render vimentin and vinculin somewhat difficult to detect immunologically. However, since vimentin presents a higher percentage of labelling in OA rat cartilage, less protein sample and/or less exposure time to chemiluminescence substrate should, in theory, be required for the illumination of vimentin, and possibly vinculin, with comparison to α-tubulin.

4.4 Cross-comparison of cell vitality assays, the presence of aggrecan and α-tubulin

Preliminary cell vitality assays, performed on control cartilage dissected from five different surface areas of the distal MCP/MTP joint (section 2.5.1), established that the central aspect of the ridge cross-section (the most inferior aspect of the joint) was most ideal for sample collection. In this region of cartilage, nearly 100% of the fluorescing cells were viable (green). On the contrary, the other four locations (section 2.5.1) presented notable amounts of dead cells (red) at 0 days PM (Figure 3.21). The lateral groove was the next best location and presented the least amount of dead cells in comparison to the posterior, medial and lateral surface areas which followed in this particular order. The lateral region presented the greatest amount of dead cells. These four surfaces areas were notably thinner in comparison to the inferior ridge, especially cartilage situated along the lateral and medial surface areas of the distal MCP/MTP bone. Variations in the amounts of dead cells present among these different surface areas can be attributed to joint mechanics, oxidative stress and normal turnover. In discussing the effects that abnormal biomechanics and modified load bearing have on the knee joints, Athanasiou and colleagues (2013) state that OA typically develops on the medial condyle of the knee where the joint experiences the greatest amount of loading pressure as a result of walking. Porcine cartilage extracted from the ridge along

the distal surface of the MCP/MTP joint is fairly central to the joint and rests within a groove on the proximal surface of the 3rd phalange. Perhaps its thickness affords the chondrocytes in the tangential/transitional zones with added protection from mechanical stress and the immediate effects of cytokines/proteases.

Majority of dead chondrocytes were clustered along the articular surface (superficial/middle zones) for all five surface areas examined. As discussed in section 1.2.2, the articular surface of cartilage possesses the greatest chondrocyte density (Drobnič *et al*., 2005; Goldring & Marcu, 2009; Moger *et al*., 2007). It is also the site of direct mechanical impact and experiences the greatest amount of trauma (Chen *et al*., 2001; Ewers *et al*. 2001; Hembree *et al*., 2007; Lewis *et al*., 2003; Morel *et al*., 2006; Quinn *et al*., 2001). Therefore, it is sensible that the superficial/middle zones of articular cartilage would bear the greatest numbers of dead cells with comparison to the underlying zones, especially for samples collected at 0 days PM.

The localisation of dead cells at the articular surface of cartilage may be an indication of age-related oxidative stress which cause a reduction in the number of viable chondrocytes over time (Carlo & Loeser, 2003; Martin & Buckwalter, 2006). When increased levels of endogenous ROS outweigh the number of antioxidant species present within the ECM, cartilage homeostasis is disrupted and results in the pathogenesis of OA. This process causes the chondrocytes to become more "susceptible to oxidant-mediated cell death" (Carlo & Loeser, 2003). Over time, this process causes a decrease in the number of viable cells within the ECM. For mature individuals, this translates to an increase in the frequency of dead chondrocytes that occur along the periphery of the articulating surfaces of cartilage where it experiences the greatest amount of mechanical stress (Martin & Buckwalter, 2006). This phenomenon could explain the presence of dead chondrocytes at the articular surface of cartilage extracted at 0 days PM. Furthermore, it seems likely that trotters interred in soil

would undergo a similar process where the hypoxic environment they are buried in would promote an increase in the amount of ROS within the decaying joint.

4.4.1 Cell vitality assay I: EXPT 7 (February 11th to March 27th, 2013)

Trotters interred during the late winter/early spring of 2013 experienced an overall ambient temperature of 2.5˚C. The rate of decomposition was slow as reflected by the thinner skin observed at 36 days PM and not the typical 21-24 days PMI as observed for earlier experiments that occurred in milder climates. Skin remained intact for five weeks with the first appearance of breaks seen occurring at 44 days PM. Despite these increasingly visible signs of PM degradation, joints remained unexposed to the surrounding soil environment. The preservation of these trotters and their cartilage was validated by the appearance of MAb 2-B-6 CRPs that indicated a presence of aggrecan for the entire duration of the experiment (Figure 3.23). Although aggrecan demonstrated a clear presence at 44 days PM, α-tubulin was only beginning to vanish at this PMI (Figure 3.16). The vitality assay substantiated the results for α-tubulin by illustrating that as much as 1% of the chondrocyte population had remained viable at 44 days PM.

A time course graph demonstrating the percentage of live cells across the weekly PMIs presented a sigmoidal curve (Figure 3.25). The appearance of this graph is similar to those obtained for an *in vitro* experiment that examined the PM viability of chondrocytes extracted from human articular cartilage (Alibegović *et al*., 2014). In the work of Alibegovic *et al*., chondrocyte extracts were stored in a biological medium (Dulbecco's Modified Eagle Medium) to maintain normal cellular activity. However, the medium was not changed in order to simulate PM conditions. The chondrocytes were incubated at several different temperatures (4˚C, 11˚C, 23˚C and 35˚C) and their viability was assessed at 3-day intervals over the course of 63 days (Ibid). The graphs for these samples started with plateaus that

varied in duration of time (7.5 to 15 days PM) based on temperature ascribed samples. These plateaus were followed by a gradual decline in cell viability and appeared almost linear before steeply tapering off as the number of live cells became drastically diminished (Alibegović *et al*., 2014). Unlike these graphs, the graph obtained for Figure 3.25 did not begin with a plateau. Instead, the PM chondrocytes presented a 30% decrease in viable cells followed by a plateau between 7 and 21 PM days where the percentage of live cells fell within a range of 60-65%. From this point forward, the shape of the graph appeared identical to those reported by Alibegović *et al*. (2014).

The slight discrepancies between the initial appearance of their graphs and the one obtained for EXPT 7 PM trotters is owed to the conditions under which both experiments occurred. The experiments conducted by Alibegović and colleagues (2014) occurred in a laboratory setting where a number of variables were controlled for. The graph presented here is derived from samples that underwent decomposition in a more natural setting where chondrocytes were examined within the context of their ECM. This initial decrease in cell vitality before plateauing may be explained as the physiological response of chondrocytes to changes in the temperature. This is an appropriate argument given that during the first week of interrment, the average ambient temperature reached a low approximating 0.5˚C (Table 3.7). Cartilage samples that are frozen at 0˚C or below results in chondrocyte death (Chen *et al*., 2001; Dean *et al*., 1984; Lewis *et al*., 2003). Conversely, another explanation may be that the chondrocytes used in the experiments conducted by Alibegović *et al*. (2014) may have already died before measurements were taken.

4.4.2 Cell vitality assay II: EXPT 8 (April 15th to May 28th, 2013)

A second cell vitality assay was conducted approximately two weeks later. During this time, the average ambient temperature reached an overall high of 9.5˚C and was seven

degrees warmer on average than for EXPT 7. The effect of this change in temperature was observed first-hand by noting that joint exposure to the soil environment had occurred earlier at a PMI of 28 days. This PMI is comparable with the initial experiments conducted for EXPTs 1 and 2 where joint exposure occurred at the same PMI (section 3.2.6). A Western blot image of MAb 2-B-6 detected aggrecan illustrated 230kDa CRPs for samples 0 to 22 days PM (Figure 3.27). With increasing PMI, the number of heterogeneous CRP subpopulations located between 175-58kDa showed that a decrease in number and intensity was contrary to previous observations. Nonetheless, this PM observation continued to reflect the general trend where the presence of the aggrecan 230kDa CRP gradually diminishes as PMI increases. The intensity of heterogeneous aggrecan subpopulations that are seen among samples 0-14 days PM may be attributed to the biological age of the porcine specimens at the time of death and over-exposing the protein samples to chemiluminescence substrate which further highlighted these age-related changes.

A Western blot for α-tubulin presented 58kDa CRPs for samples disinterred 22-35 days PM. By 43 days PM, the intensity of this protein was diminished (Figure 3.17), indicating that the cellular component continued to endure despite the relatively minute quantities of aggrecan detected for samples collected 28 to 43 days PM (Figure 3.27). The corresponding cell vitality assay demonstrated viable cells up to 35 days PM (Figure 3.28) with the percentage of live cells dramatically decreased to 4%. This observation is in agreement with the intense CRP seen for α-tubulin at 35 days PM. The anti-tubulin 58kDa CRP faintly seen at 43 days PM is reflected by the presence of dead chondrocytes that continue to persist within the cartilage ECM. This suggests that, despite cell death, the cytoskeleton of chondrocytes continues to endure after aggrecan PGs have degraded. Otsuki and colleagues (2008) reported that chondrocyte death was closely associated with the loss of GAGs after demonstrating that Ch'ABC treated cartilage resulted in increased cell death after

experiencing strain in comparison to control cartilage that maintained its GAG-rich content. They concluded that apart from its biomechanical properties, GAGs may also function to maintain chondrocyte survival.

The graph obtained for this assay appeared somewhat sigmoidal, approaching a polynomial shape (Figure 3.29). Unlike the previous graph obtained for the first cell vitality assay, there was no distinct plateau seen during the first few weeks observed. Instead, there was a gradual decline in the percentage of live cells from 0-14 days PM followed by a rapid decrease from 14-22 days PM, which is denoted by a steeper slope in comparison to that obtained for EXPT 7 (Figure 3.25), that resulted in an overall 90% decrease in the percentage of viable cells. From this point forward, the percentage of live cells that existed gradually levelled off from 7% at 22 days PM to 0% at 43 days PM. This rapid decline in the percentage of chondrocyte viability may reflect the warmer change in climate and its effect on the rate of decomposition as discussed for previous experiments involving Western blot analysis of aggrecan and its appearance/disappearance (sections 4.2.3 and 4.2.4). Van't Hoff's Law, also known as the law of 10 or Q_{10}, asserts that the rate at which bodies decompose is related to the speed at which chemical reactions occur and that the rate of decomposition doubles with every 10˚C increase in temperature (Jenkinson, 1981 in Hopkins, 2008; Vass, 2011).

4.4.3 Cell vitality assay III: EXPT 9 (June 3rd to July 15th, 2013)

EXPT 9 trotters were interred during the summer season and were subjected to an overall average ambient temperature of 15.0˚C, nearly five degrees warmer than that for EXPT 8. The warmer climate resulted in a much more rapid decline in the PM integrity of the trotters' soft tissue components. By 14 days PM, the skin of trotters were pallid, wrinkled and exhibited markedly thinner skin with one trotter illustrating a break in its skin around its

MCP/MTP joint. However, the joint remained intact. Joint exposure to the soil environment occurred among trotters disinterred at 21 days PM. The lack of detectable aggrecan at this PMI and onwards (Figure 3.30) gives credence to the extent of soft tissue degradation and increased microbial activity that rapidly ensued as a result of the warmer climate. Like the Western blot for EXPT 8, EXPT 9 samples showed an increase in the number and intensity of heterogeneous subpopulations for aggrecan from 0-7 days PM. The 230kDa and aggrecan subpopulation CRPs for cartilage extracts collected at 14 days PM were the least intense.

Alpha-tubulin CRPs were visibly detected by Western blot analysis for samples 0-42 days PM although the CRP seen for the control sample (0 days PM) was due to overloading and the CRP present for samples extracted at 7 PM days was dimly seen (Figure 3.18). The cell vitality assay performed for these PM specimens displayed viable cells for up to 14 days PM (Figure 3.32). No live cells were detected thereafter. These results are comparable with the Western blot analysis conducted for these samples using MAb 2-B-6 to detect aggrecan (Figure 3.30). Aggrecan and viable cells were not detected from 21-42 days PM. On the other hand, the presence of α-tubulin outlasted the appearance of both live and dead cells as presented by the cell vitality assay. This finding is rather interesting, especially since the percentage of dead cells detected at 21 days PM was noticeably diminished. These remaining dead cells that continued to fluoresce appeared in the most central region of the cartilage cross-section suggesting that cell death proceeds from the superficial and deep zones towards its central aspect (middle/deep zones). Otsuki *et al*. (2008) noted that the number of dead cells present in control cartilage increased from the superficial zone to the middle zone in response to increased amounts of trauma. The results obtained from this and previous Western blots for α-tubulin (sections 4.3 and 4.4) suggest that, despite PG and cellular destruction, α-tubulin lingers within the ECM for quite some time before succumbing to proteolysis. Dissolution of the microtubule likely takes place around 42 days PM or shortly

thereafter. From 28-42 days PM, no evidence of live or dead chondrocytes existed. The lack of fluorescence for these cells was attributed to "empty lacunae" (Figure 3.33).

The time course graph for the percentage of live cells remaining with increasing PMI appeared vaguely sigmoidal, adopting an exponential curve (Figure 3.34). From 0-7 days PM, the percentage of viable cells dropped to approximately half, and then to 2% the following week before absolute cell death at 21 days PM. Of the three cell vitality assays conducted for porcine cartilage, this graph demonstrated the steepest slope and illustrates the impact that increasingly warmer temperature has on PM chondrocyte survival.

4.4.4 Cell vitality assay IV: EXPT 10 – Bovine (July 4th to August 15th, 2013)

The overall ambient temperature experienced bovine samples interred for EXPT 10 was 18.0˚C. Skinned bovine tail samples exhibited very soft muscle tissues, especially at the periphery, by 24 days PM and showed signs of liquefaction among the muscles, tendons and fat. At 31 days PM, the physical state of the soft tissues had worsened and demonstrated the onset of skeletonisation where the transverse processes of the spine began to show through. Western blot analyses for the immunodetection of aggrecan displayed 230kDa and 38 kDa CRPs (Figure 3.36). However, the Western blot images showed variable results at different protein concentrations. These results can be ascribed to the region-specific locations of aggrecan for which the nucleus pulposus (the central region of the IVJ) contains the highest concentration of type II collagen, aggrecan and chondrocytes and bares an ECM similar to hyaline articular cartilage, whereas the annulus fibrosus (outer region surrounding the nucleus pulposus) is mostly comprised of type I collagen and possesses very small amounts of chondrocytes (Iatridis *et al*., 2012; Masuda *et al*., 2003; Roughley, 2006; Sive *et al*., 2002; Sztrolovics *et al*., 1997). These factors were not taken into account upon extraction of cartilage samples from the entire IVJ surface. Therefore, it is highly possible that sample

extracts were randomly collected from regions consisting of the annulus fibrosus and would serve to explain the variable results obtained for bovine aggrecan. Despite these inconsistencies, the samples of bovine IVJ cartilage in Figure 3.36a demonstrates the same PM trend observed for porcine hyaline cartilage. The 230kDa CRP showed an increase in intensity from 10 to 17 days PM and then gradually decreased from 24 to 31 days PM. These results imply that the PM processes which govern the destruction of articular cartilage in porcine are reproducible for fibrocartilage and other mammalian species. In support of the latter claim, various studies have reported that various amino acid sequences for aggrecan are highly conserved among higher mammals (Caterson *et al*., 2000; Doege *et al*., 1991; Dudhia, 2005; Dudhia *et al*., 1996; Kiani *et al*., 2002; Roughley & Mort, 2014; Watanabe *et al*., 1998). Hence, the shared biochemistry between pigs and humans suggests that similar results should be obtained for human articular cartilage.

Regardless of increasing the protein concentration loaded per well to a maximum of 60µg protein per 20µl of sample buffer, no α-tublin CRPs were detected for the bovine cartilage extracts representing samples 0-31 days PM (Figure 3.19). A 58kDa CRP was solely present for a specimen of positive control, HG (10µg protein). The lack of α-tubulin CRPs for cartilage extracts removed from the IVJs of bovine tail is not entirely a surprise. Fibrocartilage in these joints are known to contain far less chondrocytes within its ECM in comparison to hyaline articular cartilage (Masuda *et al*., 2003; Roughley, 2006).

The cell vitality assay performed for the PM specimens of bovine IVJ cartilage showed relative overlap with EXPT 9 porcine samples in terms of time frame for which all chondrocytes have undergone apoptosis. For the bovine specimens, no live chondrocytes were seen at 17 days PM (Figure 3.37), whereas all chrondrocytes were established as dead by 21 days PM for porcine specimens (Figure 3.32). These PMIs are within four days of each other. The earlier cell death for bovine IVJ cartilage can be credited to the generally

warmer climate experienced by these PM samples. Unlike EXPT 9 samples, dead chondrocytes continued to fluoresce up to 31 days PM. This difference in the PM survival of nuclei derived from the fibrous cartilage of the IVJ and that for hyaline articular cartilage might have to do with the fact that chondrocytes are even more sparsely populated in IVJ cartilage. The movement of degradative enzymes to neighbouring cells in the IVJ cartilage may require more time to elicit catabolic responses. The graph for this data set is polynomial and bears the semblance of a sigmoidal curve (Figure 3.38). It bears a steep slope between the 10-17 days PMI for which the percent of live cells rapidly decline from 80% to 0%. Although this graph illustrates similarities in the PM trend for chondrocyte death, it is only reflective of data collected from a single experiment. Furthermore, the population numbers and distribution of chondrocytes within this connective tissue should also be taken into consideration as it is likely that these factors will contribute to variable results.

The work presented by Alibegović and colleagues (2014), Drobnič *et al*. (2005) and Lasczkowski *et al*. (2002) shows that the rate of PM survival for chondrocytes is greatly influenced by time and temperature. At warmer temperatures, the rate at which chondrocytes die also increases. The results obtained from the cell vitality assays conducted with porcine articular cartilage and bovine IVJ fibrocartilage supports the findings presented by Alibegović *et al*. (2014). However, the general appearance of the graphs obtained for this study gradually changed from sigmoidal to exponential for temperatures that ranged from 2.5˚C to 15˚C. Cell viability was prolonged for up to 35 days PM at an average ambient temperature of 2.5˚C and for up to 14 PM day at an average temperature of 15˚C. These discrepancies in the rates of cell death and overall appearance of the graphs is owed to a combination of other imposing factors, such as soil chemistry, moisture levels and microbial activity, that also affect the rate at which decomposition occurs. Furthermore, the cell vitality assay conducted for EXPT 7 also demonstrated that cooler temperatures have the ability to

accelerate cell death. Therefore, cell vitality assays may not be an appropriate forensic tool for bodies buried in extremely cold or hot climates.

4.4.5 Statistical reports on measures of association between PMI, average temperature and average precipitation for the percentage of live cells

Statistics derived from the Pearson product-moment correlation coefficient test for each of the independent variable assessed (Table 3.16) support the conclusions made by Alibegović *et al*. (2014), Drobnič *et al*. (2005) and Lasczkowski *et al*. (2002). They provide a general indication of the direction and strength of influence that each independent variable imposes on the PM survivability of chondrocytes. Of the three independent variables looked at, the passing of time had the greatest influence on the percentage of live cells that persisted with increasing PMI (section 3.3.4). Average temperature moderately influenced chondrocyte viability, whereas precipitation posed a relatively weak effect. These results imply that endogenous processes that take place during the PM decomposition of remains (for instance, the autolysis of cells, enzymatic activities, putrefaction) are responsible for the decline in live chondrocytes within the ECM. Numerous studies have proven this case (Carlo & Loeser, 2003; Dudhia, 2005; Goldring *et al*., 2011; Loeser, 2009; Martin & Buckwalter, 2006). Temperature (Carter *et al*., 2008) (section 4.2.4) and, to a lesser extent, moisture (section 4.2.3) affects the rate of enzyme activity which, in turn, influences the rate at which PM decay occurs.

A multiple linear regression analysis evaluated the magnitude of the relationships between the independent variables (PMI, average temperature, and average precipitation) and their effects on chondrocyte survival (percentage of live cells) (Table 3.17, section 3.3.4). The statistical output determined that PMI was the most significant factor bearing the greatest influence on changes in the percentage of viable cells and that average ambient temperature

and average precipitation had little effect. An explanation for the statistics for ambient temperature and average precipitation is that both factors do no directly impact chondrocyte survival. Rather, their effects are experienced indirectly through their direct influences on enzyme and microbial activities. Since microbial biomass and enzyme activity were not accounted for or evaluated as dependent variables affected by temperature and moisture, it is likely that the results obtained for this multiple linear regression is valid. In general, this output corroborates results obtained for the Pearson correlation test which identifies PMI as the major factor influencing cell death.

4.5 Trotters and fungal activity in buried soil environments

4.5.1 Soil environment and its effect on the extent of fungal growth

Proteolysis within the PM body is variable. Some proteins decompose during the early PM phase, whereas others decay during the later PM stage. It was assumed that this systematic degradation of the body's organs would result in the release of different protein compounds with time. During the early phase of PM decomposition, proteins comprising the neuronal and epithelial tissues, such as the lining found within the gastro-intestinal tract, are the first to undergo proteolysis. On the other hand, proteins that form the skin, muscles, reticulin and collagen, for instance, demonstrate a little more resilience to proteolytic processes (Dent *et al.*, 2004). Hypothetically, this activity might encourage microbial succession to take place whereby various species of soil microbes would be sequentially attracted to cadavers over time. However, the results obtained for a long-term (6 PM weeks) and short-term (1-7 PM days) burials suggested that microbial succession may be an impractical forensic tool for determining PMI during the first several weeks of interment.

Unlike previous studies which have reported evidence of EP fungal succession (Carter & Tibbett, 2003; Griffin, 1960; Sagara *et al*., 2008; Sagara, 1992; Suzuki, 2009; ten Broek, 2009), the results obtained in this study did not support these findings. Long-term burials conducted over a period of 42 days (EXPT 2, Table 2.1) with trotters interred in two different soil environments did not demonstrate notable patterns of fungal succession. Observations of PM fungal activity within the moist, nutrient-rich soil of CMP and the dry nutrient-deficient soil of HLT, both characterised as sandy silt loam (section 3.1), illustrated that environmental conditions impacted the growth of fungi.

Fungal samples collected from soil encrusted trotters (section 3.4) demonstrated growth characteristic of zygomycota (white, filamentous and fast-spreading) and ascomycota (tightly woven mycelia/filaments bearing sac-like cells called asci, slower growth rate). At 7 days PM, a white hyphal growth was noted at the dismembered ends of trotters from CMP. However, from 14-42 days PM, this growth was not discernible. On the contrary, HLT trotters disinterred around the same time period exhibited a similar hyphal growth from 7 to 21 days PM. At weekly intervals during this time frame, the hyphal growth became increasingly diminished as PMI increased. The physical appearance of this hyphal growth ceased at 30 days PM. This growth pattern may be indicative of environmental modifications affecting the soil environment, such as changes in ambient temperature, moisture levels, soil chemistry, pH and/or other microbial activity (Carter & Tibbett, 2008a; Forbes, 2008; Hopkins, 2008; Janaway, 2008; Rodriguez, 1997; Rogers *et al*., 2011). Fungal growth occurs soon after an influx of ammonium enters the soil environment (Carter & Tibbett, 2003, 2008a; Sagara *et al*., 2008; Tibbett & Carter, 2003). This increase in the concentration of ammonium begins to develop soon after the deposition of remains (Carter & Tibbett, 2008a) yet can also occur spontaneously in response to excess microbial respiration (Carter & Tibbett, 2003; Sagara *et al*., 2008). Bodies interred below ground have the propensity to

modify the soil environment's pH, causing it to become basic. Shortly thereafter, the pH of the environment gradually transforms to one that is acidic (Carter & Tibbett, 2008a). This change in pH transpires as the body continues to decompose and purge itself of its internal fluids. For this reason, it is reasonable to assume that the appearance and disappearance of the hyphae seen among PM trotters disinterred from the CMP and HLT burial plots came about in response to the basic soil environment generated by the decomposing trotters themselves. The gradual decline in the appearance of the hyphae as seen for trotters from HLT may have occurred as a result of the steady release of decomposition fluids generated as a result of autolytic and soil microbial processes. However, this rationale does not explain the lack of visible hyphae for trotters disinterred from CMP at 14 days PM and beyond. Therefore, differences in the moisture level of the soil environments may explain this discrepancy. As pointed out by Vass (2011), water serves several important functions in the process of decomposition, one of which is to act as a pH buffer. Rainfall experienced at CMP from 7 days PM and onwards, could have altered the initial pH of the soil at the time of interment. The growth characteristic of the fungi in question may express sensitivity to changes in water levels whereby levels above and/or below its optimal growth conditions might impede its development. Weekly changes in the soil's pH were not taken into account while carrying out this research study. In hindsight, this information would have been useful for understanding the decomposition-related changes that occur within in the soil environment and how these changes in pH affect saprophytic fungal growth. Another rationalisation for the lack of visible hyphal growth at later PMIs is the presence of soil microbes that are capable of competing with any fungi present. It is possible that the presence of microorganisms in the soil environment at HLT were not as abundant as those at CMP for lack of soil hydration. The moisture content of the soil environment greatly impacts microbial metabolic activities, such that increased water levels promotes microbial activity

and decreased water levels supress their metabolism (Carter & Tibbett, 2008a; Carter *et al.*, 2007; Hopkins, 2008) (section 4.2.3). With soil at CMP characterised as moist and nutrient-rich, increased microbial activity would explain the rapid decline in visible hyphal growth and, whereas a reduced microbial population would allow for the persistence of this fungus at HLT where the soil is characterised as dry and nutrient deficient.

For EXPT 3 trotters disinterred from CMP (section 3.4), the extent of hyphal growth at 7 days PM was far less than that which appeared for trotters disinterred from CMP for the same PMI (EXPT 2, section 3.4). The differences in the extent of hyphal growth are attributed to differences in the moisture content of the soil. Based on these observations as shown in Figure 3.42, the fungus found growing in association with the soil covered trotters is highly affected by changes in water levels. Excess moisture or lack of moisture and nutrients results in minimal growth (Carter & Tibbett, 2008a; Hopkins, 2008; Sagara *et al.*, 2008). EXPT 2 trotters from CMP demonstrated that fungus flourishes in moist, nutrient-rich soil, but not nutrient-rich soil that is saturated. These results implicitly demonstrate that the degree of fungal growth varies considerably in response to changing water levels within a soil environment.

4.5.2 Observance of fungal species present and their patterns of colonisation

Comparative analysis of trotters from EXPTs 2 and 3 (section 3.4) underwent further examination for the presence of microscopic fungi. Fungal samples collected from visible hyphae or soil in very close proximity to the skin of trotters presented several different species, three of which appear to be common to both CMP and HLT burial plots. For EXPT 2 trotters disinterred from CMP, fungal species were consistently observed from 7-42 days PM. These species were labelled Species 1 and Species 2 (Figure 3.43). Species 1 is the hyphal growth that was detectable upon disinterment of trotters. Its presence was detected

for 7-28 days PM, while Species 2 was present at 7-21 and 42 days PM. It is possible that Species 2 was present at 28 and 35 days PM but was not collected among the fungal samples retrieved with a needle point dissection probe. However, it is also likely that changes in the soil environment might have resulted in unfavourable conditions for the development of this particular species. As noted in section 4.5.1, changes in the moisture content of the soil environment impacted the growth rate and, therefore appearance, of fungal Species 1. The short-term observations of fungal colonies found in association with PM trotters (section 3.4.1, Figure 3.48) demonstrated the same randomness in terms of the appearance/disappearance of the fungal species detected. These findings suggest that fungal succession may not be an ideal forensic tool for establishing PMI during the early stages of cadaver decomposition. This is owing to the numerous environmental factors that impact their metabolic activities. The succession from EP fungi to LP fungi, as described by Carter and Tibbett (2003) and Suzuki (2009), was not observed among the PM trotters investigated for this experiment. The fungal species observed for EXPTs 2 and 3 are members belonging to Zygomycota and Ascomycota phyla which are characterised as EP fungi (Ibid). As mentioned in section 1.3.5, EP fungi are typically observed for up to 10 months and up to four years for LP PPF. Since this experiment was only carried out for a period 42 days, it is difficult to establish whether patterns of fungal colonisation are likely to exist and requires investigating larger sample sets for PMIs that go well beyond 42 days PM.

The sporulating structures of fungal Species 1-3 underwent microscopic analysis (Figures 4.43, 4.45 and 4.47) and established that the samples observed from CMP and HLT soil environments were likely to be identical. The similarity in fungal species present for both soil environments provides supporting evidence that they share a common chemistry. In addition, an attempt at determining the genuses for each species was undertaken. Species 1 was identified as *Varicosporium sp.*; Species 2 as *Aspergillus sp.*; and Species 3 as

Monilochaetes sp. (section 3.4.1). However, DNA analysis is necessary for confirming the genus of these fungi and establishing the actual identities of these species.

In summary, Species 1 and 2 were the most prominent fungi found in association with decomposing trotters. The rate and extent of growth observed for the white hyphae discovered growing on decomposed trotters was greatly affected by the soil environment and expressed variability as seen among trotters disinterred at 7 days PM from the same soil environment at different times. Species 1 demonstrated the appearance of hyphae at approximately one week PM. Furthermore, no particular trend illustrating the temporal colonisation of the fungi was observed among the fungal species examined.

Conclusion

Chapter 5

5.0 Conclusion

5.1 A summary of the research objectives

The overall aim of this research project was to explore the PM properties of cartilage at the molecular level and to examine the colonisation patterns of fungi associated with buried remains in order to determine their forensic worth. In general, the purpose for carrying out these studies was to determine whether or not PM cartilage and fungi could be used as alternative or supplementary tools to establish PMIs for bodies discovered beyond 48 hours. Despite the fact that numerous methods exist for estimating PMI, those that are typically considered most reliable involve examination of early PM changes among cadaver soft tissues (section 1.1.2). As PMI increases, the accuracy of these methods decreases especially since the rate at which PM changes among bodies occurs are greatly affected by a multitude of exogenous and endogenous factors. Furthermore, these methods do not take into account bodies buried in soil environments.

5.2 Cartilage degradation is an ordered process

Cartilage is an impressive soft tissue. This is owing to its physiological properties. Its sturdy ECM, comprised of durable type II collagen fibres and highly electronegative PGs, coupled with its sparsely populated chondrocytes that generate low metabolic activity, makes it well-adapted for strenuous conditions. This is proven by its ability to withstand the immediate and ongoing effects of PM decomposition long after the rapid decline of other soft tissues. More importantly, the PM degradation of cartilage is a remarkably ordered process. For these reasons, cartilage is an ideal candidate for forensic studies.

In this study, the biomolecular breakdown of cartilage demonstrated systematic changes in colour and robustness, an increase in the heterogeneity of aggrecan subpopulations and decreases in chondrocyte viability with increasing PMI. Depending on environmental conditions, these changes were observed for as long as 6 PM weeks. In addition, the durability of cartilage was further substantiated by evidence of water retention among samples collected 0-42 days PM and from different soil environments, where PM cartilage maintained percentages close to the average (70%) obtained for control samples. Together, these results indicate that the PM degradation of cartilage occurs as a domino reaction where there is a gradual and progressive destruction of the tissue with increasing time.

The PM degradation of cartilage is relatively unaffected by the external environment (soil, water submersed, exposure to air) as the surrounding skin, muscle tissues, tendons and synovium provide a substantial barrier between the joint tissue and the soil environment, therefore providing cartilage with extended protection. Once the joint is exposed to the soil environment, cartilage becomes accessible to soil microbes that metabolise aggrecan and render the protein undetectable soon after. In warm climates with temperatures ranging from 10˚C-15˚C, joint exposure was observed from 21-32 days PM. This process is directly governed by the autolysis of skin and muscle tissues, where increases in temperature causes accelerated enzymatic and ROS activities that hasten proteolysis of these tissues and results in joint exposure. However, soil moisture also plays a role in this PM process by generating an influx of soil microorganisms that aid with the decomposition of soft tissues leading to joint exposure. An increase in both temperature and soil water content produces favourable conditions for microbial activity. In summary, the PM processes that affect the rate of joint exposure are simultaneously occurring from within and outside of trotters.

Destruction of the cartilage cellular matrix also proceeds in an orderly manner. Like aggrecan, chondrocyte vitality is affected by autolysis and, to a lesser extent, climate conditions. Nonetheless, cell death proceeds at an extremely slower rate than observed by other cells within the body. In cooler climates (3˚C), chondrocytes are capable of surviving for up to 35 PM days. At temperatures close to or below 0˚C, the rate of chondrocyte death also increases. Cartilage subjected to an average temperature of 15˚C demonstrates the presence of live chondrocytes for up to 14 PM days and shows a notable reduction in the presence of nuclei by 21 days PM. Therefore, the rate of chondrocyte death is accelerated as ambient temperatures become increasingly warmer, or approaches 0˚C.

Western blot detection of chondrocytes using anti-α-tubulin revealed that the ECM of PM cartilage remains fairly intact for approximately 1-2 weeks and then loosens. The chondrocytes become accessible for immunodetection and are consistently present at relatively the same amounts thereafter. Furthermore, chondrocyte death does not equate with the complete destruction of cellular components. Even though cells had undergone apoptosis, the α-tubulin microfilament did not begin to diminish until roughly 6 weeks PM, making this protein more resilient to PM decompositional processes. Alpha-tubulin consistently appeared diminished or completely undetectable at this PMI and may indicate that the destruction of this protein is time-dependent. However, further testing should be done to confirm this result.

For samples of IVJ cartilage from bovine, Western blot and cell vitality analyses proved that similar results are obtainable using a different type of cartilage (fibrocartilage). Although this is possible, IVJ cartilage is not considered ideal for examining PM changes in the ECM and cellular matrix since the location of aggrecan and chondrocytes are generally region-specific. This was made obvious by lack of, or variations in, immunodetection for

aggrecan and the inability to detect α-tubulin. Cell vitality assays revealed rather isolated cells in comparison to articular cartilage for which the chondrocytes appeared more densely populated.

The discoveries made about the PM destruction of cartilage illustrates that there is potential to expand the 48-hours limitations currently imposed by other softer tissues. In addition, the process of cartilage degradation does not appear to be affected by its immediate environment. The analogous structural arrangement of the cartilage ECM and its chondrocytes, as well as the conservation of numerous amino acid sequences along the aggrecan protein core, offers further support to claims that pigs are good forensic models for human decomposition because of their shared biogeochemistry. The PM destruction of this soft tissue also shows similarities in terms of the mechanisms involved with the progression of degenerative joint diseases. Nonetheless, investigations of PM cartilage samples from human cadavers are crucial for validating the appropriateness and practicality of these findings.

5.3 The activity of soil fungi is greatly impacted by changes in the immediate environment

The saprophytic, white hyphae observed growing among PM trotters showed development by 7 days PM. Its ability to proliferate is governed by the nutrients available in the soil and moisture content. In moist nutrient-rich environments, this fungus is capable of rapidly spreading, whereas in nutrient-deficient soil the extent and rate of its growth is retarded. Its growth is also hindered in saturated and extremely dry soil environments. This fungal species demonstrates sensitivity to changes in the immediate soil environment.

Trotters interred in the CMP and HLT burial plots demonstrated similarities in the species of colonising soil fungi as a result of comparable soil chemistry. Between the two plots, Species 1 and 2 were the most prevalent and were observed for up to 42 days PM and indicates that soils demonstrating a similar chemical make-up are likely to exhibit common fungal species. The rare occurrences of Species 3 and 4 may reflect their rarity in the natural soil environment or signify their strict requirements for certain environmental condition in order to proceed with their development. In terms of colonisation patterns, Species 1 was consistently present for the first three weeks of interment at CMP and for the first four at HLT. Beyond these PMIs their presence among trotters disinterred from both burial plots was no longer observed and may be revealing about PM changes that are taking place among the decomposing trotters and their immediate soil environment. Species 2, on the other hand, was not consistently present over the course of 42 days PM. Its presence was variable and lacked consistency which may be an indication of its sensitivity to the alterations in the soil environment and may have less to do with the effects of degrading tissue. The random colonisation of Species 1 and 2 were most notable during the first week of interment. These results suggest that early phase soil fungi do not express distinct growth patterns that can be deemed useful for estimating PMI. However, the length of time that this study was carried out for and the technique used for sample collection may have affected the ability to obtain an overall, general picture of fungal colonisation. Nonetheless, it appears that fungal succession is problematic for remains that are interred for up to 42 days PM.

5.4 Future research and other implications

This research study presents new opportunities for exploring the PM degradation of cartilage and its ability to be employed as a forensic tool. The investigation of aggrecan

involved looking at roughly 87% of its PG protein core which does not account for its remaining structure that consists of the IGD, link protein, GAGs (such as keratin which is known to be quite resistant to PM destruction) (Dent *et al*., 2004) and a HA backbone (Knudson & Knudson, 2001). Therefore, the remaining 13% has yet to be explored. For this reason, antibodies designed to detect these specific regions should be further investigated on cartilage samples for similar periods of time in order to obtain a comprehensive picture of the PM destruction that ensues for cartilage PG. Moreover, the data collected would provide a better understanding of the entire PM processes that transpire after death and allow the forensic community to evaluate the relevance of this tissue for PM examinations.

Chondrocytes have also proven their capacity to withstand harsh environments and the immediate effects that various endogenous and exogenous factors impose on various soft tissues that comprise the body. Their ability to survive for as long as 35 PM days implies that the rate at which these cells die may be useful for providing estimates of time since death. In this particular study, the statistical analyses conducted for the PM viability of chondrocytes (sections 3.3.3 and 3.3.4) offers the forensic community an additional method that has potential to repudiate the criticism that forensic science is a subjective discipline. Furthermore, the presence of viable cells, long after death, offers an opportunity to investigate cartilage as a source of DNA to assist with the PM identification of unknown persons, especially after other soft tissues, like muscle, are rendered useless. Therefore, the ability to establish a positive identification for unknown decedents, especially in cases where dental evidence is missing, may be a possibility long after decompositional processes have rendered the cellular content of other soft tissues useless for DNA extraction and/or examination.

Similarities in the structural arrangement and amino acid sequence of aggrecan for porcine and human subjects validate the use of pigs as models for human decomposition.

Although it is known that the decomposition of pigs closely resembles that for humans because of their shared biogeochemistry and that porcine tissue is more readily accessible than human tissue, examination of human cartilage is still required to substantiate the use of pigs as their models. The results obtained for porcine and bovine specimens can prove useful in criminal cases that conern crimes against animals that may involve food, endangered species or illegal trade crimes (Gupta *et al*., 2013).

The ability to decipher sequential patterns of fungal colonisation has proven to be quite a difficult task. The activity of fungi found in close proximity to PM trotters in buried soil environments is greatly influenced by many extrinsic factors. Which of these factors bear the greatest influence on their activity is a question that has yet to be answered. In retrospect, measures of soil moisture content, and pH with increasing PMI might have helped to formulate a clearer picture of the phenomena affecting fungal colonisation. Furthermore, the length of time for which these observations were carried out was relatively short in comparison to the aforementioned previous studies conducted by Carter and Tibbett (2003) and Suzuki (2009) which examined the PM colonisation of fungi over the course of 10 months to four years. Therefore, more long-term experiments are required to examine the PM changes that occur among the fungal assemblages that colonise cadavers buried in soil environments over time. As it stands, the transition for soil chemistry from a basic to acidic environment is a gradual process that is greatly affected by numerous environmental factors, such as fluctuations in precipitation and temperature.

Overall, the research presented in this thesis demonstrates that articular cartilage is an excellent candidate for forensic taphonomic research. As it stands, this cartilage is a more robust soft tissue than its softer counterparts and has the potential to indicate PMIs that surpass the 48 and 100-hours limitations of other soft tissues and biological fluids. In general, it presents an opportunity to establish PMIs as long as 6 PM weeks (42 days PM).

Cartilage may prove to be a useful tool in forensic situations where typical indicators of PMI, such as insect activity, are lacking and/or bodies have been discovered well after the crucial 48 and 100-hours after death. Moreover, the long-term viability of PM chondrocytes also provides an avenue for exploring the use of these cells as sources of DNA for identification purposes. The results obtained for the growth rate of the fungal hyphae observed and the inability to distinguish successive patterns of fungal colonisation should not rule out the use of fungi as tools for forensic investigations. On the contrary, the results obtained for the experiments conducted serve to illustrate the complexities involved with studying the relationship between these microorganism and cadavers buried in soil environments. As a result, future studies should attempt to include observations regarding soil moisture content and pH levels in order to understand how these variables influence the rate and patterns of the fungi observed in this experiment.

References

Abeyweera, T. P., Chen, X. and Rotenberg, S. A. (2009) Phosphorylation of alpha6-tubulin by protein kinase Calpha activates motility of human breast cells. *The Journal of Biological Chemistry*, **284**(26), 17648–56.

Adjutantis, G. and Coutselinis, A. (1972) Estimation of the time of death by potassium levels in the vitreous humour. *Forensic Science*, **1**(1), 55–60.

Ahi, R. S. and Garg, V. (2011) Role of vitreous potassium level in estimating postmortem interval and the factors affecting it. *Journal of Clinical and Diagnostic Research*, **5**(1), 13–15.

Alibegović, A., Balažic, J., Petrovič, D., Hribar, G., Blagus, R. and Drobnič, M. (2014) Viability of human articular chondrocytes harvested postmortem: changes with time and temperature of in vitro culture conditions. *Journal of Forensic Sciences*, **59**(2), 522–8.

Althaus, L. and Henßge, C. (1999) Rectal temperature time of death nomogram: sudden change of ambient temperature. *Forensic Science International*, **99**, 171–178.

Anderson, B., Meyer, J. and Carter, D. O. (2013) Dynamics of ninhydrin-reactive nitrogen and pH in gravesoil during the extended postmortem interval. *Journal of Forensic Sciences*, **58**(5), 1348–52.

Armstrong, C. G. and Mow, V. C. (1982) Variations in the intrinsic mechanical properties of human articular cartilage with age, degeneration, and water content. *The Journal of Bone and Joint Surgery. American Volume*, **64**(1), 88–94.

Arner, E. C. (2002) Aggrecanase-mediated cartilage degradation. *Current Opinion in Pharmacology*, **2**(3), 322–9.

Arner, E. C., Pratta, M. A., Trzaskos, J. M., Decicco, C. P. and Tortorella, M. D. (1999) Generation and Characterization of Aggrecanase: a soluble, cartilage-derived aggrecan-degrading activity. *The Journal of Biological Chemistry*, **274**(10), 6594–6601.

Aspberg, A. (2012) The different roles of aggrecan interaction domains. *The Journal of Histochemistry and Cytochemistry*, **60**(12), 987–996.

Athanasiou, K. A., Darling, E. M., DuRaine, G. D., Hu, J. C. and Reddi, A. H. (2013) *Articular Cartilage*. Boca Raton: CRC Press Taylor and Francis Group.

Barnett, H. L. and Hunter, B. B. (1972) *Illustrated Genera of Imperfect Fungi*. 3rd ed. Minneapolis: Burgess Publishing Company.

Bayliss, M. T. and Ali, S. Y. (1978a) Age-Related Changes in the Composition and Structure of Human Articular-cartilage Proteoglycans. *Biochemical Journal*, **176**, 683–693.

Bayliss, M. T. and Ali, S. Y. (1978b) Isolation of proteoglycans from human articular cartilage. *Biochemical Journal*, **169**, 123–132.

Beckett, S. (2009) Forensic Ecology: CSI hedgerow. *The Telegraph* [online] 12 February 2009. Retrieved September 12, 2014, from http://www.telegraph.co.uk/gardening/4579283/Forensic-Ecology-CSI-hedgerow.html

Bradley, D. A., Kaabar, W., Gundogdu, O., Farquharson, M. J., Janousch, M., Bailey, M. and Jeynes, C. (2010) Synchrotron and ion beam studies of the bone–cartilage interface. *Nuclear Instruments and Methods in Physics Research Section A: Accelerators, Spectrometers, Detectors and Associated Equipment*, **619**(1-3), 330–337.

Bryant, V. M. (2013) Analytical techniques in forensic palynology. In *Encyclopedia of Quaternary Science*. Elsevier.

Bunch, A. W. and Shine, C. C. (2009) Science contextualized: the identification of U.S. MIA of the Vietnam war from two perspectives. *in* Steadman, D. W. (ed.) *Hard evidence: case studies in forensic anthropology*. 2nd ed. New Jersey: Prentice Hall, pp. 52–61.

Byers, S. N. (2005) *Introduction to forensic anthropology: a textbook*. 2nd ed. Boston: Pearson Education, Inc.

Capín-Gutiérrez, N., Talamás-Rohana, P., González-Robles, A., Lavalle-Montalvo, C. and Kourí, J. B. (2004) Cytoskeleton disruption in chondrocytes from a rat osteoarthrosic (OA)-induced model: its potential role in OA pathogenesis. *Histology and Histopathology*, **19**, 1125–1132.

Carlo, M. D. and Loeser, R. F. (2003) Increased oxidative stress with aging reduces chondrocyte survival correlation with intracellular glutathione levels. *Arthritis & Rheumatism*, **48**(12), 3419–3430.

Carter, D. O. and Tibbett, M. (2003) Taphonomic mycota: fungi with forensic potential. *Journal of Forensic Sciences*, **48**(1), 168–171.

Carter, D. O. and Tibbett, M. (2008a) Cadaver decomposition and soil: processes. *in* Tibbett, M. and Carter, D. O. (eds.), *Soil analysis in forensic taphonomy: chemical and biological effects of buried human remains*. Boca Raton: CRC Press Taylor and Francis Group, pp. 29–51.

Carter, D. O. and Tibbett, M. (2008b) Does repeated burial of skeletal muscle tissue (*Ovis aries*) in soil affect subsequent decomposition? *Applied Soil Ecology*, **40**(3), 529–535.

Carter, D. O., Yellowlees, D. and Tibbett, M. (2007) Cadaver decomposition in terrestrial ecosystems. *Die Naturwissenschaften*, **94**(1), 12–24.

Carter, D. O., Yellowlees, D. and Tibbett, M. (2008) Temperature affects microbial decomposition of cadavers (*Rattus rattus*) in contrasting soils. *Applied Soil Ecology*, **40**(1), 129–137.

Caterson, B., Flannery, C. R., Hughes, C. E. and Little, C. B. (2000) Mechanisms involved in cartilage proteoglycan catabolism. *Matrix Biology: Journal of the International Society for Matrix Biology*, **19**(4), 333–44.

Catts, E. P. (1992) Problems in estimating the postmortem interval. *Journal of Agricultural Entomology*, **9**(4), 245–255.

Chen, C. T., Burton-Wurster, N., Borden, C., Hueffer, K., Bloom, S. E. and Lust, G. (2001) Chondrocyte necrosis and apoptosis in impact damaged articular cartilage. *Journal of Orthopaedic Research*, **19**(4), 703–11.

Clark, M. A., Worrell, M. B. and Pless, J. E. (1997) Postmortem changes in soft tissues. *in* Haglund, W. D. and Sorg, M. H. (eds.), *Forensic taphonomy: the postmortem fate of human remains*. Boca Raton: CRC Press Taylor and Francis Group, pp. 151–170.

Coe, J. I. (1989) Vitreous potassium as a measure of the postmortem interval: an historical review and critical evaluation. *Forensic Science International*, **42**, 201–213.

Deacon, J. W. (2006) *Fungal Biology*. 4th ed. Oxford: Wiley-Blackwell Publishing Ltd.

Dean, R. T., Roberts, C. R., Forni, L. G. and Al, D. E. T. (1984) Oxygen-centred free radicals can efficiently degrade the polypeptide of proteoglycans in whole cartilage. *Bioscience Reports*, **4**(12), 1017–1026.

Dent, B. B., Forbes, S. L. and Stuart, B. H. (2004) Review of human decomposition processes in soil. *Environmental Geology*, **45**(4), 576–585.

Dirkmaat, D. C. and Adovasio, J. M. (1997) The role of archaeology in the recovery and interpretation of human remains from an outdoor forensic setting. *in* Haglund, W. D. and Sorg, M. H. (eds.), *Forensic taphonomy: the postmortem fate of human remains*. Boca Raton: CRC Press Taylor and Francis Group, pp. 39–64.

Doege, K. J., Sasaki, M., Kimura, T., Yamada, Y., Doegesq, K. J., Sasakill, M. and Kimurajj, T. (1991) Complete coding sequence and deduced primary structure of the human cartilage large aggregating proteoglycan, aggrecan. *The Journal of Biological Chemistry*, **266**(2), 894–902.

Drobnič, M., Marš, A., Alibegović, A., Bole, V., Balažic, J., Grubič, Z. and Brecelj, J. (2005) Viability of human chondrocytes in an ex vivo model in relation to temperature and cartilage depth. *Folia Biologica (Praha)*, **51**, 103–108.

Drolet, R., D'Allaire, S. and Chagnon, M. (1990) The evaluation of postmortem ocular fluid analysis as a diagnostic aid in sows. *Journal of Veterinary Diagnostic Investigation*, **2**(1), 9–13.

Dudhia, J. (2005) Aggrecan, aging and assembly in articular cartilage. *Cellular and Molecular Life Sciences : CMLS*, **62**(19-20), 2241–56.

Dudhia, J., Davidson, C. M., Wells, T. M., Vynios, D. H., Hardingham, T. E. and Bayliss, M. T. (1996) Age-related changes in the content of the C-terminal region of aggrecan in human articular cartilage. *The Biochemical Journal*, **313**, 933–40.

Ewers, B. J., Dvoracek-Driksna, D., Orth, M. W. and Haut, R. C. (2001) The extent of matrix damage and chondrocyte death in mechanically traumatized articular cartilage explants depends on rate of loading. *Journal of Orthopaedic Research: Official Publication of the Orthopaedic Research Society*, **19**(5), 779–84.

Ferreira, M. T. and Cunha, E. (2013) Can we infer post mortem interval on the basis of decomposition rate? A case from a Portuguese cemetery. *Forensic Science International*, **226**(1-3), 298.e1–6.

Fitzpatrick, R. W. (2008) Nature, distribution, and origin of soil materials in the forensic comparison of soils. *in* Tibbett, M. and Carter, D. O. (eds.), *Soil analysis in forensic taphonomy*. Boca Raton: CRC Press Taylor and Francis Group, pp. 1–28.

Flannery, C. R., Little, C. B. and Caterson, B. (1998) Molecular cloning and sequence analysis of the aggrecan interglobular domain from porcine, equine, bovine and ovine cartilage: comparison of proteinase-susceptible regions and sites of keratan sulfate substitution. *Matrix Biology*, **16**(8), 507–511.

Forbes, S. L. (2008a) Decomposition chemistry in a burial environment. *in* Tibbett, M. and Carter, D. O. (eds.), *Soil analysis in forensic taphonomy*. Boca Raton: CRC Press Taylor and Francis Group, pp. 203–223.

Forbes, S. L. (2008b) Potential determinants of postmortem and postburial interval of buried remains. *in* Tibbett, M. and Carter, D. O. (eds.), *Soil analysis in forensic taphonomy: chemical and biological effects of buried human remains*. Boca Raton: CRC Press Taylor and Francis Group, pp. 225–246.

Forbes, S. L., Stuart, B. H. and Dent, B. B. (2002) The identification of adipocere in grave soils. *Forensic Science International*, **127**(3), 225–230.

Fortier, L. A, Barker, J. U., Strauss, E. J., McCarrel, T. M. and Cole, B. J. (2011). The role of growth factors in cartilage repair. *Clinical Orthopaedics and Related Research*, **469**(10), 2706–15.

Galloway, A. (1997) The process of decomposition: a model from the arizona-sonoran desert. *in* Haglund, W. D. and Sorg, M. H. (eds.), *Forensic taphonomy: the postmortem fate of human remains*. Boca Raton: CRC Press Taylor and Francis Group, pp. 139–150.

Gannon, K. and Gilbertson, D. L. (2014) *Case studies in drowing forensics*. Boca Raton: CRC Press Taylor and Francis Group.

Gendron, C., Kashiwagi, M., Lim, N. H., Enghild, J. J., Thøgersen, I. B., Hughes, C., Caterson, B. and Nagase, H. (2007) Proteolytic activities of human ADAMTS-5:

comparative studies with ADAMTS-4. *The Journal of Biological Chemistry*, **282**(25), 18294–306.

Gill-King, H. (1997). Chemical and ultrastructural aspects of decomposition. *in* Haglund, W. D. and Sorg, M. H. (eds.), *Forensic taphonomy: the postmortem fate of human remains*. Boca Raton: CRC Press Taylor and Francis Group, pp. 93–108.

Gino, S., Robino, C., Bonanno, E. and Torre, C. (2003) DNA typing from epiglottic cartilage of exhumed bodies. *International Congress Series*, **1239**, 885–887.

Goldring, M. B. and Marcu, K. B. (2009) Cartilage homeostasis in health and rheumatic diseases. *Arthritis Research & Therapy*, **11**(3), 224.

Goldring, M. B., Otero, M., Plumb, D. A., Dragomir, C., Favero, M., El Hachem, K., Hashimoto, K., Roach, H. I., Olivotto, E., Borzì, R. M. and Marcu, K. B. (2011) Roles of inflammatory and anabolic cytokines in cartilage metabolism: signals and multiple effectors converge upon MMP-13 regulation in osteoarthritis. *European Cells & Materials*, **21**, 202–220.

Griffin, D. M. (1960) Fungal colonization of sterile hair in contact with soil. *Transactions British Mycological Society*, **43**(4), 583–596.

Gupta, S. K., Kumar, A., Hussain, S. A., Vipin and Singh, L. (2013) Cytochrome b based genetic differentiation of Indian wild pig (*Sus scrofa cristatus*) and domestic pig (*Sus scrofa domestica*) and its use in wildlife forensics. *Science & Justice: Journal of the Forensic Science Society*, **53**(2), 220–2.

Haelewaters, D. (2013) Hebeloma, pioneer genus in forensic mycology. *Fungi*, **6**(3), 47–48.

Haskell, N. H., Hall, R. D., Cervenka, V. J. and Clark, M. A. (1997) On the body: insects' life stage presence and their postmortem artifacts. *in* Haglund, W. D. and Sorg, M. H. (eds.), *Forensic taphonomy: the postmortem fate of human remains*. Boca Raton: CRC Press Taylor and Francis Group.

Haslam, T. C. F. and Tibbett, M. (2009) Soils of contrasting pH affect the decomposition of buried mammalian (*Ovis aries*) skeletal muscle tissue. *Journal of Forensic Sciences*, **54**(4), 900–4.

Hawksworth, D. L. (2001) The magnitude of fungal diversity: the 1.5 million species estimate revisited. *Mycological Research*, **105**(12), 1422–1432.

Hawksworth, D. L. and Wiltshire, P. E. J. (2011) Forensic mycology: the use of fungi in criminal investigations. *Forensic Science International*, **206**(1-3), 1–11.

Hayes, A. J., Hughes, C. E. and Caterson, B. (2008) Antibodies and immunohistochemistry in extracellular matrix research. *Methods (San Diego, Calif.)*, **45**(1), 10–21.

Heinegård, D. and Oldberg, Å. (1989) Structure and biology of cartilage and bone matrix noncollagenous macromolecules. *FASEB Journal*, **3**, 2042–2051.

Hembree, W. C., Ward, B. D., Furman, B. D., Zura, R. D., Nichols, L. A., Guilak, F. and Olson, S. A. (2007) Viability and apoptosis of human chondrocytes in osteochondral fragments following joint trauma. *The Journal of Bone and Joint Surgery. British Volume*, **89**(10), 1388–95.

Henrotin, Y., Kurz, B. and Aigner, T. (2005) Oxygen and reactive oxygen species in cartilage degradation: friends or foes? *Osteoarthritis and Cartilage/Osteoarthritis Research Society*, **13**(8), 643–54.

Henßge, C. (1988) Death time estimation in case work. I. The rectal temperature time of death nomogram. *Forensic Science International*, **38**(3-4), 209–36.

Henßge, C. and Madea, B. (2007) Estimation of the time since death. *Forensic Science International*, **165**(2-3), 182–4.

Herreros, L., Rodríguez-Fernandez, J. L., Brown, M. C., Alonso-Lebrero, J. L., Cabañas, C., Sánchez-Madrid, F., Longo, N., Turner, C. E. and Sánchez-Mateos, P. (2000) Paxillin localizes to the lymphocyte microtubule organizing center and associates with the microtubule cytoskeleton. *The Journal of Biological Chemistry*, **275**(34), 26436–40.

Hilbert, N., Schiller, J., Arnhold, J. and Arnold, K. (2002) Cartilage degradation by stimulated human neutrophils: elastase is mainly responsible for cartilage damage. *Bioorganic Chemistry*, **30**(2), 119–32.

Hitosugi, M., Ishii, K., Yaguchi, T., Chigusa, Y., Kurosu, A., Kido, M., Nagai, T. and Tokudome, S. (2006) Case report: fungi can be a useful forensic tool. *Legal Medicine (Tokyo, Japan)*, **8**(4), 240–2.

Hoffman, A. (1987) Microdetermination of proteoglycans and glycosaminoglycans in the presence of guanidine hydrochloride sepharose CL-4B column chromatogra-. *Analytical Biochemistry*, **161**, 103–108.

Honjyo, K., Yonemitsu, K. and Tsunenari, S. (2005) Estimation of early postmortem intervals by a multiple regression analysis using rectal temperature and non-temperature based postmortem changes. *Journal of Clinical Forensic Medicine*, **12**(5), 249–53.

Hopkins, D. W. (2008) The role of soil organisms in terrestrial decomposition. *in* Tibbett, M. and Carter, D. (eds.), *Soil analysis in forensic taphonomy*. Boca Raton: CRC Press Taylor and Francis Group, pp. 53–66.

Hopkins, D. W., Wiltshire, P. E. J. and Turner, B. D. (2000) Microbial characteristics of soils from graves: an investigation at the interface of soil microbiology and forensic science. *Applied Soil Ecology*, **14**(3), 283–288.

Howard, G. T., Duos, B. and Watson-Horzelski, E. J. (2010) Characterization of the soil microbial community associated with the decomposition of a swine carcass. *International Biodeterioration & Biodegradation*, **64**(4), 300–304.

Huculak, M. A. and Rogers, T. L. (2009) Reconstructing the sequence of events surrounding body disposition based on color staining of bone. *Journal of Forensic Sciences*, **54**(5), 979–84.

Iatridis, J. C., Godburn, K., Wuertz, K., Alini, M. and Roughley, P. J. (2012) Region-dependent aggrecan degradation patterns in the rat intervertebral disc are affected by mechanical loading in vivo. *Spine*, **36**(3), 203–209.

Ikram, N., Hassan, K. and Tufail, S. (2004) Cytokines. *International Journal of Pathology*, **2**(1), 47–58.

Inagawa, K., Oohashi, T., Nishida, K., Minaguchi, J., Tsubakishita, T., Yaykasli, K. O., Ohtsuka, A, Ozaki, T., Moriguchi, T. and Ninomiya, Y. (2009) Optical imaging of mouse articular cartilage using the glycosaminoglycans binding property of fluorescent-labeled octaarginine. *Osteoarthritis and Cartilage/OARS, Osteoarthritis Research Society*, **17**(9), 1209–18.

Ishii, K., Hitosugi, M., Kido, M., Yaguchi, T., Nishimura, K., Hosoya, T. and Tokudome, S. (2006) Brief communication: analysis of fungi detected in human cadavers. *Legal Medicine (Tokyo, Japan)*, **8**(3), 188–90.

Ishii, K., Hitosugi, M., Yaguchi, T. and Tokudome, S. (2007) Letter to the editor: the importance of forensic mycology. *Legal Medicine (Tokyo, Japan)*, **9**(5), 287.

Ismail, E. C., Kaabar, W., Garrity, D., Gundogdu, O., Bunk, O., Pfeiffer, F., Farquharson, M. J. and Bradley, D. A. (2010) X-ray phase contrast imaging of the bone-cartilage interface. *Applied Radiation and Isotopes: Including Data, Instrumentation and Methods for Use in Agriculture, Industry and Medicine*, **68**(4-5), 767–71.

Jaggers, K. A. and Rogers, T. L. (2009) The effects of soil environment on postmortem interval: a macroscopic analysis. *Journal of Forensic Sciences*, **54**(6), 1217–22.

Janaway, R. C. (2008) The decomposition of materials associated with buried cadavers. *in* Tibbett, M. and Carter, D. O. (eds.), *Soil analysis in forensic taphonomy*. Boca Raton: CRC Press Taylor and Francis Group, pp. 154–201.

Janssen, W. (1984) *Forensic histopathology*. 1st ed. New York: Springer.

Jashnani, K. D., Kale, S. A. and Rupani, A. B. (2010) Vitreous humor: biochemical constituents in estimation of postmortem interval. *Journal of Forensic Sciences*, **55**(6), 1523–7.

Kakizaki, E., Takahama, K., Seo, Y., Kozawa, S., Sakai, M. and Yukawa, N. (2008) Marine bacteria comprise a possible indicator of drowning in seawater. *Forensic Science International*, **176**(2-3), 236–47.

Kaliszan, M., Hauser, R. and Kernbach-Wighton, G. (2009) Estimation of the time of death based on the assessment of post mortem processes with emphasis on body cooling. *Legal Medicine (Tokyo, Japan)*, **11**(3), 111–7.

Kashiwagi, M., Enghild, J. J., Gendron, C., Hughes, C., Caterson, B., Itoh, Y. and Nagase, H. (2004) Altered proteolytic activities of ADAMTS-4 expressed by C-terminal processing. *The Journal of Biological Chemistry*, **279**(11), 10109–19.

Kheir, E. and Shaw, D. (2009) Hyaline articular cartilage. *Orthopaedics and Trauma*, *23*, 450–455.

Kiani, C., Chen, L., Wu, Y. J., Yee, A. J. and Yang, B. B. (2002) Structure and function of aggrecan. *Cell Research*, **12**(1), 19–32.

Knight, B. (1987) *Legal Aspects of Medical Practice*. 4th ed. Edinburgh: Churchill Livingstone.

Knudson, C. B. and Knudson, W. (2001) Cartilage proteoglycans. *Seminars in Cell & Developmental Biology*, **12**(2), 69–78.

Koshimizu, T., Kawai, M., Kondou, H., Tachikawa, K., Sakai, N., Ozono, K. and Michigami, T. (2012) Vinculin functions as regulator of chondrogenesis. *The Journal of Biological Chemistry*, **287**(19), 15760–75.

Kuettner, K. E. (1992, June) Biochemistry of articular cartilage in health and disease. *Clinical Biochemistry*.

Lange, N., Swearer, S. and Sturner, W. Q. (1994) Human postmortem interval estimation from vitreous potassium: an analysis of original data from six different studies. *Forensic Science International*, **66**(3), 159–174.

Lasczkowski, G. E., Aigner, T., Gamerdinger, U., Weiler, G. and Bratzke, H. (2002) Visualization of postmortem chondrocyte damage by vital staining and confocal laser scanning 3D microscopy. *Journal of Forensic Sciences*, **47**(3), 663–6.

Lewis, J. L., Deloria, L. B., Oyen-Tiesma, M., Thompson, R. C., Ericson, M. and Oegema, T. R. (2003) Cell death after cartilage impact occurs around matrix cracks. *Journal of Orthopaedic Research : Official Publication of the Orthopaedic Research Society*, **21**(5), 881–7.

Ley, S. C., Verbi, W., Pappin, D. J., Druker, B., Davies, A. A. and Crumpton, M. J. (1994) Tyrosine phosphorylation of alpha tubulin in human T lymphocytes. *European Journal of Immunology*, **24**(1), 99–106.

Li, S., Cao, J., Shi, Z., Chen, J., Zhang, Z., Hughes, C. E. and Caterson, B. (2008) Promotion of the articular cartilage proteoglycan degradation by T-2 toxin and selenium protective effect. *Journal of Zhejiang University. Science. B*, **9**(1), 22–33.

Little, C. B., Hughes, C. E., Curtis, C. L., Janusz, M. J., Bohne, R., Wang-Weigand, S., Taiwo, Y. O., Mitchell, P. G., Otterness, I. G., Flannery, C. R. and Caterson, B. (2002). Matrix metalloproteinases are involved in C-terminal and interglobular domain processing of cartilage aggrecan in late stage cartilage degradation. *Matrix Biology: Journal of the International Society for Matrix Biology*, **21**(3), 271–88.

Loeser, R. F. (2009) Aging and osteoarthritis: the role of chondrocyte senescence and aging changes in the cartilage matrix. *Osteoarthritis and Cartilage/OARS, Osteoarthritis Research Society*, **17**(8), 971–9.

Lüsse, S., Claassen, H., Gehrke, T., Hassenpflug, J., Schünke, M., Heller, M. and Glüer, C. C. (2000) Evaluation of water content by spatially resolved transverse relaxation times of human articular cartilage. *Magnetic Resonance Imaging*, **18**(4), 423–30.

Madea, B., Herrmann, N. and Henßge, C. (1990) Precision of estimating the time since death by vitreous potassium - comparison of two different equations. *Forensic Science International*, **46**, 277–284.

Madea, B. and Rödig, A. (2006) Time of death dependent criteria in vitreous humor: accuracy of estimating the time since death. *Forensic Science International*, **164**(2-3), 87–92.

Madigan, M. T. and Martinko, J. M. (2006) *Brock: Biology of microorganisms*. 11th ed. Upper Saddle River: Pearson Prentice Hall.

Marks, M., Love, J. and Dadour, I. R. (2009) Taphonomy and time: estimating the post-mortem interval. *in* Steadman, D. W. (ed.), *Hard evidence: case studies in forensic anthropology*. 2nd ed., New Jersey: Prentice Hall, pp. 165–178.

Martin, J. A. and Buckwalter, J. A. (2006) Post-traumatic osteoarthritis: the role of stress induced chondrocyte damage. *Biorhe*, **43**(3-4), 517–521.

Mason, N. (2013) *Identifying and enhancing forensic science skills in the investigation and prosecution of war criminals within international proceedings*. University of Central Lancashire.

Masuda, K., Takegami, K., An, H., Kumano, F., Chiba, K., Anderson, G. B. J., Schmid, T. and Thonar, E. (2003) Recombinant osteogenic protein-1 upregulates extracellular matrix metabolism by rabbit annulus fibrosus and nucleus pulposus cells cultured in alginate beads. *Journal of Orthopaedic Research*, **21**(5), 922–930.

McDevitt, C. A. (1973) Biochemistry of articular cartilage. Nature of proteoglycans and collagen of articular cartilage and their role in ageing and in osteoarthrosis. *Annals of the Rheumatic Diseases*, **32**(4), 364–378.

McDowall, K. L., Lenihan, D. V, Busuttil, A. and Glasby, M. A. (1998) The use of absolute refractory period in the estimation of early postmortem interval. *Forensic Science International*, **91**(3), 163–70.

McKinley, J. and Ruffell, A. (2007) Contemporaneous spatial sampling at scenes of crime: advantages and disadvantages. *Forensic Science International*, **172**(2-3), 196–202.

Michaud, J. and Moreau, G. (2011) A statistical approach based on accumulated degree-days to predict decomposition-related processes in forensic studies. *Journal of Forensic Sciences*, **56**(1), 229–32.

Moger, C. J., Barrett, R., Bleuet, P., Bradley, D. A., Ellis, R. E., Green, E. M., Knapp, K. M., Muthuvelu, P. and Winlove, C. P. (2007). Regional variations of collagen orientation in normal and diseased articular cartilage and subchondral bone determined using small angle X-ray scattering (SAXS). *Osteoarthritis and Cartilage/OARS, Osteoarthritis Research Society*, **15**(6), 682–7.

Morel, V., Berutto, C. and Quinn, T. M. (2006) Effects of damage in the articular surface on the cartilage response to injurious compression in vitro. *Journal of Biomechanics*, **39**(5), 924–30.

Moskowitz, R. W. (1984) The biochemistry of osteoarthritis. *British Journal of Rheumatology*, **23**(3), 170–2.

Mow, V. C., Ratcliffe, A. and Poole, A. R. (1992) Cartilage and diarthrodial joints as paradigms for hierarchical materials and structures. *Biomaterials*, **13**(2), 67–97.

Muñoz Barús, J. I., Suárez-Peñaranda, J., Otero, X. L., Rodríguez-Calvo, M. S., Costas, E., Miguéns, X. and Concheiro, L. (2002) Improved estimation of postmortem interval based on differential behaviour of vitreous potassium and hypoxantine in death by hanging. *Forensic Science International*, **125**(1), 67–74.

Murata, H., Ikuta, Y. and Murakami, T. (1993) An anatomic investigation of the elbow joint, with special reference to aging of the articular cartilage. *Journal of Shoulder and Elbow Surgery*, **2**(4), 175–81.

Murphy, G. and Lee, M. H. (2005) What are the roles of metalloproteinases in cartilage and bone damage? *Annals of the Rheumatic Diseases*, **64**, 44–7.

Myburgh, J., L'Abbé, E. N., Steyn, M. and Becker, P. J. (2013) Estimating the postmortem interval (PMI) using accumulated degree-days (ADD) in a temperate region of South Africa. *Forensic Science International*, **229**, 1–6.

Nawrocki, S. P. (1996) An outline of forensic taphonomy. *Univeristy of Indianapolis Archaeology and Forensics Laboratory*.

Nguyen, Q., Murphy, G., Hughes, C. E., Mort, J. S. and Roughley, P. J. (1993) Matrix metalloproteinases cleave at two distinct sites on human cartilage link protein. *The Biochemical Journal*, **295**, 595–8.

Nordin, M. and Frankel, V. H. (2001) *Basic biomechanics of the musculoskeletal system*. 3rd ed. Philadelphia: Lippincott Williams & Wilkins.

Norkin, C. C. and Levangie, P. K. (1992) *Joint structure & function: a comprehensive analysis*. 2nd ed. Philadelphia: F. A. Davis Company.

Ogawa, R. (2011) Recent patents on stem cell-mediated cartilage regeneration and repair. *Recent Patents on Regenerative Medicine*, **1**(1), 118–122.

Otsuki, S., Brinson, D. C., Creighton, L., Kinoshita, M., Sah, R. L., D'Lima, D. and Lotz, M. (2008) The effect of glycosaminoglycan loss on chondrocyte viability: A study on porcine cartilage explants. *Arthritis and Rheumatism*, **58**(4), 1076–85.

Passos, M. L. C., Santos, A. M., Pereira, A. I., Santos, J. R., Santos, A. J. C., Saraiva, M. L. M. F. S. and Lima, J. L. F. C. (2009) Estimation of postmortem interval by hypoxanthine and potassium evaluation in vitreous humor with a sequential injection system. *Talanta*, **79**(4), 1094–9.

Pearle, A. D., Warren, R. F. and Rodeo, S. A. (2005) Basic science of articular cartilage and osteoarthritis. *Clinics in Sports Medicine*, **24**(1), 1–12.

Plaas, A., Osborn, B., Yoshihara, Y., Bai, Y., Bloom, T., Nelson, F., Mikecz, K. and Sandy, J. D. (2007) Aggrecanolysis in human osteoarthritis: confocal localization and biochemical characterization of ADAMTS5-hyaluronan complexes in articular cartilages. *Osteoarthritis and Cartilage/OARS, Osteoarthritis Research Society*, **15**(7), 719–34.

Pokines, J. T. (2009) Forensic recoveries of U.S. war dead and the effects of taphonomy and other site-altering processes. *in* Steadman, D. W. (ed.), *Hard evidence: case studies in forensic anthropology*. 2nd ed. New Jersey: Prentice Hall, pp. 141–153.

Poloz, Y. O. and O'Day, D. H. (2009) Determining time of death: temperature-dependent postmortem changes in calcineurin A, MARCKS, CaMKII, and protein phosphatase 2A in mouse. *International Journal of Legal Medicine*, **123**(4), 305–14.

Poposka, V., Gutevska, A., Stankov, A., Pavlovski, G., Jakovski, Z. and Janeska, B. (2013) Estimation of time since death by using algorithm in early postmortem period. *Global Journal of Medical Research Interdisciplinary*, **13**(3), 17–26.

Portron, S., Merceron, C., Gauthier, O., Lesoeur, J., Sourice, S., Masson, M., Fellah, B. H., Geffroy, O., Lallemand, E., Weiss, P., Guicheux, J. and Vinatier, C. (2013) Effects of in vitro low oxygen tension preconditioning of adipose stromal cells on their in vivo chondrogenic potential: Application in cartilage tissue repair. *PLOS ONE*, **8**(4), 1–10.

Pounder, D. J. (1995) Time of death. *University of Dundee*. Retrieved August 14, 2014, from www.dundee.ac.uk/forensicmedicine/notes/timedeath.pdf

Powers, R. H. (2005) The decomposition of human remains: a biochemical perspective. *in* Rich, J., Dean, D. E. and Powers, R. H. (eds.), *Forensic medicine of the lower extremity: human identification and trauma analysis of the thigh, leg, and foot*. Totowa: The Humana Press Inc., pp. 3–15.

Pratta, M. A., Tortorella, M. D. and Arner, E. C. (2000) Age-related changes in aggrecan glycosylation affect cleavage by aggrecanase. *The Journal of Biological Chemistry*, **275**(50), 39096–102.

Pratta, M. A., Yao, W., Decicco, C., Tortorella, M. D., Liu, R., Copeland, R. A., Magolda, R., Newton, R. C., Trzaskos, J. M. and Arner, E. C. (2003) Aggrecan protects cartilage collagen from proteolytic cleavage. *The Journal of Biological Chemistry*, **278**(46), 45539–45.

Quinn, T. M., Allen, R. G., Schalet, B. J., Perumbuli, P. and Hunziker, E. B. (2001) Matrix and cell injury due to sub-impact loading of adult bovine articular cartilage explants: Effects of strain rate and peak stress. *Journal of Orthopaedic Research: Official Publication of the Orthopaedic Research Society*, **19**(2), 242–9.

Rao, S., Aberg, F., Nieves, E., Band Horwitz, S. and Orr, G. A. (2001) Identification by mass spectrometry of a new alpha-tubulin isotype expressed in human breast and lung carcinoma cell lines. *Biochemistry*, **40**(7), 2096–103.

Rengel, Y., Ospelt, C. and Gay, S. (2007) Proteinases in the joint: clinical relevance of proteinases in joint destruction. *Arthritis Research & Therapy*, **9**(5), 221.

Rivers, D. B. and Dahlem, G. A. (2014) *The Science of Forensic Entomology*. Chichester: John Wiley & Sons, Ltd.

Rodriguez, W. (1997) Decomposition of buried and submerged bodies. *in* Haglund, W. D. and Sorg, M. H. (eds.), *Forensic taphonomy: the postmortem fate of human remains*. Boca Raton: CRC Press Taylor and Francis Group, pp. 459–468.

Rogers, C. J. (2010) *Dating death: forensic taphonomy and the postmortem interval thesis submitted for the Degree of doctor of philosophy*. Ph. D. Thesis, University of Wolverhampton.

Rogers, C. J., Clark, K., Hodson, B. J., Whitehead, M. P., Sutton, R. and Schmerer, W. M. (2011) Postmortem degradation of porcine articular cartilage. *Journal of Forensic and Legal Medicine*, **18**(2), 52–6.

Rogers, C. J., Ten Broek, C. M. A., Hodson, B., Whitehead, M. P., Schmerer, W. M. and Sutton, R. (2014). Identification of crystals forming on porcine articular cartilage: a new method for the estimation of the postmortem interval. *Journal of Forensic Sciences*, **59**(6), 1575–82.

Rognum, T. O., Hauge, S., Øyasaeter, S. and Saugstad, O. D. (1991) A new biochemical method for estimation of postmortem time. *Forensic Science International*, **51**(1), 139–146.

Roughley, P. J. (2006) The structure and function of cartilage proteoglycans. *European Cells & Materials*, **12**, 92–101.

Roughley, P. J. and Mort, J. S. (2014) The role of aggrecan in normal and osteoarthritic cartilage. *Journal of Experimental Orthopaedics*, **1**(1), 8.

Sachdeva, N., Rani, Y., Singh, R. and Murari, A. (2011) Review research paper estimation of post-mortem interval from the changes in vitreous biochemistry. *Journal of Indian Academy of Forensic Medicine*, **33**(2), 171–174.

Sagara, N. (1992) Experimental disturbances and epigeous fungi. *in* Carroll, G. C. and Wicklow, D. T. (eds.), *The fungal community: its organisation and role in the ecosystem* New York: Marcel Dekker, Inc., pp. 427–454.

Sagara, N., Yamanaka, T. and Tibbett, M. (2008) Soil fungi associated with graves and latrines: toward a forensic mycology. *in* Tibbett, M. and Carter, D. O. (eds.), *Soil analysis in forensic taphonomy: chemical and biological effects of buried human remains*. Boca Raton: CRC Press Taylor and Francis Group, pp. 67–107.

Schultz, M. (1997) Microscopic investigation of excavated skeletal remains: a contribution to paleopathology and forensic medicine. *in* Haglund, W. D. and Sorg, M. H. (eds.), *Forensic taphonomy: the postmortem fate of human remains*. Boca Raton: CRC Press Taylor and Francis Group, pp. 201–222.

Schwarcz, H. P., Agur, K. and Jantz, L. M. (2010) A new method for determination of postmortem interval: citrate content of bone. *Journal of Forensic Sciences*, **55**(6), 1516–22.

Scott, K. R., Morgan, R. M., Jones, V. J. and Cameron, N. G. (2014) The transferability of diatoms to clothing and the methods appropriate for their collection and analysis in forensic geoscience. *Forensic Science International*, **241**, 127–37.

Sidrim, J. J. C., Moreira Filho, R. E., Cordeiro, R. A., Rocha, M. F. G., Caetano, E. P., Monteiro, A. J. and Brilhante, R. S. N. (2010) Fungal microbiota dynamics as a postmortem investigation tool: focus on Aspergillus, Penicillium and Candida species. *Journal of Applied Microbiology*, **108**(5), 1751–6.

Simmons, T., Adlam, R. E. and Moffatt, C. (2010) Debugging decomposition data--comparative taphonomic studies and the influence of insects and carcass size on decomposition rate. *Journal of Forensic Sciences*, **55**(1), 8–13.

Sive, J. I., Baird, P., Jeziorsk, M., Watkins, A., Hoyland, J. A. and Freemont, A. J. (2002) Expression of chondrocyte markers by cells of normal and degenerate intervertebral discs. *Journal of Clincial Pathology: Molecular Pathology*, **55**, 91–97.

Sorg, M. H., Dearborn, J. H., Monahan, E. I., Ryan, H. F., Sweeney, K. G. and Edward, D. (1997) Forensic taphonomy in marine contexts. *in* Haglund, W. D. and Sorg, M. H. (eds.), *Forensic taphonomy: the postmortem fate of human remains*. Boca Raton: CRC Press Taylor and Francis Group, pp. 567–604.

Steadman, D. W. (1997) Interpretation of taphonomy and trauma. *in* Haglund, W. D. and Sorg, M. H. (eds.), *Forensic taphonomy: the postmortem fate of human remains*. Boca Raton: CRC Press Taylor and Francis Group, pp. 155–164.

Steadman, D. W. and Andersen, S. A. (2009) The Marty Miller case: Introducing forensic anthropology. *in* Steadman, D. (ed.), *Hard evidence: case studies in forensic anthropology*. 2nd ed. New Jersey: Prentice Hall, pp. 8–28.

Suzuki, A. (2002) Fungal succession at different scales. *Fungal Diversity*, **10**, 11–20.

Suzuki, A. (2009) Propagation strategy of ammonia fungi. *Mycoscience*, **50**, 39–51.

Suzuki, A. and Bärlocher, F. (2009) Editorial for the special feature: propagation strategy of fungi. *Mycoscience*, **50**(1), 1–2.

Swift, B. (2010) Methods of time since death estimations within the early post-mortem interval. *The Journal of Homicide and Major Incident Investigation*, **6**(1), 97–112.

Sztrolovics, R., Alini, M., Roughley, P. J. and Mort, J. S. (1997) Aggrecan degradation in human intervertebral disc and articular cartilage. *The Biochemical Journal*, **326**, 235–41.

Ten Broek, C. M. A. (2009) *Post mortem degradation of articular cartilage and fungal succession on buried pig trotters: exploring possibilities in the field of forensic taphonomy*. M.Sc. Thesis. University of Wolverhampton.

Tersigni-Tarrant, M. A. and Shirley, N. R. (2013) Forensic anthropology today. *in* Tersigni-Tarrant, M. A. and Shirley, N. R. (eds.), *Forensic anthropology: an introduction*. Boca Raton: CRC Press Taylor and Francis Group, pp. 25–32.

Thaik-Oo, M., Tanaka, E., Oikawa, H., Aita, K., Tanno, K., Yamazaki, K. and Misawa, S. (2002) No significant differences in the postmortem interval in Myanmar and Japanese using vitreous potassium levels. *Journal of Clinical Forensic Medicine*, **9**(2), 70–73.

Thierauf, A., Musshoff, F. and Madea, B. (2009) Post-mortem biochemical investigations of vitreous humor. *Forensic Science International*, 192(1-3), 78–82.

Tibbett, M. and Carter, D. O. (2003) Mushrooms and taphonomy: the fungi that mark woodland graves. *Mycologist*, **17**(1), 20–24.

Tibbett, M., and Carter, D. O. (eds.) (2008) *Soil analysis in forensic taphonomy: chemical and biological effects of buried human remains*. Boca Raton: CRC Press Taylor and Francis Group.

Towbin, H., Staehelin, T. and Gordon, J. (1992) Electrophoretic transfer of proteins from polyacrylamide gels to nitrocellulose sheets: Pprocedure and some applications. 1979. *Biotechnology (Reading, Mass.)*, **24**(9), 145–9.

Tranchida, M. C., Centeno, N. D. and Cabello, M. N. (2014) Soil fungi: their potential use as a forensic tool. *Journal of Forensic Sciences*, **59**(3), 785–9.

Turchetto, M. and Vanin, S. (2004) Forensic entomology and climatic change. *Forensic Science International*, **146**, S207–9.

Ubelaker, D. H. (1997) Taphonomic applications in forensic anthropology. *in* Haglund, W. D. and Sorg, M. H. (eds.), *Forensic taphonomy: the postmortem fate of human remains*. Boca Raton: CRC Press Taylor and Francis Group, pp. 77–90.

Van de Voorde, H. and van Dijck, P. J. (1982) Determination of the time of death by fungal growth. *Zeitschrift Für Rechtsmedizin*, **89**, 75–80.

Vass, A. A. (2011) The elusive universal post-mortem interval formula. *Forensic Science International*, **204**(1-3), 34–40.

Vass, A. A. (2012). Odor mortis. *Forensic Science International*, **222**(1-3), 234–41.

Vass, A. A., Bass, W. M., Wolt, J. D., Foss, J. E. and Ammons, J. T. (1992) Time since death determinations of human cadavers using soil solution. *Journal of Forensic Sciences*, **37**(5), 1236–53.

Vass, A. A., Smith, R. R., Thompson, C. V, Burnett, M. N., Dulgerian, N. and Eckenrode, B. A. (2008) Odor analysis of decomposing buried human remains. *Journal of Forensic Sciences*, **53**(2), 384–91.

Vass, A. A., Smith, R. R., Thompson, C. V, Burnett, M. N., Wolf, D. A., Synstelien, J. A., Dulgerian, N. and Eckenrode, B. A. (2004) Decompositional odor analysis database. *Journal of Forensic Sciences*, **49**(4), 760–9.

Vaz, S. (2001). *Multivariate and spatial study of the relationships between plant diversity and soil properties in created and semi-natural hay meadows*. Ph.D. Thesis. University of Wolverhampton.

Voss, S. C., Forbes, S. L. and Dadour, I. R. (2008) Decomposition and insect succession on cadavers inside a vehicle environment. *Forensic Science, Medicine, and Pathology*, **4**(1), 22–32.

Wang, Q., Yang, Y., Niu, H., Zhang, W., Feng, Q. and Chen, W. (2013) An ultrasound study of altered hydration behaviour of proteoglycan-degraded articular cartilage. *BMC Musculoskeletal Disorders*, **14**(1), 289.

Watanabe, H., Yamada, Y. and Kimata, K. (1998) Roles of aggrecan, a large chondroitin sulfate proteoglycan, in cartilage structure and function. *Journal of Biochemistry*, **124**(4), 687–93.

Wells, T., Davidson, C., Mörgelin, M., Bird, J. L. E., Bayliss, M. T. and Dudhia, J. (2003) Age-related changes in the composition, the molecular stoichiometry and the stability of proteoglycan aggregates extracted from human articular cartilage. *The Biochemical Journal*, **370**(Pt 1), 69–79.

Willey, P. and Leach, P. (2009) The skull on the lawn: trophies, taphonomy, and forensic anthropology. *in* Steadman, D. W. (ed.), *Hard evidence: case studies in forensic anthropology*. 2nd ed.. New Jersey: Prentice Hall, pp. 179–189.

Wilson, A. S., Janaway, R. C., Holland, A. D., Dodson, H. I., Baran, E., Pollard, A. M. and Tobin, D. J. (2007) Modelling the buried human body environment in upland climes using three contrasting field sites. *Forensic Science International*, **169**(1), 6–18.

Wilson, L. T. and Barnett, W. W. (1983) Degree-days: an aid in crop and pest management. *California Agriculture*, **37**(1), 4–7.

Wilson-Taylor, R. J. (2013) Time since death estimation and bone weathering: the postmortem interval. *in* Tersigni-Tarrant, M. A. and Shirley, N. R. (eds.), *Forensic anthropology: an introduction*. Boca Raton: CRC Press Taylor and Francis Group, pp. 339–380.

Wiltshire, P. E. J., Hawksworth, D. L., Webb, J. A. and Edwards, K. J. (2014) Palynology and mycology provide separate classes of probative evidence from the same forensic samples: a rape case from southern England. *Forensic Science International*.

Yasuda, T. (2006) Cartilage destruction by matrix degradation products. *Modern Rheumatology/the Japan Rheumatism Association*, **16**(4), 197–205.

Yasumoto, T. (2003) The G1 domain of aggrecan released from porcine articular cartilage forms stable complexes with hyaluronan/link protein. *Rheumatology*, **42**(2), 336–342.

Zhang, J. and An, J. (2007) Cytokines, inflammation and pain. *International Anesthesiology Clinics*, **45**(2), 27–37.

Zhou, B., Zhang, L., Zhang, G., Zhang, X. and Jiang, X. (2007) The determination of potassium concentration in vitreous humor by low pressure ion chromatography and its application in the estimation of postmortem interval. *Journal of Chromatography. B, Analytical Technologies in the Biomedical and Life Sciences*, **852**(1-2), 278–81.

Appendix

Calculated Accumulated Degree Days for Experiments 1-5

Table A.1 ***EXPT 1*** Comparison of ADDs experienced by trotter samples disinterred from HLT and CMP during the spring of 2011 (March 28 to May 10, 2011).

Date of Extraction for Hilton	Number of Days PM	Accumulated Degree-Days (ADD)	Date of Extraction for Compton	Number of Days PM	Accumulated Degree-Days (ADD)
March 28	0	6*	March 29	0	8*
April 4	7	81	April 5	7	88
April 11	14	165	April 12	14	169
April 18	21	238	April 19	21	245
April 27	30	357	April 28	30	360
May 3	36	433	May 4	36	440
May 9	42	531	May 10	42	541

Table A.2 ***EXPT 2*** Comparison of ADDs experienced by trotter samples disinterred from HLT and CMP during the summer of 2011 (June 20 to August 7, 2011).

Date of Extraction for Hilton	Number of Days PM	Accumulated Degree-Days (ADD)	Date of Extraction for Compton	Number of Days PM	Accumulated Degree-Days (ADD)
June 20	0	13*	June 21	0	17*
June 27	7	134	June 28	7	136
July 6	16	281	July 7	16	284
July 11	21	360	July 12	21	364
July 18	28	511	July 19	28	519
August 1	42	755	August 2	42	763
August 7	49	872	August 8	49	N/A

Table A.3 ***EXPT 3*** ADDs for trotter specimens disinterred daily for a short-term (7-days) experiment conducted at CMP from October 31 to November 7, 2011.

Date of Extraction for Compton	Number of Days PM	Accumulated Degree-Days (ADD)	Date of Extraction for Compton	Number of Days PM	Accumulated Degree-Days (ADD)
October 31	0	15*	November 4	4	60
November 1	1	24	November 5	5	68
November 2	2	33.5	November 6	6	74
November 3	3	47.5	November 7	7	80

* This ADD value was not taken into consideration for control cartilage extracted on the day of slaughter but was included among calculations for all experimental trotters disinterred.

Table A.4 ***EXPT 4*** ADDs for trotters disinterred over a 32-days period (weekly for the first three weeks and bi-weekly thereafter) from the HLT burial plot (September 17 to October 19, 2012).

Date of Extraction for Hilton	Number of Days PM	Accumulated Degree-Days (ADD)	Date of Extraction for Hilton	Number of Days PM	Accumulated Degree-Days (ADD)
September 17	0	13*	October 11	24	262
September 24	7	84	October 15	28	291
October 1	14	163	October 19	32	331
October 8	21	233			

Table A.5 ***EXPT 5*** ADDs for trotters disinterred weekly for a period of 42 PM days from the HLT burial plot (October 8 to November 19, 2012).

Date of Extraction for Hilton	Number of Days PM	Accumulated Degree-Days (ADD)	Date of Extraction for Hilton	Number of Days PM	Accumulated Degree-Days (ADD)
October 8	0	10*	November 6	29	266
October 16	8	78	November 12	35	369
October 23	15	154	November 19	42	430
October 30	22	217			

* This ADD value was not taken into consideration for control cartilage extracted on the day of slaughter but was included among calculations for all experimental trotters disinterred.